McGRAW-HILL
CHEMICAL ENGINEERING SERIES

TEXTS AND REFERENCE WORKS OUTLINED
BY THE FOLLOWING COMMITTEE

THE SERIES

BADGER AND BAKER—
Inorganic Chemical Technology

BADGER AND McCABE—
Elements of Chemical Engineering

EDWARDS, FRARY AND JEFFRIES
The Aluminum Industry (in Two Volumes)
Aluminum and Its Production
Aluminum Products and Their Fabrication

GROGGINS—
Unit Processes in Organic Synthesis

LEWIS AND RADASCH—
Industrial Stoichiometry

MANTELL—
Industrial Electrochemistry

NELSON—
Petroleum Refinery Engineering

PERRY (EDITOR)—
Chemical Engineers' Handbook

PROCHAZKA—
Accounting and Cost Finding for the Chemical Industries

SHERWOOD—
Absorption and Extraction

TYLER—
Chemical Engineering Economics

VILBRANDT—
Chemical Engineering Plant Design

WALKER, LEWIS AND McADAMS
Principles of Chemical Engineering

ABSORPTION AND EXTRACTION

BY

THOMAS K. SHERWOOD

Associate Professor of Chemical Engineering,
Massachusetts Institute of Technology

FIRST EDITION
SECOND IMPRESSION

McGRAW-HILL BOOK COMPANY, INC.
NEW YORK AND LONDON
1937

THE MAPLE PRESS COMPANY, YORK, PA.

PREFACE

The physical aspects of chemical engineering have to do principally with the transfer of heat and the interphase diffusion of material. Of the unit operations of chemical engineering, absorption, extraction, drying, humidification, and dehumidification are diffusional processes, and others may be cited in which diffusion plays a large part. It is the purpose of the present book to outline the underlying theory of these important processes and to deal particularly with the engineering problems connected with the design and operation of equipment for absorption and extraction.

In a technical article published recently in an English journal there appeared the statement: "Considering that absorption towers are as old as the chemical and certain allied industries, it is a remarkable fact that practically *all* those in use today are designed on the 'rule of thumb' and 'trial and error' methods. Few people understand the mechanism of absorption, and fewer still can *design* an absorption tower with any assurance. . . . " This is an obvious exaggeration, but it is nevertheless true that the relative complexity of the necessary theoretical background of the subject has retarded the accumulation of useful design data in the literature. It is hoped that the present work may encourage the publication of such information in a form suitable for the purposes of a general correlation.

The book may be divided roughly into three parts: The theoretical aspects of diffusion and the underlying theory of the design of absorption equipment; a summary of the available performance data on various types of equipment; and a section dealing with the basic principles of solvent extraction. The first presents the important relations derived from the kinetic theory and explains their applicability to the interphase transfer of materials. Graphical methods for design calculations are treated in detail, and a chapter is devoted to the design of absorption equipment for multicomponent systems, so important in the petroleum industry. The latter chapter includes tables of pre-

viously unpublished equilibrium data derived from the Lewis fugacity charts. The two chapters on absorption equipment include brief descriptions of the principal types, as well as the physical characteristics, allowable gas and liquor rates, and pressure-drop data for the more important packing materials. Absorption coefficients for the various systems have been collected from various sources and are summarized and presented in a single standard set of units. The final chapter deals with the underlying principles of solvent extraction, and explains the general methods of calculation employed both for three-component systems and for the solvent refining of lubricating oils.

The first two chapters, dealing with the theoretical aspects of diffusion and its relation to the kinetic theory, employ the c.g.s. system of units. The remaining chapters use English units, as being more appropriate to the engineering problems discussed. No apology is offered for introducing the two systems in a single text, as it is assumed that the present-day chemical engineer is necessarily proficient in the use of both. The principal nomenclature is consistent throughout the book. The various symbols used are explained both in the text and in the tables of nomenclature which appear at the end of each chapter. The bibliography appearing in the Appendix is not intended to be a complete list of the relevant material but includes only those sources referred to in the text.

The author is greatly indebted to his colleagues in the Department of Chemical Engineering at the Massachusetts Institute of Technology for encouragement and helpful advice. Thanks are due T. H. Chilton of the duPont Company and H. F. Johnstone of the University of Illinois for permission to use unpublished data, and T. H. Chilton for his critical review of Chapter V.

THOMAS K. SHERWOOD.

CAMBRIDGE, MASS.,
January, 1937.

CONTENTS

ABSORPTION AND EXTRACTION

CHAPTER I

DIFFUSION

True diffusion may be defined as the spontaneous intermingling of miscible fluids placed in mutual contact, accomplished without the aid of mechanical mixing. For example, a lump of sugar placed in the bottom of an unstirred cup of coffee will dissolve and diffuse slowly throughout the solution. If convection currents were entirely eliminated, the distribution of the sugar throughout the cup of coffee would require a very long time. Slight convection currents, due either to temperature differences within the solution or to residual or undamped mechanical motion, or to both, are invariably present to some slight extent in an apparently quiescent solution, so that even in the laboratory it is possible only to minimize these effects and so approach the conditions of true diffusion. The persistence of mechanical convection is greater in a gas than in a liquid, because of the greater viscosity of the latter. Because gases have large temperature coefficients of expansion and low viscosities, thermal convection currents are easily set up. For these reasons true diffusion in gases is even more difficult to approach than in liquids.

It is important to note that mixing by convection does not necessarily occur simply because the fluid is in motion. Viscous fluids at low velocities move in straight-line motion, with all particles moving along parallel paths. In such a moving fluid it is quite possible to have the process of true diffusion. At high velocities the motion of all fluids becomes turbulent, characterized by the development of many tiny eddies, or swirls, causing mixing of parallel streams of the fluid. True diffusion in such a

moving fluid is, of course, not possible, but mixing can and does take place, with considerably greater facility and speed than is possible by true diffusion. Thus, smoke leaving a tall chimney spreads conically with fair rapidity, owing to the eddy motion in the atmosphere, even at low wind velocities. The transference of material or the mixing of fluids by this mechanism has been termed eddy diffusion. It is much more rapid than true diffusion and is dependent principally upon the nature of the turbulent fluid and the conditions of flow. True diffusion, on the other hand, is governed principally by the nature of the fluids involved. Both true diffusion and eddy diffusion are of fundamental importance in the transfer of material in various industrial processes.

DIFFUSION IN GASES

According to the kinetic theory, a gas consists of a large number of individual molecules in rapid motion. The molecules move at random and so suffer frequent collisions with one another. The behavior of molecules at collision is not definitely known, but approximates that of hard elastic balls. Because of the frequent collisions, the molecular velocities are being continually changed in both direction and magnitude. The pressure of the gas on the walls of the containing vessel is due to the large number of impacts of impinging molecules. The temperature is determined by the mean kinetic energy of the individual molecules and hence by their weight and mean speed. For oxygen at 0°C. this mean speed corresponding to the mean kinetic energy of the molecule is approximately 462 m./sec., although there may be present molecules having speeds anywhere from zero to several thousand meters per second. The extremely high molecular speeds explain why pressure differences in a gas are equalized with such great rapidity.

At first thought it might seem that interdiffusion of gases must be very rapid if molecular speeds are in reality several hundred meters per second. Because of the large number of molecules present, however (2.8×10^{19} per cc. at 0°C. and 1 atm.), the collisions are extremely frequent, amounting to several billion per second, and the equalization of molecular distribution, or concentration, is relatively slow. Diffusion is more rapid at high temperatures because of the greater molecular velocities. It is similarly more rapid at low pressures because the average

distance between the molecules is greater and because the collisions are less frequent. Small molecules diffuse rapidly, primarily because of their greater molecular speeds, and also because the chance for collisions is not so great as for large molecules. The various experimental data on diffusion in gases are in remarkable agreement, both qualitatively and quantitatively, with the theoretical relations derived from the kinetic theory. Confirmation of the theory by the data on diffusion in gases is, in fact, one of the principal pieces of supporting evidence for the kinetic theory as a whole.

The theory of diffusion in gases was developed as a part of the kinetic theory* and is due principally to Maxwell[139] and to Stefan[177,178] with later important contributions from O. E. Meyer, Sutherland, Langevin, Chapman, Enskog, and Jeans. Maxwell's basic concept is that of a resistance to diffusion proportional to the number of molecules of the diffusing gas A; proportional to the number of molecules of the gas B through which diffusion takes place; proportional to the difference between the velocity u_A of the diffusing gas in the direction of net diffusion, and the velocity u_B of the second gas, and so to $(u_A - u_B)$; and proportional to the length of the path in the direction of diffusion. The number of molecules of each gas may be taken as proportional to the partial molal densities, ρ_A/M_A, and ρ_B/M_B, where ρ_A and ρ_B represent the partial densities as weight per unit volume, and M_A and M_B represent the molecular weights of the two gases. For diffusion to take place, the frictional resistance to the diffusion of the gas A must be overcome by a drop in concentration or partial pressure p_A of the diffusing gas, in the direction of diffusion. Neglecting external forces, and the acceleration of the molecules of gas A, this basic concept may be expressed algebraically as

$$-dp_A = \alpha_{AB}\frac{\rho_A\rho_B}{M_AM_B}(u_A - u_B)\,dx \qquad (1)$$

* For a readable outline of the kinetic theory, see "The Kinetic Theory of Gases" by O. E. Meyer, translated from the 2d rev. ed., 1899, by R. E. Baynes (Longmans, Green & Company, London). Perhaps the best general treatment of diffusion is Maxwell's article[141] under the title "Diffusion" in the 9th ed. of the "Encyclopaedia Britannica," 1877. The best discussion of diffusion, according to the kinetic theory, is believed to be found in Chap. XIII of Jeans' "Dynamical Theory of Gases," 3d ed., 1921 (Cambridge University Press).

where $-dp_A$ = decrease in partial pressure of the gas A in the length dx in the direction of diffusion.

α_{AB} = a proportionality constant for the diffusion of A through B.

The derivation of this equation is outlined by Lewis and Chang,[120] who also give integrations for various special cases.

If N_A be used to represent the rate of diffusion of the gas A as mols per unit time per unit area, then

$$N_A = \frac{u_A \rho_A}{M_A} \tag{2}$$

where M_A = molecular weight of the gas A.

Restricting the treatment to the case of equal molal diffusion of A and B in opposite directions, for which $N_A = -N_B$, then

$$\frac{u_A \rho_A}{M_A} = -\frac{u_B \rho_B}{M_B} \tag{3}$$

Combining this equality with Eq. (1), and remembering that $p_A + p_B = P$, one obtains

$$\frac{u_A \rho_A}{M_A} = -\frac{u_B \rho_B}{M_B} = -\frac{RT}{\alpha P}\frac{dp_A}{dx} = -\frac{R^2T^2}{\alpha M_A P}\frac{d\rho_A}{dx} \tag{4}$$

where α represents either α_{AB} or α_{BA}, depending on how the substitution is made. Since the interdiffusion of the two gases is dependent equally on the nature of both gases, it should be clear that $\alpha_{AB} = \alpha_{BA} = \alpha$, as suggested by the foregoing derivation. The relation between p_A and ρ_A is: $\rho_A = M_A p_A / RT$, which assumes the perfect gas laws, where T is the absolute temperature, and R the gas constant.

For any small element of volume of the gas, input must equal output plus accumulation; consequently

$$\frac{\partial \rho_A}{\partial \theta} + \frac{\partial}{\partial x}(u_A \rho_A) = 0 \tag{5}$$

which is termed the "equation of continuity."* In this equation θ represents time.

* Consider a small element of volume dx of unit cross section in the direction of diffusion. The weight of gas A contained in this element is $\rho_A\, dx$,

Combining Eqs. (4) and (5), the result is

$$\frac{\partial \rho_A}{\partial \theta} = \frac{R^2T^2}{\alpha P}\frac{\partial^2 \rho_A}{\partial x^2} \tag{6}$$

Maxwell substitutes D for the group $R^2T^2/\alpha P$, whence

$$\frac{\partial \rho_A}{\partial \theta} = D\frac{\partial^2 \rho_A}{\partial x^2} \tag{7}$$

or, in terms of partial pressures,

$$\frac{\partial p_A}{\partial \theta} = D\frac{\partial^2 p_A}{\partial x^2} \tag{8}$$

This is the equation which is encountered most frequently in discussions of the theory of diffusion in gases. It must be remembered, however, that it applies only to equal-molal diffusion of two gases in opposite directions, and not to the diffusion of one gas through a second stagnant one. The latter case will be discussed below. The constant D is termed the "diffusivity" or "diffusion coefficient" for the pair of gases in question. In differentiating Eq. (4) to obtain (6), α and therefore D are assumed independent of x and consequently of concentration. As brought out below, the experimental data indicate but slight variation of D with gas concentration and so justify this step.

Unsteady-state Diffusion of Two Gases.—If the partition separating two gas quantities is removed, the gases tend to diffuse into each other, and eventually the concentration becomes the same throughout the gas space. The rate at which the concentration equalizes is a function of the diffusivity, pressure, and

---

and the rate of depletion of A from the element is:

$$-\frac{\partial}{\partial \theta}(\rho_A)\, dx$$

The rate of diffusion of A to the element is $u_A\rho_A$, and the rate of diffusion from the element is:

$$u_A\rho_A + \frac{\partial}{\partial x}(u_A\rho_A)\, dx$$

Equating the depletion to the increase in diffusion rate across the element,

$$-\frac{\partial}{\partial \theta}\rho_A\, dx = \frac{\partial}{\partial x}(u_A\rho_A)\, dx$$

from which Eq. (5) follows.

dimensions of the container. Expressions relating concentration and time may be obtained by integration of Eq. (7) and form the basis of the standard method of determining diffusivities experimentally for the permanent gases.

Equations and plots are given by A. S. Smith,[172] showing the time required for mixing of two gases by diffusion in a commercial gas cylinder 125 cm. high. If such a cylinder is originally half full of helium and half full of methane at a total pressure of 5 atm., nearly 2½ hr. will be required for the average mol fraction of methane to fall to 0.7 in one half, and to rise to 0.3 in the other half of the cylinder. The calculation assumes mixing to be solely by true diffusion, with convection currents completely absent. Because of the low molecular weight of helium the diffusivity for the system helium-methane is high, and other gases require much longer times to mix by diffusion. The case treated by Smith is of practical interest in the preparation of gas mixtures for experimental purposes by forcing a second gas into a cylinder of the first.

Steady-state Diffusion of One Gas through a Second Stagnant Gas.—Most of the industrial operations to be discussed in later chapters involve steady-state operation, *i.e.*, continuous flow through an apparatus with steady conditions of temperature, pressure, and concentrations at any one point. Diffusion under such conditions implies the continuous supply and removal of the diffusing material. The usual conditions are those of a steady supply of the gas A at a plane x_1, with steady removal at the same rate at a plane x_2. In addition to the gas A there is present a second stagnant gas B which is neither supplied nor removed. The total pressure P is constant throughout the mixture. Thus $u_B = 0$, and Eq. (1) becomes

$$-\frac{dp_A}{dx} = \alpha\frac{\rho_A\rho_B}{M_AM_B}u_A = \alpha\frac{\rho_Au_A}{M_A}\frac{\rho_B}{M_B} \tag{9}$$

The general differential equation for the diffusion of one component at constant total pressure is obtained by differentiating Eq. (9) with respect to x, and combining with the equation of continuity; whence

$$\frac{\partial\theta}{\partial} = \frac{}{\partial x}\left(\frac{}{p_B}\frac{}{dx}\right) \tag{10}$$

It should be noted that this equation, and not Eq. (8), is the fundamental differential equation for the unidirectional diffusion of a single component through a second stagnant gas. Equation (8) is frequently used by mistake for this case, although the error involved in so doing is not large if p_B and P are nearly equal.

For steady-state operation, since

$$\frac{\rho_A u_A}{M_A} = N_A \qquad \text{and} \qquad \frac{\rho_B}{M_B} = \frac{p_B}{RT}$$

Eq. (9) may be written

$$N_A = -\frac{RT}{\alpha p_B}\frac{dp_A}{dx} \tag{11}$$

Introducing D as defined above, and substituting dp_B for $-dp_A$,

$$N_A = \frac{DP}{RTp_B}\frac{dp_B}{dx} \tag{12}$$

Integrating between the limits x_1 and x_2 in the direction of diffusion,

$$N_A = \frac{DP}{RT(x_2 - x_1)} \ln \frac{p_{B2}}{p_{B1}} \tag{13}$$

where p_{B2} and p_{B1} are the partial pressures of the gas B at the planes x_2 and x_1, respectively. The logarithmic mean of the values p_{B2} and p_{B1} is defined as

$$p_{BM} = \frac{p_{B2} - p_{B1}}{\ln \dfrac{p_{B2}}{p_{B1}}} \tag{14}$$

Combining this with Eq. (13) and letting the length of path $x_2 - x_1 = x$, one obtains

$$N_A = \frac{DP}{RTx}\frac{(p_{B2} - p_{B1})}{p_{BM}} = \frac{k}{x}\frac{(p_{B2} - p_{B1})}{p_{BM}} \tag{15}$$

or

$$N_A = \frac{DP}{RTx}\frac{(p_{A1} - p_{A2})}{p_{BM}} = \frac{k}{x}\frac{(p_{A1} - p_{A2})}{p_{BM}} \tag{16}$$

where $k = DP/RT$. This states that the rate of diffusion is directly proportional to the decrease in partial pressure of the diffusing gas A, and inversely proportional to the length of the path and to the logarithmic mean of the extreme values of the partial pressure of the interfering inert gas B. This

equation is the relation found to be most generally applicable to diffusion in gas films, as encountered in commercial absorption equipment.

Illustration 1.—Ammonia gas is diffusing at a constant rate through a layer of stagnant air 1 mm. thick. Conditions are fixed so that the gas contains 50 per cent ammonia by volume at one boundary of the stagnant layer. The ammonia diffusing to the other boundary is quickly absorbed, and the concentration is negligible at that plane. The temperature is 20°C. and the pressure atmospheric, under which conditions the value of D for the ammonia air may be assumed to be 0.18 cm.²/sec. Calculate the rate of diffusion of ammonia through the air layer.

Solution.—The conditions are those of steady-state diffusion of one gas through a second stagnant gas, and Eq. (16) applies. At one boundary of the gas layer the concentration is 50 per cent ammonia, and the partial pressure p_B of air and the partial pressure p_A of ammonia are each 0.5 atm. At the other boundary of the layer the concentration and consequently the partial pressure of ammonia are assumed to be zero, and the partial pressure of air is 1 atm. Hence

$$p_{A1} = 0.5, \qquad p_{A2} = 0, \qquad p_{B1} = 0.5, \qquad p_{B2} = 1.0 \text{ atm.},$$

and

$$p_{BM} = \frac{p_{B2} - p_{B1}}{\ln \frac{p_{B2}}{p_{B1}}} = \frac{1 - 0.5}{\ln \frac{1}{0.5}} = 0.72 \text{ atm.}$$

Substituting in Eq. (16),

$$N_A = \frac{DP}{RTx} \frac{p_{A1} - p_{A2}}{p_{BM}} = \frac{0.18 \times 1 \times (0.5 - 0)}{82.07 \times 293 \times 0.1 \times 0.72}$$
$$= 5.21 \times 10^{-5} \text{ g. mols/(sec.)(cm.}^2\text{)}$$

Equation (11) brings out the fact that for steady-state diffusion at constant total pressure, p_A is not linear in x, but the slope (dp_A/dx) is directly proportional to p_B, and therefore to $P - p_A$. A plot of p_A *vs.* x is consequently concave to the x-axis, as shown in Fig. 1. This plot indicates the type of pressure gradients obtained in the steady-state diffusion of a gas A through a second stagnant gas B.

At first thought it seems impossible for A to diffuse without a simultaneous diffusion of B, since the gradients are similar for both gases. The explanation lies in the fact that the pressure gradient of the gas B is maintained by the diffusion of A. It is the friction of the moving molecules of A that increases the concentration of B molecules at the second boundary, and the result may be explained by stating that the number of molecules of B carried toward x_2 by this friction is exactly equal to the

number of molecules of B diffusing toward x_1 under the influence of the partial-pressure gradient so set up. The net diffusion of B is zero.

Steady-state Diffusion of Both Components of a Binary Mixture.[120]—In absorption practice it is frequently necessary to treat a mixture of two or more gases, both or all of which are soluble to varying degrees in the absorbing medium. Such a case is one of simultaneous diffusion of two or more gases in the same direction. In other cases the absorbing medium may evaporate into the gas to be treated, resulting in simultaneous diffusion of two gases in opposite directions. The diffusion of each gas is affected by the presence of the molecules of the other gas and hindered if the gases are diffusing in opposite directions. The equations for diffusion of both gases of a binary mixture are easily obtainable in a manner similar to the derivation of Eq. (16). Substituting Mp/RT for the partial densities, and NM/ρ for u in Eq. (1),

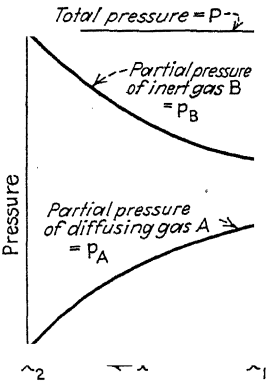

FIG. 1.—Partial-pressure gradients in layer of inert gas B through which gas A is diffusing.

$$-\frac{dp_A}{dx} = \frac{\alpha}{RT}(p_B N_A - p_A N_B)$$
$$= \frac{RT}{DP}(p_B N_A - p_A N_B) = \frac{1}{k}(p_B N_A - p_A N_B) \qquad (17)$$

For a constant total pressure, $P = p_B + p_A$, and

$$-\frac{dp_A}{dx} = \frac{1}{k}(PN_A - p_A N_A - p_A N_B) \qquad (18)$$

Under given conditions of steady-state diffusion, N_A and N_B are constants, and (18) may be integrated between the limits $p_A = p_{A1}$ at $x = 0$, and $p_A = p_{A2}$ at $x = x$:

$$\ln \frac{1 - \left(1 + \frac{N_B}{N_A}\right)\frac{p_{A2}}{P}}{1 - \left(1 + \frac{N_B}{N_A}\right)\frac{p_{A1}}{P}} = \frac{x}{k}(N_A + N_B) \qquad (19)$$

For parallel diffusion, N_A and N_B will have the same signs; for counterdiffusion, N_A and N_B will have opposite signs. For equal-molal counterdiffusion of two vapors, as is approximated in rectification, $N_A = -N_B$. For this special case, integration of Eq. (18) leads to

$$N_A = \frac{k}{x}\left(\frac{p_{A1} - p_{A2}}{P}\right) \tag{20}$$

which differs from the equation for one diffusing gas only by the substitution of P for p_{BM}. Unless some relation between N_A and N_B is known (as may be given, for example, by a heat balance), it is impossible to determine both N_A and N_B from the single Eq. (19).

Illustration 2.—A simple rectifying column consists of a vertical tube supplied at the bottom with a mixture of benzene and toluene as vapor. At the top a reflux condenser condenses and returns some of the product as reflux which flows in a thin film down the inner wall of the tube. The tube is sufficiently insulated so that heat loss may be neglected. At one point in the column the vapor contains 70 mol per cent benzene and the adjacent liquid reflux contains 59 mol per cent benzene. The temperature at this point is 90°C. Assuming the diffusional resistance to vapor transfer between vapor and liquid to be equivalent to the diffusional resistance of a stagnant vapor layer 0.2 mm. thick, calculate the rate of interchange of benzene and toluene between vapor and liquid. The molal latent heats of vaporization of benzene and toluene may be assumed to be equal. The vapor pressure of toluene at 90°C. is 404.6 mm., and the diffusivity for toluene-benzene may be assumed to be 0.051 cm.²/sec.

Solution.—In a rectifying column operating without heat loss, the liquid will be at its boiling point. As a result, the toluene condensed liberates sufficient heat to vaporize an equal number of mols of benzene. At any point in the column, therefore, $N_A = -N_B$, and Eq. (20) applies.

Since the vapor composition at the point in question is 70 mol per cent benzene, the partial pressure of toluene in the vapor p_{A1} is 0.3 atm. The value of p_{A2} is obtained from Raoult's law as the vapor pressure of toluene in equilibrium with the liquid:

$$p_{A2} = (1.0 - 0.59)\frac{404.6}{760} = 0.218 \text{ atm.}$$

$$N_A = \frac{DP}{RT\,x}\frac{(p_{A1} - p_{A2})}{P} = \frac{0.051 \times 1 \times (0.3 - 0.218}{82.07 \times 363 \times 0.02 \times 1}$$

$$= 7.06 \times 10^{-6} \text{ g. mol toluene/(sec.)(cm.}^2\text{)}$$

Simultaneous Diffusion of Two Gases through a Third Stagnant Gas.—The fundamental differential equations of the type of Eq. (1) are, for this case:

$$-\frac{dp_A}{dx} = \alpha_{AB}\frac{\rho_A\rho_B}{M_AM_B}(u_A - u_B) + \alpha_{AC}\frac{\rho_A\rho_C}{M_AM_C}(u_A - u_C) \quad (21)$$

and

$$-\frac{dp_B}{dx} = \alpha_{BA}\frac{\rho_A\rho_B}{M_AM_B}(u_B - u_A) + \alpha_{BC}\frac{\rho_B\rho_C}{M_BM_C}(u_B - u_C) \quad (22)$$

Let the stagnant gas be C, then $u_c = 0$. Substituting $\rho u = MN$, $\rho = Mp/RT$, $P = p_A + p_B + p_C$, and $\alpha_{AB} = \alpha_{BA}$, one obtains

$$-\frac{dp_A}{dx} = (r_{AB} - r_{AC})N_Ap_B - (r_{AB}N_B + r_{AC}N_A)p_A + r_{AC}N_AP \quad (23)$$

and

$$-\frac{dp_B}{dx} = (r_{AB} - r_{BC})N_Ap_A - (r_{AB}N_A + r_{BC}N_B)p_B + r_{BC}N_BP \quad (24)$$

where $r_{AB} = 1/k = \alpha_{AB}/RT$, etc.

A solution of these equations in the form of two simultaneous equations has been obtained by E. R. Gilliland.[67] The equations are

$$r_{AC}N_A + r_{BC}N_B = \frac{1}{x}\ln\frac{p_{C2}}{p_{C1}} \quad (25)$$

and

$$N_A + N_B = \frac{k_{AB}}{x}\ln \left[\frac{\left(\frac{r_{AB} - r_{AC}}{r_{AB} - r_{BC}}\right)\frac{N_A + N_B}{N_B}p_{B2} - \frac{N_A + N_B}{N_A}p_{A2} + \left(\frac{r_{AC} - r_{BC}}{r_{AB} - r_{BC}}\right)P}{\left(\frac{r_{AB} - r_{AC}}{r_{AB} - r_{BC}}\right)\frac{N_A + N_B}{N_B}p_{B1} - \frac{N_A + N_B}{N_A}p_{A1} + \left(\frac{r_{AC} - r_{BC}}{r_{AB} - r_{BC}}\right)P}\right] \quad (26)$$

Although apparently unwieldy, these equations are not overly difficult to use in actual numerical calculation. For various special cases they simplify considerably, as for example, when $p_c = 0$, they reduce to Eq. (19). In using Eqs. (25) and (26) it is important to place N_A and N_B positive if diffusing in the direction of increasing x, and negative if diffusing in the opposite direction; also note that $p_A = p_{A1}$ at $x = 0$, and $p_A = p_{A2}$ at $x = x$, with a similar convention for the other components.

Illustration 3.—Ammonia is diffusing from an air-ammonia mixture into water under a total pressure of 0.2 atm. Assume the diffusion to take place through a stagnant gas layer at an average temperature of 55°C. At one point in the apparatus the gas contains 3 per cent ammonia by volume, and

the concentration of the ammonia in the water is so low that the partial pressure of ammonia over the solution may be neglected at the point under consideration. The air is dry.

What percentage error would be made in calculating the rate of diffusion of ammonia if the simultaneous vaporization of the water were overlooked?

Data and Assumptions.

Assume the vapor pressure of the water to be 55.2 mm. Hg.

Diffusivity of ammonia in air = 1.075 cm.²/sec.

Diffusivity of water vapor in air = 1.245 cm.²/sec.

Diffusivity of water vapor in ammonia = 1.47 cm.²/sec.

These values were calculated for a total pressure of 0.2 atm., using Eq. (31).

Solution.

Total pressure = 0.2 atm. = P.

Let A refer to ammonia, B to water vapor, and C to air.

Neglecting water vaporization, this is a case of the diffusion of one gas, ammonia, through a second stagnant one, air, and Eq. (16) applies.

Allowing for water vaporization, this becomes a case of simultaneous diffusion of two gases, ammonia and water vapor, through a third stagnant gas, air, and the two simultaneous Eqs. (25) and (26) should be used.

Since the problem is to find the percentage error made in calculating the rate of ammonia diffusion without allowing for the simultaneous diffusion of water vapor, it is allowable to calculate the percentage deviation of any variable which is proportional to the rate of ammonia diffusion. An inspection of the equations shows that the solution would be expedited by solving for a new variable $y = N_A x RT$, which is proportional to the rate of ammonia absorption, N_A. The product xRT is a constant and is the same in both cases.

Neglecting water-vapor diffusion, substitution in Eq. (16) gives

$$N_A = -\frac{1.075 \times 0.2}{RTx} \frac{(0.2 \times 0.03 - 0)}{\ln \frac{0.2}{0.194}} = -\frac{0.00655}{RTx}$$

or,

$$N_A x RT = y = -0.00655.$$

Allowing for simultaneous diffusion of water vapor, and using Eqs. (25) and (26),

$$r_{AC} = \frac{1}{k_{AC}} = \frac{RT}{D_{AC}P} = \frac{RT}{1.075 \times 0.2} = \frac{RT}{0.215} = 4.65\ RT$$

$$r_{AB} = \frac{RT}{1.47 \times 0.2} = 3.4\ RT$$

$$r_{BC} = \frac{RT}{1.245 \times 0.2} = 4.01\ RT$$

$$\frac{r_{AB} - r_{AC}}{r_{AB} - r_{BC}} = \frac{3.4\ RT - 4.65\ RT}{3.4\ RT - 4.01\ RT} = 2.05$$

$$\frac{r_{AC} - r_{BC}}{r_{AB} - r_{BC}} = \frac{4.65\ RT - 4.01\ RT}{3.4\ RT - 4.01\ RT} = -1.05$$

$$\text{At } x = 0 \begin{cases} p_{A1} = 0.0 \text{ atm.} \\ p_{B1} = \dfrac{55.2}{760} = 0.0727 \text{ atm.} \\ p_{C1} = 0.2 - 0.0727 = 0.1273 \text{ atm.} \end{cases}$$

$$\text{At } x = x \begin{cases} p_{A2} = 0.2 \times 0.03 = 0.006 \text{ atm.} \\ p_{B2} = 0.0 \text{ atm.} \\ p_{C2} = 0.2 - 0.005 = 0.194 \text{ atm.} \end{cases}$$

Substituting in Eq. (25),

$$4.65\,RTN_A + 4.01\,RTN_B = \frac{1}{x} \ln \frac{0.194}{0.1273} = \frac{0.421}{x}$$

$$N_B = \frac{0.105}{xRT} - 1.158N_A \qquad (A)$$

Substituting in Eq. (26),

$$N_A + N_B = \frac{1.47 \times 0.2}{xRT} \ln \left[\frac{-\dfrac{N_A + N_B}{N_A}(0.006) - 1.05 \times 0.2}{2.05\left(\dfrac{N_A + N_B}{N_B}\right)(0.0727) - 1.05 \times 0.2} \right] \qquad (B)$$

Substituting Eqs. (*A*) in (*B*), and substituting $y = N_A xRT$, and rearranging,

$$0.357 - 0.540\,y = \ln \frac{0.242y^2 - 0.02122y - 0.0000661}{0.2195\,y^2 - 0.00639y} \qquad (C)$$

Since the value of y obtained without allowing for water-vapor diffusion is approximately correct, it may be substituted in the left side of Eq. (*C*) to facilitate solving. Substituting,

$$0.357 - 0.540(-0.00655) = \ln \frac{0.242y^2 - 0.02122y - 0.0000661}{0.2195y^2 - 0.00639y}$$

Solving, $y = -0.0057$, or -0.160.

The effect of simultaneous water-vapor diffusion is to reduce the rate of ammonia diffusion, N_A; hence -0.0057 is the correct value of y. Recalculation using this value on the left-hand side of Eq. (*C*) would not change the result appreciably.

Therefore

$$N_A = -\frac{0.0057}{xRT}$$

Substituting this value of N_A back in Eq. (*A*),

$$N_B = \frac{0.105 + 1.158(0.0057)}{xRT} = \frac{0.1116}{xRT}$$

Neglecting ammonia diffusion, and using Eq. (16),

$$p_{BM} = \frac{0.0727}{\ln \dfrac{0.2}{0.1273}} = 0.161 \text{ atm.}$$

$$N_B = \frac{1.245 \times 0.2 \times 0.0727}{xRT\ 0.161} = \frac{0.1124}{xRT}$$

SUMMARY OF RESULTS

	Calculated allowing for counterdiffusion	Calculated counterdiffusion	error
(ammonia)...	-0.0057		14.9
$N_B x RT$ (water vapor).	0.1116	0.1124	0.7

The effect of counterdiffusion of solvent is ordinarily less than indicated by this example, since the error involved in neglecting it is exaggerated by the low pressure and by the high driving force for water-vapor diffusion. In the usual cases met with in absorption practice the simpler Eq. (16) is sufficiently accurate.

THEORETICAL EQUATIONS FOR DIFFUSION COEFFICIENTS IN GASES

Because of its intimate association with the kinetic theory of gases, the development of a theory of diffusion from the concepts of the kinetic theory has been a subject of great interest to physicists. The first theoretical expression connecting the diffusion coefficient with the molecular properties of the two diffusing gases was derived by Maxwell[140] and is

$$D = \frac{W}{n} + \frac{1}{w_B} \tag{27}$$

where D = diffusion coefficient for the system.
W = "velocity of mean square" of the hydrogen molecule at 0°C.
n = number of molecules per cubic centimeter in a gas at standard conditions.
S = distance between the centers of two unlike molecules at collision.
w = molecular weight relative to that of hydrogen as unity.

This equation was apparently intended to apply at standard conditions only. Substituting for W and n their equivalent functions of temperature and pressure, the above equation becomes

$$D = \left(\frac{R^{\frac{3}{2}}}{\sqrt{\pi}}\right)\frac{T^{\frac{3}{2}}}{PS^2}\sqrt{\frac{1}{M_A} + \frac{1}{M_B}} \tag{28}$$

where M_A and M_B = ordinary molecular weights of the two gases.
P = total pressure.
R = gas constant.
A = Avogadro's number.

Jeans[101] gives the same relation but with a slightly different constant, $8/3\pi$ times that given by Maxwell. Chapman's derivation[32] leads to a constant 3/4 of that obtained by Maxwell.

The most important modification of the Maxwell equation is due to Sutherland,[180] who introduced the factor $\left(1 + \frac{C}{T}\right)$ in the denominator of Eq. (28) to allow for the intermolecular attraction at low temperatures. The "Sutherland constant" C for the system depends only on the natures of the two kinds of molecules and is obtained from the individual values of C for each gas, which are in turn obtained preferably from viscosity data on the pure gases. Methods of estimating C for any gas system are discussed by Arnold.[3]

O. E. Meyer[143] has derived a theoretical equation which indicates a variation of the diffusion coefficient with the ratio of the quantities of the two gases present. Several investigators have carried out series of experiments to discover such an effect, if present, and their results show such a small variation of D with gas composition that it seems entirely allowable to neglect it in engineering computation.

In attempting to use the Maxwell or Sutherland equations for D, it is, of course, necessary to have values of S for the system. Arnold has compared various experimental data on diffusion coefficients with the Sutherland equation, obtaining values of S from the molecular volumes by the Titani equation. However, since this last relation is empirical, it seems best to rewrite Eq. (28) as

$$D = B\frac{T^{\frac{3}{2}}}{P(V_A^{\frac{1}{3}} + V_B^{\frac{1}{3}})^2}\sqrt{\frac{1}{M_A} + \frac{1}{M_B}}, \tag{29}$$

or

$$D = B'\frac{T^{\frac{3}{2}}}{P(V_A^{\frac{1}{3}} + V_B^{\frac{1}{3}})^2\left(1 + \frac{C}{T}\right)}\sqrt{\frac{1}{M_A} + \frac{1}{M_B}} \tag{30}$$

where V represents the molecular volume (see below), and then to obtain the best values of B or B' empirically by comparison with experimental diffusion data. This has been done by Gilliland,[68] who has collected the published results of some 400 experimental determinations. Gilliland has himself obtained values in air for a number of vapors, including diphenyl and mer-

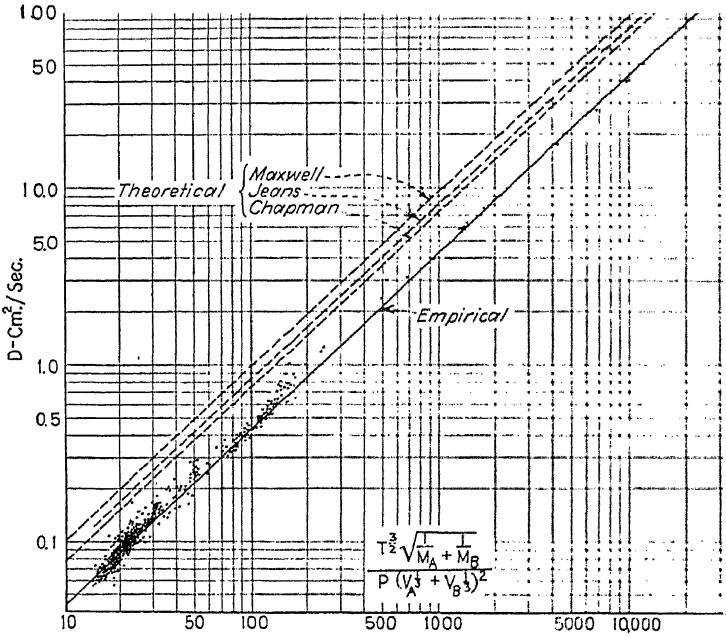

FIG. 2.—Experimentally determined diffusion coefficients compared with the theoretical equations based on the kinetic theory.

cury at elevated temperatures, using the evaporative technique outlined below. The data plotted against the groups suggested by Eqs. (29) and (30) are shown in Figs. 2 and 3. In calculating the group plotted as abscissa in Fig. 3, the values of C used were obtained as suggested by Arnold,[3] using values of C for the pure gases obtained from viscosity determinations or, where those were lacking, values estimated from the empirical equation

$$C = 1.47T_b$$

where T_b = normal boiling point, °K.

Each plot shows a wide band of points, with considerable deviation from the mean line. This is to be expected from the rather poor precision obtained by the experimental methods so far developed for obtaining diffusion coefficients. There is, however, no definite trend of deviation with molecular weight

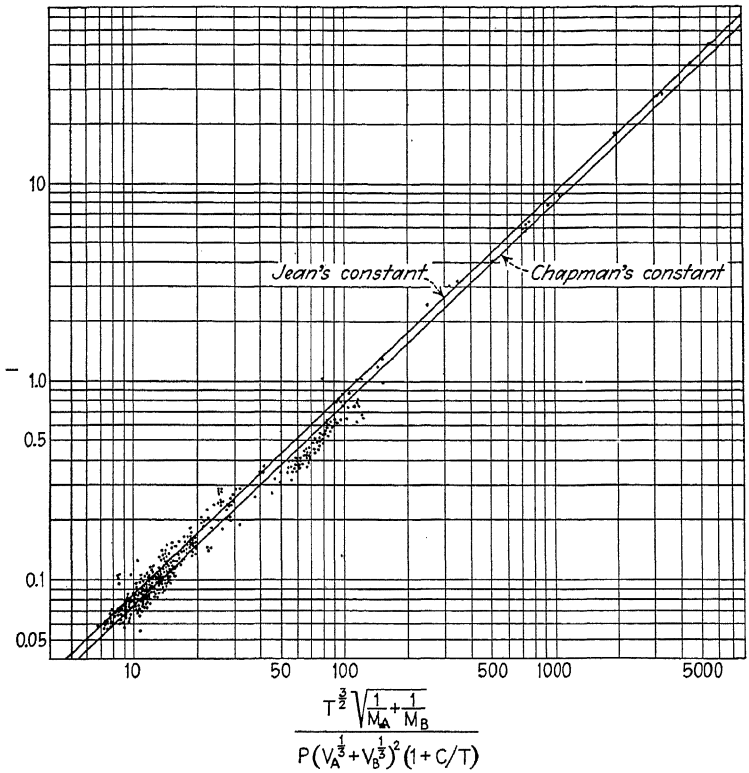

FIG. 3.—Experimentally determined diffusion coefficients compared with the Sutherland equation.

or with pressure, both of which were varied over quite wide ranges in the data plotted. Comparison of the two plots shows the first to give the better correlation. The temperature range covered was narrow, being only from 0 to 100°C., except for a few points; therefore it is not possible to show whether the poorer correlation with the Sutherland group is due to the temperature

function being incorrect, or to the use of incorrect values of C in calculating the groups plotted. In obtaining an empirical relation the first plot is the more satisfactory from a practical point of view, since it not only shows a better correlation of the data but does not involve the uncertain quantity C. Inspection of Fig. 2 shows the empirical constant to be 0.0043, and the relation is, therefore,

$$D = 0.0043 \frac{T^{\frac{3}{2}}}{P(V_A^{\frac{1}{3}} + V_B^{\frac{1}{3}})^2} \sqrt{\frac{1}{M_A} + \frac{1}{M_B}} \qquad (31)$$

where D = diffusion coefficient, cm.^{2}/sec.
T = absolute temperature, °K.
M_A, M_B = molecular weights of the two gases,
P = total pressure, atm.
V_A, V_B = molecular volumes (see below).

Sutherland himself,[180] on analyzing certain of von Obermayer's data for several pairs of gases, found a greater variation in B' than in B. For six pairs of gases he found B to vary from 0.0038 to 0.0047. Arnold, however, prefers the Sutherland type of equation for which he recommends Jean's value of 0.00837 for B'.

In using Eq. (31), values of V should be obtained in the same way as were those used by Gilliland in preparing Fig. 2. For this plot, the values of V were obtained using Kopp's law of additive volumes, with the rules and values for each element given by LeBas, as outlined by Arnold.[3] The principal values and rules are given in Table I. Thus for SO_2, V = 25.6 + 7.4 + 7.4 = 40.4.

TABLE I.—ATOMIC VOLUMES

Bromine	27.0	Hydrogen	3.7
Sulfur	25.6	Nitrogen	15.6
Oxygen	7.4	In primary amines	10.5
In methyl esters	9.1	In secondary amines	12.0
In higher esters and ethers	11.0	For benzene ring formation deduct 15; naphthalene deduct 30	
In acids	12.0		
Carbon	14.8		
Chlorine	24.6	For the hydrogen molecule use V = 14.3, and for air use V = 29.9.	

Equation (31) is recommended for use in estimating values of D in cases where no good experimental data exist. Reliable experimental data are, of course, to be preferred to an estimate obtained from such an empirical equation.

Illustration 4.—Estimate the diffusivity for ethyl alcohol in air at 0°C. and at atmospheric pressure.

Solution.—The problem is simply that of substitution in Eq. (31). Using the values for atomic volumes given in Table I, for ethyl alcohol,

$$V_A = 2 \times 14.8 + 6 \times 3.7 + 7.4 = 59.2;$$

for air, $V_B = 29.9$.

$$D = 0.0043 \times \frac{(273)^{\frac{3}{2}}}{\left[(59.2)^{\frac{1}{3}} + (29.9)^{\frac{1}{3}}\right]^2 \times 1} \sqrt{\frac{1}{46} + \frac{1}{29}} = 0.093$$

The I.C.T. give 0.102 cm.²/sec. for D at 0°C. and 1 atm. for ethyl alcohol in air. In this case the estimated value is approximately 9 per cent lower.

SELF-DIFFUSION

The rate of diffusion of molecules of a gas through other molecules of the same gas is obviously impossible to determine experimentally. It is of interest, however, that for this case the various theoretical equations developed from the kinetic theory reduce to

$$\frac{\rho D}{\mu} = E \tag{32}$$

where E is a numerical constant and μ and ρ represent gas viscosity and density, respectively. Maxwell's theory of molecules repelling as the fifth power of the distance leads to a value of E of 1.504, whereas Chapman's theory for elastic spheres gives $E = 1.20$. Jeans[101] quotes Lord Kelvin's analysis of the data of Loschmidt, in which the coefficients of self-diffusion for four gases were calculated from the data on interdiffusion of several pairs of the four gases, and the value of E was found to vary from 1.34 to 1.50. This confirmation of Eq. (32) supports the conclusions from the kinetic theory that for a mixture of gases, $\rho D/\mu$ is independent of temperature, a relation which will be found useful in the calculations of the next chapter.

EXPERIMENTAL DETERMINATIONS OF DIFFUSION COEFFICIENTS IN GASES

Several different methods have been devised for the measurement of diffusion coefficients in gases. The principal ones are described very briefly below.

1. Evaporation of Liquids in Narrow Tubes.—One of the two components, in the liquid state, is placed in a small glass tube, filling the tube to within 1 to 5 cm. of the top. The tube and liquid are held at constant temperature and the second gas passed over the top of the tube. The rate of diffusion is obtained by measuring the rate of fall of liquid in the tube. This technique, devised and used by Stefan, is perhaps the best and most widely used of the experimental methods. It is limited, however, to a fairly narrow range of temperature for any one system, since one component must be liquid, and the precision is poor at very low or very high vapor pressures.

2. Unsteady-state Interdiffusion of Two Gases.—The two gaseous components are placed in separate sections of a tube, and diffusion is allowed to take place by removing the partition separating the sections. After a definite time interval the gas from various portions of the tube is analyzed and the results compared with an integrated form of Eq. (8). This method has been widely used for systems of the permanent gases but gives results somewhat less reliable than those obtained by the first method.

3. Miscellaneous Methods.—Diffusion coefficients for iodine in air have been obtained by measuring the rate of evaporation of a small sphere of iodine suspended in air. It seems probable that convection currents in the air make this method unreliable. Mullaly and Jacques[146] placed iodine and mercury, respectively, at the two ends of a tube filled with nitrogen at low pressure. The diffusion coefficients of both iodine and mercury were calculated from the measured amount, composition, and location of the deposit of mercurous and mercuric iodides formed. Special methods of this type are useful only for special types of systems.

Figure 4 shows data* on the diffusion coefficients for a number of gases diffusing in air at 0°C. and 1 atm., plotted as D *vs.* molecu-

* Data from the International Critical Tables.[98] The experimental values, obtained in most cases at temperatures from 10 to 50°C., have been extrapolated to 0°C.

lar weight. The plot shows a rather striking correlation of the data for any one class of compounds, and a trend of decreasing

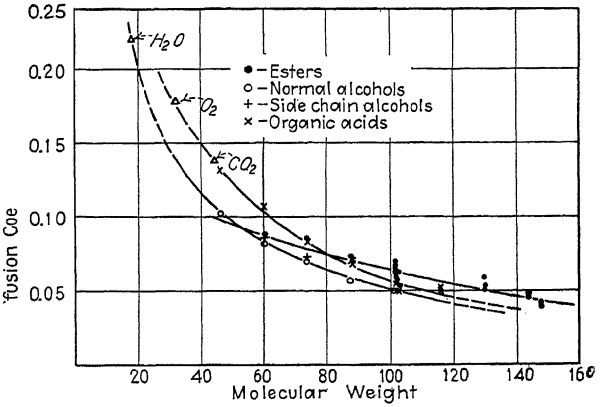

FIG. 4.—Diffusion coefficients for various gases in air at 0°C. and 1 atm.

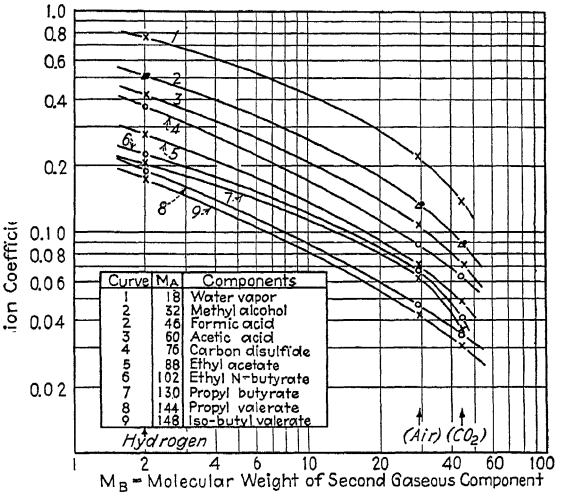

FIG. 5.—Relation between the diffusion coefficients for various gases and the molecular weight of the second gas.

values of D with increased molecular weight in each case. The points for carbon dioxide and for oxygen fall, by chance perhaps, on a continuation of the line for organic acids. Similarly, the

point for water vapor falls on a continuation of the line for normal alcohols.

Figure 5 shows values of the diffusion coefficient for several vapors through hydrogen, air, and carbon dioxide. The values of D at 0°C. and 1 atm. are shown plotted *vs.* molecular weight M_B of the second gas, using logarithmic coordinates. The same trend is indicated as in Fig. 4, showing the decrease in D with increase in molecular weight of either component.

DIFFUSION IN LIQUIDS

Diffusion takes place very much more slowly in liquids[179] than in gases. Because of the greater density of the liquid phase, the resistance to diffusion is much greater, and days are required for equalization of a concentration difference in a liquid, where a similar change in the gas phase would require but a few seconds. Because of the closer spacing of the molecules, molecular attraction plays an important part, and the kinetic theory of liquids has been but partially developed. There are consequently no theoretical equations for diffusion coefficients in liquids comparable with the Maxwell equation (27). The mechanism of molecular diffusion is similar in both liquids and gases, however, and by analogy to Eq. (1), we may write for liquids

$$-\frac{dc_A}{dx} = \beta c_A c_B (u_A - u_B) \tag{33}$$

where c_A and c_B = partial molal densities of the two components,
β = a new proportionality constant.

For the special case of equal molal diffusion of A and B in opposite directions

$$N_A = u_A c_A = -N_B = -u_B c_B \tag{34}$$

Combining Eqs. (33) and (34),

$$N_A = -\frac{1}{\beta(c_A + c_B)} \frac{dc_A}{dx} \tag{35}$$

Using the above nomenclature, the equation of continuity becomes

$$\frac{\partial c_A}{\partial \theta} + \frac{\partial}{\partial x}(u_A c_A) = 0 \tag{36}$$

which may be combined with Eq. (35) to give

$$\frac{\partial c_A}{\partial \theta} = \frac{1}{\beta(c_A + c_B)} \frac{\partial^2 c_A}{\partial x^2} \tag{37}$$

This step introduces the assumption that β and $(c_A + c_B)$ do not vary with x. Letting

$$D = \frac{1}{\beta(c_A + c_B)} \tag{38}$$

$$\frac{\partial c_A}{\partial \theta} = D\frac{\partial^2 c_A}{\partial x^2} \tag{39}*$$

which is obviously analogous to Eq. (8) for gases.

Steady-state Diffusion of a Solute through a Stagnant Solvent. Let A refer to the diffusing solute, and B refer to the solvent which is assumed not to diffuse. Then $u_B = 0$, and from Eq. (33)

$$N_A = u_A c_A = -\frac{1}{\beta c_B}\frac{dc_A}{dx} = -D\frac{(c_A + c_B)}{c_B}\frac{dc_A}{dx} \tag{40}$$

For dilute solutions, where c_A is small compared with c_B, or in any case where D and $(c_A + c_B)/c_B$ may be assumed constant, this may be integrated to give

$$N_A = D\frac{(c_A + c_B)}{c_B}\frac{(c_{A1} - c_{A2})}{x} \tag{41}$$

analogous to Eq. (16) for gases.

In case D and $(c_A + c_B)$ may be assumed constant, although c_B varies, integration of Eq. (40) gives

$$N_A = \frac{D}{x}(c_A + c_B)\ln\frac{c_{B2}}{c_{B1}} = \frac{D}{x}(c_A + c_B)\frac{(c_{B2} - c_{B1})}{c_{BM}} \tag{42}$$

which is seen to be similar to Eq. (13) for gases.

Equation (42) is to be preferred to Eq. (41) because the assumption on which the integration is based is somewhat more justifiable. In the case of a solution of sodium chloride in water, for example, over the concentration range from zero to saturation at 18°C., the variation in $(c_A + c_B)/c_B$ is 11 per cent, whereas the variation in $(c_A + c_B)$ is only 2 per cent. Over this range of concentrations the variation in D is found experimentally to be about 28 per cent.

DIFFUSION COEFFICIENTS FOR LIQUIDS

Diffusion coefficients for most of the common organic and inorganic materials in the usual solvents, such as water, methyl

* It seems possible that published experiments on diffusion in liquids, indicating peculiar variations of D, have been interpreted erroneously by Eq. (39), which makes no allowance for the variation of $(c_A + c_B)$.

and ethyl alcohols, and benzene at room temperature, lie in the range from 0.3 to 1.5×10^{-5} cm.^{2}/sec. Table II gives a summary of experimental values for typical systems. More complete tables of such data are to be found in Vol. 5 of the International Critical Tables. Where no experimental data are available, an estimation of the diffusion coefficient may be obtained by employing the empirical equation published by J. H. Arnold.[4]

TABLE II.—REPRESENTATIVE VALUES FOR DIFFUSION COEFFICIENTS IN THE LIQUID PHASE (I.C.T.)

Solute	Solvent	Temperature, °C.	Concentration, g. mols/l.	$D \times 10^5$ (cm.^{2}/sec.) $\times 10^5$
H_2	Water	16	0*	4.7
N_2	Water	22	0*	2.0
CO_2	Water	20	0*	1.8
Cl_2	Water	12	0.1	1.4
Br_2	Water	12	0.1	0.9
NH_3	Water	12	1.0	1.6
HCl	Water	12	0.1	2.3
H_2SO_4	Water	20	0.1	1.73
HNO_3	Water	20	0.1	2.6
NaCl	Water	18	0.1	1.24
			0.4	1.20
			1.0	1.24
			3.0	1.36
KCl	Water	18	0.1	1.52
			0.4	1.49
			1.0	1.59
			3.0	1.92
Acetic acid	Water	17	0.47	0.95
Ethyl alcohol	Water	15	0*	1.0
Glycerol	Water	15	0*	0.7
Saccharose	Water	15	0*	0.38
Urea	Water	20	1.0	1.14
CO_2	Ethyl alcohol	17	0*	3.2
Phenol	Ethyl alcohol	20	0.1	0.8
Sodium acetate	Methyl alcohol	14	0.1	0.9
Sodium iodide	Methyl alcohol	14	0.1	1.0

* Indicates diffusion in very dilute solutions.

Nomenclature for Chapter I

A = Avogadro's number = 6.06×10^{23}.
B = constant in Eq. (29).
B' = constant in Eq. (30).
c = partial molal density, g. mols/cc.
C = Sutherland constant.
D = diffusion coefficient, or diffusivity, cm.^{2}/sec.
E = $\rho D/\mu$ [see Eq. (32)].
k = constant in Eq. (15), = DP/RT.
M = molecular weight.
n = number of molecules per cubic centimeter in a gas at standard conditions (0°C., 1 atm.).
N = rate of diffusion, g. mols/(sec.)(sq. cm.).
p = partial pressure of one component, atm.
P = total pressure, atm.
r = $1/k = RT/DP$.
R = gas-law constant = 82.07 (cc.)(atm.).
S = the distance between centers of two unlike molecules at collision.
T = absolute temperature, °K. = 273 + °C.
T_b = boiling temperature at 1 atm. pressure, °K.
u = velocity of diffusion, cm./sec.
V = molecular volume, see Table I.
w = molecular weight relative to that of hydrogen as unity.
W = velocity of mean square of the hydrogen molecule at 0°C.
x = distance in the direction of diffusion, cm.
α_{AB} = proportionality constant in Eq. (1) for interdiffusion of components A and B = $\alpha_{BA} = \alpha$.
β = proportionality constant in Eq. (33) for diffusion in liquids.
θ = time, sec.
μ = absolute viscosity, g./(sec.)(cm.).
ρ = partial density of one component, g./cc.

Subscripts

A, B, C referring to components A, B, or C of a mixture of several substances.

1, 2 referring to positions of planes at right angles to the direction of diffusion.

CHAPTER II

TRANSFER OF MATERIAL BETWEEN PHASES

It is a common observation that separate phases brought into contact tend to approach a state of equilibrium. Thus a hot piece of metal dropped in a bath of water dissipates heat to the water, and in time the temperatures of water and metal become the same. The phase equilibrium approached requires that the temperatures of metal and of water be identical. If, instead of a lump of metal, a mass of salt crystals be dropped into water, a thermal equilibrium is again reached at which the temperatures of the water and of the salt are the same. At the same time, however, salt dissolves in the water, building up the salt concentration in the solution until a concentration equilibrium is reached at which the salt concentrations in the solid salt phase and in the liquid solution are widely different. When pure water is placed in contact with dry air, water evaporates until the air becomes saturated, and air is absorbed by the water until the liquid is saturated with oxygen and nitrogen. At equilibrium the temperatures of the two phases will be the same, but the concentration of air, expressed in any of the ordinary units, will be less in solution in the water than in the gas phase, and the water concentration will be very much less in the gas phase than in the liquid. At 20°C., for example, air saturated with water vapor carries approximately 0.000017 g. water per cc., whereas the liquid with which it is in equilibrium contains approximately 1.0 g./cc. It is apparent from these examples that there is a sharp concentration drop across the interface between two phases in contact and in equilibrium.

If an exploration is made of the region immediately adjacent to the interphase boundary, it is found that the concentration gradient is surprisingly steep as compared with the corresponding gradient at points further removed from the interface. An example of an experimental concentration gradient is shown in Fig. 6, which represents the data obtained by Black and Monroe[15] in a vertical wetted-wall pipe. Water was vaporized from a thin

film on the inner wall of an iron pipe 183 cm. long and 5.15 cm. i.d. Air was supplied at the bottom through a long dry vertical calming section, and water supplied at the top and removed at the bottom at the junction with the calming section. The temperature and humidity of the air, and the water temperature, were measured at inlet and outlet. Figure 6 represents a humidity gradient obtained under flow conditions at a plane 15 cm. from the top. A capillary metal tube was used to obtain samples of air for analysis from various points across the diameter of the pipe at the plane described. It is apparent from the plot that the slope of the humidity gradient is many times as great in the vicinity of the pipe wall as in the main body of the gas stream, indicating that the principal resistance to vapor transfer exists in a narrow zone near the wall. The gradient is relatively flat across the middle section of the pipe, showing the resistance to vapor transfer to be small in this region. This conforms with the concept of rapid transfer by mixing or eddy diffusion in the main turbulent stream.

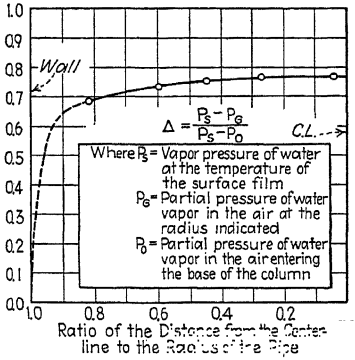

:G. 6.—Moisture gradients in an air

The molecules of fluid actually in contact with the wall are believed to be entirely at rest (or in the case of the wetted-wall tower, the relative velocity of gas and liquid is zero). The degree of turbulence thus increases from zero at the wall to a maximum in the central turbulent "core," and the mechanism of vapor transfer changes from true diffusion through the stagnant air at the wall to pure eddy diffusion in the main turbulent stream. The slowness of true diffusion and the rapidity of eddy diffusion explain the wide variations of the observed slopes of the humidity curve. It is true that both cross-sectional area and rate of transfer vary across the diameter, but the net effect of these variables is in no way sufficient to explain the observed gradient on the basis of a single mechanism of diffusion. It may be concluded that the principal resistance to interphase

transfer is to be found in a thin "film" of relatively stagnant fluid next to the interface between phases.

The film concept has been of inestimable service in providing a mental picture of the surface resistances encountered in interphase transfer of momentum (as in viscous friction), of materials (interphase diffusion), and of heat. The word "film" is somewhat misleading, however, since it is frequently inferred that the resistance is offered wholly by a layer of absolutely stationary fluid at the interphase boundary. The gradients of Fig. 6 show the error of this conclusion. It is possible, however, to imagine a purely stagnant fluid film, of such a thickness that it would offer the same resistance as is usually encountered in transfer between the phases. The thickness of such a fictitious "film" is best termed the "effective film thickness."

Temperature and velocity traverses in fluids flowing in turbulent motion yield curves similar to the concentration curves of Fig. 6. McAdams[131] quotes the data of a number of investigators who determined gas velocities at various distances from a flat plate in a turbulent stream of air. Several investigators employed special techniques enabling them to determine the velocity at points very close to the wall. The results show the velocity to be an approximately linear function of the distance, up to 0.1 to 1.0 mm., after which the curves flatten off to roughly 1/7-power curves in the main gas stream. Since a linear relation between velocity and distance from the wall is characteristic of viscous, or streamline flow, it seems reasonable to infer that a thin layer of fluid in contact with the wall is moving in viscous motion, but that beyond the outer boundary of this film the flow is turbulent or eddying. Such a concept is the basis for the Prandtl and the Colburn theoretical equations for heat flow and mass transfer, respectively, as explained below. Close examination of the velocity gradients, however, reveals a definite trend away from the linear relation in the "laminar" film, and it seems doubtful that the evidence at hand is sufficient to prove whether there is continuous change from viscous to turbulent motion (and so from true diffusion to eddy diffusion) from wall to main fluid stream, or whether there is a sharp break from viscous to turbulent flow at the outer boundary of a truly laminar film.

Interesting microscopic observations of the nature of turbulent flow have been reported by Fage and Townend.[59] Highly

illuminated ultramicroscopic solid particles, carried by water flowing through a horizontal square brass pipe, were observed through a microscope and one of two quartz windows cemented flush with the inner side and top surfaces of the pipe. The particles passing through the field of vision appeared as bright streaks, and provision was made for measuring the angle between these streaks and the axis of the pipe. The angles were measured in both vertical and horizontal planes at various points along a horizontal axis at right angles to the direction of flow. By means of a sharp-focusing microscope with micrometer attachment, it was possible to make such determinations up to within an extremely short distance from the wall. Typical results, obtained at a water velocity about seven times the critical value, are shown in Fig. 7. The x-axis represents the principal axis of the pipe; the y-axis the horizontal center line, across which the traverse was made, and the z-axis the vertical center line. The subscripts indicate the plane in which the angle is measured. The abscissa represent the location along the horizontal center line, or y-axis, as a fraction of the distance from center to wall.

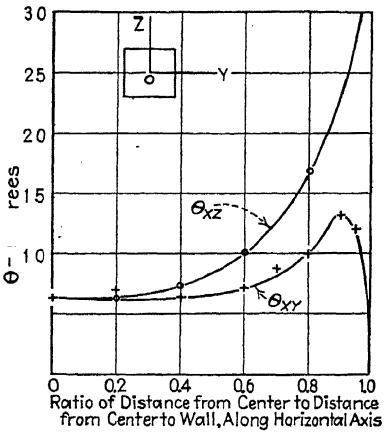

FIG. 7.—Data of Fage and Townend on angles between particle paths and pipe axis.

The measured values of θ may be taken as indicative of the degree of turbulence in a given plane. The θ_{xy} curve is seen to reach a maximum and then drop off to zero at the wall. This indicates that very near the wall the fluid is moving in parallel planes and that flow is, therefore, laminar in character. The particles are not moving in straight lines within each plane or lamina, however, as shown by the increasing values of θ_{xz}. The flow at the wall, therefore, may be laminar, but is not rectilinear. Fage and Townend write: "At the wall itself, it was found that while the flow tended to the laminar type, the motions of particles in the laminae were sinuous, even to within a distance of

1/4000 in. from the wall. No particle was seen to move in a rectilinear path."

In concluding the qualitative discussion of the film concept, it should be emphasized that whereas the principal resistance to interphase transfer of heat or material is encountered in a narrow zone very near the interface, an appreciable resistance is also encountered in the main turbulent fluid stream. The relative magnitudes of these resistances will be discussed in connection with the Colburn theoretical equation.

EQUATIONS OF DIFFUSION THROUGH FILMS

In the quantitative treatment of diffusion between phases it is customary to employ the equations for true diffusion developed in Chap. I. This procedure has little theoretical justification, since from the derivations it is evident that such relations apply only to diffusion in truly stagnant fluid layers. We have just seen that the molecules of fluid are stationary only at the immediate interface, and the equations for true diffusion may consequently be supposed to apply as the interface is approached more and more closely. However, even in the turbulent layers, the rate of eddy diffusion may be assumed to be proportional to the partial-pressure gradient, as in true diffusion, and the equations of Chap. I have, in fact, been applied with considerable success to interphase diffusion, involving transfer across both the eddy layer and the laminar layer. Thus for water evaporating into a stream of air, Eq. (16) becomes

$$N_A = \frac{DP}{RTx} \frac{(p_i - p_0)}{p_{BM}} \tag{43}$$

where p_i = vapor pressure of water at the interface.
p_0 = partial pressure of water vapor in the main gas stream.
x = "effective film thickness."

Since the coefficients for eddy diffusion of various vapors in a given gas are doubtless in different ratios to each other than for true diffusion, the molal-diffusion rates of two different vapors are not found to be in the same ratio as the true diffusion coefficients D. This important point will be discussed in detail in connection with a later analysis of experimental data on the vaporization of several different vapors into air streams.

THEORETICAL RELATIONS BETWEEN HEAT FLOW, FRICTION, AND DIFFUSION THROUGH FILMS*

For the case of fluids moving in viscous motion, it is frequently possible to calculate the velocity of the fluid particles at any point in the stream. With the equations of motion known, it is possible then to calculate the rate of heat conduction into the moving fluid, and so develop a theoretical equation for heat transfer between fluid and solid. Such an equation has been derived for heat flow between the wall of a round pipe and a fluid moving in viscous motion through the pipe. An analogous equation for diffusion into a fluid passing in viscous motion through a round pipe is discussed below.

In interphase diffusional processes, however, the flow is usually turbulent, for which the eddy motion is extremely complicated and haphazard, and the equations of motion are not known. Consequently, no theoretical relations for heat flow or diffusion into fluid streams have been developed along the lines of those for viscous flow mentioned above.†

There is available, however, the Reynolds analogy between heat transfer and fluid friction in turbulent flow, which leads to a theoretical expression for the surface coefficient of heat transfer in terms of the surface coefficient of friction. This relation has been found to fit the data within about 10 per cent, for the case of heat flow between a round pipe and a gas flowing in turbulent motion through the pipe. The basic assumption on which the derivation rests is that the head lost due to friction, divided by the momentum of the stream, is equal to the ratio of the actual heat transferred in the section to the heat which would be transferred were the fluid to come to thermal equilibrium with the wall of the pipe. An analogous relation may be derived for diffusion, based on a corresponding assumption that the head lost due to friction, divided by the momentum of the stream, is equal to the ratio of the actual material transferred between phases, to the material which would be transferred were the stream to come to equilibrium with the other phase. For the

* The remainder of the chapter may be omitted by readers not concerned with the more theoretical aspects of diffusion in films.

† See, however, the semitheoretical analysis of Murphree[148] for heat transfer in turbulent flow. The application of a similar treatment to diffusional processes is suggested.

differential length of pipe of radius a, this assumption may be expressed algebraically as

$$\frac{\pi a^2 dP}{Wu/g} = \frac{dC_G}{C_G - C_i} \tag{44}$$

where P = total pressure.
W = weight rate of flow of the fluid mixture.
u = average velocity.
g = acceleration due to gravity.
C_G = partial molal density of the diffusing component in the fluid stream.
C_i = equilibrium partial molal density at the phase boundary.

The material balance

$$N_A = \text{mols/(sec.)(sq. cm.)} = \frac{W dC_G}{\rho 2\pi a dL} \tag{45}$$

and the Fanning equation for turbulent friction

$$dP = \frac{f\rho u^2 dL}{ga} \tag{46}$$

may be combined with Eq. (44) to give

$$\frac{N_A}{C_G - C_i} = \frac{fu}{2} \tag{47}$$

For gases, where $C = p/RT$, this becomes

$$\frac{N_A}{p - p_i} = k_G = \frac{fu}{2RTM} = \frac{f\rho u}{2RTM} \text{ g. mols/(sec.)(sq. cm.)(atm.)} \tag{48}$$

This equation may be expected to apply under the same conditions as does the corresponding equation for heat transfer, *i.e.*, in gas flow, under conditions where the friction factor represents the true skin friction, and not a combination of skin friction and turbulence losses.

The Colburn Equation.—In a modification of the Reynolds equation for heat transfer, Prandtl[154] has applied the basic Reynolds assumption to the "core" or eddy layer of the moving fluid, and treated the heat flow through the assumed laminar film as a process of pure conduction. Then equating the frictional force as given by the Fanning equation to the shear on

the viscous laminar layer, he obtained an equation for the surface coefficient of heat transfer which involved the ratio r of the fluid velocity at the boundary between laminar and eddy layers, to the average velocity of the main fluid stream.

Colburn[38] has treated the problem of interphase material transfer through a gas in turbulent motion in an entirely analogous manner, and obtained an equation for interphase gas diffusion similar to the Prandtl equation for heat flow. He applies the basic Reynolds assumption to the eddy layer and treats the transfer through the laminar layer as a process of true diffusion. The resulting equation is

$$k_G = \frac{f\rho u}{2p_{BM}M_M\phi_D} \tag{49}$$

where k_G = a coefficient of material transfer, g. mols/(sec.)(sq.cm.)(atm.).

f = friction factor in the Fanning equation (46).

ρ = density of the main gas stream, g./cc.

M_M = average molecular weight of the main gas stream.

p_{BM} = mean partial pressure of the nondiffusing or inert gas in the laminar layer.

$\phi_D = 1 - r + r\left(\frac{\mu_f}{\rho D}\right)$.

r = ratio of the fluid velocity at the boundary between laminar and eddy layers, to the average velocity u of the main fluid stream.

μ_f = average absolute viscosity of the laminar layer, g./(sec.)(cm.).

D = diffusion coefficient of gas A through the inert gas B, cm.^{2}/sec.

The value of r is given approximately by the equation[113]

$$r = 5.9\sqrt{f} \tag{50}$$

The effect of gas velocity on the coefficient k_G is indicated by the variation of the terms f, u, and r. For most gases the variation in r and ϕ_D is small, and Eq. (49) indicates a variation of k_G with the product fu. Since in turbulent flow f is approximately proportional to the velocity to the -0.2 power, the net result is an indicated variation of k_G as the 0.8 power of the fluid velocity. It is well known that the surface coefficients of heat

transfer for fluids flowing in pipes vary directly as the 0.8 power of the fluid velocity.

From the derivation of Eq. (49) it follows that

$$\frac{p_G - p_f}{p_f - p_i} = \frac{1 - r}{r(\mu_f/\rho D)} \tag{51}$$

in which p_G, p_f, and p_i are the partial pressures of the diffusing gas in the main gas stream at the boundary of the laminar layer and at the interface between phases, respectively. Since the diffusion rate is the same through both eddy and laminar layers, and the respective resistances of eddy and laminar layers may be taken as proportional to the driving forces $(p_G - p_f)$ and $(p_f - p_i)$, it follows that the right-hand side of Eq. (51) represents the ratio of eddy or core to laminar film resistance. Thus $1 - r$ represents the resistance of the former, and $r\mu_f/\rho D$ represents the resistance of the laminar layer.

J. H. Arnold[5] has made the logical assumption that the effective thickness of the assumed laminar layer may be the same for heat transfer and for diffusion, providing, of course, that the turbulence conditions are the same. If this assumption is made, then from the foregoing resistance ratios the relation between the effective total film thickness for heat flow and that for diffusion is

$$\frac{x_H}{x_D} = \frac{k_H}{D\rho c}\left[\frac{1 - r + r(c\mu_f/k_H)}{1 - r + r(\mu_f/\rho D)}\right] \tag{52}$$

x_H represents the thickness of a stagnant gas layer which would offer the same thermal resistance as is actually encountered in interphase heat transfer. x_D is a similar value for diffusion, and represents the value of x which, used in Eq. (43), would lead to the correct value for the rate of interphase diffusion. Values of $\mu/\rho D$ for various vapors and air at 0°C. are given in Table III. According to the kinetic theory $\mu/\rho D$ does not vary with temperature, so values of this group from Table III may be used for temperatures other than 0°C.

The assumption made by Arnold may be employed to give a relation between rates of diffusion of different gases in a dilute mixture with a given carrier gas under similar turbulence conditions. It follows from the above that the ratio of the effective film thickness for one gas A to that for a second gas C, is given by

$$\frac{x_A}{x_C} = \frac{D_A\,[1 - r +}{D_C\,[1 - r + r(\mu_f/\rho D_C)]} \tag{53}$$

Arnold has employed the relations (52) and (53) to develop a new theory of the wet-bulb psychrometer. Under similar conditions of total and inert gas pressure, driving force, temperature, and

TABLE III.—VALUES OF D AND $\mu/\rho D$ FOR VARIOUS VAPORS IN AIR AT 0°C. AND 1 ATM.

Vapor	D cm.²/sec. [Calc. from Eq. (31)]	D cm.²/sec. (I.C.T.)	based on calc. values of D*
Ammonia	0.170		0.78
Benzene	0.072	0.077	1.84
Brombenzol	0.066	.....	2.00
Carbon dioxide	0.121	0.138	1.09
Carbon tetrachloride	0.062		2.13
Chlorobenzene	0.063		2.10
Ethyl acetate	0.068	0.072	1.94
Ethylene bromide	0.068		1.94
Ethylene tetrachloride	0.058		2.27
Ethyl propionate	0.061	0.065	2.16
Methyl alcohol	0.120	0.133	1.10
n-Propyl acetate	0.061		2.16
n-Propyl alcohol	0.080	0.085	1.65
Sulfur dioxide	0.103		1.28
Toluene	0.065	0.071	2.03
Water	0.188	0.220	0.60†

* Using μ and ρ for pure air (μ/ : 0.132 cm.²/sec.).
† Based on I.C.T. value for D.

turbulence conditions, the molal rates of diffusion will be in the ratio

$$\frac{N_A}{N_C} = \frac{1 - r +}{1 - r +} \tag{54}$$

Under such conditions the molal rates become equal as D_A becomes equal to D_C, just as in the case of the simple concept of a single stagnant film offering all of the resistance to diffusion.

The Chilton and Colburn Modification of the Reynolds Analogy.—The Prandtl theoretical modification of the Reynolds analogy between heat transfer and fluid friction introduced the group $\phi_H = 1 - r + r(c\mu_f/k_H)$, which supposedly served to

correlate the data on heat transfer to various fluids. Actually, the correlation on this basis between heat transfer to liquids and heat transfer to gases was poor, although the correlation between friction and heat transfer for gases was good. Colburn[40] has shown that an empirical function of $c\mu_f/k_H$ serves to correlate the friction data with data on heat transfer to both liquids and gases at high Reynolds numbers (above about 10,000). His suggested relation is

$$\left[j_H = \frac{h}{cu\rho}\left(\frac{c\mu_f}{k_H}\right)^{\frac{2}{3}} \right] = \frac{1}{2}f \tag{55}$$

For flow in conduits this modified analogy between heat transfer and friction fails at Reynolds numbers below about 10,000, but a graphical correlation of heat-transfer data for low Reynolds numbers is given, involving the Grashof group, the ratio of tube length to diameter, and the ratio of film viscosity to viscosity in the main body of the fluid. Plots are given showing the recommended correlation for flow in conduits, over tubes and tube banks, and between parallel planes.

Chilton and Colburn[35] have since proposed an analogous treatment for diffusion through gas films, for which

$$j_D = \frac{k_G p_{BM} M_M}{u\rho}\left(\frac{\mu_f}{\rho D}\right)^{\frac{2}{3}} \tag{56}$$

k_G = film coefficient for diffusion or mass transfer g. mols/(sec.)(sq. cm.)(atm.).

$u\rho$ = mass velocity of fluid, g./(sec.)(sq. cm.).

M_M = average molecular weight of the main fluid stream.

They find that the previous correlation of values of j for heat transfer may be used to predict values of j for diffusion through gas films, as shown by comparison of the predicted values with data on absorption and evaporation in wetted-wall columns, absorption on cylinders placed at right angles to a gas stream, and on vaporization from a plane surface.

Even though sources of heat-transfer data other than Colburn's curves be used, the method is of considerable value in estimating absorption and vaporization coefficients. Thus, if $j_H = j_D$,

$$k_G = \frac{h}{cp_{BM}M_M}\left(\frac{c\rho D}{k_H}\right)^{\frac{2}{3}} \tag{57}$$

This equation may be used directly to predict k_G from values of h obtained in a similar apparatus. The relation is dimensionally correct, so any consistent set of units may be employed. Since $c\mu/k$ for all gases is approximately 0.74, the group in parentheses may be obtained by dividing 0.74 by the appropriate value of $\mu/\rho D$.

Since the Chilton-Colburn analogy provides a relation between heat transfer and diffusion in gas films, it can be used as a semi-theoretical basis for the analysis of the wet-bulb psychrometer. This point has been discussed by Colburn.[39]

EXPERIMENTAL DATA ON THE DIFFUSION OF VARIOUS VAPORS THROUGH AIR FILMS

The influence of the nature of the diffusing gas or vapor is shown clearly by the experimental data of Gilliland[69] who measured the rate of vaporization of a number of liquids in a wetted-wall column through which air was forced at various velocities and pressures. The apparatus used consisted of a vertical pipe, 2.67 cm. i.d., 117 cm. long, vaporization taking place from a liquid falling film covering the pipe's inner surface. Above and below the wetted-wall section were straight approach or "calming" sections, each 115 cm. long, which served to minimize turbulence effects in the entering air stream. The liquid was fed at the top through a cylindrical wire gauze and withdrawn through a slot at the bottom, allowing no liquid to pass to the lower calming section. The apparatus is shown diagrammatically in Fig. 8. The liquid leaving the lower tee was returned to the apparatus through a calibrated reservoir. The rate of vaporization was determined by noting the rate of fall of the liquid level in this reservoir. The temperatures of gas and liquid entering and leaving the apparatus were measured, and the mean driving force Δp

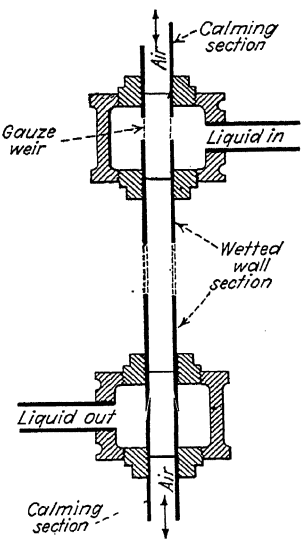

FIG. 8.—Wetted-wall column used by Gilliland.

calculated from the known vapor pressures of the liquids used. The mean Δp was taken as the logarithmic mean of the differences between the vapor pressure of the liquid and the partial pressure of vapor in the main gas stream at top and bottom of the column. The results were expressed in terms of the effective film thickness x obtained by substitution in Eq. (43). In each test the air sup-

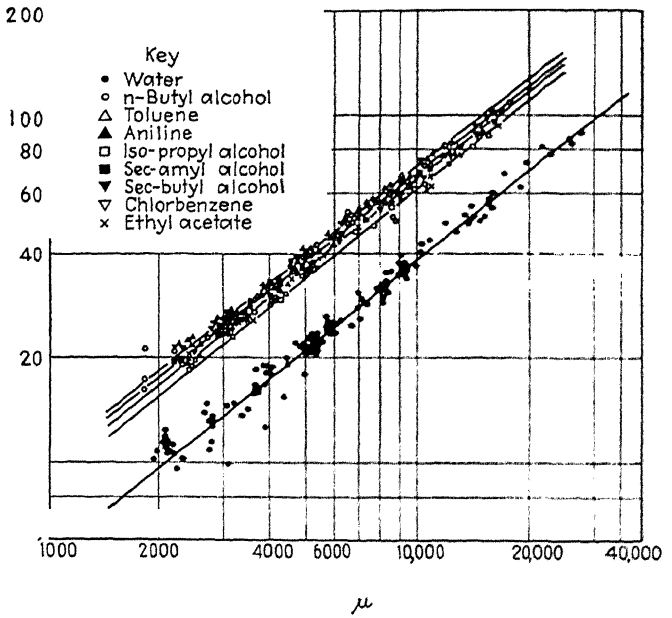

FIG. 9.—Experimental data on vaporization of various liquids into a turbulent air stream in a wetted-wall column.

plied was heated to approximately the same temperature as the liquid.

The results obtained with air flowing in turbulent motion are shown in Fig. 9, in which the calculated values of d/x are plotted *vs.* the Reynolds group $du\rho/\mu$ using logarithmic coordinates. The ratio d/x corresponds to the group hd/k_H for heat transfer, since the ratio of the thermal conductivity k_H to the surface coefficient h is equal to the effective film thickness for heat transfer. d represents the inside diameter of the duct, u the average velocity of the main gas stream, ρ the gas density, and

μ its viscosity. The data plotted include results for both parallel and countercurrent flow of liquid and gas, showing a good correlation for both types of experiments.*

The data for the various liquids plotted on Fig. 9 fall on parallel straight lines having slopes of approximately 0.8. This is entirely

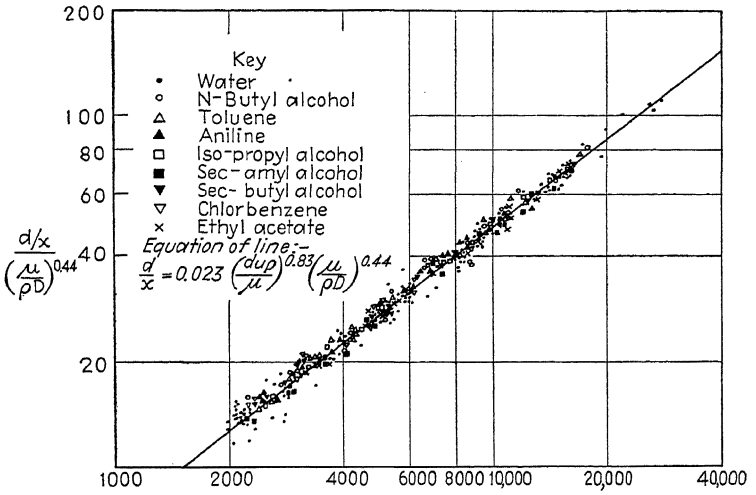

FIG. 10.—Empirical correlation of data on vaporization of liquids into air.

analogous to the corresponding plot for heat transfer to liquids in pipes, where hd/k_H is plotted *vs.* the Reynolds group for each of several liquids. The spread of the points shows that at a given Reynolds number, the effective film thickness for one gas may be nearly twice that for a second gas.

The corresponding plot of k_G *vs.* $du\rho/\mu$ shows similar parallel lines but with the order reversed. The lack of correlation for

* At first thought it might seem that in correlating the data of Fig. 9 the Reynolds group should be based on the velocity of the air relative to the surface of the liquid film. On calculating the liquid surface velocities, however, and using the corrected Reynolds number in replotting the data, a much poorer correlation was obtained for each liquid than shown by Fig. 9. It is possible that this would not be found true of results obtained in an apparatus having different principal dimensions. The values of u used in the plots represent the velocity of the gas relative to the pipe, *i.e.*, volume per second divided by free cross section of the pipe.

the various vapors is clearly due to the omission of an important variable or group of variables representing the physical properties of gas and diffusing vapor. Both dimensional analysis and the Colburn equation suggest that the missing group is $\mu/\rho D$, representative of the properties of the "film." The data of Fig. 9 are, in fact, brought together by the introduction of the group $(\mu/\rho D)^{0.44}$. This is shown by Fig. 10, in which $\frac{d/x}{(u/\ldots}$ plotted *vs.* the Reynolds group, with a resulting single line for the various vapors. The equation of this line is

$$\frac{d}{x} = 0.023\left(\frac{du\rho}{\mu}\right)^{0.83}\left(\frac{\mu}{\rho D}\right)^{0.44} \tag{58}$$

in which the groups are dimensionless, and any self-consistent set of units may be employed. This equation, which is of general applicability under conditions of turbulent gas flow in wetted-wall towers, is strikingly similar to the corresponding general equation recommended by McAdams[131] for heat transfer to liquids flowing in turbulent motion in pipes,

$$\frac{hd}{k_H} = 0.0225\left(\frac{du\rho}{\mu}\right)^{0.8}\left(\frac{c\mu}{k_H}\right)^{0.4} \tag{59}$$

Illustration 5.—The following data were obtained by Cogan and Cogan[47] on the absorption of ammonia from air in a laboratory wetted-wall column. The air-ammonia mixture was blown downward parallel to the falling-water film on the inside of the pipe.

Diameter of gas passage	4.09 cm.
Length of wetted surface	91.5 cm.
Water temperature, inlet	13.3°C.
Water temperature, outlet	18.6°C.
Average gas velocity, gas inlet	216 cm./sec.
Calculated downward velocity of liquid surface	51.8 cm./sec.
Gas temperature, inlet	25.5°C.
Gas temperature, outlet	24.0°C.
p_{AG}, gas inlet	122 mm. Hg
p_{Ai}, gas inlet	0 mm. Hg
p_{Ai}, gas outlet	3.8 mm. Hg
Absorption rate	7.18 g./min.
Barometer	756 mm. Hg

a. Calculate the effective film thickness x in cm.

b. Compare with the value calculated from the Gilliland equation (Eq. 58).

c. Compare with the effective film thickness for heat transfer to gas flowing in a dry pipe at the same Reynolds number.

d. Compare with the value calculated from friction data using the Colburn theoretical equation.

e. Compare with the value predicted from the Arnold theory based on the value calculated under (*c*) for heat transfer.

Solution.

$$\text{Air flow} = \frac{216}{22{,}400} \times 3600 \times \frac{\pi}{4}(4.09)^2 \times \frac{273}{298.5} \times \frac{756}{760} \times \frac{634}{756} = 348 \text{ g. mols/hr.}$$

$$\text{NH}_3 \text{ in inlet gas} = 348 \times \frac{122}{634} = 67 \text{ g. mols/hr.}$$

$$\text{NH}_3 \text{ absorbed} = \frac{7.18 \times 60}{17} = 25.3 \text{ g. mols/hr.}$$

$$\text{NH}_3 \text{ in exit gas } (67 - 25.3) = 41.7 \text{ g. mols/hr.}$$

$$p_{AG} \text{ in exit gas} = \frac{41.7}{348 + 41.7} \times 756 = 81 \text{ mm.}$$

$$\text{At top } p_{BM} = 756 - \frac{122}{2} = 695 \text{ mm.}$$

$$\text{At bottom } p_{BM} = \frac{(756 - 3.8) + (756 - 81)}{2} = 714 \text{ mm.}$$

$$p_{BM} \text{ average} = \frac{695 + 714}{2} = 704 \text{ mm.}$$

$$\text{Wetted surface} = 4.09 \times \pi \times 91.5 = 1172 \text{ sq. cm.}$$

$$N_A = \frac{7.18}{17 \times 60 \times 1172} = 0.0000060 \text{ g. mols/(sec.)(cm.}^2\text{).}$$

$$\Delta p \text{ at top} = 122 \text{ mm.}$$

$$\Delta p \text{ at bottom} = 81 - 3.8 = 77.2 \text{ mm.}$$

$$\Delta p_{av} = \frac{122 - 77.2}{\ln \frac{122}{77.2}} = 98 \text{ mm.}$$

$$D = \frac{0.0043(273 + 20.3)^{\frac{3}{2}} \sqrt{\frac{1}{17} + \frac{1}{29}}}{\frac{756}{760}\left(26.7^{\frac{1}{3}} + 29.9^{\frac{1}{3}}\right)^2} = 0.179 \text{ cm.}^2\text{/sec.}$$

Solving for x, in Eq. (16),

$$x = \frac{DP\Delta p}{N_A R T p_{BM}} = \frac{0.179 \times (756/760) \times 98}{0.0000060 \times 82.07 \times 293.3 \times 704} = 0.172 \text{ cm.}$$

b. Using the Gilliland equation (58),

$$\frac{d}{x} = 0.023\left(\frac{du\rho}{\mu}\right)^{0.83}\left(\frac{\mu}{\rho D}\right)^{0.44}$$

$$u\rho = \frac{348 \times 29 + \left(67 - \frac{25.3}{2}\right)17}{3600 \times \frac{\pi}{4} \times (4.09)^2} = 0.233 \text{ g./(sec.)(cm.}^2\text{).}$$

$$\mu(\text{at } 20°\text{C.}) = 0.000185 \text{ g./(cm.)(sec.)}$$

$$Re = \frac{du\rho}{\mu} = \frac{4.09 \times 0.233}{0.000185} = 5{,}160$$

$$\text{Average molecular weight of gas} = \frac{348 \times 29 + \left(67 - \frac{25.3}{2}\right) \times 17}{348 + \left(67 - \frac{25.3}{2}\right)} = 27.4$$

$$\frac{\mu}{D\rho} = 0.78 \text{ (Table III)}$$

Substituting in Eq. (58)

$$\frac{d}{x} = 0.023 \times (5160)^{0.83} \times (0.78)^{0.44} = 24.7$$

$x = 4.09/24.7 = 0.165$ cm., *vs.* 0.172 cm. calculated from the experimental data.

c. Using the McAdams equation (59):

$$\frac{hd}{k_H} = \frac{d}{x} = 0.0225\left(\frac{du\rho}{\mu}\right)^{0.8}\left(\frac{c\mu}{k_H}\right)^{0.4}$$

For diatomic gases, $\frac{c\mu}{k_H} = 0.74$, approximately.

$$\frac{d}{x} = 0.0225 \times (5160)^{0.8} \times (0.74)^{0.4} = 18.7$$

$$x = \frac{4.09}{18.7} = 0.218 \text{ cm. } \textit{vs.} \text{ 0.172 cm. from absorption data}$$

d. Using the Colburn theoretical Eq. (49):

$$k_G = \frac{f\rho u}{2p_{BM}M_M\phi_D}$$

Then, since

$$x = \frac{DP'\Delta p}{RTp_{BM}N_A} \tag{16}$$

and

$$N_A = k_G\Delta p$$

$$x = \frac{DP\Delta p}{RTp_{BM}k_G\Delta p} = \frac{DP2p_{BM}M_M\phi_D}{RTp_{BM}f\rho u} = \frac{DP2M_M\phi_D}{RTf\rho u} \tag{A}$$

$$\phi_D = 1 - r + r\left(\frac{\mu}{\rho D}\right)$$

At $Re = 5160$,

$$f = 0.0096 \text{ for smooth pipes}$$

$$r = 5.9\sqrt{f} = 5.9\sqrt{0.0096} = 0.58$$

$$\phi_D = 1 - 0.58 + 0.58/0.78 = 0.872$$

Substituting in Eq. (*A*),

$$x = \frac{0.179 \times 756 \times 2 \times 27.4 \times 0.872}{82.07 \times 760 \times 293 \times 0.0096 \times 0.233} = 0.158 \text{ cm.}$$

Using the Arnold theory [Eq. (52)]:

$$x_D = \frac{(c\mu/k_H)[1 - r + r(\mu/\rho D)]x_H}{(\mu/\rho D)[1 - r + r(c\mu/k_H)]} \qquad (B)$$

$$\frac{c\mu}{k_H} = 0.74 \text{ (Part } c\text{)}$$

$$\frac{\mu}{\rho D} = 0.78 \text{ (Table III)}$$

$$1 - r + r\left(\frac{\mu}{\rho D}\right) = 0.872 \text{ (Part } d\text{)}$$

$$x_H = 0.173 \text{ cm. (Part } c\text{)}$$

$$r = 0.58 \text{ (Part } d\text{)}$$

$$1 - r + r\left(\frac{c\mu}{k_H}\right) = 1 - 0.58 + 0.58 \times 0.74 = 0.85$$

Substituting in Eq. (*B*),

$$x_D = \frac{0.74 \times 0.872 \times 0.173}{0.78 \times 0.85} = 0.168 \text{ cm.}$$

The values of x calculated by the last three methods check reasonably well with the value calculated from the experimental data.

Effect of Total Pressure.—The wetted-wall column described above was operated over a range of total pressures from 110 to 2,330 mm., and the data consequently serve as an excellent test of the theoretical effect of pressures called for by Eq. (43). This relation calls for a variation in rate of diffusion N_A with DP/p_{BM}. However, since D varies inversely with P, N_A should vary inversely with p_{BM}. The value of x calculated from the experimental data should not vary with pressure, since proper values of p_{BM} were used in Eq. (43) in calculating the results. This prediction is verified by Fig. 11, which shows d/x, corrected for variations in Reynolds number by dividing by $(du\rho/\mu)^{0.83}$, plotted *vs.* total pressure. No trend of variation with pressure is evident, and the data consequently substantiate the use of the diffusion Eq. (43) for interphase transfer through gas films. The dotted lines shown represent the empirical Eq. (58) for each of three liquids. It follows that k_G varies inversely as the partial pressure of inerts, p_{BM}, since

$$k_G = \frac{N_A}{(p_G - p_i)} = \frac{DP}{RTxp_{BM}} \qquad (60)$$

and it has just been shown that DP/x is independent of pressure. The same conclusion was reached by Hanks and McAdams[76] who varied solute gas concentration over a wide range at constant total pressure.

Illustration 6.—By what percentage would the rate of absorption be increased or decreased by increasing the total pressure from 1 to 2 atm. for the following cases?

a. The absorption of NH_3 from a mixture of NH_3 and air containing 10 per cent NH_3 by volume, using pure water as solvent. Assume that when absorbing NH_3 the gas film is the controlling resistance to diffusion.

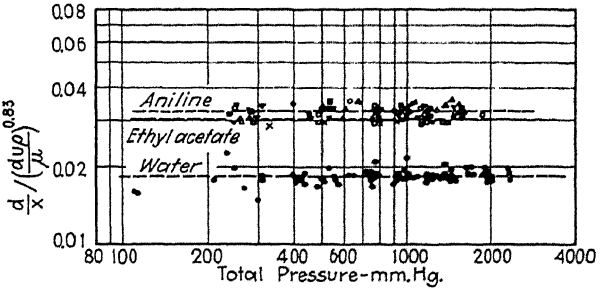

FIG. 11.—Effect of pressure on effective film thickness for diffusion.

b. The absorption of NH_3 from a mixture of NH_3 and air containing 10 per cent NH_3 by volume, using a solution of NH_3 in water as a solvent. The vapor pressure of NH_3 over the solution is 0.05 atm.

c. The absorption of SO_2 by pure water from a mixture of SO_2 and air containing 10 per cent SO_2 by volume. Assume that at 1 atm. the resistance of gas and liquid films are equal, *i.e.*, that the partial pressure drops across gas and liquid films are equal.

Solution.

a. Using the Stefan equation (13):

$$N_A = \frac{DP}{RTx} \ln \frac{p_{B2}}{p_{B1}}$$

$$\frac{N_A(1 \text{ atm.})}{N_A(2 \text{ atm.})} = \frac{\left[\frac{DP}{RTx}\left(\ln \frac{p_{B2}}{p_{B1}}\right)\right]_{1 \text{ atm.}}}{\left[\frac{DP}{RTx}\left(\ln \frac{p_{B2}}{p_{B1}}\right)\right]_{2 \text{ atm.}}} = \frac{\left[\ln \frac{p_{B2}}{p_{B1}}\right]_{1 \text{ atm.}}}{\left[\ln \frac{p_{B2}}{p_{B1}}\right]_{2 \text{ atm.}}} \qquad (A)$$

It was noted previously that the product DP is independent of pressure.

At 1 atm.:

$$p_{B1} = 0.9 \text{ atm.} \qquad p_{B2} = \text{0.1 atm.} \simeq \text{1.0 atm}$$

At 2 atm.:

$$p_{B1} = 0.90 \times 2 = 1.8 \text{ atm.} \qquad p_{B2} = 2 \text{ atm.}$$

Substituting in Eq. (*A*),

$$\frac{N_A(1 \text{ atm.})}{N_A(2 \text{ atm.})} = \frac{\ln \frac{1}{0.9}}{\ln \frac{2}{1.8}} = 1$$

There is no effect of pressure on the absorption rate.

b. Equation (*A*) also applies in this case.

At 1 atm.:

$$p_{B1} = 0.9 \text{ atm.} \qquad p_{B2} = 1 - 0.05 = 0.95 \text{ atm.}$$

At 2 atm.:

$$p_{B1} = 1.8 \text{ atm.} \qquad p_{B2} = 2 - 0.05 = 1.95 \text{ atm.}$$

Substituting in Eq. (*A*),

$$N_A(2 \text{ atm.}) = \frac{\left(\ln \frac{p_{B2}}{p_{B1}}\right)_{2 \text{ atm.}}}{\left(\ln \frac{p_{B2}}{p_{B1}}\right)_{1 \text{ atm.}}} \times N_A(1 \text{ atm.}) = \left(\frac{\ln \frac{1.95}{1.8}}{\ln \frac{0.95}{0.9}}\right) \times N_A(1 \text{ atm.}) =$$

$$1.480 \times N_A(1 \text{ atm.})$$

The increase in pressure results in a 48.0 per cent increase in absorption rate.

c. At 1 atm.:

$$p_{A1} = 0.1 \text{ atm.} \qquad p_{A2} = 0.05 \text{ atm.}$$
$$p_{B1} = 0.9 \text{ atm.} \qquad p_{B2} = 0.95 \text{ atm.}$$

At 2 atm.:

$$p_{A1} = 0.2 \text{ atm.} \qquad p_{A2} = \text{to be determined}$$
$$p_{B1} = 1.8 \text{ atm.} \qquad p_{B2} = 2 - p_{A2}$$

From Eq. (*A*) for gas film:

$$\frac{N_A(2 \text{ atm.})}{N_A(1 \text{ atm.})} = \frac{\ln \frac{2 - p_{A2}}{1.8}}{\ln \frac{0.95}{0.90}} \qquad (B)$$

For liquid film:

$$\frac{N_A(2 \text{ atm.})}{N_A(1 \text{ atm.})} = \frac{p_{A2} - 0}{0.05 - 0} = \frac{p_{A2}}{0.05} \qquad (C)$$

Combining Eqs. (*B*) and (*C*) and solving, $p_{A2} = 0.066$ atm.

Therefore

$$\frac{N_A(2 \text{ atm.})}{N_A(1 \text{ atm.})} = \frac{0.066}{0.05} = 1.32$$

The increased pressure results in a 32 per cent increase in absorption rate.

Comparison of Experimental Data with the Colburn Theoretical Equation.—The Colburn theoretical Eq. (49) may be rewritten as

$$\frac{k_G p_{BM}}{\mu} = \frac{\frac{f}{2}\left(\frac{du\rho}{\mu}\right)}{M_M d\phi_D} \tag{61}$$

In order to compare the turbulent flow data of Gilliland with this relation, the left-hand side has been plotted *vs.* the group on the right-hand side, as shown in Fig. 12. The values of r used in calculating ϕ_D were obtained from Eq. (50). Values of f were

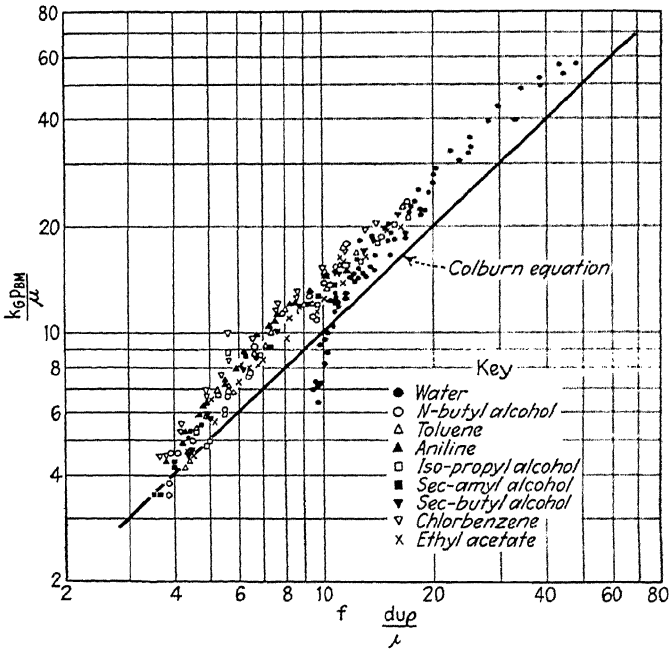

FIG. 12.—Comparison of Gilliland's data on vaporization with the Colburn analogy to friction.

obtained experimentally from pressure-drop measurements, and the relation between f and $du\rho/\mu$ ascertained for the apparatus in which the vaporization tests were made. The correlation of the points on Fig. 12 is good, but the line representing the theoretical equation falls roughly 30 per cent below the data. This is apparently not due to the use of incorrect values of f, for these were determined experimentally, and check within a few per cent the best correlations of data on turbulent-flow friction.[54] Some-

what better agreement would be obtained if the values of r used were greater than those given by Eq. (50). The maximum value of r is unity, however, so that only a limited improvement could be made by using other values of this ratio.

The same data may be used to test Arnold's assumption that the effective thickness of the laminar film is the same for heat transfer as for diffusion of any vapor. If B_D represent the

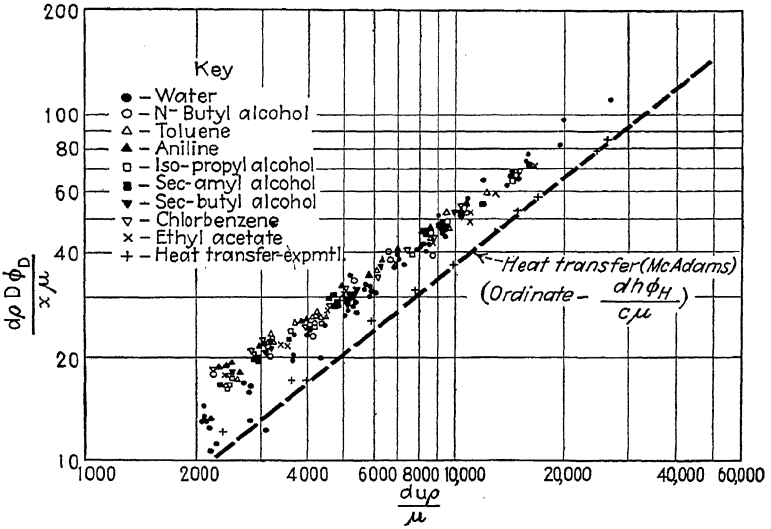

FIG. 13.—Heat transfer and diffusion in round pipes compared on the basis of the Arnold theory.

effective thickness of the laminar layer, from the point of view of diffusion, then from Eq. (51),

$$B_D = \frac{r\mu_f/\rho D}{\frac{r\mu_f}{\rho D} + (1 - r)} x = \frac{r\mu_f}{\rho D \phi_D} x \tag{62}$$

where x is the effective total film thickness. B_D/d should be a function of Reynolds number only, as is the ratio r. Hence, for each vapor, $d\rho D\phi_D/x\mu_f$ should be the same function of the Reynolds group. Figure 13 shows this group plotted *vs.* $du\rho/\mu$ for the turbulent-flow data obtained by Gilliland, and it may be seen that the correlation is very good, indeed. Similarly, for

heat transfer, if B_H represents the effective thickness of the laminar layer, then

$$\frac{x_H}{I} = \frac{}{\phi_H h}$$

where $\phi_H = 1 - r + r(c\mu_f/k_H)$.

x_H = effective total film thickness for heat transfer.

Arnold assumes that $B_D = B_H$, whence it follows that the groups $d\rho D\phi_D/x\mu_f$ and $dh\phi_H/c\mu_f$ should be the same function of the Reynolds number. In addition to the diffusion data, Fig. 13 shows a line representing Eq. (59) recommended by McAdams[131] for heat transfer to gases in pipes, and also the data obtained by Gilliland on heat transfer to air flowing in the same apparatus in which the vaporization tests were carried out. On this basis, $1/B_H$ appears to be some 30 to 35 per cent less than $1/B_D$. This may be compared with the analysis by Sherwood and Comings[166] of Mark's data on wet-bulb measurements for various liquids, which showed a deviation from the Arnold theory of some 15 to 25 per cent in the opposite direction.

The good correlation obtained in Fig. 13 on the basis of the Arnold theory supports the use of Eq. (53) for the purpose of estimating gas-film resistance for one gas, from the experimentally determined resistance to the diffusion of a second gas. The alternative method of calculation is the use of the empirical Eq. (58).

Gas Films Outside Pipes.—The data of Vint[187] are available on the vaporization of water, toluene, and *n*-butyl alcohol from the outer surface of a 5.08-cm. tube, past which air was blown at right angles. The tube was covered with a thin cloth sleeve, down which the liquid flowed in a thin film. The apparatus was placed in a small wind tunnel, through which air was forced at 1 to 4 m./sec. at 20° to 40°C. The data are shown on Fig. 14 plotted as $d\rho D\phi_D/x\mu$ *vs.* $du\rho/\mu$, which are the same coordinates used in Fig. 13. The slope of the line is considerably less than that of Fig. 13 for turbulent flow of gases inside pipes. This is analogous to the effect noted in heat transfer, for which the exponent on the Reynolds number is greater for turbulent flow in pipes than for turbulent flow outside and at right angles to pipes. The correlation is not so good as that of Fig. 13, but the discrepancies between the data for the three vapors are not excessive.

The dotted line represents the data of Reiher,[157] on heat transfer between a single tube and air flowing outside and at right angles in turbulent motion. The ordinate in this case is $dh\phi_H/c\mu$. As in the case of flow inside pipes, the heat flow and diffusion data check reasonably well when plotted on this basis.

Figure 14 shows also the data of Lorisch[128] on the absorption from air of water vapor and ammonia vapor on the outer surface of vertical tubes placed in a cross air current. For water-vapor

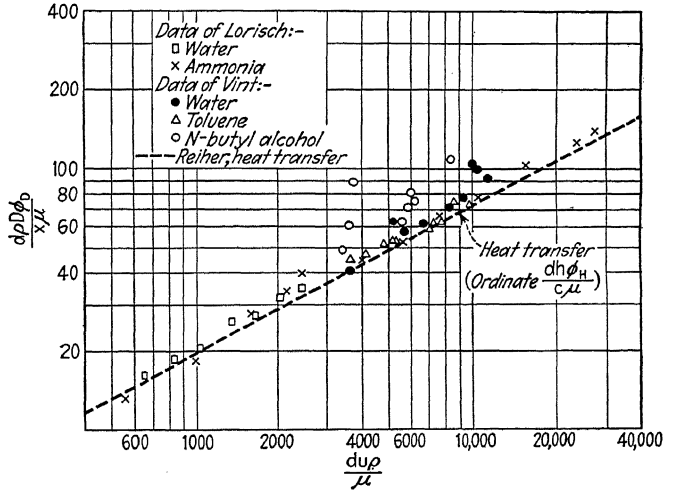

FIG. 14.—Heat transfer and diffusion outside vertical tubes compared on the basis of the Arnold theory.

absorption the tubes consisted of sticks of solid caustic, and for ammonia absorption glass tubes were wrapped with blotting paper saturated with phosphoric acid. The data fall in well with those of Vint and Reiher, checking the heat-transfer data better, in fact, than Vint's data on vaporization. These data consequently lend additional support to Arnold's hypothesis outlined above.

In preparing Fig. 14, ϕ_D and ϕ_H were calculated using a constant value of r of 0.50. This procedure was followed since the variation of r with Reynolds number was not known for the case of gas flow outside pipes.

Wetted-wall Column Experiments with Air Flowing in Viscous Motion.—At values of $du\rho/\mu$ below about 2,300, the flow in a

tube becomes viscous or streamline, and the central turbulent core or eddy layer disappears. Since with this type of flow there is no mixing of successive layers of fluid moving parallel to the wall, the laws of true diffusion may be expected to apply, provided proper allowance is made for the velocity gradient across the stream. For diffusion in one direction of one gas through a second stagnant gas, the basic differential equation is

$$\frac{p_A}{\partial\theta} = \frac{\partial}{\partial x}\left[\frac{DP}{p_B}\frac{dp_A}{dx}\right.$$

In many cases the partial pressures of the diffusing gas are small compared to the total pressure P. Under such conditions p_B may be assumed constant and equal to P, whence

$$\frac{\partial p_A}{\partial\theta} = D\frac{\partial^2 p_A}{\partial x^2} \tag{8}$$

The corresponding equation for diffusion in three directions may be integrated to give an equation for diffusion into a viscous stream flowing in a round pipe. The procedure is the same as that followed in deriving the similar relations for heat transfer.[70,53]

For rodlike flow, *i.e.*, assuming a uniform velocity across the diameter of the pipe, the integration leads to the equation

$$\frac{p_{AG2} - p_{AG1}}{p_{Ai} - p_{AG1}} = 1 - \sum_{1}^{\infty} \frac{1}{\alpha_n^2} e^{-\frac{\alpha^2 n \pi D \rho L}{W}} \tag{64}$$

where p_{AG2} = partial pressure of the diffusing gas in the main gas stream at the outlet.

p_{AG1} = partial pressure of the diffusing gas in the main gas stream at the inlet.

p_{Ai} = partial pressure of the diffusing gas at the phase boundary (inner surface of the tube), assumed constant throughout the length L.

D = diffusion coefficient, cm.²/sec.

π = 3.1416.

W = weight rate of gas flow, g./sec.

L = tube length, cm.

ρ = density of main gas stream, g./cc.

α_n = nth root of the Bessel function $J_0(x) = 0$.

In isothermal viscous flow, the velocity is a parabolic function of the distance from the central axis, and the cylinders of fluid near the axis have a greater vapor-carrying capacity than those near the wall of the pipe. If the parabolic velocity gradient is allowed for in the derivation, the result is somewhat more complicated than (64), but may be reduced[52] to

$$\frac{p_{AG2} - p_{AG1}}{p_{Ai} - p_{AG1}} = 1 - 0.10238e^{-14.6272\left(\frac{\pi}{4}\right)\frac{D\rho L}{W}} - 0.01220e^{-89.22\left(\frac{\pi}{4}\right)\frac{D\rho L}{W}} - \cdots \qquad (65)$$

In the derivation of Eqs. (64) and (65), the partial pressure p_{Ai} is assumed constant throughout the length of the pipe, and diffusion in a direction parallel to the axis of the pipe is neglected.

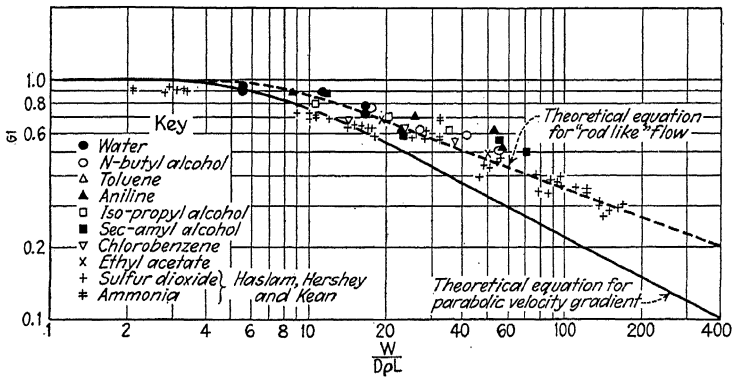

FIG. 15.—Absorption and vaporization in wetted-wall columns under conditions of viscous flow of the main gas stream.

Both theoretical equations are shown plotted in Fig. 15 as

$$\frac{p_{AG2} - p_{AG1}}{p_{Ai} - p_{AG1}} \text{ vs. } \frac{W}{D\rho L}$$

The maximum value of the ordinate is unity, which corresponds to equilibrium at the wall, and is approached at low velocities, in long tubes, or for large values of D. On the same plot are shown the vaporization data obtained in the viscous flow region by Gilliland, and the data on absorption of sulfur dioxide and ammonia obtained by Haslam, Hershey, and Kean,[79] using a wetted-wall column with air flowing below its critical velocity.

Both vaporization and absorption data fall together on the line representing the theoretical equation for rodlike flow. Since the flow was viscous, a parabolic velocity doubtless existed, and the data would be expected to check the lower line for Eq. (64). In a similar way, the data on heat transfer in viscous flow check the equation for rodlike flow better than they do the theoretical equation based on a parabolic velocity gradient. This effect in heat transfer was ascribed[53] to free convection effects caused by temperature gradients through the fluid, or to the fact that the parabolic velocity gradient is but partially attained in a short length of pipe. In Gilliland's tests, however, the flow was substantially isothermal and the tube vertical; consequently, free convection eddies should have been at a minimum. The vaporization data plotted represent both parallel- and counter-flow tests, so the falling film could not have been a disturbing factor. The agreement of the data with the theoretical equation for rodlike flow is not justified theoretically, but the theoretical line shown represents an empirical correlation of the data.

In cases where the vapor concentrations are large, and p_B and P differ considerably, a better approximation will be obtained in using the dotted curve of Fig. 15, if the actual value of D be multiplied by the ratio of P to some average value of p_B.

SIMULTANEOUS DIFFUSION AND HEAT TRANSFER—THE WET-BULB HYGROMETER

Simultaneous transfer between phases of both heat and material is of considerable engineering importance in drying, humidification, dehumidification, and other unit operations. Various data on evaporation of liquids confirm the use of the basic diffusion equations with or without simultaneous heat transfer across the same air film. Occasionally, however, there are evidences of complicating effects, and the correlation based on the diffusion equations is poor. Combs and Simons,[41] for example, found values of d/x, when both water and air were at 19 to 24°C., to be 33 per cent greater than when the air was at 17 to 25°C. and the water at 37 to 43°C., at the same Reynolds number. These results were obtained when vaporizing water into air in a 2-in. wetted-wall column. Similar discrepancies are indicated for data on dehumidification of air by contact with cold surfaces.

No good explanation for these discrepancies is available, although in some cases they are doubtless connected with fog formation within the surface gas film.

The Lewis equation

$$h/k' = s \tag{66}$$

has proved of considerable utility in connection with vaporization problems. As originally presented,[116] it was based on a theoretical derivation, and served to confirm Carrier's conclusion that the wet-bulb temperature was identical with the temperature of adiabatic saturation.[31] Although the original derivation is now known to be in error,[118] the relation given above holds reasonably well for the evaporation of water into air, but not for other systems studied. The use of the adiabatic cooling lines of the Grosvenor humidity chart for the interpretation of wet- and dry-bulb measurements hinges on the validity of this relation, and it follows that these lines for psychrometric work may be used as a good approximation for water and air only.

In Eq. (66), h represents the surface coefficient of heat transfer, s the specific or "humid" heat of the air stream, and k' the vaporization coefficient in the simplified diffusion equation

$$N_A M_A = k'(H_i - H_G) \tag{67}$$

H_i represents the absolute humidity (g. vapor per g. bone-dry gas, or lb. vapor per lb. bone-dry gas) corresponding to saturation at the temperature of the liquid surface, and H_G the corresponding absolute humidity of the ambient gas stream. By definition

$$H_i - \left[\frac{p_i}{P - p_i} - \frac{p_G}{P - p_G}\right]\frac{M_A}{M_B}$$

and since in most cases p_i and p_G are small compared to P, $P - p_i$ is approximately equal to $P - p_G$, and each is approximately equal to the mean inert pressure, p_{BM}, whence

$$H_i - H_G = \frac{M_A}{M_B}\frac{(p_i - p_G)}{p_{BM}}$$

Combining this last with the basic Eq. (16),

$$k' = \frac{N_A M_A}{(H_i - H_G)} - \frac{kM_B}{x_D}$$

Writing h as k_H/x_H, the ratio of the thermal conductivity to the effective thickness of the gas film for heat transfer,

$$\frac{h}{k'} = \frac{k_H}{kM_H} \frac{x_D}{x_H}$$

Combining this last with the Arnold relation (52), and remembering that $k = DP/RT$, $\rho = M_H P/RT$, and $c = s$ (approximately), there results

$$\frac{h}{k'} = c\frac{\phi_D}{\phi_H} \tag{68}$$

where $\phi_D = 1 - r + r(\mu/\rho D)$, and $\phi_H = 1 - r + r(c\mu/k_H)$

For water vapor and air, $\mu/\rho D$ is approximately 0.60, $c\mu/k_H$ is 0.74, c is 0.24, and taking r as 0.5, Eq. (68) reduces to $h/k' = 0.22$. Experimental data indicate that h/k' is somewhat greater than this, and for water and air in general h/k' approximates s so closely that the adiabatic cooling lines of the standard humidity charts may be used for the interpretation of wet- and dry-bulb readings in all engineering calculations. Data on wet-bulb determinations with various liquids show fairly good agreement with Eq. (68), and this relation, based on the Arnold proposal for relating x_H and x_D, is probably the best present theory[5] of the wet-bulb hygrometer. Values of h/k', based on wet-bulb measurements with various liquids in air, are tabulated in Table IV. For dry air, c is 0.24, and the failure of the original Lewis relation for the various organic liquids is apparent.

It may be noted that a simple heat balance[188] on the wet-bulb gives

$$\frac{h}{k'} = \frac{r_w(H_i - H_G)}{(t_G -} \tag{69}$$

This relation may be employed when using the values of h/k' given in Table IV for the interpretation of wet- and dry-bulb readings (see Illustration 7).

The Chilton-Colburn analogy between heat transfer and diffusion in gas films was shown to give the relation (57) between k_G and h. For small concentrations of vapors in an inert gas this reduces to

$$\frac{h}{k'} = c\left(\frac{\mu/\rho D}{c\mu/k_H}\right)^{\frac{2}{3}} \tag{70}$$

TABLE IV.—SUMMARY OF AVERAGE VALUES OF h/k' CALCULATED FROM WET-BULB DETERMINATIONS IN AIR*

Vapor	Mark[136]	Sherwood and Comings[166]	Awberry and Griffiths[8]	Hilpert[89]	Arnold[5]	Calculated from Arnold Theory [Eq.(68)]	Calculated from Chilton-Colburn Analogy [Eq.(70)]
Benzene	0.41	0.40	....	0.49	....	0.39	0.44
Brombenzol	....	....	....	0.46	....	0.41	0.47
Carbon tetrachloride	0.44	0.50	....	0.50	....	0.43	0.49
Chlorobenzene	0.44	....	....	0.51	....	0.43	0.48
Ethyl acetate	0.42	....	....	....	....	0.41	0.46
Ethylene bromide	....	....	....	0.53	....	0.41	0.47
Ethylene tetrachloride	0.50	....	....	....	....	0.45	0.51
Ethyl propionate	....	....	....	....	0.50	0.44	0.46
Methyl alcohol	....	....	....	....	0.35	0.29	0.31
n-Propyl acetate	....	0.52	....	....	....	0.44	0.49
Propyl alcohol	....	....	....	....	0.43	0.37	0.41
Toluene	0.44	0.50	....	0.46	0.50	0.42	0.47
Water	0.26	0.29	0.36	....	0.27	0.22	0.21

* The values tabulated have not been corrected for radiation from the surroundings, since in most cases the conditions of the tests were not sufficiently well described to make this correction with any accuracy. Mark's data were obtained with high air velocities, and the correction is negligible; the radiation correction would reduce Arnold's experimental values by 12 to 16 per cent.

For gases, $c\mu/k$ may be taken as 0.74, and values of the group $\mu/\rho D$ may be obtained from Table III. For water vapor in air this becomes

$$\frac{h}{k'} = 0.21 \tag{71}$$

Other values of h/k' calculated in this way are tabulated in Table IV for comparison with the experimental values. It may be seen that the general agreement of the calculated and experimental values is about the same as for the Arnold theory.

Illustration 7.—A thermometer covered with a clean porous wick wet with benzene is placed in a current of a gas mixture containing air and benzene vapor. Care is used to maintain the wick adequately wet with benzene supplied at a temperature as near as practicable to the observed wet-bulb temperature. The gas velocity is sufficiently great so that radiation to the wick may be assumed to be small as compared with heat transfer by convection. Under these conditions the observed wet-bulb temperature is 19.7°C. at a dry-bulb temperature of 92°C., and under a barometric pressure of 768.4 mm. Estimate the benzene content of the gas.

Data and Assumptions.—Employ the relation between effective film thicknesses for heat transfer and diffusion suggested by Arnold, using a value of r of 0.5. Assume the physical properties of the film to be the same as those of air at the mean film temperature of 50°C. At this temperature the specific heat of air is 0.243 g. cal./(g.)(°C.), the thermal conductivity is 0.0000618 g. cal./(sec.)(cm.²)(°C.)(cm.), the viscosity is 0.000196 g./(sec.)(cm.), and the density is 0.00108 g./cc. At 19.7°C. the latent heat of vaporization of benzene is 8,100 g. cal./g. mol., and the vapor pressure is 74.5 mm. Hg.

Solution.—The wetted wick may be assumed to be in dynamic equilibrium with its surroundings, at a temperature such that the heat inflow corresponds quantitatively to the enthalpy change of the benzene vaporizing. he heat inflow from air to wick may be expressed by the conduction quation

$$q = \frac{k_H}{x_H} A(t_G - t_i) \qquad (A)$$

where k_H represents the thermal conductivity of the film, A is the surface area of the wetted wick, t_G and t_i are the dry- and wet-bulb temperatures, and x_H is the effective film thickness for heat transfer by convection.

The vapor diffusing from wick to gas may be obtained by Eq. (43)

$$N_A = \frac{DP}{RTx_D} \frac{(p_i - p_G)}{p_{BM}} \qquad (B)$$

where p_i = vapor pressure of benzene at the wet-bulb temperature.
p_G = partial pressure of benzene in the gas.
x_D = effective film thickness for diffusion.

The heat corresponding to the latent heat of vaporization must be transferred across the air film, but the smaller quantity of heat required to raise the temperature of the vapor formed need be transferred across only part of the film, since the temperature of the vapor rises as it diffuses away from the film. Since the heat of vaporization is large compared with the sensible heat required to raise the vapor temperature, and since the latter traverses only part of the film, a sufficiently good approximation may be made by equating the latent heat of vaporization of the diffusing vapor to the heat transfer across the film, thus:

$$\frac{k_H}{x_H} A(t_G - t_i) = \frac{M_A r_w DPA}{RTx_D} \frac{(p_i - p_G)}{p_{BM}} \qquad (C)$$

here $M_A r_w$ represents the molal heat of vaporization. At 50°C. the iffusivity is found by Eq. (31) to be 0.0943 cm.²/sec. Hence $\mu/\rho D = 1.92$, ad $c\mu/k_H = 0.77$. By Eq. (52),

$$\frac{x_H}{x_D} = \frac{0.0000618}{0.0943 \times 0.00108 \times 0.243} \frac{(1 - 0.5 + 0.5 \times 0.77)}{(1 - 0.5 + 0.5 \times 1.92)} = 1.51$$

Substituting in Eq. (*C*),

$$\frac{0.0000618}{1.51x_D} A(92 - 19.7) = 8{,}100 \frac{0.0943 \times 768.4A(74.5 - p_G)}{82.07 \times 323 \times 760x_D p_{BM}}$$

The partial pressure of air p_B is 768.4 − 74.5, or 693.9 mm. at the wick surface, and greater than this, but not greater than 768.4, in the air stream. The mean p_B, or p_{BM}, is consequently somewhere between 694 and about 733. Assuming p_{BM} to be 730, and substituting in the relation above, p_G is found to be 0.4 mm.

Actually, the temperatures given were observed by J. G. Mark[136] when using a wick wet with benzene in a stream of air carrying no benzene. Experimentally, therefore, $p_G = 0$, with which the calculated value checks remarkably well.

From Eq. (68), taking r as 0.5,

$$\frac{r}{k'} = 0.243\left(\frac{1 - 0.5 + 0.5 \times 1.92}{1 - 0.5 + 0.5 \times 0.77}\right) \quad 0.40$$

As compared with the value of 0.42 calculated from the data given, using Eq. (69).

It is also of interest to compare the value of p_G based on the Chilton-Colburn analogy, and to follow the method of using Eq. (70). For this purpose the heat balance expressed above as Eq. (*C*) is rewritten using k':

$$hA(t_G - t_i) = k'A(H_i - H_G)r_w \qquad (D)$$

From Eq. (70), h/k' is found to be 0.44.

Substituting in Eq. (*D*), there results

$$0.44(92 - 19.7) \quad \frac{8,100}{78}\left(\frac{74.5}{768.4 - 74.5} \times \frac{78}{29} - H_G\right)$$

from which H_G −0.017, and p_G = −4.8 mm.

EVAPORATION OF CONSTANT-BOILING MIXTURES

When a liquid mixture is boiled, the composition of the vapor formed is determined by the vapor-liquid equilibrium for the system. When the same mixture is allowed to evaporate into air or other inert gas at temperatures below the boiling point, the composition of the vapor leaving is dictated by the relative rates of diffusion of the components through the gas film on the surface. Although the diffusion of each vapor is affected by the simultaneous diffusion of the others present, the simple relation for the diffusion of a single vapor through an inert gas may be used as an approximation. Thus the rate of transfer may be assumed to be proportional to the diffusivity and the driving force, and inversely proportional to the effective film thickness. If the liquid is exposed to a turbulent current of vapor-free air, the rate of diffusion is proportional to the partial pressure over the solution and to the 0.56 power of the diffusivity. In the evaporation of a binary mixture under these conditions the

relative rates of removal of the two components A and C having vapor pressures p_A and p_C will be

$$\frac{N_A}{N_C} = \frac{p_A}{p_C}\left(\frac{D_A}{D_C}\right)^{0.56}$$

and the liquid composition will change accordingly as evaporation proceeds.

The effect of the relative diffusivities on the evaporation of constant boiling mixtures has been pointed out by Lewis, Squires, and Sanders.[124] When the relative rates of removal of the two vapors are equal to the ratio of the amounts of the two components present in the liquid, evaporation produces no change in the composition of the liquid left behind. The composition at which this occurs is termed the "constant-evaporating composition" as distinguished from the composition at the constant boiling point. At the constant-boiling point the equilibrium vapor and liquid compositions are identical, and, if Raoult's law holds, the ratio p_A/p_C is equal to the ratio of A to C in the liquid. Lewis and Squires[125] find toluene-ethanol to have a constant-evaporating mixture of 19 per cent toluene, whereas the constant-boiling mixture at the same temperature (25°C.) contains approximately 32 per cent toluene.

If A and C form a constant-boiling mixture having a minimum boiling point, the boiling of any mixture of A and C results in a progressive change of liquid composition away from the constant-boiling composition. If the same mixture is allowed to evaporate into air, however, the liquid composition may change in the opposite direction and actually *cross the constant-boiling composition* owing to the influence of the relative diffusivities. Lewis and Squires studied this effect by allowing mixtures of methanol and benzene to evaporate in a small vessel covered with a wire gauze and placed in an air current. The evaporation of a mixture initially 56 mol per cent methanol gave a liquid composition of 46 mol per cent methanol after 63 per cent by weight of the original mixture had vaporized, crossing the constant-boiling composition of 51 mol per cent methanol. The application of the diffusion equations to the problem of relating liquid composition to fraction vaporized is dealt with by Lewis and Squires.

If the evaporation is carried on in an efficient bubbler or other saturating device, so that the air-vapor mixture leaving the apparatus is at all times in equilibrium with the liquid left behind, then no time element is involved and the relative diffusivities obviously have no bearing on the result. Such a process is essentially the same as boiling at the same temperature, and the Rayleigh equations for batch distillation apply.

Nomenclature for Chapter II

a = radius of pipe.
A = surface of contact between phases.
B_D = effective thickness of the laminar film for diffusion.
B_H = effective thickness of the laminar film for heat transfer.
c = specific heat.
C_G = partial molal density of the diffusing component in the fluid stream.
C_i = equilibrium partial molal density at the phase boundary.
d = tube diameter.
D = diffusion coefficient or diffusivity, cm.^{2}/sec.
e = base of natural logarithms.
f = friction factor in Fanning equation, Eq. (46).
g = acceleration due to gravity.
h = surface coefficient of heat transfer.
H = absolute humidity, g. vapor/g. bone-dry gas, or lb. vapor/lb. bone-dry gas.
j_D = defined by Eq. (56).
j_H = defined by the first equality of Eq. (55).
$k = \frac{DP}{RT}$.
k' = vaporization coefficient, defined by Eq. (67), weight per unit time per unit area per unit driving force expressed in units of absolute humidity.
k_H = thermal conductivity.
k_G = coefficient of material transfer, g. mols/(sec.)(sq. cm.)(atm.).
L = tube length.
M = molecular weight.
M_M = average molecular weight of the main gas stream.
N_A = rate of diffusion for gas A, mols/(unit area)(unit time).
p = partial pressure of diffusing gas, atm.
p_{AG1} = partial pressure of the diffusing gas in the main gas stream at the gas inlet, atm. See Eq. (64).
p_{AG2} = partial pressure of the diffusing gas in the main gas stream at the gas outlet, atm. See Eq. (64).
p_{Ai} = partial pressure of diffusing gas at the phase boundary (inner surface of the tube), assumed constant throughout the length L. See Eq. (64).
p_B = partial pressure of the inert or nondiffusing gas, atm.

p_{BM} = log mean partial pressure of inerts at film boundaries, atm.
p_f = partial pressure of the diffusing gas at the boundary of the laminar layer, atm. [Eq. (51)].
P = total pressure, atm.
q = heat inflow from air to wick, B.t.u./hr. (See Illustration 7.)
r = ratio of the fluid velocity at the boundary between laminar and eddy layers, to the average velocity of the main fluid stream.
r_w = latent heat of vaporization at the wet-bulb temperature, g. cal./g.
R = gas-law constant.
Re = Reynolds number = $\frac{du\rho}{\mu}$.
s = humid heat, or heat capacity of humid air per unit weight of dry air content.
t = temperature, °F. or °C.
T = absolute temperature, °R. or °K.
u = average velocity of gas stream, cm./sec.
W = weight rate of flow of fluid mixture, g./sec.
x = effective total film thickness.
x_D = effective total film thickness for diffusion.
x_H = effective total film thickness for interphase heat transfer.
α_n = nth root of the Bessel function $J_0(x) = 0$.
θ = angle between axis of pipe and path of particle observed by Fage and Townend. See Fig. 7.
π = 3.1416.
ρ = gas density in the main gas stream, g./(cc.).
μ_f = average absolute viscosity of the laminar layer, g./(sec.)(cm.).

$$\phi_D = 1 - r + r\left(\frac{\mu_f}{\rho D}\right).$$

$$\phi_H = 1 - r + r\left(\frac{c\mu_f}{k_H}\right).$$

SUBSCRIPTS

A, B, C refer to components A, B, C of a mixture of several substances.
D refers to diffusion or mass transfer.
G refers to conditions in the main body of fluid.
H refers to heat transfer.
i refers to conditions at the phase boundary or interface.

CHAPTER III

PRINCIPLES OF THE DESIGN OF ABSORPTION EQUIPMENT

Good engineering design of absorption equipment must be based on a sound application of the principles of diffusion. Because of wide variations in gas and liquid compositions through the apparatus, care must be used in the interpretation and use of the experimental and plant data which must form the basis of the design. The technique of allowing for these varying compositions and diffusional rates in applying the fundamental diffusion theory will be discussed in the present chapter.

The first requirement of engineering equipment for gas absorption is that it be designed to bring two separate phases into intimate contact. Since the gas to be treated and the liquid solvent are both fluids, the material at the interface or surface of contact between the phases is not fixed but may itself be in motion. Owing to free or forced convection currents the main body of each fluid is invariably in motion with respect to the interface. There is, consequently, a fluid "film" adjoining the interface in each fluid, and the principal resistance to interphase diffusion is this double film. This concept, first proposed by W. G. Whitman,[194] has been a great aid in visualizing the process of interphase transfer between two fluids. The relative resistances of the liquid and gas films depend primarily on the nature of the fluids, their relative motion, and the solubility of the solute in the absorbing liquid. In the design of absorption equipment for any specific purpose, it is clearly of great importance to understand which of the two films may be expected to offer the major resistance to diffusion, in order that a rational attempt may be made to improve the design.

The analytical treatment of the diffusion through each of the two films[126] follows the methods described in the previous chapter, and since the films are sufficiently thin so that the solute retained by them may be neglected, it is possible to equate the rates of

diffusion through gas and liquid films. Thus, by Eqs. (16) and (41),

$$N_A = \frac{DP}{RTx_G}\frac{(p_G - p_i)}{p_{BM}} = \frac{D_L(C_A + C_B)(C_i - C_L)}{x_L C_{BM}} \qquad (72)$$

where p_G = partial pressure of the solute in the main gas phase.
p_i = partial pressure of the solute at the interface between gas and liquid.
C_i = concentration of the solute in the liquid phase at the interface.
C_L = concentration of the solute in the main body of the liquid.
D_L = diffusion coefficient for solute through the liquid phase.
D = diffusion coefficient for the solute through the gas phase.
x_G = effective thickness of the gas film.
x_L = effective thickness of the liquid film.

The other symbols represent the same quantities as in the previous chapter.

There appears to be no evidence of an appreciable diffusional resistance at the actual interface, and it seems not only reasonable, but in accord with the available data, to assume that there exists no resistance of such a character. It follows, therefore, that the gas and liquid phases at the actual interface are in equilibrium and that the relation between p_i and C_i is the equilibrium relation between the two phases for the system involved. The over-all resistance to interphase diffusion is evidently the sum of the individual gas and liquid "film resistances."

For purposes of engineering computations, many of the terms of Eq. (72) may be grouped in the form of individual "film coefficients," and the expression rewritten

$$N_A = \text{mols per unit time per unit area} = k_G(p_G - p_i) = k_L(C_i - C_L) \qquad (73)$$

where k_G is the gas-film coefficient, and k_L is the liquid-film coefficient. Obviously, k_G is a function of temperature, total pressure, mean pressure of inert, as well as of the various factors which determine the value of D and of the effective gas-film thickness. Similarly, k_L is a function of solute concentration,

and D_L and of those factors determining x_L. For these reasons the extrapolation of experimental values of k_G and k_L is usually somewhat hazardous.

Equation (73) states that the weight rate of diffusion through each film is proportional to the driving force applicable to the particular phase. In the case of the gas film the driving force is expressed in terms of partial pressures, while in the liquid film it is expressed in terms of solute concentrations. In a given case where p_G, C_L, k_G, and k_L are known, the rate of diffusion may be obtained from Eq. (73) if the equilibrium relation $p_i = f(C_i)$ is known. The ratio of the driving force $(p_G - p_i)$ to the driving force $(C_i - C_L)$ is determined by the ratio of k_L to k_G, but the actual values of p_i and C_i are determined by the equilibrium or solubility relation. For example, if $k_G = k_L$ then

$$(p_G - p_i) = (C_i - C_L)$$

If the case in question is that of a very soluble gas, then the only way for the driving forces to be equal would be for p_i to be nearly as small as p_e, the equilibrium value corresponding to C_L, since with a large value of p_i the concentration C_i would be very large, and the difference $(C_i - C_L)$ too great. Actually, if k_L and k_G are of the same order of magnitude in the units employed, then for a liquid and very soluble gas, such as water and ammonia, p_i will necessarily be practically equal to p_e, and Eq. (73) may be written

$$N_A = k_G(p_G - p_e) \tag{74}$$

It follows that the rate of diffusion is the same as though the liquid film were absent, and the gas-film resistance is said to be controlling. This conclusion is supported by experience with industrial-absorption equipment, in which it is found that the factors influencing the liquid-film resistance are of negligible consequence when handling liquids and highly soluble gases.

Pursuing a similar line of reasoning, it follows that for liquids and relatively insoluble gases, p_i becomes nearly equal to p_G and C_i nearly equal to C_e, the equilibrium value corresponding to p_G. The diffusion equation then becomes

$$N_A \quad k_L(C_i - C_L) = k_L(C_e - C_L) \tag{75}$$

The gas film is eliminated from consideration, and it is said that the liquid-film resistance is controlling. For gases of intermediate solubility, the resistance of each film must be considered.

OVER-ALL COEFFICIENTS

Where allowable, it is convenient to employ a single over-all coefficient, in place of the two film coefficients, k_G and k_L. Two over-all coefficients, K_G and K_L, are defined by the equation

$$N_A = K_G(p_G - p_e) = K_L(C_e - C_L) \tag{76}$$

where p_e is the pressure in equilibrium with the concentration C_L, and C_e is the concentration in equilibrium with the pressure p_G. K_G is the over-all coefficient in terms of pressures, and K_L is the over-all coefficient in terms of concentrations.

It is important to realize that the over-all coefficient should be employed only when $(p_G - p_e)$ remains proportional to $(C_e - C_L)$ as pressure and concentration are varied. If this proportionality does not hold, it is evident from Eq. (76) that as the concentration changes, K_L or K_G will vary. In order for the proportionality to hold, it is necessary that Henry's law should apply, *i.e.*, that

$$C = Hp \tag{77}$$

Over-all coefficients should be employed only for systems and for concentration ranges over which Henry's law applies. In systems where Henry's law does not apply, the over-all coefficients are frequently found to vary widely with concentration, and should be used with the greatest caution. Variations of k_L and k_G with concentrations, as indicated by Eqs. (72) and (73), are ordinarily negligible in engineering computations, except for the effect on k_G of large variations in mean pressure of inerts, p_{BM}. The procedure in allowing for variations in these latter factors is discussed below.

Where Henry's law applies, the relation between the over-all and the individual film coefficients[188] may be obtained by eliminating C_i and p_i from Eqs. (73) and (74):

$$\frac{1}{K_G} = \frac{1}{k_G} + \frac{1}{Hk_L} \tag{78}$$

and

$$\frac{1}{K_L} = \frac{1}{k_L} + \frac{H}{k_G} \tag{79}$$

Tne reciprocal of the over-all coefficient may be looked upon as the over-all resistance to diffusion, which is the sum of the individual film resistances, represented by the terms on the right-hand side of the equations above. Thus, in terms of pressures, $1/K_G$ represents the over-all or total resistance, $1/k_G$ the gas-film resistance, and $1/Hk_L$ the liquid-film resistance. In terms of liquid concentrations, $1/K_L$ is the over-all resistance, $1/k_L$ the liquid-film resistance, and H/k_G the gas-film resistance. The numerical values of the resistance will clearly depend on the units in which the driving force is expressed.

It is evident from Eqs. (78) and (79) that as H is made large, the gas-film resistance approaches the over-all resistance, and k_G approaches K_G. Similarly, if H is made very small the liquid-film and over-all resistances become practically equal. Since a large H corresponds to high solubility, these considerations bear out the previous general conclusions that gas-film resistance becomes controlling for highly soluble gases, but that in the case of a gas of low solubility the liquid film is the controlling resistance.

Illustration 8.—In the absorption of SO_2 from air by water at 68°F. in a wetted-wall column operated at a pressure of 1 atm., a value of K_G of 0.071 lb. mol/(hr.) (sq. ft.) (atm.) was obtained. Gas and water rates were held constant throughout the run.

Estimate the value of the coefficient K_G for the absorption at atmospheric pressure of NH_3 in water in the same wetted-wall column at 50°F., using the same gas and water rates that were used above. Assume the resistance of gas and liquid films to be equal in the absorption of SO_2.

Solution.—From Eq. (78),

$$\frac{1}{K_G} = \frac{1}{k_G} + \frac{1}{Hk_L} = \frac{1}{0.071} = 14.1$$

Since gas- and liquid-film resistances are assumed equal in the absorption of SO_2,

$$k_G = Hk_L = \frac{1}{7.05} = 0.141$$

As an approximation it will be assumed that k_L for both solutes is the same. The values of H for SO_2 at 68° and for NH_3 at 50°F., are approximately 0.15 and 2.6, respectively. Hence:

$$Hk_L \text{ for } NH_3 = 0.141 \times \frac{2.6}{0.15} = 2.44$$

The ratio of diffusion rates for SO_2 and NH_3 in the gas film is given by

$$\frac{\left[\frac{DP}{-p_i)}\right]_{NH_3}}{\left[\frac{DP}{}\right]_{NH_3}} = \frac{\left[\frac{(p_G - p_i)}{}\right]}{\left[\frac{(p_G - p_i)}{}\right]_{NH_3}}$$

For dilute gas mixtures, the mean pressure of the inerts may be assumed to be the same for the cases of both SO_2 and NH_3.

$$(k_G)_{NH_3} = (k_G)_{SO_2}\frac{[(D/xT)]_{NH_3}}{[(D/xT)]_{SO_2}} \qquad (B)$$

The ratio of the effective gas-film thicknesses may be obtained from the Gilliland equation (58), as follows:

$$\frac{(d/x)_{SO_2}}{(d/x)_{NH_3}} = \frac{[0.023(du\rho/\mu)^{0.83}(\mu/\rho D)^{0.44}]_{SO_2}}{[0.023(du\rho/\mu)^{0.83}(\mu/\rho D)^{0.44}]_{NH_3}}; \quad \text{and} \quad \frac{x_{NH_3}}{x_{SO_2}} = \left(\frac{D_{NH_3}}{D_{SO_2}}\right)^{0.44} \qquad (C)$$

Substituting Eq. (*C*) in Eq. (*B*),

$$(k_G)_{NH_3} = (k_G)_{SO_2}\left(\frac{x_{SO_2}}{x_{NH_3}}\right)\frac{(D/T)_{NH_3}}{(D/T)_{SO_2}} = (k_G)_{SO_2}\left(\frac{D_{NH_3}}{D_{SO_2}}\right)^{0.56}\frac{(T)_{SO_2}}{(T)_{NH_3}} \qquad (D)$$

Values for the diffusivities may be determined from Eq. (31). Substituting in Eq. (*D*),

$$(k_G)_{NH_3} = 0.141\left(\frac{0.169}{0.114}\right)^{0.56}\left(\frac{528}{510}\right) = 0.182$$

$$\frac{1}{K_G} = \frac{1}{0.182} + \frac{1}{2.44} = 5.5 + 0.41 = 5.91$$

Therefore

$$(K_G)_{NH_3} = 0.17 \text{ lb. mol/(hr.) (sq. ft.) (atm.)}$$

NOTE: This result may be compared with the value of 0.206 for K_G for NH_3 absorption obtained from the experimental results of Haslam, Hershey, and Kean.[79] The data given on SO_2 are taken from the results of the same workers, and the assumption of equal gas- and liquid-film resistances is based on their data. The discrepancy between the estimated and experimental values of K_G for NH_3 is no doubt partly due to the uncertainty involved in the latter assumption.

It may be noted that the values of k_G are proportional to the 0.56 power of the diffusivities. This rule is derived from Gilliland's data for a wetted-wall column, and although it has not been confirmed for use in packed towers, it is probably the best basis for estimation of k_G for one gas from data on another.

PRINCIPAL TYPES OF ABSORPTION EQUIPMENT

Industrial apparatus for gas absorption may usually be classified as one of three quite different types, each having as a principal objective the promotion of interphase contact between gas and

liquid. Many varieties and combinations of these types exist or are possible, but only the major classifications will be described briefly. A fuller description of various commercial absorption towers will be found in a later chapter.

Spray towers consist of large empty chambers through which the gas passes and into which the solvent is introduced by means of a spray or sprays. The sprays are commonly placed at the top of a cylindrical tower, and the gas passed in at the bottom and up through the tower countercurrent to the spray. The spray serves to break up the solvent into a large number of small drops, providing a very great surface of contact between gas and liquid phase. The drops falling and spinning through the tower attain a fairly high velocity relative to the gas, and the gas-film resistance is relatively low. Within the drops, however, the liquid is stationary and movement of the solute is by true diffusion. The diffusional resistance on the liquid side of the interface is consequently large. This type of apparatus is clearly best suited for use in cases where the gas-film resistance is normally the controlling resistance. Spray towers are, in fact, commonly employed for the absorption of ammonia by water, and particularly for the humidification and dehumidification of air by water. In these latter examples there is no concentration gradient in the liquid, and consequently no liquid-film resistance.

Quite opposite in principle to the spray tower are the various bubble towers, of which numerous forms are used. In one of these, the gas is introduced into the liquid in the form of numerous fine bubbles, formed in passing the gas through a porous plate placed at the bottom of the receptacle for the liquid. The small bubbles present a very large surface of contact between the phases, and interphase diffusion takes place as the bubbles rise through the liquid. Here the conditions are the reverse of those in the spray tower. The liquid-film resistance is greatly reduced by the motion of the bubble upward, but the gas-film resistance is relatively great because of the lack of turbulent mixing within the bubble. For these reasons the various forms of bubble towers are particularly suitable in cases where the liquid-film resistance is normally controlling. Porous plates are used, for example, in the aeration of sewage, in which case the liquid film is normally the controlling resistance, owing to the very low solubility of air in water.

Various other types of bubble towers are in widespread use. These are commonly designed to reduce the pressure drop due to friction, although their effectiveness in promoting interphase contact may be somewhat impaired. The most common modification is the bubble-cap column, described in detail in a later chapter.

The third general type of absorption equipment is the packed tower. This consists of a tower or chamber packed loosely with any one of a large number of different types of "packing," over which the solvent is allowed to trickle or flow in thin films, without filling the intervening spaces between the lumps or pieces. With the packings ordinarily obtainable, the interfacial area per unit of volume is much less than can be provided by spray towers or porous-plate equipment, but since both gas and liquid phases are in violent turbulence, packed towers may be used where either gas or liquid film is the controlling resistance.

OVER-ALL COEFFICIENT ON A VOLUME BASIS

The over-all coefficient K_G was defined by Eq. (76) to be the rate of interphase diffusion as mols per unit time per unit area per unit of driving force in terms of pressures. Although the wetted-wall column described in Chap. II had a definite interfacial surface area, the corresponding area in the case of the ordinary packed tower is difficult, if not impossible, to evaluate. It is usually possible to calculate the total surface of the dry packing, but this is somewhat greater than the interfacial area, because the solvent circulated tends to collect at the points of contact of the lumps of packing. For this reason it is convenient to introduce a new variable, a, which represents the interfacial area per unit of volume. Since both a and K_G depend principally on the nature of the packing, they may be combined as a product K_Ga, which represents the over-all capacity coefficient, on a volume basis, for any particular packing. Thus K_Ga represents the rate of interphase diffusion as mols per unit time per unit volume, per unit of driving force in terms of pressures. It is defined by the equation

$$N_AaV = K_GaV(p_G - p_e) = \text{mols of solute transferred per unit time} \quad (80)$$

where V represents the volume of packing. K_La is similarly defined by the equation

$$N_AaV = K_LaV(C_e - C_L) \tag{81}$$

as the rate of diffusion as mols per unit time per unit volume, per unit of driving force in terms of concentrations.

The capacity coefficients K_Ga and K_La are of fundamental importance in engineering-design calculations. For this reason these quantities will be defined and used in English units. Thus K_Ga will be expressed as pound mols per hour per cubic foot per atmosphere. K_La will be expressed as pound mols per hour per cubic foot per unit ΔC, where ΔC represents the over-all driving force as pound mols solute per cubic foot of solution. The same units will be employed in connection with the individual film coefficients on a volume basis, k_Ga and k_La.

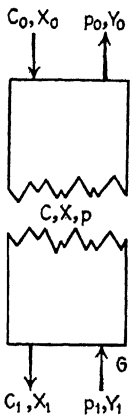

FIG. 16.—Diagrammatic sketch of countercurrent absorption tower.

GRAPHICAL DESIGN METHOD

In the application of the various rate equations to the conditions of a commercial absorption tower, it is necessary to allow for the fact that both gas and liquid concentrations may vary throughout the apparatus. Allowance for these variables is best made by the graphical method developed and described by Walker, Lewis, and McAdams.[188] The present treatment will follow these authors closely in method and nomenclature, but will employ partial pressures instead of stoichiometric units for gas concentrations, in an attempt to make the method somewhat less restricted in application, and less confusing for use with coefficients based on a driving force in partial pressures.

Consider any countercurrent absorption equipment, such as a packed tower, illustrated diagrammatically in Fig. 16. The absorbent enters at the top, containing L lb./hr. of solute-free liquid per square foot of tower cross section with X_0 lb. solute per pound of solvent. On a volume basis, the concentrations may be expressed as C_0 lb. mols solute per cubic foot of solution. In passing through the apparatus the solute concentration increases to X_1 or C_1. The gas to be treated enters at the bottom,

containing G lb./(hr.)(sq. ft.) of solute-free, or "inert" gas, and with a partial pressure of the solute gas of p_1 atm. At the top the partial pressure of the solute in the gas leaving has been reduced to p_0. If the pressure drop through the apparatus is assumed to be negligible in comparison with the total pressure P, we may write the over-all material balance

$$\frac{L}{M_A}(X_1 - X_0) = \frac{G}{M_B}\left[\frac{p_1}{P - p_1} - \frac{p_0}{P - p_0}\right] \tag{82}$$

Similarly, if the concentrations at any point in the apparatus are X and p, respectively, then

$$\frac{L}{M_A}(X_1 - X) = \frac{G}{M_B}\left[\frac{p_1}{P - p_1} - \frac{p}{P - p}\right] \tag{83}$$

If the concentrations and p_1 be fixed, and the ratio L/G known, then Eq. (83) specifies the relation between the variables X and p. If the relation between the concentration and density of the solution is known, the relation between X and C may be obtained readily. Equation (83) is based on a material balance only and involves no assumptions other than steady flow and constant conditions of the streams fed to the tower; consequently it may be relied upon as an expression for the relation between gas and liquid concentrations at any point in the apparatus.

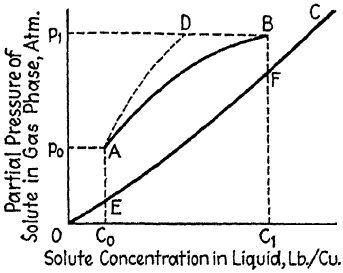

FIG. 17.—Operating lines (AB, AD) and equilibrium curve (OC) for countercurrent absorption tower.

Figure 17, curve AB, represents a typical relation between p and C. The point B represents the conditions at the gas inlet where both gas and liquid concentrations are high. The point A represents the conditions at the gas outlet, the partial pressure of solute in the gas having been reduced from p_1 to p_0. The curve AB, expressing graphically the relation between p and C, is termed the "operating line." On the same figure is shown a representative equilibrium curve OC, indicating the relation between the concentration of solute in the liquid, and the partial pressure of the solute in the gas phase in equilibrium with it.

Although the equilibrium curve may be any one of a number of shapes, the curve shown slightly concave upward is typical of the equilibrium relation for various common systems. For absorption to take place the solute concentration in the gas must be greater than in the liquid, *i.e.*, the operating line must lie above the equilibrium curve. For the reverse operation of "stripping," the operating line will lie below the equilibrium curve.

Gas-film Resistance Controlling.—In many cases the gas absorbed is highly soluble in the absorbent and the liquid-film resistance may be assumed to be negligible in comparison with the resistance of the gas film. Under such conditions the concentration drop across the liquid film may be said to be negligible. The partial pressure of the solute at the gas-liquid interface may thus be taken as the equilibrium pressure corresponding to the main body of the solution. The driving force across the gas film is obtained, therefore, as the difference between the pressures read from the operating and equilibrium curves, respectively, at any concentration C in the main body of the liquid. Similarly, the mean inert gas pressure p_{BM} at any point becomes the mean of $P - p$ and $P - p_e$, where p is the partial pressure of solute in the gas phase, and p_e is the equilibrium pressure over the solution.

The material balance leading to Eq. (83) and to the "operating line" provides the relation between p and C necessary for the integration of the diffusion equations. For the case of gas-film-resistance controlling, the rate of absorption, obtained by differentiating Eq. (83), is equated to the rate of diffusion as given by Eq. (13):

$$\frac{L}{M_A}\,dX \qquad \frac{}{M_B(P-p)^2}\,dp = \frac{ka}{x}\ln \qquad dh$$

In this equation dh is the differential tower height (volume per square foot of tower cross section), a the interphase surface per unit volume, and p_{B2} and p_{B1} are the inert gas pressures at the film boundaries. The latter are easily obtained from the known total pressure P and the curves EF and AB, and the logarithm of their ratio expressed as a function of X. Thus

$$h = \int_0^h dh = L\int_{X_0}^{X_1} \frac{\dfrac{x}{M_A ka}\,dX}{\ln \dfrac{p_{B2}}{p_{B1}}} = \frac{GP}{M_B}\int_{p_0}^{p_1} \frac{\dfrac{x}{ka}\,dp}{(P-p)^2 \ln \dfrac{p_{B2}}{p_{B1}}} \qquad (85)$$

Although it is often possible to use a simplified form of this relation, as explained below, the general relation given above must be used in any case where the inert gas pressure varies appreciably from one end of the apparatus to the other. In some cases a large fraction of the total inlet gas is absorbed, and the effective film thickness x may vary considerably because of the reduced gas velocity. If the relation between x and $k_g a$ and gas velocity is known, x may be expressed in terms of p, and its variation allowed for in the integration of Eq. (85).

An alternative and equally general procedure to the use of Eq. (85) involves first plotting p_{BM} on the graph showing the operating line and equilibrium curve. From Eq. (16) and the material balance,

$$\frac{L}{M_A}\,dX = \frac{GP}{M_B(P-p)^2}\,dp = \frac{ka}{x}\,\frac{(p-p_e)}{p_{BM}}\,dh \qquad (86)$$

whence

$$h = \frac{GP}{M_B}\int_{p_0}^{p_1} \frac{x}{ka}\,\frac{p_{BM}}{(P-p)^2(p-p_e)}\,dp = \frac{L}{M_A}\int_{X_0}^{X_1} \frac{x}{ka}\,\frac{p_{BM}}{(p-p_e)}\,dX \qquad (87)$$

Of the various alternative procedures, the preliminary calculation of the relation between ka/x and p_{BM} and X, and the graphical integration of Eq. (87), is perhaps the simplest.

The over-all capacity coefficient ka/x is defined by

$$\frac{ka}{x} = k_G a p_{BM} \qquad (88)$$

In the analysis of test data on absorption towers, $k_G a$ should be obtained by graphical integration. An approximate value may be obtained, however, by using the mean of the values of p_{BM} for the two ends of the apparatus.

Illustration 9.—An NH_3-air mixture containing 2.0 per cent NH_3 at 68°F. and 1 atm. is to be scrubbed with water in a tower packed with 1 to 2 in. quartz. The water rate will be 240 lb./(hr.)(sq. ft.), and the gas rate 240 lb./(hr.)(sq. ft.) at the gas inlet. Assume the tower temperature to remain constant at 68°F. At this temperature the partial pressure of NH_3 over aqueous ammonia solutions is as follows:

p, mm	12.0	18.2	31.7	50.0	69.6	166
C, g. NH_3 per 100 g. water	2.0	3.0	5.0	7.5	10	20

For the above packing, $K_G a$ is obtained from Chap. VI as 9.6 lb. mols/(hr.)(cu. ft.)(atm.).

Note that for absorption of dilute gases in systems obeying Henry's law, the logarithmic mean driving force should be used (see below).

a. Estimate the required height for the absorption of 98 per cent of the NH_3 in the entering gas.

b. If a 2 per cent mixture of acetone in air were passed through the tower designed for NH_3 in (*a*) under the same conditions of temperature, pressure, gas rate, and liquid rate, what percentage of the acetone would be absorbed? At 68°F., the equilibrium relation for aqueous solutions of acetone is as follows:

Mol per cent acetone	3.33	7.20	11.7	17.1
p.p. acetone, mm	30.0	62.8	85.4	103

Solution a.

$$p_1 = 0.02 \times 760 = 15.2 \text{ mm. in gas entering}$$

$$p_0 = \frac{0.02 \times 2}{98.04} \times 760 = 0.31 \text{ mm. in gas leaving}$$

$$Y_1 = \frac{2}{98} \times \frac{17}{29} = 0.012 \text{ lb. } NH_3\text{/lb. air entering}$$

$$Y_0 = 0.02 \times 0.012 = 0.00024 \text{ lb. } NH_3\text{/lb. air leaving}$$

$$NH_3 \text{ absorbed/(hr.)(sq. ft.)} = 240 \times \frac{0.012}{1.012} \times 0.98 = 2.79 \text{ lb.}$$

$$= 0.164 \text{ lb. mols/(hr.)(sq. ft. cross section)}$$

$$\text{Lb. } NH_3 \text{ per 100 lb. water leaving} = \frac{2.79 \times 100}{240} = 1.16.$$

$$p_{e1} = 1.16 \times \frac{12}{2} = 6.96 \text{ mm.} \qquad p_{e0} = 0 \text{ mm.}$$

$$\Delta p_1 = (15.2 - 6.96) = 8.24 \text{ mm.}; \qquad \Delta p_0 = (0.31 - 0) = 0.31 \text{ mm.}$$

$$\Delta p_{av} = \frac{8.24 - 0.31}{\ln \frac{8.24}{0.31}} = 2.42 \text{ mm. (log mean approximation)}$$

$$h = \frac{0.164 \times 760}{9.6 \times 2.42} = 5.4 \text{ ft.}$$

Solution b.—First it is necessary to predict a value of $K_G a$ for acetone from that of NH_3 by the method of Illustration 8.

$$D_{ac.} = \frac{0.0043 \times (293)^{\frac{3}{2}}}{(76.5^{\frac{1}{3}} + 29.9^{\frac{1}{3}})^2} \sqrt{\frac{1}{58} + \frac{1}{29}} = 0.0924 \text{ cm.}^2\text{/sec.}$$

$$D_{NH_3} = \frac{0.0043 \times (293)^{\frac{3}{2}}}{(26.7^{\frac{1}{3}} + 29.9^{\frac{1}{3}})^2} \sqrt{\frac{1}{17} + \frac{1}{29}} = 0.181 \text{ cm.}^2\text{/sec.}$$

$$(K_G a)_{ac.} = (K_G a)_{NH_3} \left[\frac{(D)_{ac.}}{(D)_{NH_3}}\right]^{0.56} = 9.6 \times \left(\frac{0.0924}{0.181}\right)^{0.56}$$

$$= 6.6 \text{ lb. mols/(hr.)(cu. ft.)(atm.).}$$

$$p_1 = 0.02 \times 760 = 15.2 \text{ mm.}$$

$$Y_1 = \frac{2}{98} \times \frac{58}{29} = 0.0408 \text{ lb. acetone/lb. air entering.}$$

$$Y_0 = \frac{p_0}{760 - p_0} \frac{58}{29} = \frac{2p_0}{(760 - p_0)}$$

Let acetone absorbed = W lb. mols/(hr.)(sq. ft.)

$$W = \frac{240}{58 \times 1.0408}\left(0.0408 - \frac{2p_0}{760 - p_0}\right) = 0.162 - \frac{7.93p_0}{760 - p_0} \qquad (A)$$

$$p_{e1} = \frac{W \times 100}{\left(W + \frac{240}{18}\right)} \times \frac{30}{3.33} = \frac{900W}{W + 13.3} \qquad (B)$$

$$\text{Height} = \frac{W \times 760}{6.6(p - p_e)_{l.m.}} = 5.4 \text{ ft.} \qquad \frac{W}{(p - p_e)_{l.m.}} = 0.0468 \qquad (C)$$

Solving by trial and error Eqs. (A), (B) and (C)

p_0 mm.	W	p_{e1}, mm.	Δp_1, mm.	Δp_0, mm.	$\Delta p_{l.m.}$, mm.	$W/\Delta p_{l.m.}$
5.0	0.109	7.34	7.86	5.0	6.35	0.0172
2.0	0.141	9.45	5.75	2.0	3.56	0.0397
1.5	0.146	9.78	5.42	1.5	3.06	0.0476
1.58	0.1455	9.73	5.47	1.58	3.13	0.0466

$$Y_0 = \frac{58}{29} \frac{p_0}{(760 - p_0)} = \frac{2 \times 1.58}{760 - 1.58} = 0.00417 \text{ lb. acetone/lb. air leaving.}$$

$$\text{Absorption} = \left[1 - \frac{0.00417}{0.0408}\right] \times 100 = 89.8 \text{ per cent}$$

Liquid-film Resistance Controlling.—Under conditions such that the liquid film offers the principal resistance to diffusion, the liquid at the interface may be assumed to be in equilibrium with the main body of the gas. The driving force, therefore, is the difference between the concentrations C_e and C, obtained from the equilibrium and operating lines, respectively, at any partial pressure p in the main body of the gas.

Combining the material balance with the diffusion equation (72), there results

$$\frac{L\,dX}{M_A} = \frac{D_L a(C_A + C_B)(C_e - C)}{x_L C_{BM}}\,dh = k_L a(C_e - C)\,dh \qquad (89)$$

whence,

$$h = \frac{L}{M_A}\int_{X_0}^{X_1} \frac{x_L C_{BM}}{D_L a(C_A + C_B)(C_e - C)}\,dX \qquad (90)$$

After constructing the operating and equilibrium curves, it is not difficult to evaluate the terms under the integral sign and carry out the integration graphically. The capacity coefficient $D_L a/x_L$ is related to the liquid film coefficient k_L by the equation

$$\frac{D_L a}{x_L} = \frac{C_{BM}}{(C_A + C_B)} k_L a \tag{91}$$

Simplified Procedure for Lean Gas Mixtures.—The general procedure described above may be simplified considerably for cases where the following conditions hold:

a. The mean partial pressure of the inert carrier gas (p_{BM}) remains essentially constant throughout the apparatus.

b. The capacity coefficient $k_G a$ and $k_L a$ remain constant throughout the apparatus.

c. The solute content of the gas and liquid phases are sufficiently low so that the partial pressure p may be taken as proportional to the concentration Y expressed in stoichiometric units (weight of solute per unit weight inert carrier gas), and the concentration C may be taken as proportional to the concentration X in stoichiometric units.

In stoichiometric units the material balance may be written

$$L(X_1 - X) = \qquad - Y) \tag{92}$$

Since this relation assumes only steady flow and constant feed strength of gas and liquid, it must hold whatever the mechanism of the diffusion may be for any tower construction or type of steady operation. Figure 18 shows the "operating line" AB representing this relation between X and Y as given by this equation. Point B represents the conditions at the gas inlet and liquid outlet, where the concentrations are Y_1 and X_1; point A represents the corresponding conditions at the gas outlet, where the concentrations are Y_0 and X_0. Since Eq. (92) is linear, only inlet and outlet concentrations are necessary to place this "operating line," representing the relation between gas and liquid concentrations throughout the apparatus.

Equilibrium data for the system may be converted into stoichiometric units and plotted on the same diagram as the operating line, as indicated by the curve OC of Fig. 18. As explained above, the operating line must be above the equilibrium curve if absorption is to take place, but for the reverse operation of

stripping, the operating line will be below the equilibrium curve. Where the gas film is controlling, the difference in concentration between gas and liquid phase, and consequently the driving force causing diffusion, is represented by the vertical distance between the curves AB and EF. The rate equation may be written

$$L\,dX = G\,dY = M_A \alpha K_G a (Y - Y_e)\,dh \tag{93}$$

in which Y and Y_e are the concentrations in the gas phase and in equilibrium with the liquid, respectively. Since the capacity coefficient $K_G a$ is expressed in terms of partial pressures, the difference $(Y - Y_e)$ is multiplied by the factor α to convert to

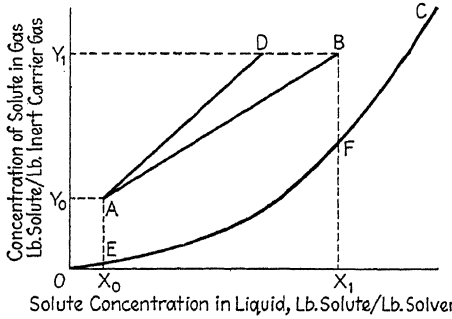

FIG. 18.—Graphical construction using stoichiometric units.

$(p - p_e)$. Since Y is not strictly proportional to p, an average value of α is used, based on the calculated values of α for the concentrations at the two ends of the apparatus. If the specified conditions of low gas concentrations actually exist, then these values of α will not be far apart, and an arithmetic mean value may be used. It is usually more convenient to integrate the rate equation with respect to X rather than Y, using the relation

$$h = \frac{L}{\alpha_{AV} K_G a M_A} \int_{X_0}^{X_1} \frac{dX}{(Y - Y_e)} \tag{94}$$

The integration is easy to perform graphically, first plotting $\left(\frac{1}{Y - Y_e}\right)$ *vs.* X, and measuring the area under the curve between the limits X_0 and X_1.

In case the liquid-film resistance is controlling, the driving force is represented by the horizontal distance between the operating

and equilibrium curves, since the equilibrium curve gives the interface concentration corresponding to any gas concentration Y. The integration may then be carried out as indicated by the equation

$$h = \frac{L}{\beta_{AV} K_L a M_A} \int_{X_0}^{X_1} \frac{dX}{X_e - X} \tag{95}$$

Because of the use of stoichiometric units for liquid concentration, the factor β is introduced to convert $(X_e - X)$ to $(C_e - C)$. For dilute solutions, an average value may be employed, as explained in the case of the factor α.

Illustration 10.—Repeat the calculation of the tower height required in Illustration 9 (*a*), using the simplified procedure for lean gas mixtures.

Solution.—Basis: 1 sq. ft. cross-sectional area of the tower.

$$Y_1 = \frac{2}{98} \times \frac{17}{29} = 0.012 \text{ lb. } NH_3\text{/lb. air}$$

$$Y_0 = 0.012 \times 0.02 = 0.00024 \text{ lb. } NH_3\text{/lb. air}$$

$$NH_3 \text{ absorbed} = 240 \times \frac{0.012}{1.012} \times 0.98 = 2.79 \text{ lb./hr.}$$

$$X_1 = \frac{2.79}{240} = 0.0116 \text{ lb. } NH_3\text{/lb. water}$$

$$X_0 = 0 \text{ lb. } NH_3\text{/lb. water}$$

$$p_1 = 0.02 \times 760 = 15.2 \text{ mm. in entering gas}$$

$$p_0 = \frac{0.02 \times 2}{98.04} \times 760 = 0.31 \text{ mm. in leaving gas}$$

$$p_{e1} = 6.96 \text{ mm.} \qquad Y_{e1} = \frac{6.96}{753} \times \frac{17}{29} = 0.00545 \text{ lb. } NH_3\text{/lb. air}$$

$$\Delta p = \alpha \Delta Y$$

Therefore

$$\left.\begin{aligned} \alpha_1 &= \frac{\Delta p_1}{\Delta Y_1} = \frac{15.2 - 6.96}{(0.012 - 0.00545) \times 760} = 1.64 \\ \alpha_0 &= \frac{\Delta p_0}{\Delta Y_0} = \frac{0.31}{(0.00024) \times 760} = 1.70 \end{aligned}\right\} \alpha_{Av.} = 1.67$$

From equilibrium data it is seen that Henry's law holds approximately through the range of concentrations encountered in this problem.

Therefore

$$p \quad \cdots \quad \cdots \quad C$$

$$H \qquad 100\frac{p}{\quad} = \frac{12 \times 100}{760 \times 2} = 0.79 \qquad p = 0.79X$$

Therefore

but $p = \alpha Y = 1.67Y$

$$1.67Y_e = 0.79X \qquad \text{and} \qquad X = 2.11Y_e$$

From a material balance,

$$L(X - X_0) = G(Y - Y_0)$$

$$Y = \frac{L}{G}(X - X_0) + Y_0 \qquad (A)$$

$$\frac{L}{G} = \frac{240}{240 \times \frac{1}{1.012}} = 1.012 \text{ lb. water/lb. air.}$$

Substituting in Eq. (*A*)

$$Y = 1.012X + 0.00024$$

Substituting in Eq. (94),

$$h = \frac{L}{K_G a M_A}\int_{X_0}^{X_1}\frac{dX}{(Y - Y_e)} = \frac{L}{\alpha_{Av.} K_G a M_A}\int_0^{0.0116}\frac{dX}{1.012X + 0.00024 - \left(\frac{X}{2.11}\right)}$$

$$= \frac{240}{1.67 \times 9.6 \times 17 \times 0.538} \ln \frac{0.0116 + 0.000446}{0.000446} = 5.4 \text{ ft.}$$

The solution outlined above is lengthened by the inclusion of the actual integration. The assumption of a logarithmic mean ΔY would have shortened the procedure considerably, and given the same result.

Limiting Gas and Liquid Rates.—It is evident from Eq. (92) that the slope of the operating line of Fig. 18 is L/G. It is also apparent from the figure that large values of L/G correspond to steep operating lines and to large values of the driving force, $X_e - X$ or $Y - Y_e$. The gas and liquid velocities consequently have a profound effect on the required size of the apparatus, quite apart from the effect on the capacity coefficients $K_G a$ and $K_L a$. The lines AD and AB of Figs. 17 and 18 represent the conditions in two absorbers operating over the same range of gas compositions, but with different ratios of liquid to gas rates. AD is further from the equilibrium curve, and the apparatus need not be so large to absorb the same weight of solute. As the ratio L/G is decreased, the operating line approaches the equilibrium curve and the driving force causing diffusion decreases. Actual touching of operating and equilibrium curves would represent equilibrium at that point in the apparatus; this would be impossible in an actual apparatus of finite length, except for special conditions which are discussed in Chap. IV. There is consequently a minimum value of the ratio L/G, below which the absorber could not operate, no matter how large it might be. For a fixed gas capacity, the liquid rate corresponding to this minimum value of L/G is termed the minimum liquid rate, and

may be used as a basis in deciding on a practical liquid rate to be used. The maximum gas and liquid rates are fixed by the tendency toward entrainment or carry-over. The latter phenomenon will be discussed in a later section.

Illustration 11.—Two hundred cubic feet per minute of an air-SO_2 mixture containing 10 per cent SO_2 by volume at 68°F. and 1 atm. are to be scrubbed with water in a countercurrent packed tower for the purpose of recovering 95 per cent of the SO_2. Cooling coils will be installed in the tower to maintain the liquor temperature constant at 68°F. Determine the minimum water rate at which the tower would operate as planned, assuming that there is no limitation on the height of packing available. Vapor pressure of SO_2 over aqueous SO_2 solution at 68°F.:

Conc., g. SO_2 per 100 g. water	0.5	1.0	2.0	3.0	5.0	10.0
p.p. SO_2, mm. Hg	26	59	123	191	336	698

Solution.

$$p_1 = 0.10 \times 760 = 76 \text{ mm.}$$

$$SO_2 \text{ absorbed} = \frac{200}{250} \times \frac{273}{292} \times 64 \times 60 \times 0.10 \times 0.95 = 190 \text{ lb./hr.}$$

By interpolation, the concentration of an aqueous SO_2 solution which has a partial pressure of SO_2 of 76 mm. is

$$1.27 \text{ lb. } SO_2/100 \text{ lb. water}$$

Therefore

$$\text{Minimum water rate} = \frac{190}{1.27} \times 100 = 15{,}000 \text{ lb./hr.}$$

Logarithmic Mean Driving Force.—Although the graphical procedure outlined above must be employed in many practical design problems, it is frequently possible to use a simple mean driving force or potential and so obviate the graphical integration. Where it is possible to assume that the equilibrium curve is linear over the range in which it is to be used, it can be shown that the logarithmic mean of the terminal potentials is theoretically correct. When the gas-film resistance is controlling the calculation then reduces to the solution of the equation

$$L(X_1 - X_0) = G(Y_1 - Y_0) = M_A \alpha_{Av.} K_G a h (Y - Y_e)_{Av.} \quad (96)$$

$$(Y - Y_e)_{Av.} = \frac{(Y - Y_e)_1 - (Y - Y_e)_0}{\ln \dfrac{(Y - Y_e)_1}{(Y - Y_e)_0}} \quad (97)$$

A proof of this relation is outlined below:

Assume that between X_0 and X_1 the equilibrium curve may be represented by the equation

$$Y_e = mX + n \quad (98)$$

Combining Eqs. (92), (93), and (98) there results

$$\frac{dY}{Y - Y_e} = \frac{dY}{Y - \frac{mG}{L}(Y - Y_0) - mX_0 - n} = \frac{G}{\left(1 - m\frac{G}{L}\right)(Y_1 - Y_0)\frac{M_A\alpha_{Av.}K_Gah}{\ln\frac{(Y - Y_e)_1}{(Y - Y_e)_0}}} = G(Y_1 - Y_0) \quad (99)$$

From the assumed relation (98), and the over-all material balance, it follows that

$$\left(1 - m\frac{G}{L}\right)(Y_1 - Y_0) = (Y - Y_e)_1 - (Y - Y_e)_0 \quad (100)$$

whence

$$G(Y_1 - Y_0) = L(X_1 - X_0) = M_A\alpha_{Av.}K_Gah\frac{(Y - Y_e)_1 - (Y - Y_e)_0}{\ln\frac{(Y - Y_e)_1}{(Y - Y_e)_0}} = M_A\alpha_{Av.}K_Gah(Y - Y_e)_{Av.} \quad (101)$$

A similar procedure may be followed to show that with liquid film controlling

$$G(Y_1 - Y_0) = L(X_1 - X_0) = \beta_{Av.}K_Lah(X_e - X)_{Av.} \quad (102)$$

where

$$(X_e - X)_{Av.} = \frac{(X_e - X)_1 - (X_e - X)_0}{\ln\frac{(X_e - X)_1}{(X_e - X)_0}} \quad (103)$$

It may be noted that with gas film controlling it is necessary that the equilibrium curve be linear between X_0 and X_1 if the logarithmic mean is to be used. With liquid film controlling, the logarithmic mean applies if the equilibrium curve is linear over the range Y_0 to Y_1.

Allowance for Resistance of Both Gas and Liquid Films.—In the absorption of sulfur dioxide in water, and in many other important cases, the resistances of both gas and liquid films must be allowed for. The graphical design method may be modified for this purpose if the individual film coefficients k_G and k_L are known.

Rewriting Eq. (73) in terms of stoichiometric units,

$$N_A = \alpha k_G(Y - Y_e) = \beta k_L(X_e - X) \quad (104)$$

from which it follows that the ratio of the potential $(Y - Y_e)$ across the gas film to the potential $(X_e - X)$ across the liquid film is equal to $\beta k_L/\alpha k_G$. Figure 19 shows operating and equilib-

rium curves similar to those of Fig. 18, with a point C representing conditions at any point in the apparatus. The conditions at the interface corresponding to the point C are represented by some point E, showing the liquid concentration to be less than the equilibrium concentration corresponding to the composition of the main body of the gas, and the gas concentration to be greater than the equilibrium concentration corresponding to the main body of the liquid. The driving force or potential across the gas film is represented by the line HE, and the liquid-film potential by GE. Since HE/GE is equal to $\beta k_L/\alpha k_G$, it follows that the point E may be located by drawing a line through

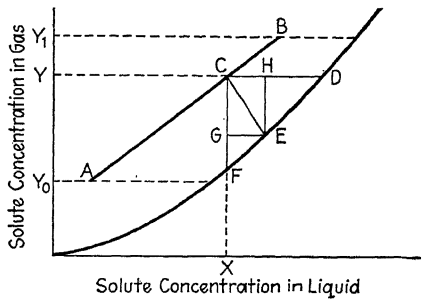

FIG. 19.—Graphical construction to allow for resistances of both gas and liquid films.

C with a negative slope of $\beta k_L/\alpha k_G$. The point E is obtained at the intersection of this line with the equilibrium curve. The graphical integration to obtain the tower height may then be carried out using the potentials HE or GE in place of $(Y - Y_e)$ or $(X_e - X)$, and the individual coefficients $\alpha_{Av}.k_G$ or $\beta_{Av}.k_L$ in place of $\alpha_{Av}.K_G$ or $\beta_{Av}.K_L$, in Eqs. (94) and (95). Allowance for variation of α or β with Y or X may be made in constructing the various lines corresponding to CE, and the integration performed in terms of $\alpha(Y - Y_e)$ or $\beta(X_e - X)$.

The method outlined above of allowing for both gas- and liquid-film resistances is somewhat limited in practical application because of the necessity of knowing the individual film coefficients k_G and k_L. Unfortunately, most experimental data are available only in the form of over-all coefficients, from which it is difficult, if not impossible, to deduce the individual film coefficients. In applying the method described to the analysis of an

experimental test of an absorption tower, the ratio of film resistances is not ordinarily known, and the lines CE cannot be drawn to locate the interface conditions. If several tests are made under varying operating conditions, it is sometimes possible to evaluate k_L and k_G by a method described in a later section.

RESTRICTIONS ON THE USE OF OVER-ALL COEFFICIENTS

In the case where both gas- and liquid-film resistances are of importance, illustrated by Fig. 19, the potential across the gas film is represented by the line HE or CG. The over-all potential from gas to liquid is represented by CF, which bears a constant relation to CG as long as the equilibrium curve is straight over the range in which it is used. Where this constant proportionality between CG and CF exists, the over-all coefficient $\alpha K_G a$ may be used in Eq. (94) with the over-all potential CF. Alternatively, the over-all coefficient $\beta K_L a$ may be used in Eq. (95) with the over-all potential CD, subject to the same restriction. It follows that the operating data may be expressed in terms of over-all coefficients, even though both gas- and liquid-film resistances are involved, provided the equilibrium curve is straight over the range of concentrations encountered. This restriction does not apply to the use of over-all coefficients at any single point in the apparatus, but only to the use of such coefficients for the tower as a whole.

CONCEPT OF THE THEORETICAL PLATE

Both packed towers and plate columns may be used for gas absorption, just as both types of equipment are found serviceable in distillation practice. Rectifying columns for distillation are more often of the plate than the packed type, however, and the traditional basis for the design of such equipment is the "theoretical plate." Also, absorption equipment is commonly of the packed-tower type, and the design of such towers is usually based on capacity coefficients such as $K_G a$ or $K_L a$. Just as the equipment is interchangeable in practice so the design methods for the two processes may be interchanged and the "theoretical plate" used as the basis for absorption-tower design, or capacity coefficients used in rectifying-column design.

The design procedure based on the theoretical plate concept may be followed by referring to Fig. 20. The use of stoichio-

metric units will be continued, although the method may be modified for rich gases, as explained above for use with capacity coefficients.

The horizontal lines *AA*, *BB*, etc., represent bubble-cap or other plates, the solvent overflowing from one plate to the next down through the column. The gas to be treated, containing *G* lb./hr. of inert carrier gas, passes up through the column, countercurrent to the flow of solvent, being brought into intimate contact with the solvent by bubble caps or other devices on each plate. In a theoretically perfect plate the contact between phases will be sufficiently good to bring the two streams into equilibrium. The gas leaving plate *CC* therefore will be in equilibrium with the liquid leaving the same plate. For a column of theoretical plates, therefore, it is possible to represent the relation between gas and liquid compositions leaving any plate by the equilibrium curve for the system. The relation between the gas and liquid compositions between any two plates, *i.e.*, the relation between the composition Y_c of the gas leaving *CC* and the composition X_B of the liquid leaving *BB*, is given by the material balance

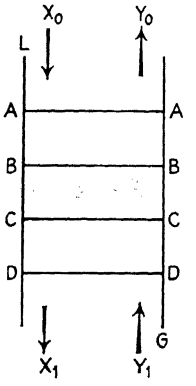

FIG. 20.—Diagrammatic sketch of plate column.

$$G(Y_1 - Y_c) = L(X_1 - X_B) \qquad (105)$$

Figure 21 shows a diagram for this case, with the operating line *AB*, and the equilibrium curve *OD*. It should be noted that the operating line now gives the relation between the composition of *gas leaving* a plate and the composition of *liquid from the plate next above*. The vapor leaving any plate *CC* will be in equilibrium with the concentration X_c of the liquid on the plate, and its composition Y_c will be determined by referring to the point *c* on the equilibrium curve. The liquid leaving the plate *BB* next above will have a composition determined by the point *b'* on the operating line, corresponding to the gas composition Y_c. The composition of the gas leaving *BB* may then be determined, and the equilibrium curves and operating line used alternately until the point *A* is reached, corresponding to conditions at the top of the column. With any fixed operating line, this step-

wise calculation may be employed to determine the compositions of liquid and gas on the various plates and, what is more important, the number of theoretical plates required.

It is obvious that, when the operating line lies close to the equilibrium curve, a large number of plates will be required. If the two curves touch, the staircase construction will indicate an infinite number of plates, because equilibrium cannot be reached in any finite flow apparatus.

Although the graphical method just described is of general applicability, it may be replaced by an algebraic procedure due

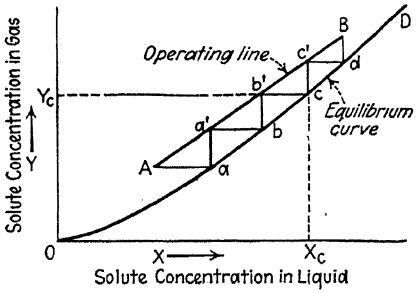

FIG. 21.—Graphical design method of theoretical plates.

to Kremser,[112] in those cases where solute concentrations in gas and liquid are low, and where the equilibrium curve is straight.

The material balance, as applied to the nth plate from the top of a plate column may be written

$$L(X_n - X_{n-1}) = G(Y_{n+1} - Y_n) \tag{106}$$

Assuming the equilibrium to be expressed by the linear relation

$$Y_n = mX_n \tag{107}$$

Kremser has derived an expression relating the compositions Y_1 and Y_0 of the gas entering and leaving the apparatus to the number of plates n. This has been modified by Souders and Brown,[175] who express the result in the form

$$\frac{Y_1 - Y_o}{Y_1 - mX_o} = \frac{\left(\frac{L}{mG}\right)^{n+1} - \left(\frac{L}{mG}\right)}{\left(\frac{L}{mG}\right)^{n+1} - 1} \tag{108}$$

The left-hand side represents the ratio of the actual change in gas composition in the column of n plates, to the change in composition which would occur if the gas leaving were in equilibrium with the solvent entering at the top. Figure 22 shows the relation plotted, with the ratio on the left as ordinate, and the ratio L/mG as abscissa, with several curves for various numbers of plates. This plot brings out clearly the relation between the amount absorbed, the number of theoretical plates, and the "absorption factor" L/mG. It is apparent that a high recovery may be obtained either by the use of a large number of plates or by employing a large value of the ratio L/mG. Since m is

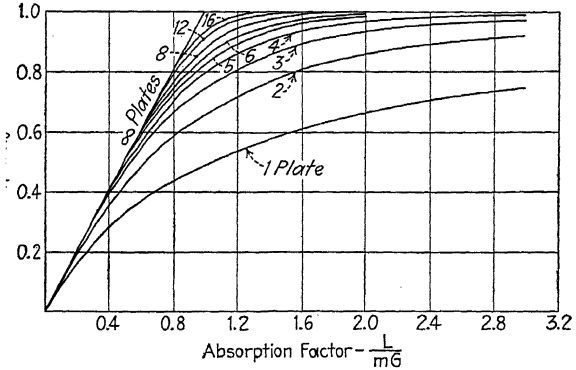

FIG. 22.—Relation between column performance and number of theoretical plates [Eq. (108)].

fixed for any given system and temperature, the "absorption factor" is proportional to the ratio of solvent to inert gas, L/G. The plot also shows that if L/G is less than m (L/mG less than unity), the absorption is definitely limited no matter how many plates may be used. This is also apparent from Fig. 21, where it is clear that if the slope of the operating line were less than the slope of the equilibrium curve, the point A could not touch the equilibrium curve, since the operating line would then be below the equilibrium curve.

Equation (108) and Fig. 22 are particularly useful in trial computations in the design of multicomponent absorbers, as outlined in the next chapter. They may be used in calculations on single solute systems where the relation $Y = mX$ approximates the true equilibrium curve. The straight line on Fig. 22

for an infinite number of plates may be used in determining the minimum "absorption factor," and so the minimum ratio L/G of solvent to gas for a given desired solute recovery. This minimum value of L/G is a useful basis for a decision as to the actual values of L and G to be used.

It may be noted that Eq. (108) is equally valid if X and Y are defined as mol fractions of solute in liquid and gas, and L and G as total mols of liquid and gas, respectively, including solute. Because absorption takes place, the total mols of both liquid and gas varies, and L/G varies from one end of the apparatus to the other.

Plate Efficiency.—The number of plates required in an actual absorber is usually greater than the number of theoretical plates indicated by the method of calculation just outlined. Various types of "plate efficiencies" have been defined, of which the simplest is an over-all efficiency equal to the ratio of the number of theoretical to the number of actual plates required. Few data are available on the efficiencies of bubble-cap columns used in gas absorption (see page 191), although considerable data on such plates used in distillation indicate efficiencies of 65 to 95 per cent and higher. In other words, the number of theoretical plates must be multiplied by 1.0 to 1.5 to obtain the actual number of plates required. The efficiency will obviously vary with the type of construction, increasing with the intimacy of contact between phases on the plate. Any construction which breaks the gas stream up into small bubbles in passing through the liquid will give high plate efficiencies. Considerable interphase reaction doubtless occurs in the spray occasioned by the splashing of the liquid above the plate. The liquid on the plates may be maintained at any level, but the depth at which the bubbles are released is a factor of secondary importance in determining plate efficiency. Data are available which indicate that most of the interphase diffusion takes place as the bubble is formed, and before its release, and that but little increase in efficiency is obtainable by increasing the liquid head on the plates. The liquid levels are consequently maintained at only 1 to 3 in., in order to minimize the pressure drop of the gas passing through the column.

The efficiency concept may be applied to each individual plate with a somewhat different result than the use of the over-all plate efficiency. Thus Murphree[147] has defined the efficiency as

the ratio of the change in gas composition on the plate to the change in composition corresponding to attainment of equilibrium. This ratio may be expressed as $\frac{Y_B - Y_C}{Y_{Be} - Y_C}$, where $Y_B - Y_C$ represents the actual change in gas concentration across plate *BB*, and Y_{Be} is the gas composition in equilibrium with X_B of the liquid *leaving* the plate. If the efficiency on this basis is known, the stepwise procedure may be followed as before, but reducing the length of the vertical steps, *aa'*, *bb'*, etc., to correspond to the actual efficiency. It may be seen from the diagram (Fig. 21) that if the Murphree efficiency is constant throughout the apparatus and if the equilibrium curve is parallel to the operating line over the range involved, then the Murphree and over-all efficiencies will be the same.

The Murphree efficiency for absorption may be expressed in terms of partial pressures in place of stoichiometric units, and should be so used when operating and equilibrium curves are plotted as partial pressure *vs.* liquid compositions. If liquid film is known to be controlling, the efficiency represents the fractional approach to equilibrium on the basis of the liquor analyses, and it is the horizontal lengths *a'b*, *b'c*, etc., which are reduced to correspond to the actual efficiency.

In the usual plate construction it is common for the liquid to flow from one side to the other before overflowing to the next plate below. The result is something in between a true countercurrent action and the assumed single contact, and it is possible for the average composition of the gas leaving the plate to be less rich than would correspond to equilibrium with the liquid leaving the plate at one side. Consequently it is possible, and not uncommon, for either the Murphree or the over-all plate efficiencies as defined above to be greater than 100 per cent. This point is discussed fully by W. K. Lewis, Jr.,[127] in relation to rectifying columns.

Illustration 12.—A 10-plate bubble-cap column is to be employed to recover acetone from an acetone-air mixture by absorption in water at 68°F. Fifty cubic feet per minute of gas enter at 68°F., containing 9.0 per cent acetone by volume, and it is desired to obtain a liquor containing 20.0 per cent acetone by weight. At 68°F., the equilibrium relation for aqueous solutions of acetone is as follows:

Mol per cent acetone	3.33	7.20	11.7	17.1
p.p. acetone, mm	30.0	62.8	85.4	103

Assuming isothermal operation at 68°F. and an over-all plate efficiency of 60 per cent, calculate the percentage recovery of acetone to be expected, if the tower is operated to obtain the desired liquor strength.

Solution a.—Let x = mol fraction acetone in water, then

$$X \quad \frac{x}{(1-x)}\frac{58}{18} = \frac{3.22x}{1-x} \text{ lb. acetone/lb. water.}$$

$$Y \quad \frac{p}{(760-p)}\frac{58}{29} = \frac{2p}{(760-p)} \text{ lb. acetone/lb. air.}$$

Using these conversion factors, the equilibrium data are plotted as Y *vs.* X, as shown on Fig. 23.

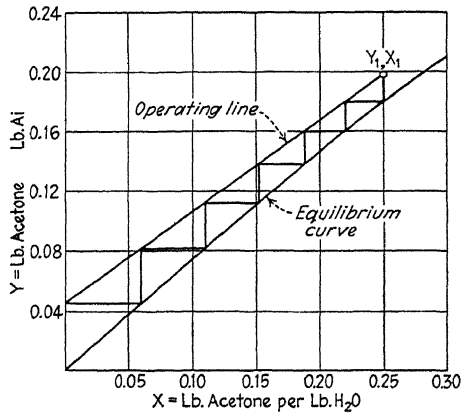

FIG. 23.—Graphical construction for Illustration 12.

Data for operating line:

$$Y_1 = \frac{0.09 \times 58}{0.91 \times 29} = 0.198 \text{ lb. acetone/lb. air.}$$

$$\frac{20}{80} = 0.250 \text{ lb. acetone/lb. water.}$$

Ten actual plates are equivalent to $10 \times 0.60 = 6$ perfect plates. Since the above data locate the upper end of the operating line and all of the equilibrium curve, and the column must have six perfect plates, the conditions at the top of the column, corresponding to the left end of the equilibrium curve, may be determined. It is known that $X_o = 0$, so that the slope of the operating line may be determined by trial and error, such that six perfect plates may be drawn in between the operating line and equilibrium curve.

From the plot (Fig. 23), $Y_o = 0.045$ lb. acetone/lb. air.

$$\text{Recovery of acetone} = \frac{0.198 - 0.045}{0.198} \times 100 = 77.3 \text{ per cent.}$$

Solution b.—The problem may also be solved by the use of Eq. (108) and an average value of the slope m, although a trial-and-error calculation is involved since L/G is not known.

Since the solvent is water containing no acetone, X_o is zero. The left-hand side of (108) represents the fraction recovery of acetone, which will be represented by E. Thus

$$E = \frac{\left(\frac{L}{mG}\right)^{7} - \frac{L}{mG}}{\left(\frac{L}{mG}\right)^{7} - 1} \qquad (A)$$

The value of m for the concentration range involved is calculated from the equilibrium data of Fig. 23 to be 0.72. By a material balance on acetone

$$E \times 0.198 \times G = 0.25L \qquad (B)$$

Solving the simultaneous equations (A) and (B),

$E = 0.79$; or acetone recovery = 79 per cent.

THE H.E.T.P.

In order to apply the theoretical plate concept to a packed tower, it is necessary to picture a certain height of packing as accomplishing the same separation as one theoretical plate. The *height of packing equivalent to one theoretical plate* has been termed by Peters[153] the "H.E.T.P." and its numerical value is an indication of the capacity of the apparatus, as are the capacity coefficients $K_G a$ and $K_L a$. It should be noted, however, that large values of $K_G a$ or $K_L a$ correspond to small values of H.E.T.P.

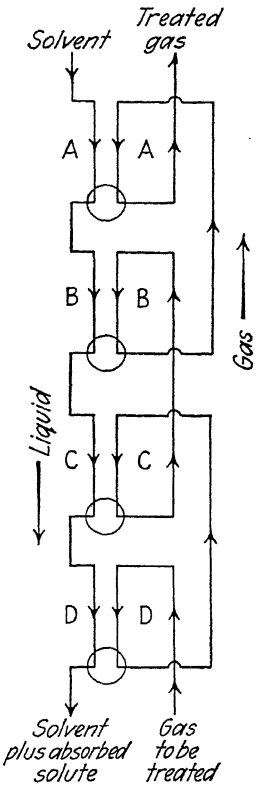

FIG. 24.—Diagrammatic sketch of the operation of a plate column with countercurrent flow of l[illegible] and gas.

Let Fig. 20 now represent a packed tower, and the packing between BB and CC perform the same separation as one theoretical plate. Let AB and CD represent other imaginary divisions of the column into theoretical plates. From the definition of a perfect plate, the gas leaving the section BC at BB will be in equilibrium with liquid leaving the same section at CC. Analysis of the process on the basis of the theoretical plate concept assumes the flow to be somewhat as pictured in Fig. 24. On each

plate the liquid from the plate above and the gas from the plate below come together, and are separated at the points circled, where the two streams are assumed to be in equilibrium. In an actual packed column the flow is countercurrent throughout, but the analysis based on the theoretical plate concept does not introduce serious error if the sections are sufficiently small, *i.e.*, if H.E.T.P. is small compared to the total height of the column. If we assume the gas-film resistance to be controlling, the potential or driving force at *BB* will be represented on Fig. 21 by *b'b*. At *CC* the corresponding potential will be represented by *c'c*. These potentials will be referred to as $(Y - Y_e)_b$ and $(Y - Y_e)_c$. Assuming the equilibrium curve to be straight over the short range *bc*, the logarithmic mean may be used, and the equation written

$$G(Y_D - Y_C) = G(Y - Y_e)_c = L(X_C - X_B) = M_A \alpha K_G a h \frac{(Y - Y_e)_b - (Y - Y_e)_c}{\ln \dfrac{(Y - Y_e)_b}{(Y - Y_e)_c}} \quad (109)$$

Let

$$\frac{(Y - Y_e)_b}{(Y - Y_e)_c} = J$$

Then

$$h = \text{H.E.T.P.} = \frac{G \ln J}{M_A \alpha K_G a (J - 1)} \quad (110)$$

If m represents the slope of the equilibrium curve over the range of concentrations of the plate in question, then

$$J = \frac{Gm}{L} \quad (111)$$

which may be used to simplify Eq. (108). Even when the slopes of the operating and equilibrium curves differ considerably, it is usually allowable to employ the arithmetic in place of the logarithmic mean potential. The result is

$$\text{H.E.T.P.} = \frac{2G}{M_A \alpha K_G a (J + 1)} = \frac{2GL}{M_A \alpha K_G a (L + mG)} \quad (112)$$

For the special case where J is substantially unity, both Eqs. (110) and (112) reduce to

$$\text{H.E.T.P.} = \frac{G}{M_A \alpha K_G a} \quad (113)$$

For a very dilute gas, in which p_G is negligible compared with P, the conversion factor α becomes equal to PM_B/M_A, and the relation simplifies further to

$$\text{H.E.T.P.} = \frac{G}{M_B P K_G a} \tag{114}$$

This may be compared with the "H.T.U." discussed below. Equations (110) and (112) bring out the important point that the ratio of slopes of operating and equilibrium curves is involved in the relation between $K_G a$ and the H.E.T.P. For this reason the H.E.T.P. is clearly not as fundamental as the coefficient $K_G a$, and it is quite possible for the H.E.T.P. to vary widely over the range of concentrations involved in a single apparatus. No such variations in $K_G a$ may be expected, unless there are large variations in temperature, pressure, or p_{BM}.

Because it substitutes a stepwise calculation for integration, the theoretical plate method for absorption-tower design is allowable only when the number of plates is large, and is inaccurate for less than five to six theoretical plates. It is simpler than the graphical integration, however, and when proper values of H.E.T.P. are available it may be used to advantage. Since the method assumes essentially parallel flow of liquid and vapor across each "plate," and makes no allowance for the countercurrent action above the top "plate," it gives inaccurate results for the composition of the vapor product, in cases where this is the desired unknown quantity.

THE TRANSFER UNIT AND THE H.T.U.

A third alternative design method, having many of the advantages of the plate concept, but not subject to the limitations described in the last paragraph, has been described by Chilton and Colburn.[36] Rewriting Eq. (86), and integrating,

$$\int_{p_0}^{p_1} \frac{dp}{p - p_e} \frac{p_{BM}}{P - p} = \frac{ka}{x} \frac{(P - p)_{\text{Av.}} M_B h}{PG} \tag{115}$$

in which $PG/(P - p)_{\text{Av.}} M_B$ represents the average total mols of solute plus inert gas passing through the apparatus in unit time. Chilton and Colburn point out that the left-hand side of Eq. (115) represents a measure of the difficulty of the desired separation, and define this quantity as the number of "transfer units." The height of column corresponding to one transfer unit thus

becomes

$$\text{H.T.U.} = \frac{PG}{(ka/x)(P - p)_{\text{Av.}} M_B} \tag{116}$$

Like the H.E.T.P., the H.T.U. is small when ka/x or $k_G a$ is large. Its numerical value increases with increasing gas velocity through the column, provided $k_G a$ increases as less than the first power of G. Since the H.T.U. concept is based on a sound integration of the basic diffusion equation, the H.T.U. should not vary with solute concentration in the gas, as does the H.E.T.P. Although this method is basically the same as the use of capacity coefficients such as $k_G a$, it has the advantage that the H.T.U. has only one dimension (length), and does not vary widely with change in gas velocity.

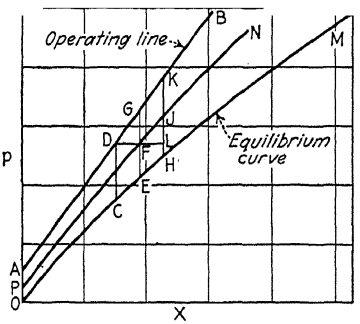

FIG. 25.—Graphical determination of the number of transfer units.

A method of graphically stepping off the number of transfer units has been proposed by Baker[11] and may be followed by reference to Fig. 25. The line PN is placed with ordinates midway between those of the operating line AB and the equilibrium curve OM. Starting at any point D on the operating line the horizontal line DF is drawn to PN, and continued an equal distance to L, such that $DF = FL$. The vertical line KL is drawn through L. The performance of one transfer unit is thus obtained as the change in p from D to K.

The construction is based on the definition of a transfer unit as corresponding to a change in partial pressure equal to the mean driving force. This follows from Eq. (115), where the left-hand side is equal to unity, and p_{BM} is taken as equal to $P - p$. Over the small section of the diagram corresponding to one transfer unit the equilibrium curve is essentially straight, and the arithmetic mean Δp may be employed. This mean is represented on the diagram by the vertical distance GE. The increase in p is LK, which by similar triangles is $2GF = GE$. Thus the construction locates K such that the change in p is equal to the mean Δp, and the step DK corresponds to one trans-

fer unit. If the operating and equilibrium lines are parallel, L will coincide with H and the transfer unit and theoretical plate are identical.

The H.T.U. and the H.E.T.P. differ appreciably only when operating and equilibrium lines are far from parallel, *i.e.*, when J is less than about 0.5 or greater than 2. If the gas contains very little solute, p is small compared with P, and Eq. (116) reduces to

$$\text{H.T.U.} = \frac{G}{(ka/x)M_B} = \frac{G}{K_G a P M_B} \tag{117}$$

which is identical with Eq. (114) for the H.E.T.P. Thus when operating and equilibrium lines are parallel and the gas dilute, the H.E.T.P. and H.T.U. become identical.

The above treatment applies only when gas film is controlling, or when an over-all coefficient $K_G a$ may be used. A similar treatment is possible for the cases when liquid film controls, and the method can be applied to solvent extraction. Chilton and Colburn have described in detail its application to rectification.

ALLOWANCE FOR HEAT EFFECTS

The graphical design method outlined in the preceding pages has implicitly assumed isothermal operation, the equilibrium curve in each example being constructed for a single average tower temperature. In actual practice there are many cases in which the temperature of the solvent flowing through the absorption tower rises or falls quite appreciably. An extreme case would be the drying of air by concentrated sulfuric acid, the heat of solution of water vapor in acid causing a large rise in temperature of the acid. In gas-recovery processes the "stripped" or "denuded" solvent frequently is returned to the absorption tower at a temperature considerably above that of the surroundings. In passing down the tower, the solvent cools and may leave the bottom 20 to 30°F. cooler than when fed at the top. In rich gas absorption this cooling due to heat loss may be largely offset by the heat of condensation of the vapor absorbed.

In most cases it is a relatively simple matter to correct for the change in temperature due to the heat of solution or condensation of the vapor. This correction is possible because the heat liberated is a function of the change in composition of the liquid,

so if the heat capacity of the solvent is known, the relation between temperature rise and concentration may be calculated quite easily. An equilibrium curve of gas composition *vs.* liquid composition may then be constructed, which takes into account the temperature variation through the column.

Figure 26 shows the change in position of the equilibrium curve caused by the changing liquid temperature. Curve *OED* represents the equilibrium curve corresponding to the temperature of the liquid feed. As the liquid composition increases from X_0 to X_1, the temperature of the liquid rises in proportion to the heat liberated, and the curve *OFC* represents the equilibrium curve corresponding to the temperature of the liquid leaving the apparatus. The equilibrium curve *EF*, corresponding to the actual temperatures existing in the column, is located by first calculating the temperature rise for each value of X from X_0 to X_1. The curve *EF* is then used in the design calculations. If the liquid film is controlling the points *E* and *F* will be moved up to the ordinates Y_0 and Y_1, but the procedure will be the same. The variation of the liquid film resistance with temperature may be allowed for in the graphical integration, since the relation between temperature and liquid concentration is obtained in order to place the equilibrium curve.

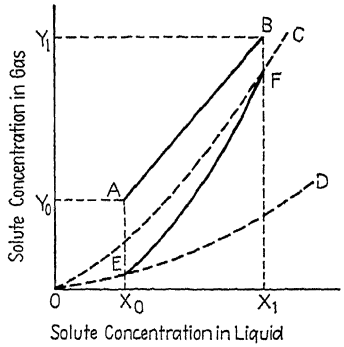

FIG. 26.—Displacement of equilibrium curve due to thermal effects.

Allowance for cooling of the solvent due to heat loss from the column is more complicated, because the cooling is a function of column length, rather than liquid composition. The equilibrium curve may be placed by trial, however, until a graphical integration shows a relation between length and concentration which leads to a temperature-concentration relation agreeing with the assumed location of the equilibrium curve.

Illustration 13.—A gas containing 41.6 per cent NH_3 by volume at 68°F. is to be scrubbed with water to recover 99 per cent of its NH_3 content. If the water enters at 68°F. and heat loss from the absorber is assumed to be negligible, what will be the minimum water rate, as pounds water per pound

gas mixture treated? What will be the corresponding maximum liquor strength obtainable?

For heats of solution, see I.C.T., Vol. 5, p. 213.

Solution.

$$NH_3 \text{ (gas)} + n\ H_2O \text{ (liq.)} \rightarrow (NH_3 + n\ H_2O) \text{ solution}$$

At 68°F.:

$$45.8676 + n(286.103) = a' + nb' + Q$$

n	a'	b'	$-Q$(Kilojoules/ g. mol)*	B.t.u./lb. NH_3	lb. NH_3/ 100 lb. H_2O	Temp. rise, °F.
1	66.12	293.4	27.55	698	94.5	338
2.33	76.17	287.13	32.69	829	40.5	238
4	78.09	286.46	33.62	861	23.6	164
9	79.68	286.17	34.41	873	10.5	83
19	80.31	286.11	34.64	879	4.97	41.6
49	80.64	286.11	35.77	906	1.93	17.1

* $-Q$ = heat of solution.

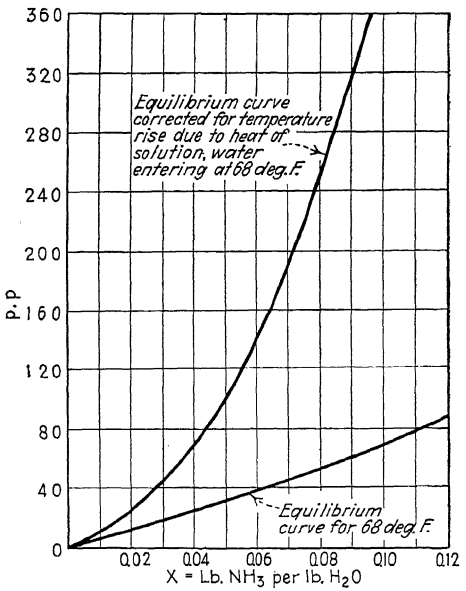

FIG. 27.—Equilibrium curve modified to allow for heat of solution (Illustration 13).

The liquor temperature is obtained by adding the temperature rise to the inlet temperature of 68°F. The partial pressure is then plotted *vs.* liquor strength, each point corresponding to the actual temperature resulting from the heat of solution. The result is shown by the upper curve of Fig. 27.

$$p_1 = 0.416 \times 760 = 316 \text{ mm.}$$

$$p_0 = \frac{41.6 \times 0.01 \times 760}{58.4 + 0.4} = 5.39 \text{ mm.}$$

$$Y_1 = \frac{41.6}{58.4} \times \frac{17}{29} = 0.418 \text{ lb. } NH_3\text{/lb. air.}$$

$$Y_0 = 0.418 \times 0.01 = 0.00418 \text{ lb. } NH_3\text{/lb. air.}$$

$$NH_3 \text{ absorbed/lb. gas mixture} = \frac{0.418 - 0.00418}{1.418} = 0.292 \text{ lb.}$$

Reading from equilibrium curve of Fig. 27 where $p = 316$ mm., $x = 0.0893$ lb. NH_3/lb. H_2O, which is the maximum liquor strength. Minimum water rate = 0.292/0.0893 = 3.27 lb. H_2O/lb. entering gas mixture, corresponding to the maximum liquor strength (and equilibrium at gas inlet).

Maximum liquor strength = 0.0893 lb. NH_3/lb. H_2O.

Nomenclature for Chapter III

a = area of interphase contact, sq. ft./cu. ft.
C_A = concentration of solute in liquid phase, lb. mols/cu. ft.
C_B = concentration of solvent in liquid phase, lb. mols/cu. ft.
C_{BM} = log mean of C_B at film boundaries.
C_e = concentration of solute in liquid phase corresponding to equilibrium with gas, lb. mols/cu. ft.
C_i = solute concentration in the liquid at the interphase boundary, lb. mols/cu. ft.
C_L = solute concentration in the main body of the liquid, lb. mols/cu. ft.
C_0 = solute concentration in the liquid fed to the top of a countercurrent absorption apparatus, lb. mols/cu. ft.
C_1 = solute concentration in the liquid leaving the bottom (gas inlet), lb. mols/cu. ft.
D = diffusion coefficient for gas (see Chap. I).
D_L = diffusion coefficient in liquid phase (see Chap. I).
G = gas flow, lb. solute-free gas/(hr.)(sq. ft. of column cross section).
h = height of column, ft.
H = Henry's law constant = C/p.
J = ratio of the slope of the operating line to that of the equilibrium curve.
$\frac{aDP}{\quad}$

k_G = gas-film coefficient, lb. mols/(hr.)(sq. ft.)(atm.).
k_Ga = gas-film coefficient, lb. mols/(hr.)(cu. ft.)(atm.).
k_L = liquid-film coefficient, lb. mols/(hr.)(sq. ft.)(unit ΔC).
K_G = over-all coefficient, lb. mols/(hr.)(sq. ft.)(atm.).
K_L = over-all coefficient, lb. mols/(hr.)(sq. ft.)(unit over-all ΔC).

K_Ga = over-all coefficient, lb. mols/(hr.)(cu. ft.)(atm.).
K_La = over-all coefficient, lb. mols/(hr.)(cu. ft.)(unit over-all ΔC).
L = liquor rate, lb. solute-free solvent/(hr.)(sq. ft. column cross section).
m = slope of equilibrium curve $= \frac{dYe}{dX}$.
M_A = molecular weight of solute.
M_B = molecular weight of inert or carrier gas.
n = number of theoretical plates.
N_A = diffusion rate, mols/(unit time)(unit area); [lb. mols/(hr.)(sq. ft.)].
p_{BM} = log mean of inert gas pressures at film boundaries, atm.
p_{B1}, p_{B2} = partial pressures of inert gas at film boundaries, atm.
p_G = partial pressure of solute in main gas stream, atm.
p_i = partial pressure of solute at liquid-gas interface, atm.
p_e = pressure of solute in equilibrium with concentration of main body of liquid, atm.
p_0 = partial pressure of solute in main gas stream at gas outlet, atm.
p_1 = partial pressure of solute in gas entering, atm.
P = total pressure on system, atm.
R = gas-law constant (= 1,544 in English units).
T = absolute temperature, ° Rankine.
V = volume of absorption apparatus, cu. ft.
x_G = effective thickness of the gas film.
x_L = effective thickness of the liquid film.
X = solute concentration in liquid, lb. solute/lb. solvent.
X_e = solute concentration corresponding to equilibrium with the solute concentration in the main body of the gas, lb. solute/lb. solvent.
X_n = solute concentration in the liquid on the nth plate from the top of the column, lb. solute/lb. solvent.
X_0 = solute concentration of the liquid fed at the top (gas outlet), lb. solute/lb. solvent.
X_1 = solute concentration of the liquid leaving the bottom (gas inlet), lb. solute/lb. solvent.
Y = solute concentration in gas, lb. solute/lb. inert gas.
Y_e = solute concentration in gas corresponding to equilibrium with the concentration of the main body of the liquid, lb. solute/lb. inert gas.
Y_n = solute concentration in gas leaving the nth plate from the top of the column, lb. solute/lb. inert gas.
Y_0 = solute concentration of gas leaving the top of the column, lb. solute/lb. inert gas.
Y_1 = solute concentration of the gas entering the column, lb. solute/lb. inert gas.
$\alpha = (p - p_e)/(Y - Y_e)$.
$\beta = (C_e - C)/(X_e - X)$.
ΔC = driving force causing diffusion in liquid phase, lb. mols solute/cu. ft. solution.

CHAPTER IV

DESIGN PRINCIPLES FOR MULTICOMPONENT SYSTEMS

The principles of the design calculations for the absorption of a single solute gas have been treated in the previous chapter. The graphical design method there described may be extended without great difficulty to the treatment of design problems where several solute gases are absorbed simultaneously. Operating and equilibrium curves for each component are drawn on the same diagram, and the design is fixed by the fact that the calculation for each component must indicate the same tower volume or number of plates. The principle of the method is fairly simple, but practical difficulties are encountered in locating the equilibrium curves exactly, since each solute acts as a solvent for the other solutes.

Multicomponent absorption is sometimes encountered in the recovery of mixed solvent vapors, but it is in the recovery of natural gasoline and in the treatment of refinery gases that the problem is one of tremendous importance industrially. In these absorption problems of the petroleum industry, the gas to be treated ordinarily consists of a mixture of methane and several of the lower hydrocarbons, principally aliphatics and olefins. The solvent used is almost invariably a light hydrocarbon oil, in which the hydrocarbons to be absorbed are so highly soluble that the gas film may be assumed to be controlling. In the petroleum industry the apparatus used is usually of the plate type, and it is convenient, though not necessary, to employ the theoretical plate concept in the design calculations. The effect of simultaneous diffusion of the several vapors on their respective diffusion rates will be ignored, since its effect is doubtless small (see Illustration 3, page 11) and within the precision of the plate efficiencies employed.

EQUILIBRIA FOR HYDROCARBON-OIL SYSTEMS

Before taking up the application of the graphical design method to multicomponent systems, it will be necessary to discuss the

equilibrium relations employed in using the method for absorption problems of the petroleum industry. These relations are based on the laws of ideal solutions modified according to certain generalizations of the properties of the hydrocarbons encountered. At low pressures Raoult's law, $p = P_v x$, and Dalton's law, $P = \Sigma p$, may be combined with Avogadro's law to give the equilibrium relation

$$p = P_v x = Py \tag{118}$$

In these equations, p is the partial pressure of the solute in the gas phase, P_v is the vapor pressure of the pure component, P is the total pressure, and x and y represent the mol fraction of the solute in liquid and gas, respectively. Σp represents the sum of the partial pressures of the various components. Under conditions where the above relation applies, the compositions of vapor and liquid in equilibrium may be calculated. Even under atmospheric conditions, the deviations from Raoult's law may be appreciable, and at pressures of 400 to 500 lb./sq. in., at which many absorbers operate, Eq. (118) breaks down completely. The equation may be used to give correct results, however, if fugacities[122,176] are employed in place of the pressure terms P_v and P. The term fugacity is defined by a thermodynamic equation for isothermal reversible work of compression, and is discussed fully by Lewis and Randall.[115] In the present section we need be interested only in the use of the term in the calculation of high-pressure equilibria. At pressures low enough for the gas laws to apply, the fugacity becomes equivalent to the partial pressure. Substituting for P_v, the fugacity f_P of the liquid, and for P, the fugacity f_π corresponding to the total pressure, the solution law becomes

$$f_P x = f_\pi y \tag{119}$$

f_P and f_π may be looked upon as pressures corrected for the deviations of the compressibility from the perfect gas laws, at the vapor pressure and at the total pressure, respectively. The fugacities to be used in this relation have been determined in two ways: by calculation from P-V-T data on the pure hydrocarbons and by direct determination of vapor-liquid equilibria.

The P-V-T data on the simpler straight-chain hydrocarbons have been satisfactorily correlated on the basis of the critical values of the individual hydrocarbons, *i.e.*, by a reduced equation

of state.[42,119] This correlation is in terms of the reduced pressure, P_R, which is the ratio of the pressure to the critical pressure P_c of the particular hydrocarbon; the reduced temperature, T_R, which is the ratio of the absolute temperature T to the critical temperature T_c; and reduced volume, V_R, or ratio of the specific volume to the specific volume at the critical conditions. The fugacities to be employed in Eq. (119) may be calculated from the P-V-T data, if it be assumed that hydrocarbon liquids mix isothermally without heat effect or change in volume, and that

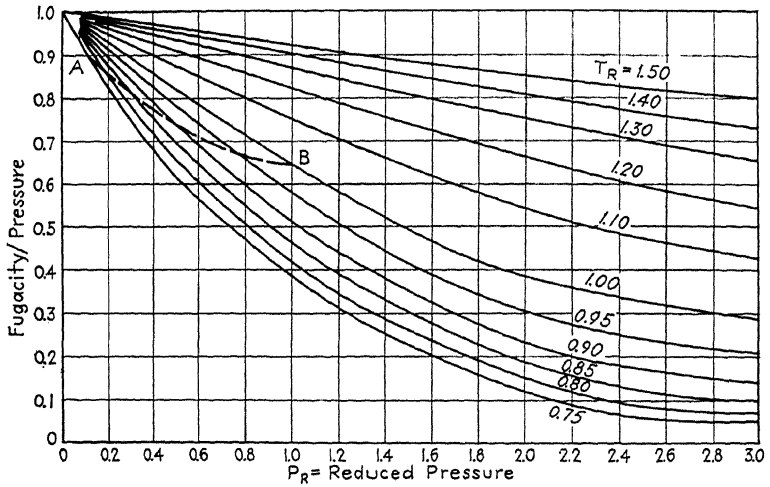

FIG. 28.—Fugacities of hydrocarbons correlated on a reduced basis.

the same is true of hydrocarbon vapors at constant pressure. It is found that the fugacities calculated in this way may be correlated in terms of reduced pressure and reduced temperature, as was the case for the data on reduced volumes.[122,165] Curves representing the resulting correlation, given by Lewis and Kay,[121] are reproduced in Fig. 28. The ordinate is the ratio of fugacity to pressure, and the units of fugacity are those of the pressure by which the ratio is multiplied to get the fugacity. The curves above the line AB are based on the considerable amount of P-V-T data on the simpler straight-chain hydrocarbons. The curves below the line AB and for values of T_R less than 1.0 are based on equilibrium data for several binary systems of the same hydrocarbons. In plotting the latter data, f_P is obtainable

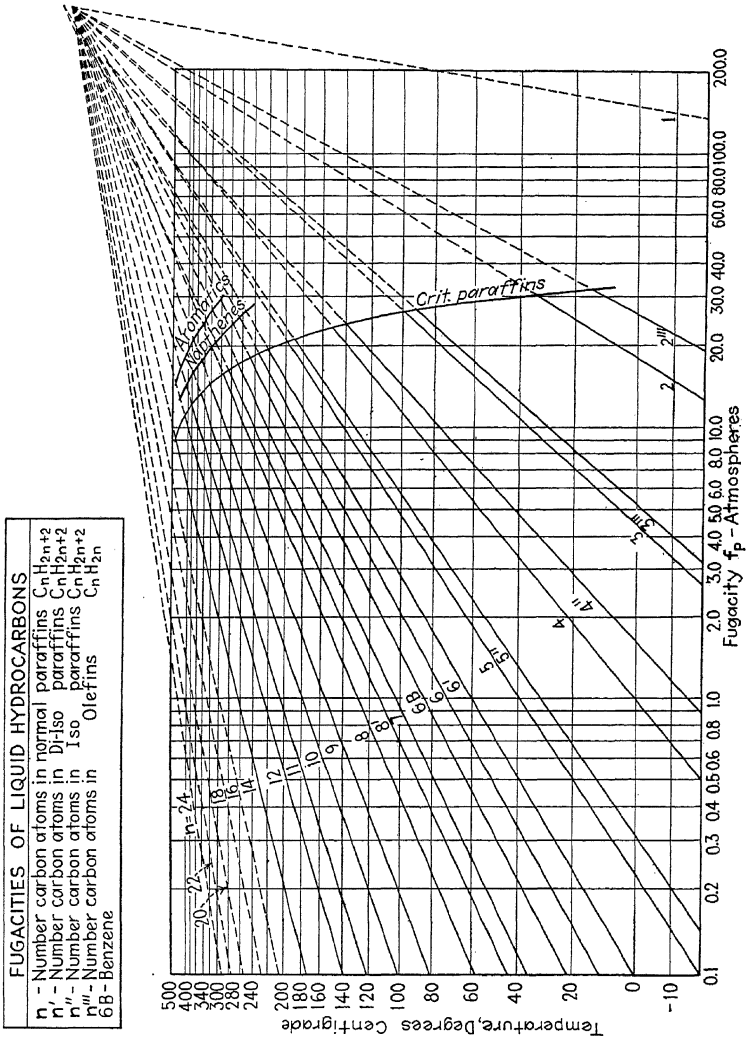

FIG. 29.—Fugacities of liquid hydrocarbons.

from the plot in the region based on P-V-T data, and the other term calculated from the data using Eq. (119). This procedure is equivalent to a definition of the fugacity f_P of the liquid at temperatures above the critical. Using the reverse procedure, the plot may be employed to calculate equilibria for hydrocarbons containing more than two carbon atoms (propane and higher) with an accuracy of 5 to 8 per cent.[121] The deviations are greatest when the hydrocarbons differ appreciably in structure, as in a mixture of aromatic and paraffinic compounds.

The fugacity of the liquid may be obtained from the vapor pressure and Fig. 28, or obtained directly from Fig. 29. This latter is a plot of f_P *vs.* temperature constructed by W. C. Kay[107] in the manner of a Cox chart of vapor pressures. (As pointed out above, f_P approaches the vapor pressure at low temperatures.) The use of an extrapolated vapor pressure together with Fig. 28 for f_P for methane leads to serious error, because ordinary temperatures are well above the critical temperature (191°K.), and at high values of T_R the correlation for the lower hydrocarbons is poor. In this range there appears to be a trend of deviations with the nature of the solvent and with the hydrocarbon. Thus Frölich's[65] data on the solubility of methane at 25°C. in various hydrocarbons gave values of f_P ranging from 143 to 191 atm. when the solvent was butane, pentane, hexane, or octane at 18 to 100 atm. total pressure; and values of f_P from 270 to 555 atm. when the solvent was cyclohexane or benzene. These data are insufficient to show the variation of f_P with the character of the solvent, and the effect can only be estimated. The error involved in extrapolating vapor pressures above the critical may be reduced by carrying out the extrapolation on a plot of f_P *vs.* $1/T_R$ on semilogarithmic coordinates. Figure 30 shows such a plot for methane, with the critical point indicated. The lower right end up to the critical is based on vapor-pressure data, converted to f_P by Fig. 28. The upper dotted section is an extrapolation of the lower branch. The range of Frölich's data on the solubility of methane is indicated in the upper part of the plot. The extrapolated curve goes through the methane data for paraffin hydrocarbons, but the variation with solvent is evident.

The fugacity plots represent a correlation of the physical properties of the common hydrocarbons, useful not only in the

calculation of equilibria, but also as a basis for the calculation of various thermal properties. For convenience in using these plots, Table V summarizes the critical constants as given by the International Critical Tables.[99] In absorption and distillation

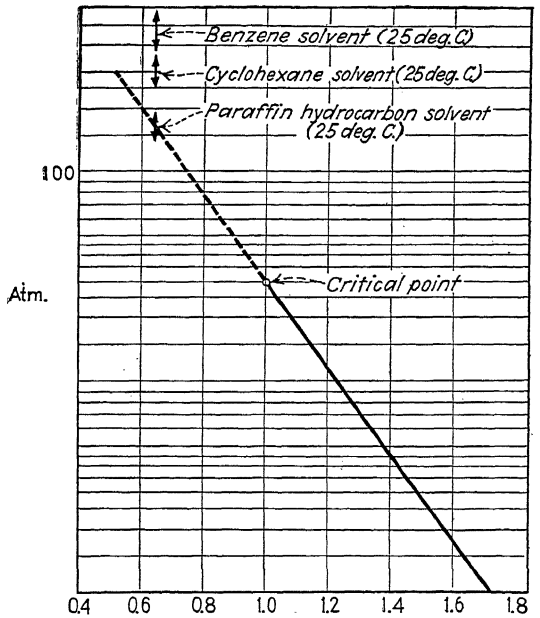

FIG. 30.—Fugacities of methane extrapolated beyond the critical and compared with Frolich's solubility data.

practice, however, the relations plotted are of interest principally as a means of calculating the important equilibrium relations, for which purpose Eq. (119) may be written

$$y = \left(\frac{f_P}{f_\pi}\right)x = Kx \tag{120}$$

The procedure in obtaining values of K from the plots is simple but time consuming, and for convenience tabulated values*

* However, considerable work is under way at present to obtain dependable equilibrium data for hydrocarbon mixtures, and it is probable that these tables will have to be revised from time to time as new data appear.

of K are given for various common hydrocarbons in Table VI. In each case the value of f_π was obtained from the Lewis curves of Fig. 28. For temperatures below the critical, f_P was obtained from Fig. 29. For temperatures above the critical, f_P was obtained from plots of f_P *vs.* $1/T_R$ given by Luke.[129] These are similar to Fig. 30.

TABLE V.—CRITICAL CONSTANTS FOR HYDROCARBONS

Compound	Critical temperature, °K.	Critical pressure, Atm.
CH_4, methane	190.6	45.8
C_2H_4, ethylene	282.8	50.9
C_2H_6, ethane	305.2	48.8
C_3H_6, propylene	365.4	45.0
C_3H_8, propane	368.7	43.0
C_4H_{10}, *n*-butane	426	36.0
C_4H_{10}, iso-butane	407	37.0
C_5H_{12}, *n*-pentane	470.3	33.0
C_5H_{12}, iso-pentane	461	32.8
C_6H_6, benzene	561.6	47.7
C_6H_{14}, *n*-hexane	508	29.5
C_7H_{16}, *n*-heptane	540	26.8
C_8H_{18}, *n*-octane	569	24.6

Illustration 14.—Calculate the value of $K(= y/x)$ for *n*-butane at 5 atm. and 150°F.

Solution.—From Table V the critical temperature and pressure of *n*-butane are 426°K. and 36.0 atm., respectively.

$$T_R = \frac{(150 + 460)}{(1.8 \times 426)} = 0.795$$

$$P_R = \frac{5}{36} = 0.139$$

From Fig. 28, $f_\pi/P = 0.88$; $f_\pi = 0.88 \times 5 = 4.4$ atm.
From Fig. 29, at 150°F. (65.6°C.); $f_P = 6.15$ atm.
$K = f_P/f_\pi = 6.15/4.4 = 1.4$, as given in Table VI.

Illustration 15.—Luke[129] has experimentally determined the compositions of both gas and liquid phases for a mixture of hydrocarbons brought together and maintained at constant temperature and pressure until equilibrium was reached. A typical experiment showed the following vapor and liquid

TABLE VI.—VALUES OF K FOR THE LOWER HYDROCARBONS, CALCULATED FROM THE FUGACITY CURVES

Pressure, atm.	60°F.	80°F.	100°F.	150°F.	200°F.	300°F.
			Methane, CH_4			
0.5	296	340	380	490	610	870
1	148	170	190	250	305	440
2	74	85	95	122	154	220
5	30	34	38	49	61	87
10	15	17	19	25	31	44
25	6.2	7.1	7.9	10	12.4	18
50	3.2	3.7	4.1	5.2	6.3	8.9
			Ethylene,			
0.5	73	87	101	150	204	350
1	37	43	51	75	101	170
2	18.5	22	26	37	51	87
5	7.5	8.9	10.4	15	21	35
10	3.9	4.6	5.3	7.7	10.5	20
15	1.8	2.0	2.3	3.3	4.4	7.3
50	1.1	1.2	1.4	1.8	2.3	3.8
			Ethane, C_2H_6			
0.5	48	56	68	100	140	250
1	24	28	34	49	70	124
2	12	14	17	25	36	62
5	4.9	5.8	7.0	10	14.5	25
10	2.6	3.0	3.6	5.2	7.4	13
25	1.2	1.4	1.6	2.3	3.3	5.2
50	0.83	0.93	1.0	1.3	1.75	2.8
			Propylene, C_3H_6			
0.5	15	20	24	39	61	120
1	7.7	10	12.2	20	31	59
2	4.0	5	6.3	10	15	30
5	1.7	2.2	2.6	4.1	6.2	12.3
10	0.94	1.15	1.4	2.2	3.3	6.3
25	0.50	0.60	0.73	1.05	1.5	2.7
50	0.40	0.49	0.57	0.76	1.0	1.5

TABLE VI.—VALUES OF K FOR THE LOWER HYDROCARBONS, CALCULATED FROM THE FUGACITY CURVES.—(*Continued*)

Pressure, atm.	60°F.	80°F.	100°F.	150°F.	200°F.	300°F.
			Propane, C_3H_8			
0.5	13.2	17	21	35	52	100
1	6.8	8.6	10.8	17	25	50
2	3.4	4.4	5.5	8.7	13	24
5	1.5	1.8	2.3	3.6	5.3	10.3
10	0.8	1.0	1.23	1.9	2.8	5.3
25	0.44	0.54	0.65	0.95	1.3	2.3
50	0.37	0.44	0.53	0.72	0.91	1.34
			n-Butane, C_4H_{10}			
0.5	3.5	4.9	6.6	12.8	21	45
1	1.8	2.5	3.4	6.4	10.4	23
2	0.91	1.25	1.7	3.3	5.3	11.4
5	0.41	0.55	0.75	1.4	2.3	4.7
10	0.24	0.32	0.43	0.80	1.24	2.5
25	0.14	0.19	0.26	0.45	0.68	1.23
50	0.16	0.20	0.26	0.44	0.61	0.87
			iso-Butane, C_4H_{10}			
0.5	5.4	7.2	9.5	16.6	26	56
1	2.7	3.6	4.8	8.5	13	28
2	1.4	1.85	2.5	4.3	6.7	14
5	0.61	0.81	1.05	1.8	2.8	5.8
10	0.35	0.46	0.50	1.0	1.5	3.1
25	0.21	0.27	0.35	0.55	0.70	1.4
50	0.23	0.27	0.34	0.51	0.65	0.95
			n-Pentane, C_5H_{12}			
0.5	0.92	1.4	2.0	4.6	8.5	23
1	0.48	0.71	1.0	2.3	4.4	11.6
2	0.25	0.36	0.53	1.2	2.2	5.9
5	0.11	0.16	0.23	0.53	0.97	2.5
10	0.062	0.094	0.14	0.31	0.55	1.4
25	0.045	0.064	0.091	0.19	0.33	0.75
50	0.057	0.080	0.11	0.22	0.35	0.65

TABLE VI.—VALUES OF K FOR THE LOWER HYDROCARBONS, CALCULATED FROM THE FUGACITY CURVES.—(*Concluded*)

Pressure, atm.	60°F.	80°F.	100°F.	150°F.	200°F.	300°F.
			iso-Pentane, C_5H			
0.5	1.2	1.8	2.6	5.6	10.3	26
1	0.62	0.91	1.3	2.9	5.2	13
2	0.32	0.47	0.67	1.5	2.6	6.7
5	0.15	0.21	0.30	0.65	1.1	2.8
10	0.09	0.127	0.18	0.38	0.65	1.4
25	0.058	0.081	0.11	0.23	0.39	0.80
50	0.076	0.10	0.14	0.26	0.40	0.70
			n-Hexane,			
0.5	0.26	0.43	0.68	1.8	3.6	12.0
1	0.13	0.22	0.35	0.90	1.9	6.0
2	0.071	0.11	0.18	0.46	1.0	3.1
5	0.032	0.052	0.080	0.21	0.43	1.3
10	0.021	0.033	0.051	0.126	0.26	0.77
25	0.015	0.024	0.036	0.089	0.17	0.46
50	0.025	0.037	0.055	0.12	0.21	0.50
			n-Heptane, C_7H_{16}			
0.5	0.075	0.13	0.22	0.69	1.6	6.3
1	0.039	0.067	0.114	0.36	0.82	3.2
2	0.020	0.035	0.059	0.18	0.43	1.6
5	0.0094	0.016	0.027	0.085	0.20	0.72
10	0.0061	0.0106	0.018	0.053	0.12	0.43
25	0.0048	0.0081	0.014	0.040	0.087	0.28
50	0.011	0.017	0.027	0.070	0.14	0.36
			n-Octane,			
0.5	0.025	0.044	0.076	0.27	0.77	3.4
1	0.013	0.023	0.039	0.14	0.39	1.7
2	0.0067	0.012	0.021	0.070	0.21	0.90
5	0.0032	0.0056	0.0096	0.032	0.093	0.40
10	0.0021	0.0037	0.0064	0.022	0.062	0.24
25	0.0018	0.0036	0.0051	0.017	0.045	0.18
50	0.015	0.021	0.030	0.064	0.11	0.29

analyses (mol fractions) after the two phases had come to equilibrium with each other at 81°F.

Component		y
CH_4..	0.041	0.315
C_2H_4.	0.015	0.033
C_2H_6.	0.200	0.323
C_3H_6.	0.115	0.072
C_3H_8.	0.310	0.175
	0.095	0.029
	0.224	0.053

The observed temperature and pressure were 81°F. and 22 atm., respectively.

From the vapor analysis calculate the total pressure and the liquid analysis, and compare with the measured values. From the liquid analysis calculate the total pressure and the vapor analysis, and make a similar comparison. Repeat, using Raoult's and Dalton's laws in place of the calculation from fugacities.

Solution.—The procedure in calculating the pressure from the vapor analysis is to tabulate values of K for an assumed pressure, and calculate values of x. If the assumed pressure is incorrect, the sum of the values of x will not equal unity. Assume, for example, a pressure of 10 atm., and tabulate values of K obtained from Table VI.

Component	y	K	$x = y/K$
CH_4	0.315	17.6	0.018
C_2H_4	0.033	4.6	0.007
C_2H_6	0.323	3.0	0.107
C_3H_6	0.072	1.15	0.063
C_3H_8	0.175	1.0	0.175
i-C_4H_{10}	0.029	0.45	0.063
n-C_4H_{10}	0.053	0.33	0.162
Total	.....	.....	0.598

By trial it is found that at a pressure of 21 atm., the sum of the calculated values of x is very nearly unity:

Component	y	K	x (calculated)	x (observed)
CH_4	0.315	8.6	0.037	0.041
C_2H_4	0.033	2.4	0.014	0.015
C_2H_6	0.323	1.62	0.199	0.200
C_3H_6	0.072	0.68	0.106	0.115
C_3H_8	0.175	0.60	0.292	0.310
i-C_4H_{10}	0.029	0.28	0.103	0.095
n-C_4H_{10}	0.053	0.21	0.252	0.224
Total	.....	....	1.003	1.000

The calculated pressure, found by trial to be approximately 21 atm., checks the observed pressure of 22 atm. well within the accuracy of the values of K. The above table shows the excellent agreement of the calculated and observed liquid analysis.

Starting with the liquid analysis and following a similar procedure, it is found that the vapor compositions total unity when values of K are employed for a pressure of 22 atm.

Component		K	y (= Kx)	y (observed)
CH_4....	0.041	8.2	0.336	0.315
C_2H_4...	0.015	2.3	0.035	0.033
C_2H_6...	0.200	1.56	0.312	0.323
C_3H_6...	0.115	0.62	0.072	0.072
C_3H_8...	0.310	0.58	0.180	0.175
i-C_4H_{10}.	0.095	0.28	0.026	0.029
n-C_4H_{10}	0.224	0.21	0.047	0.053
Total	1.000		1.008	1.000

The check obtained for both pressure and vapor analysis is probably within the accuracy of the methods of analysis employed.

In calculating the corresponding quantities using Raoult's law, the vapor pressures are tabulated, and y/P_v calculated for each component. The sum of these ratios is the reciprocal of the total pressure [Eq. (118)].

Component	y	P atm.	y/P_v	x (calculated)	x (observed)
CH_4.....	0.315	250*	0.00126	0.021	0.041
C_2H_4.....	0.033	70*	0.00047	0.008	0.015
C_2H_6.....	0.323	37.5	0.00862	0.146	0.200
C_3H_6.....	0.072	12.1	0.00595	0.099	0.115
C_3H_8.....	0.175	10.4	0.0168	0.284	0.310
i-C_4H_{10}.....	0.029	4.1	0.0708	0.121	0.095
n-C_4H_{10}.....	0.053	2.8	0.0190	0.321	0.224
Total.....	.....	.....	0.0592		

* Extrapolated considerably beyond critical.

The calculated pressure is the reciprocal of 0.0592, *i.e.*, 16.9 atm. Neither pressure nor composition as calculated check well with the observed values.

The corresponding computation, starting with the liquid analysis, is as follows:

Component			y (calculated)	y (observed)
CH_4	0.041	10.3	0.42	0.315
C_2H_4	0.015	1.05	0.043	0.033
C_2H_6	0.200	7.5	0.306	0.323
C_3H_6	0.115	1.39	0.057	0.072
C_3H_8	0.310	3.23	0.132	0.175
	0.095	0.39	0.016	0.029
	0.224	0.63	0.026	0.053

$$P = 24.49$$

This time the calculated pressure is only 11 per cent high, but the calculated analysis of the vapor is appreciably in error.

GRAPHICAL DESIGN METHOD

The graphical design method described in Chap. III, was first applied to multicomponent systems by W. K. Lewis,[117] and it is a slight modification of Lewis's method that is outlined below. For convenience, concentrations will be expressed in molal stoichiometric units; X' representing the mols of one solute per mol of solvent, and Y' the mols of solute in the gas phase per mol of rich gas to be treated. The liquid rate will be represented by L', the mols of solvent per unit time, and the gas rate by G', the mols of gas to be treated per unit time. As before, the subscripts 1 and 0 will be used in referring to the rich and lean end of the column, respectively. The material balance for any one component may be written

$$L'(X' - X_0') = G'(Y' - Y_0') \tag{121}$$
$$L'(X_1' - X') = G'(Y_1' - Y') \tag{122}$$

and Y' represent the concentrations in liquid and gas phases at any point in the column. In terms of molal stoichiometric units the equilibrium equation (120) becomes

$$\frac{Y'}{\Sigma Y'} = K\frac{X'}{1 + \Sigma X'} \tag{123}$$

or

$$Y' = KX'\left(\frac{\Sigma Y'}{1 + \Sigma X'}\right) \tag{124}$$

where $\Sigma Y'$ = sum of the values of Y' for each component present.
$\Sigma X'$ = sum of the values of X' for each component except the solvent present in the liquid phase (X' is unity for the solvent).

In the special case of absorption from lean gases with large amounts of solvent Eq. (124) reduces to

$$Y' = KX' \tag{125}$$

The operation of a column treating a *lean gas* may be represented by a plot of Y' *vs.* X', with straight equilibrium curves for each

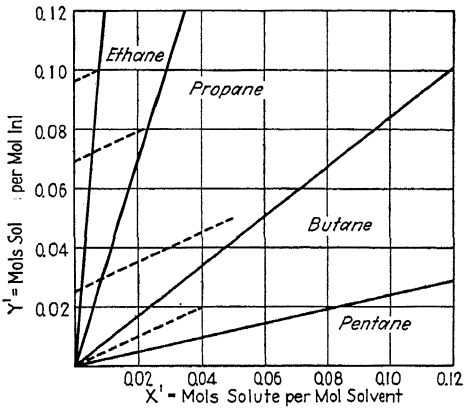

FIG. 31.—Graphical construction for absorption of a lean gas containing several soluble constituents present in small amounts.

component. Each equilibrium curve will pass through the origin and have a slope K. Each component will have its own straight operating line, and these lines will be parallel, since the slope of each is L'/G'. Assuming the capacity coefficients on a molal basis to be the same for the various components, the ratio of the amount absorbed to the mean driving force must be the same for each component, and the location of each operating line is thus fixed by the size of the column. A typical diagram for absorption from a lean gas is shown as Fig. 31. The oil used as a solvent is assumed to be completely denuded ($X_0' = 0$), and the lower ends of the operating lines, at their intersections with the ordinate scale, indicate the composition of the treated gas with respect to

each component. The percentage of each component absorbed may be determined by comparison of the values of Y' at the two ends of each operating line. Thus 50 per cent of the butane is absorbed, and the oil leaves the tower containing 0.05 mols butane per mol of solute-free oil. The operating line for propane is drawn parallel to that for butane, and is placed so that the change in Y', $(Y_1' - Y_0')$, divided by the mean driving force $\Delta Y'$ (mean vertical distance between operating and equilibrium lines) is the same as for butane. In the case illustrated by Fig. 31 the equilibrium lines are straight and a logarithmic mean $\Delta Y'$ may be employed. This may be obtained for butane by calculating the logarithmic mean of the values of $\Delta Y'$ at the two ends of the butane operating line. The propane line is then placed by trial so that the $(Y_1' - Y_0')/\Delta Y'$ for propane is equal to the corresponding ratio for butane. It is evident from the plot that the upper end of the operating line for propane must be very near the propane equilibrium curve, since the large slope of the latter curve reduces the amount absorbed and at the same time increases the driving force at the lean end of the column. In other words, the oil leaving the column is very nearly saturated with propane. In the case of ethane, the equilibrium curve is still steeper, and the oil leaving will be even more nearly saturated with ethane. The slope of the equilibrium curve for pentane is less than the slope of the operating line, so that the driving force is largest at the rich end of the column. The driving force at the rich end is fairly large compared with the total amount of pentane absorbed, and the operating and equilibrium curves will approach each other at the lean end, *i.e.*, the pentane content of the gas leaving the column is essentially in equilibrium with the oil entering. The "key component," in this case the butane, is defined as that component absorbed in appreciable amount, whose equilibrium curve falls most nearly parallel to the operating line, *i.e.*, the component having a value of K most nearly equal to L'/G'. In general, the composition of the gas with respect to components more volatile than the key component approaches equilibrium with the liquid phase at the rich end of the column, and the composition of the gas with respect to components less volatile than the key component approaches equilibrium with the oil entering. Varying the oil-gas ratio will clearly change the nature of the key component.

The theoretical plate method may be employed[175] to fix the various operating lines, as indicated by Fig. 32. This plot is quite similar to Fig. 31, with the addition of the steps used in counting theoretical plates. Assuming any one operating line to be fixed, as may be done by fixing the oil-gas ratio and fraction of the butane absorbed, the other operating lines must be drawn with the same slope, and placed to give the same number of theoretical plates. Except for the method of placing the various operating lines, the construction is the same as that of Fig. 31.

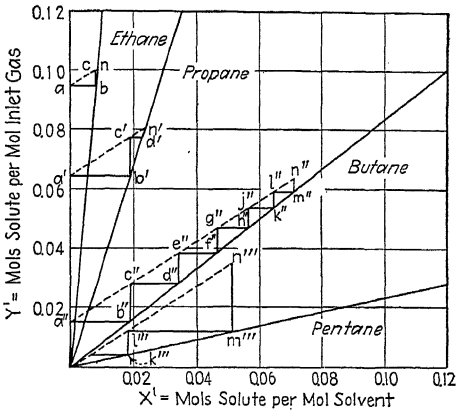

FIG. 32.—Construction for counting theoretical plates in multicomponent absorption.

Figure 32 serves to illustrate the differences in absorption distribution through the column for the various components. Starting at the ordinate scale at the left (representing the top of the column) and counting off one step for each component, the points *c*, *c'*, *c''*, etc., on the various operating lines represent the composition of the gas entering and of the liquid leaving the top plate of the column. For ethane the composition of the gas entering the top plate (point *c*) is nearly equal to the composition of the gas entering the column, Y_1'. For pentane it is evident that no appreciable change occurs in the gas composition in passing through the top plate. It follows that the absorption of the more volatile components takes place in the upper part of the column, and that the less volatile components are absorbed in the lower section. The analysis of the oil-solute mixture on

any plate may be determined by reading from the plot the values of X' for each of the various components on that plate.

ALGEBRAIC METHOD

The method of calculation outlined above based on the theoretical plate concept may be followed algebraically, using the Kremser formula[112,176] discussed in the preceding chapter. In terms of the molal stoichiometric units, this equation becomes

$$\frac{Y_1' - Y_0'}{Y_1' - mX_0'} = \frac{\left(\frac{L'}{mG'}\right)^{n+1} - \left(\frac{L'}{mG'}\right)}{\left(\frac{L'}{mG'}\right)^{n+1} - 1} \tag{126}$$

where, as before, n represents the number of theoretical plates. It applies only when the equilibrium curve is a straight line through the origin with a slope m. In the case of lean gas absorption with a large amount of solvent, Eq. (125) applies and $m = K = y/x$. The left-hand side represents the ratio of the amount of solute absorbed to the amount which would be absorbed were the gas to leave in equilibrium with the entering oil, and consequently represents the efficiency of absorption of any one component. If the oil enters solute-free, as in Figs. 31 and 32, this ratio becomes equal to the fraction of the component entering the column which is absorbed. Where n, L', and G' are fixed, the fraction absorbed may be computed directly for each component, and the operating lines need not be placed by trial and error.

It is apparent from Eq. (126) that where m is greater than L'/G' and n is large, the result is

$$\frac{Y_1' - Y_0'}{Y_1' - mX_0'} = \frac{L'}{mG'} \tag{127}$$

This is also evident from Fig. 22, which represents Eq. (126), if the coordinates are replaced by

$$\frac{Y_1' - Y_0'}{Y_1' - mX_0'} \quad \text{and} \quad \frac{L'}{mG'}, \text{ respectively.}$$

The same conclusion may be reached by referring to Figs. 31 or 32, from which it follows easily by simple geometry that in those cases where equilibrium is reached at the rich end of the column,

the change in Y', divided by Y_1', is equal to the ratio of slopes of operating and equilibrium curves. It is usually convenient to estimate the fraction absorbed for each of the more volatile components by use of Eq. (127). The procedure is satisfactory in the case of those components for which the value of m is three to four times the value of m for the key component.

Furthermore, it is apparent that where m is small compared with L'/G', and n is large, the right-hand side of Eq. (126) reduces to unity, which means that the gas leaves in equilibrium with the entering oil. This is also shown by Fig. 22, and is apparent by inspection from Figs. 31 and 32. For the least volatile components, therefore, equilibrium at the lean end of the column may be assumed. If the oil used is solute-free, this corresponds to complete absorption of these components.

It is seen that the computations are quite simple for the relatively volatile and nonvolatile components. It is only for the key component, and the components on either side of the key component with respect to volatility, that the graphical method or the use of Eq. (126) is necessary.

APPLICATION OF GRAPHICAL METHOD TO THE ABSORPTION OF RICH GASES—GENERAL CASE

Because of the variation through the column of the amount of solutes carried by the oil, the equilibrium lines are curved, their curvature depending on the fraction of the gas absorbed and on the relative amounts of gas and liquid. This is evident from the equilibrium relation

$$Y' = KX'\left(\frac{\Sigma Y'}{1 + \Sigma X'}\right) \tag{124}$$

For lean gases and high oil rates, the term in parentheses may be assumed to approximate unity, as was done in the preceding section, but for rich gas or low oil rates, the variations in the terms $\Sigma Y'$ and $(1 + \Sigma X')$ must be allowed for. Where the column is supplied with oil containing no dissolved solute, the equilibrium line may be located by two facts: (*a*) the slope at the origin is $K(\Sigma Y_0')$, as found by differentiating Eq. (124), and (*b*) the equilibrium curve for conditions at the rich end of the column is determined by substituting Y_1' or X_1', $\Sigma Y_1'$, and $\Sigma X_1'$ in Eq. (124). $\Sigma Y_1'$ is unity by definition, and $\Sigma X_1'$ may be

calculated if the total mols of all components absorbed in the column is known. In almost all practical problems the curvature of the equilibrium lines is not serious, and the lines may be placed with sufficient accuracy if the slope at the origin and the location at the rich end are known in each case. The error involved in locating these lines is negligible except for the key component, for which certain additional calculations described below may be necessary.

The exact location of the equilibrium lines is determined by the total absorption and the amount absorbed is dependent on the equilibrium relations. Consequently the procedure is necessarily by trial and error, although it is possible to reduce greatly the computations necessary if a logical method is employed for the first estimates. For the volatile components, the absorption is determined by the location of the equilibrium curve at the rich end of the column, and the shape and exact location of the remainder of the curve are unimportant. For the absorption of these volatile components from a lean gas, the performance of the column was shown above to be

$$\frac{Y_1' - Y_0'}{Y_1' - mX_0'} = \frac{L'}{mG'} \tag{127}$$

In Eq. (127), m represents the slope of a straight line through the origin and through a point on the equilibrium curve at the rich end of the column, *i.e.*, $m = Y_1'/X_1'$. It applies even though the equilibrium line is curved, so long as equilibrium is reached at the rich end of the column. If the solvent supplied is solute-free, X_0' is zero, and the relation gives the fraction absorbed. Allowing for the solvent effect of dissolved solute, and neglecting the solute content of the liquid feed, this becomes

$$\frac{Y_1' - Y_0'}{Y_1'} = \frac{L'(1 + \Sigma X_1')}{K(\Sigma Y_1')G'} = \frac{L'(1 + \Sigma X_1')}{KG'} \tag{128}$$

where $K\dfrac{\Sigma Y_1'}{(1 + \Sigma X_1')}$ has replaced m [Eq. (124)].

The mols of total gas to be treated, G', is usually specified, but the mols absorbed, $L'(\Sigma X_1')$, must first be estimated. This is best done by assuming straight equilibrium curves of slope K, and using Eq. (126) to estimate the fraction absorbed for each

component. If the performance of the tower with respect to one component be specified, Eq. (126) may be used first to estimate the required number of perfect plates, and then to estimate the absorption of the other components. This procedure leads to an estimate of the total absorption of all components, and consequently of the value of $\Sigma X_1'$, which may be employed to repeat the calculation, this time using

$$\frac{L'(1 + \Sigma X_1')}{KG'}$$

in place of L'/mG'.

This second calculation will be very nearly correct, except for the key component and possibly one component on either side of the key component. For these it is necessary to construct a plot, placing the equilibrium lines from the known slope at the origin, and from the known location of the curve at the rich end, and placing the operating lines by trial until the correct number of plates are counted. A new value of the total absorption is obtained by addition. If this is appreciably different from that obtained by the first trial, a third calculation should be made, using the corrected value of $\Sigma X_1'$.

In many cases it is possible to make a rough guess of the total absorption by inspection from the gas analysis. Where this can be done the first trial calculation using straight equilibrium curves may be omitted. More than three trials are very seldom required, and in cases where the total mols of oil leaving the column is approximately the same as the total mols of gas entering, the equilibrium curves are nearly straight, and the first trial is sufficient.

The use of the inlet gas as a "basis" for all gas compositions is simple and convenient. The distance from equilibrium at any point in the tower expressed as a $\Delta Y'$, is not, however, strictly proportional to the diffusional driving force called for by the diffusional equations. The plate concept is commonly used in this type of absorber, however, and the choice of basis has no effect on the calculation of the number of theoretical plates.

The design calculation outlined above for multicomponent systems may be summarized in the form of a list of steps given below in order. This tabulation assumes that the problem is to calculate the performance of a given column, having given the

operating conditions, solvent and gas rates, and composition of the feed gas. Minor modifications of this procedure allow the calculation of the number of theoretical plates when the performance of the column is specified, etc.

1. Determine from Table VI, or other sources, the values of K for each component for the conditions prevailing in the column.

2. Calculate L' and G', the mols of solvent and inlet gas per unit time.

3. Make a rough estimate of the total absorption, as mols per 100 mols feed gas.

4. Calculate $\Sigma X_1'$, based on this estimate of the total absorption. Calculate values of $L'(1 + \Sigma X_1')/KG'$ and employ Eq. (126) using these ratios in place of L'/mG' to obtain a second estimate of the absorption of the very volatile and the nonvolatile components.

5. For the key component (or components) construct a plot of Y' *vs.* X', and draw a line with a slope $K(\Sigma Y_0')$ through the origin.* Locate the point Y_1', X_1' (equilibrium) from Eq. (124), and draw the equilibrium curve in its approximate position.

6. Locate the operating line for the key component with a slope L'/G', and in a position above the equilibrium curve corresponding to the proper number of theoretical plates. From this line read off Y_0' for the key component, and calculate the mols of that component absorbed.

7. Add up the mols of each component absorbed to obtain a third estimate of the total absorption. If this differs appreciably from the value obtained under 4, repeat steps 4, 5, and 6.

The procedure just outlined is not difficult to follow, but it is suggested that the following illustrative problem be studied carefully if a clear understanding of the method of calculation is desired.

Illustration 16.—A 24-plate absorber is designed to operate at 470 lb./sq. in. gauge, treating 18,780,000 cu. ft. (1 atm., 60°F.) per 24 hr., of a gas containing 83.02 per cent CH_4, 8.41 per cent C_2H_6, 4.76 per cent C_3H_8, 0.84 per cent iso-C_4H_{10}, 1.66 per cent n-C_4H_{10}, 0.61 per cent iso-C_5H_{12}, 0.16 per cent n-C_5H_{12}, and 0.54 per cent C_6H_{14} and higher. The tower will be supplied with 111,840 gal. per 24 hr. of a denuded oil having a density of 0.8363 at the temperature at which it is metered, and an average molecular

* This assumes the oil fed to contain none of the key component. Where this is not the case, the procedure must be modified as indicated in a later section.

weight of 161. The tower will operate with an average oil temperature of 87°F. Assuming Atkins and Franklin's value of 18 per cent for the over-all plate efficiency (see below), calculate the composition of the treated gas.

Solution.

$$\text{Inlet gas} = \frac{18{,}780{,}000}{359} \times \frac{492}{520} \left| \frac{\text{lb. mols/day}}{\dfrac{1}{24 \times 60}} \right. = 34.4 \text{ lb. mols/min.}$$

$$\text{Inlet oil} = \frac{111{,}840}{24 \times 60} \left| \frac{\text{g.p.m.}}{\dfrac{8.33 \times 0.8363}{161}} \right. = 3.36 \text{ lb. mols/min.}$$

$$\text{Operating pressure} = 1 + \frac{470}{14.7} = 33 \text{ atm.}$$

Because of the high proportion of methane and ethane in the gas, the total absorption will not be large, even at this relatively high pressure. Assume 10 mols absorbed per 100 mols inlet gas. Values of K are obtained from Table VI by interpolation (graphically) for 87°F. at 33 atm. The tabulation of the values of K completes steps 1, 2, and 3.

$$\Sigma X_1' = \frac{10}{100} \times 34.4 \left| \frac{\text{mols absorbed per minute}}{\times \dfrac{1}{3.36}} \right. = 1.02 \text{ mols/mol oil}$$

$$\frac{L'(1 + \Sigma X_1')}{G'} = \frac{3.36(1 + 1.02)}{34.4} = 0.197$$

Values of $L'(1 + \Sigma X_1')/KG'$ are tabulated, and used in place of L'/mG' in Eq. (126) to calculate the absorption of each component. The number of theoretical plates, n, is taken as 4.3, corresponding to the assumed plate efficiency of 18 per cent. For $n-C_4H_{10}$, for example,

$$\text{Fraction absorbed} \quad \frac{0.94^{5.3} - 0.94}{0.94^{5.3} - 1.0} \quad 0.79$$

Component	Mol per cent	K	$\dfrac{L'(1 + \Sigma X_1')}{KG'}$	Per cent absorbed	Mols absorbed
CH_4	83.02	5.7	0.035	3.5	2.9
C_2H_6	8.41	1.2	0.164	16.4	1.4
C_3H_8	4.76	0.51	0.386	38.6	1.8
i-C_4H_{10}	0.84	0.27	0.73	67	0.6
n-C_4H_{10}	1.66	0.21	0.94	79	1.3
i-C_5H_{12}	0.61	0.09	2.19	100	0.6
n-C_5H_{12}	0.16	0.072	2.74	100	0.2
$C_6H_{14}+$	0.54	.....	.....	100	0.5
	Total mols absorbed = 9.3				

Since the total absorption checks closely the assumed value of 10 mols the calculation may be continued with step 5, a more careful treatment of the key component. The previous calculation showed the key component to be normal butane, for which it is necessary to plot equilibrium and operating lines. The slope of the equilibrium curve at the origin is

$$K(\Sigma Y_0') = 0.21 \times (1 - 0.093) = 0.19$$

The dotted line OB of Fig. 33 is drawn with this slope. The value of X' in equilibrium with Y_1' is obtained from Eq. (124):

$$X' \text{ (equilibrium)} = \frac{0.0166}{0.21}\left[1 + \frac{9.3}{100} \times \frac{34.4}{3.36}\right] = 0.156$$

This locates one point on the equilibrium curve near the rich end of the column, as shown by the point A on Fig. 33. (The value of $1 + \Sigma X'$ used

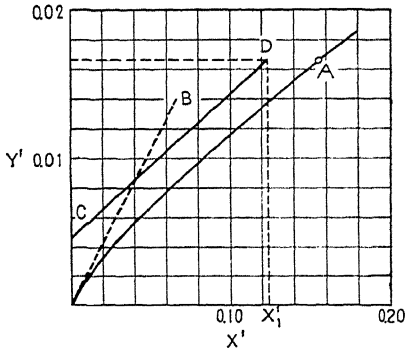

FIG. 33.—Curved equilibrium line for key component obtained in case of low oil rate (Illustration 16).

in this last calculation really applies at the abscissa X_1', but the error involved is negligible). The equilibrium curve is drawn in its approximate position, starting at the origin with the slope OB, and curving off to pass through A.

The slope of the operating line is $L'/G' = 3.36/34.4 = 0.0975$. A straight line with this slope is placed by trial in a position such that 4.3 steps corresponding to theoretical plates can be stepped off between operating and equilibrium curve.

The n-butane content of the gas leaving the column is read as the intercept of the operating line with the Y' axis as $Y_0' = 0.0045$. The mols n-butane absorbed is consequently $1.66 - 0.45 = 1.21$, *vs.* 1.3 previously estimated. The corrected total absorption is 9.2 mols checking the original estimate sufficiently closely so that further computations are not necessary.

The composition of the gas leaving the column may now be calculated.

Component	Feed, mol per cent	Mols absorbed	Mols in exit gas	Mol per cent in exit gas (calculated)	Mol per cent in exit gas (observed)
CH_4.....	83.02	2.9	80.1	88.4	88.7
C_2H_6.....	8.41	1.4	7.0	7.7	6.9
C_3H_8.....	4.76	1.8	3.0	3.3	3.5
i-C_4H_{10}.....	0.84	0.56	0.28	0.31	0.42
n-C_4H_{10}.....	1.66	1.21	0.45	0.49	0.47
i-C_5H_{12}.....	0.61	0.6	0		
n-C_5H_{12}.....	0.16	0.2	0		
C_6H_{14+}.....	0.54	0.5	0		
Total.....	.....	....	90.83		

The conditions described in the problem are those of a test reported by Brown and Souders[21] in which an actual natural gasoline absorber was tested under the conditions described. The measured analysis of the exit gas is given in the last column of the table for comparison with the calculated composition. The agreement between calculated and observed compositions of the treated gas is seen to be quite good. The calculations show 73 per cent absorption for n-butane, whereas the actual absorption was about 69 per cent. This discrepancy is probably within the accuracy of the analysis for the small quantity of n-butane in the lean gas. Reliable test data[74] on stabilizers and other rectifying columns give plate efficiencies from 60 to over 100 per cent, but relatively few data are available from which plate efficiencies for absorbers may be calculated (see page 191). The reported butane content in the lean gas in the case of the above test would correspond to a plate efficiency of only about 15 per cent, and Atkins and Franklin[7] report efficiencies of 18 per cent for absorbers operating at lower pressures. It seems probable that plate efficiencies in absorbers do run much lower than in stabilizers, and decrease as the molecular weight of the absorbent oil increases.[74] The absorption of all but the key component is almost independent of the plate efficiency, since a relatively large number of plates is always used.

The equilibrium curve for the key component may be placed much more accurately if an additional point is located corresponding to the middle of the column. The absorption of the

components more volatile than the key component will take place in the upper part of the column; the absorption of the less volatile will take place on the lower plates. Consequently $(1 + \Sigma X')$ for the middle plate may be estimated closely, and by using Eq. (124) the coordinates of a point on the equilibrium curve at about the middle of the column can be found. This additional calculation removes some of the uncertainty in placing the curved equilibrium line for the key component, and improves the accuracy of the method. If the key component is one of the least volatile constituents, almost all of the curvature will occur near the origin (see Fig. 33); if the key component is one of the most volatile constituents the equilibrium line will follow the original slope (*OB* of Fig. 33) for a considerable distance from the origin. Where necessary the equilibrium curve may be located reasonably exactly by trial and error, until the values of $\Sigma X'$ and $\Sigma Y'$ calculated for each individual plate correspond with the location of the equilibrium curves at the same plates. For example, on the top plate in the column, the values of X' and Y' for each component may be obtained by counting one step from the left-hand end of the operating lines. Adding these to obtain $\Sigma X'$ and $\Sigma Y'$, Eq. (124) may be employed in checking the location of the curves used in measuring off one step or plate. By trial the curves can be adjusted until a check is obtained. Proceeding to the second plate and on down the column by the same method, the equilibrium curves may be located with a precision well within the accuracy of the equilibrium data. This procedure is time consuming and is necessary only when L' is but a small fraction of G', in which case the equilibrium lines are considerably curved, or when the oil fed contains considerable amounts of the key solutes.

ALLOWANCE FOR THERMAL EFFECTS

The latent heats of condensation of the common hydrocarbons are relatively small, and the heat of mixing of the liquids is negligible; consequently, the temperature rise of the solvent passing through the column is usually not large. Furthermore, natural gasoline columns ordinarily operate at temperatures somewhat above the temperature of the surroundings, and some of the heat of condensation is dissipated. The temperature rise of the oil may be quite appreciable, however, if the oil rate

is low compared with the total mols of solutes absorbed. Low oil rates are ordinarily employed at high pressures, and since the latent heats of condensation decrease rapidly with increased pressure, the heat effect is still small in spite of the greater condensation per mol of oil. Figure 34 may be used to estimate this temperature rise of the solvent. The curves shown are based on molal latent heats at 68°F. at 1 and at 34 atm., read from a curve of the Hildebrand function.[188] The lean oil is assumed to be solute-free, and the rich oil is assumed to have a

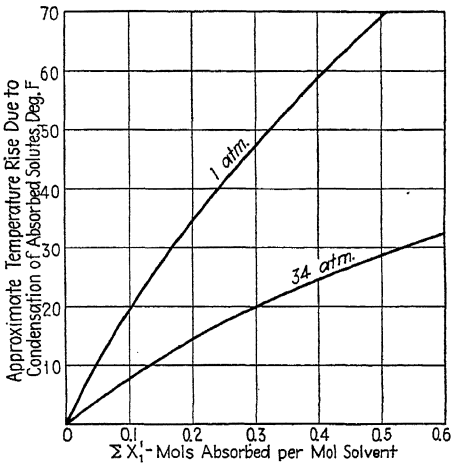

FIG. 34.—Temperature rise due to absorption of dissolved solutes; oil absorption of light hydrocarbons.

specific heat of 0.5, with an average molecular weight of 180. The temperature rise estimated from the total absorption may be obtained from this plot and added to the inlet oil temperature to obtain the outlet oil temperature. If desired, corrections may be made for the heat lost to the surroundings, and for the temperature change of the gas. An average of inlet and outlet oil temperatures is usually satisfactory as a basis for the choice of values of K in the design calculations. It is entirely possible, though unnecessary for most purposes, to allow for the changing oil temperature in constructing the equilibrium curves of Figs. 31 and 32. The procedure would be to adjust the curves by trial, using a different set of values of K for each plate, until the tem-

perature change from one plate to the next corresponded with the total absorption between the two sections. Except in special circumstances, however, the heat liberated by condensation is sufficiently small so that this more complicated procedure is uncalled for.

It sometimes happens that the rise in oil temperature due to condensation is sufficient to cause stripping of one or more components previously absorbed in the cooler upper section. The composition of the oil with respect to these particular

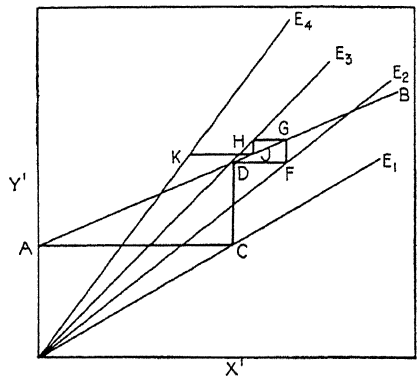

FIG. 35.—Nonisothermal conditions, with stripping on the lower plates.

components goes through a maximum on the middle plate of the column. The effect is illustrated by Fig. 35, on which the lines E_1, E_2, E_3, E_4 are equilibrium lines for the temperatures prevailing on the top four plates. AB represents the operating line, and $ACDFG$ is the usual construction for stepping off the first two plates. The abscissa at F represents the composition of the liquid on the second plate, and the ordinate at G the gas rising from the third plate. The composition of the liquid on the third plate is next determined by moving to the left to the E_3 line at H. Beyond the point G the operating line is below the equilibrium curves, and the component is stripped from the oil. The concentration in the oil of the component in question is a maximum on the second plate, where the concentration is indicated by the abscissa at F.

The stripping action in the lower section of an absorption tower is not obtained in the adiabatic absorption of a single

solute, except in some cases where the gas enters hot. The stripping effect is obtained for certain components in a multicomponent mixture only because the temperature of the solvent increases as it flows through the apparatus, owing to condensation of other components. Heat supplied to the column from outside would cause the same effect.

The effect just described should not be confused with the occurrence of maximum concentration with respect to one component frequently obtained in the central portion of a multicomponent column due to the varying concentrations of other components. In an isothermal column it is quite possible for the composition of the oil, with respect to a component of intermediate volatility to reach a maximum near the middle of the column because of the diluent effect of the nonvolatile components absorbed in the lower section. In this case the concentration of the particular components falls off in the lower section, although the amount of the component dissolved in the oil may continue to increase on the lower plates. The concentration decreases, although no stripping occurs.

Nomenclature for Chapter IV

f_p = fugacity of a pure liquid corresponding to a total pressure equal to its vapor pressure, at the temperature T.
f_π = fugacity of a pure vapor corresponding to the total pressure at the temperature T.
G' = gas rate, mols inlet gas per unit time.
K = y/x = ratio of mol fraction of a component in the vapor to the mol fraction of the same component in a liquid which is in equilibrium with the vapor.
L' = liquid rate, mols pure solvent per unit time.
n = number of theoretical plates.
p = partial pressure, atm.
P = total pressure, atm.
P_c = critical pressure, atm.
P_R = reduced pressure, $= \frac{P}{P_c}$, or $\frac{P_v}{P_c}$.
P_v = vapor pressure, atm.
T = absolute temperature, °K. or °R.
T_c = critical temperature, °K. or °R.
T_R = reduced temperature, $= \frac{T}{T_c}$.
V_R = reduced volume.
x = mol fraction in liquid.

X' = liquid composition, mols solute/mol pure solvent.
y = mol fraction in gas.
Y' = gas composition, mols of one component per mol of gas entering.
$\Delta Y'$ = driving force in stoichiometric units = Y' minus equilibrium value of Y' corresponding to liquid composition at the same point in the tower.
$\Sigma X'$ = sum of the various solute concentrations expressed in stoichiometric units.
$\Sigma Y'$ = sum of concentrations of the various gases, expressed in stoichiometric units.

Subscript 1 refers to the conditions at the rich end of the column, where the gas enters and the solvent is removed.

Subscript 0 refers to the lean end of the column, where the gas is withdrawn and the solvent enters.

CHAPTER V

GAS ABSORPTION EQUIPMENT

Filters, heat exchangers, stills, dryers, and many other types of chemical-engineering equipment are ordinarily designed and built by equipment companies, to be purchased by the manufacturing plant. Absorption equipment is frequently, if not usually, designed and built by engineers connected with the plant in which it is to be installed. As a result of this practice and of the wide variety of purposes and specifications of absorption equipment, there are hardly two units alike, and a very large number of quite different types have been built and used. The objective of each design, however, is the provision for intimate contact of gas and liquid over a large interphase surface, with a low first cost and low operating costs. The various types may be divided roughly into three groups: (*a*) packed towers, (*b*) bubble-cap or plate towers, and (*c*) miscellaneous types, including spray towers. The first cost includes foundations, tower, packing, solvent charge, pumps, blowers, piping, ducts, and accessory heaters, coolers, and heat exchangers. The operating costs include power for circulating gas and solvent, maintenance, labor, steam, cooling water, and solvent make-up.

PACKED TOWERS

The most common type of absorption equipment is the packed tower. It consists of a vertical shell set on an adequate foundation, and filled with one of numerous types of inert packing material. The operation is usually countercurrent, the solvent being distributed over the packing at the top of the tower and passing down over the packing in thin liquid films, while the gas passes up through the free space between the wetted particles of packing. In place of one very tall tower it is customary to employ several shorter towers in series, the gas passing from the top of the first tower to the bottom of the second, and so on, while the liquor is pumped in the opposite direction as from the

bottom of the second to the top of the first, etc. This type of operation is common practice in the absorption of hydrogen chloride and of nitric oxide in the manufacture of hydrochloric and nitric acids.

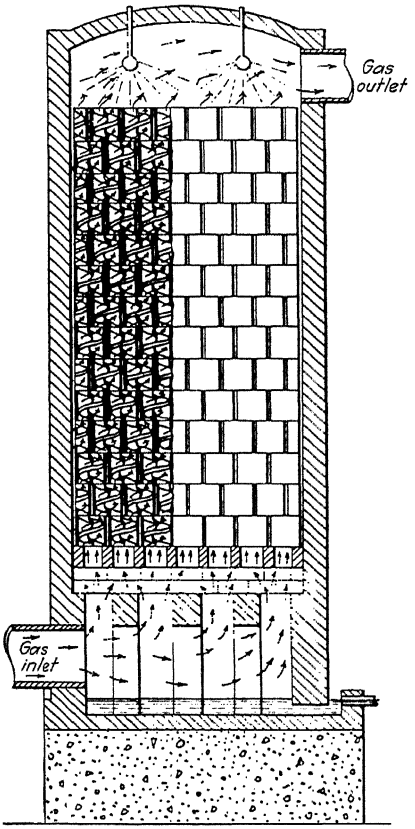

FIG. 36.—Absorption tower packed with manufactured ring packing.

In some cases the liquor rate is necessarily small compared to the gas flow, and if the tower has a cross section adequate to handle the gas, there may not be enough liquid thoroughly to wet the packing. One method of overcoming this difficulty is to recirculate the liquor through the tower so that the liquor circulated is several times the actual throughput. When this

is done in a single tower the advantage of countercurrent action is largely lost, and the use of several shorter towers is resorted to in an effort to simulate true countercurrent action. With this design the liquor moves from tower to tower, countercurrent to the flow of gas. If the liquor throughput is small compared to the liquor recirculated, the change in liquor concentration from top to bottom of any one tower will be small, and it is not

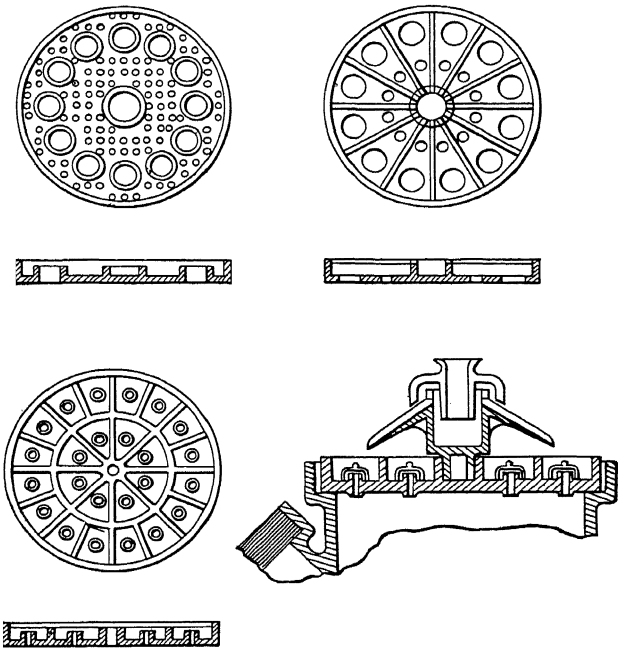

FIG. 37.—Liquid-feed distributor plates. (*Maurice A. Knight.*)

important that the gas pass up through each tower. In order to save on gas mains in such cases the gas may be allowed to pass alternately up and then down through successive towers.

Individual towers may be as high as 80 ft. and as large as 30 ft. in diameter. Because of the enormous weight of the wetted packing in large towers, and the necessity of allowing for wind pressure, the foundations are heavy and costly. The requirements of foundations for self-supporting towers are discussed by Sandstrom.[164] It is advisable to have the diameter small com-

pared to the packed height, and where the ratio of diameter to height is greater than one-fifth, special care must be taken to ensure proper distribution of gas and liquor flow through the packing. The packing rests on a brick checkerwork or metal grid below which the gas is introduced. Above the packing is the liquor-feed distributor, which may be any one of several types (see Fig. 37).

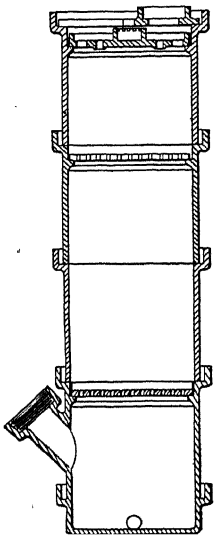

FIG. 38.—Tower construction using acidproof stoneware sections.

Since absorption towers find their widest application in chemical plants, particularly for acid manufacture, the most common construction material is acidproof ceramic ware. Towers up to 5 ft. in diameter are constructed of cylindrical tower sections which fit together. Larger towers are made of acidproof brick, or of steel lined with an acidproof brick or special plastic lining. Chamber sulfuric acid plants use lead shells lined with acidproof brick. Modern plants producing nitric acid by oxidation of ammonia employ towers having shells made of chromium-steel alloy, and towers for this purpose were among the first large structures fabricated with stainless steel in this country. Ordinary steel is used in the petroleum industry, where the corrosion difficulties are less serious, and plate towers more common than packed.

The acidproof brick for the shells of the larger towers are bonded with an acidproof mortar usually having a sodium silicate base. Various grades of chemical stoneware may be obtained, that for contact with acid being high in silica, low in iron oxide, alumina, and alkaline earths, thoroughly vitrified, and nonabsorbent. In general the more porous grades are more resistant to temperature changes, and denser materials more resistant to acid. In addition to packing material and shells for the smaller towers it is possible to obtain acidproof chemical-stoneware pipes, liquor-distributing plates, valves, pumps, and blowers. Pipes, valves, and other small pieces may also be had in hard rubber. A general discussion of tower construction for acid plants is given by Fairlie.[60]

PACKING MATERIALS

A very large number of packing materials have been used or suggested for use in absorption towers. The earliest packings were lump materials such as coke or broken rock, screened to size to eliminate small particles which might plug the gas passages. These materials are still used, but in recent years a number of manufactured packings have been placed on the market and have found favor, particularly where acid-resistant materials are required. The individual particles of the manufactured packings have general dimensions of from 1/2 to 6 in. and are usually hollow so that when dumped or packed in a tower there will be less tendency for channeling of gas and liquor than in the case of the broken materials, the resistance to gas flow will be low, and the wetted surface per unit volume will be large. Most of these newer packings are patented, and their first cost is considerably greater than for broken materials.

The various criteria of an ideal packing are discussed in detail by Butcher,[26] Fairlie,[60] and by Badger and McCabe.[9] Basically, however, the requirements are three:

1. Low cost per cubic foot.
2. High absorption capacity as indicated by high allowable gas and liquor, rates, and high capacity coefficients K_La or K_Ga under the operating conditions.
3. Low maintenance, implying low resistance to gas flow.

In addition, the packing must naturally have a long life under the existing corrosion and thermal conditions. Manufacturers of packings can usually supply data on percentage of free volume, surface per unit volume, etc., but seldom have the really fundamental data on resistance to gas flow, and the capacity coefficients for the purpose at hand. Since high-capacity coefficients are usually obtained with the smaller packing sizes for which the resistance to gas flow is large, the best packing is necessarily a compromise having moderate absorption capacity and moderate resistance to gas flow.

Figure 39 illustrates a few of the many types of manufactured packings, and Table VII summarizes the physical characteristics of those pictured as well as of several not shown. The weight per cubic foot is important in connection with the design of the foundations, shell, and supporting grid for the packing. The

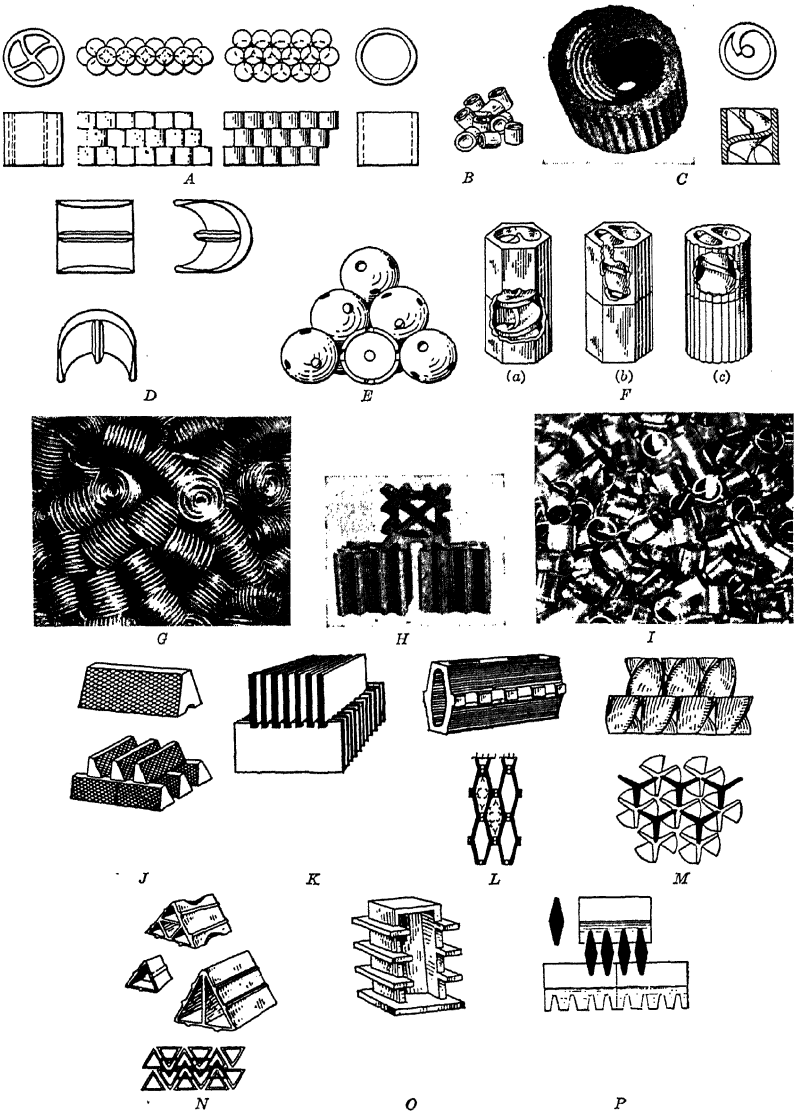

FIG. 39.—Various typical manufactured packings. (*Most of the individual illustrations shown are the copyright of Charles H. Butcher, London, reproduced by permission.*) *A.* Partition rings. *B.* Plain Raschig rings. *C.* (Photo *and* diagram) Spiral rings. *D.* Berl saddles. *E.* Hollow balls. *F.* Helical packers: (*a*) single-spiral hexahelix blocks, (*b*) double-spiral hexahelix blocks, (*c*) double-spiral cyclohelix blocks. *G.* Bregeat multiple spirals. *H.* Hechenbleikner blocks. *I.* Metal Lessing rings. *J.* Prismic packing. *K.* Grids. *L.* Guttmann cells. *M.* Nielson "propeller" packing. *N.* Prym triangular packing. *O.* "Obsidianite" packers. *P.* Scherfenberg bricks.

percentage of free volume is roughly indicative of the resistance to gas flow, although frequently misleading in this respect. For example, 1/4-in. spheres have a very much greater resistance

TABLE VII.—PHYSICAL CHARACTERISTICS OF VARIOUS PACKING MATERIALS
(SEE ALSO TABLE X)
(Copyright by C. H. Butcher, London, reproduced from *The Industrial Chemist*,[26,27,28] by permission)

Material	Key (Fig. 39)	Dimensions, in.	Bulk density, lb./cu. ft.	Dry surface, sq. ft./cu. ft.	Per cent free volume	Number of pieces per cu. ft.
Coke, dumped	..	6	10	5.5	57	
		3	24	12	50	
Quartz, dumped	..	6	87	6.3	48	
		4	90	9.7	46	
		3	92	13.7	43	
		2	100	22.7	37	
Raschig rings, dumped	*B*	1 × 1	58	58	73	1,350
		1/2 × 1/2	49	132	68	11,000
		2 × 2	35	14.4	73	170
Raschig rings, packed	*B*	4 × 3	52	20	64	38
Partition rings (double-crossed partition), packed	*A*	6 × 6	64	18	54	8
same	*A*	3 × 3	80	37	42	70
Single spiral rings, packed	*C*	6 × 6	53	15	58	8
same	*C*	3 × 3	53	29	64	64
Triple spiral rings	..	3 1/4 × 3 1/4	55	37	60	55
"Propeller" twisted prisms	*M*	6 × 6	40	16	78	13
Hollow balls	*E*	2 1/2	52	19	33	140
"Hechenbleikner" blocks, packed	*H*	6 × 6 × 6	52	14	62	8
"Hexahelix" units, packed	*F*	4 × 4	60	20	60	28
"Prym" triangles, packed	*N*	3 1/4 × 3 1/4	60	40	72	55
Stoneware single-partition rings, packed	..	1 × 1	35	66	92	1,145
Metal Lessing rings, dumped	*I*	2 × 2	...	37	95	160
		1 × 1	...	74	93	1,300
		1/2 × 1/2	...	130	91	9,000
"Bregeat" wire spirals	*G*	1/2 × 7/8	57	144	83	9,350
		1 1/4 × 1 1/4	45	81	91	620
Vertical tubes	..	1 in. diam. on 1 3/8 in. centers	...	40		
		1/2 in. diam. on 11/16 in. centers	...	160		
Berl saddles	*D*	1.0	...	79	75	2,260

to gas flow than 3-in. spheres, and yet the percentage of free volume is the same for both, providing the arrangement of the

packing is the same. The packings with the larger percentages of free volume usually give the lower pressure drop per foot of height, but since the tower height will usually be greater for these packings, the advantage may not be so great as would be expected. The data on surface per cubic foot of tower volume are roughly indicative of the absorption capacity, but the values given are for dry packing, and are much larger than the active wetted area, as discussed below. The stability of the packing, or angle of repose of a pile, is of importance in designing the tower shell. Some of the larger cylindrical and rectangular shapes are practically self-supporting, and exert little side thrust on the walls.

Possibly the most popular packing is the hollow cylinder or Raschig ring. These are made of glass, carbon, ceramic material, or metal. They are usually "dumped" into the tower, although the larger sizes may be "packed" in regular horizontal tiers or courses. Packing is usually reserved for the larger spiral and partition tiles. Raschig rings, Lessing rings, and other cylindrical pieces are almost always made with height equal to diameter. When dumped into the tower the mass is homogeneous and there is little tendency for channeling of either gas or liquid stream. Packing constructed of slats, tiles, or glass plates on edge have both high surface per cubic foot and high free volume, but are not so widely used as Raschig rings because of the labor of stacking and the channeling resulting from broken units. In comparing first costs of packing the installation costs should always be included. The shape of the individual piece will sometimes suggest the likelihood of the liquor following its natural tendency of working over to the walls of the tower (see below). Stacked or packed hollow cylinders, for example, provide little opportunity for the liquor to work sidewise in the tower, whereas dumped packings provide the liquor with a possible velocity component toward the wall.

The mechanical-energy loss corresponding to the pressure drop of the gas goes partly to turbulence and partly to true skin friction. In a packed tower most of the loss is in turbulence, since the gas changes direction so frequently. Either increased turbulence or increased skin friction tends to thin the surface-air film and promote interphase diffusion, but experience in heating air with heating surfaces of various shapes shows clearly that a

given energy loss due to skin friction is more efficient in promoting heat transfer than is the same loss due to turbulence in the main body of the gas. By analogy, therefore, it would appear that the best packings might be those for which the pressure drop due to skin friction is high compared to that due to turbulence. This is true in streamline sections, in which the gas does not change direction, and high coefficients are obtained by using high gas velocities. A simple packing meeting these conditions is a bundle of vertical tubes without headers, with spacers to maintain passages between the tubes having the same hydraulic mean radius as the interior of the tubes. A preliminary test of this packing has been made by the author, and it was found to give excellent capacity coefficients with very low pressure drop.

LIQUOR DISTRIBUTION IN PACKED TOWERS

The grouping of the coefficient K_G or K_L with the area factor a is convenient in the case of packed towers because of the difficulty of measuring either quantity separately. The two are equally important, however, and the variables influencing the latter are well worth consideration. The factor a is defined as the square feet of active wetted surface per cubic foot of packed volume. It is necessarily an average value, since the degree of wetting of the packing varies from point to point within the column. It is by no means proportional to the total surface of dry packing, although the smaller packing sizes will naturally tend to give more wetted surface per unit volume. This lack of proportionality is due primarily to three causes: (*a*) uneven distribution of liquor over the cross section of the column, (*b*) failure of the liquid to wet all of the individual particle, and (*c*) inactive surface at points of contact of packing particles, at which the liquor remains stagnant and soon becomes saturated with solute.

An experimental study of liquor distribution over various packings has been reported by Baker, Chilton, and Vernon[12] in a recent paper. These investigators passed air and water through a number of common packing materials, and collected the water draining from the bottom at each of several small cross-sectional areas of the column. By using various heights of packing they obtained data indicating the liquor distribution over the tower cross section at different distances from the top. In all tests they used a water rate of 500 lb./(hr.) (sq. ft.).

With packing particles large compared to the tower diameter, the data confirmed the previous results of Kirschbaum[109] in showing a marked tendency for the liquor to concentrate near the walls and for the center of the column to run nearly dry. With large ratios of tower diameter to packing size, this tendency was negligible. For example, in a 6-in. column in which water was fed through a single central-point inlet over 1/2-in. broken-stone packing, the water had assumed a fairly uniform distribution at a point 4 ft. from the top, and the distribution did not change appreciably between points 4 and 15 ft. from the top. When the same packing was used in a 3-in. column, however, over 70 per cent of the water was found in the 25 per cent of the cross section adjoining the wall, at the same elevation 4 ft. from the top. Using a 3/4-in. broken-stone packing, definite segregation of water near the wall was observed when using the 6-in. tower. Baker, Chilton, and Vernon conclude that reasonably uniform liquor distribution is obtained with either regular or irregular solid packing materials, providing the ratio of tower diameter to packing size is greater than 8 to 1. When this ratio was greater than 8 they found that multiple-point liquor distribution at the top improved the uniformity of flow only in the top 4 ft. of packing of the 3-in. and 6-in. towers. With a 12-in. tower, using 3/4-in. spheres and a central-point liquor feed, uniform distribution was not obtained until a depth of nearly 10 ft. was reached. This result indicates the necessity of proper feed distribution in the larger towers, in which channeling due to poor initial distribution would be serious unless the tower were very tall.

In tests with fabricated rings and other hollow packing, the results were similar to those obtained with solid packings in that the water was driven to the walls of the column if the ratio of column diameter to particle size was small. With 1-in. Lessing rings in a 12- or 24-in. tower fairly uniform liquor distribution was obtained, although multiple-point feed distributors were found to be necessary. Variations in gas or vapor velocity were found to have little effect on liquor distribution in the packing except as the flooding point was approached, when more even distribution was obtained. Changes in liquor rate over the ordinary range had but little effect on the uniformity of distribution.

In the absorption of a very soluble gas from a dilute mixture with other inert gases it is sometimes desirable to operate with a

very low liquor-gas ratio. With a reasonable gas rate the liquor rate per square foot of tower cross section will then be very low and uniform distribution of the liquor feed over the packing almost impossible. One solution of this difficulty, as described above, is to recirculate the solution through the tower, returning several times as much liquor as is actually fed to the system. This has the disadvantage that the average liquor strength throughout the tower is increased, and the gas leaving is not in contact with fresh solvent. For a specified recovery the tower must then be larger. Another method is to flood the tower at intervals with accumulated feed liquor, allowing the gas to react with the liquor draining from the packing while another liquor-feed charge is collecting. This intermittent feed method requires a special feed device.

Even when the liquor is flowing over the packing with a uniform distribution over the tower cross section there is no guarantee that the packing surface is thoroughly wetted. The extent to which the packing is wetted has been the subject of an ingenious study by Mayo, Hunter, and Nash.[142] These investigators employed a small tower packed first with 1/2- by 1/2-in. and then with 1- by 1-in. Raschig rings made of paper, and circulated water containing a red dye. After running the apparatus for 10 or 15 min., the liquor feed was stopped, the packing removed, dried, and the wetted surface estimated by measuring the colored areas of the paper. The rings were made of double thicknesses of paper, so that they might be divided and the dyed areas measured on both inner and outer surfaces of the cylinders. The tower was fitted with a paper liner, so that the wetted surface of the tower wall could be measured. In many ways their results substantiate the work of Baker, Chilton, and Vernon described above.

Since they used a perforated-plate distributor for the feed, the uniformity of distribution was best near the top of the tower. Using 1/2-in. rings, the surface was almost perfectly wetted at the top of the tower, but the percentage of surface wetted fell off to about 40 below a point 9 in. from the top, being very nearly the same for both inside and outside surfaces of the rings. Below the same point the tower surface was 60 per cent wetted. In the packing itself the percentage of the surface wetted was greatest near the walls, although this tendency toward nonuniformity of

distribution did not increase below a point a few inches from the top. The percentage of total surface wetted increased steadily as the liquor-feed rate was increased up to the flooding point, being 70 per cent for the 1/2-in. rings and 45 per cent for the 1-in. rings for a water rate of 8,300 lb./(hr.)(sq. ft.) at a point two ring diameters from the top of the tower. The gas rate had no measurable effect on the wetted surface, up to the flooding point.

These results emphasize the point that the surface of the packing is only partially wetted, even though the liquor is flowing over the packing with a uniform distribution over the cross section of the tower.

The third factor listed above as influencing the factor a, namely, the extent to which the wetted surface may be inactive owing to stagnant liquid films at points of contact of the packing, has not been the subject of a quantitative study. Mayo, Hunter, and Nash estimate that some 10 per cent of the actual wetted surface may be inactive for this reason.

PRESSURE DROP THROUGH PACKINGS

Apart from general maintenance, the power required to force the gas up through the packing frequently represents the principal operating cost of a packed tower. The power cost is proportional to the product of the gas rate and the pressure drop through the tower, so data on pressure drops at various gas rates are of first importance for design purposes. The data available are not sufficient to give a really satisfactory correlation, but may be used as a basis for most engineering computations.

Chilton and Colburn,[34] in 1931, made an excellent survey of the data then available, and added certain new data on various solid packings, mostly of small sizes. They pointed out that most of the pressure drop is due to contraction and expansion losses in the gas flow through the irregular orifices formed by the packing particles, and estimate that only some 10 per cent of the drop is due to true skin friction. Contraction losses, expansion losses, and skin friction are all proportional approximately to the square of the gas rate, so an empirical correlation based on the Fanning equation for friction in pipes is not unsound. The relation is written

$$\Delta P = \frac{2f' A_w A_p A_L \rho u_0^2 h}{g d_p} \tag{129}$$

where ΔP = pressure drop in the height h.
u_0 = linear velocity of the gas based on the total cross section of the tower.
ρ = gas density.
A_w = "wall-effect factor."
A_p = a correction factor for hollow packing.
g = acceleration due to gravity.
d_p = nominal particle size of the packing.
A_L = a correction for the wetting of the packing by the solvent circulated; unity for dry packing.

Figure 40 shows Chilton and Colburn's correlation for solid particles, in which the friction factor f' is plotted *vs.* a modified

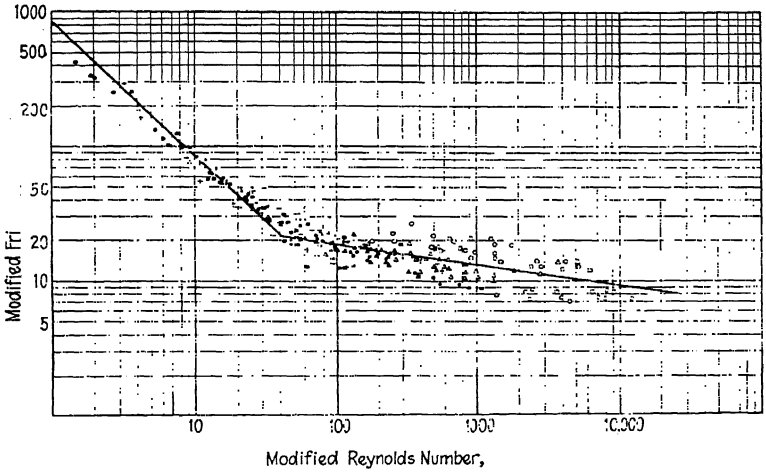

FIG. 40.—Correlation of friction factors for solid-packing particles.

Reynolds number $d_p u_0 \rho/\mu$, following the method of plotting commonly used for friction in pipes. The pipe diameter is replaced by nominal particle size as being more convenient for calculations than the diameter corresponding to the mean hydraulic radius of the irregular gas passage. Equation (129) is dimensionally sound, and both f' and $d_p u_0 \rho/\mu$ are dimensionless, so any consistent set of units may be employed. In English units (pounds, feet, seconds) ρ/μ for air 70°F. and 1 atm. is 6,170, from which $d_p u_0 \rho/\mu$ may be obtained by substituting d_p in feet and u_0 in feet per second [cu. ft./(sec.)(sq. ft. of tower cross section)].

The figure shows the correlation to be not particularly good, but it must be remembered that the plot includes data[25,66,16,6] on irregular-shaped broken particles as well as geometrically similar shapes such as spheres. The solid line passing through the band of points is recommended for *dry solid particles.* The two branches of the curve are typical of friction-factor plots, the left branch with a negative slope of 1.0 representing the viscous-flow region in which ΔP varies as the first power of u_0, the first power of μ, and inversely as the square of d_p.

When large particles are packed in a small tower, as, for example, when 2-in. spheres are placed in a 6-in. cylindrical tower, the region near the walls has a higher fraction voids than in the main body of the packing, and the gas passage near the walls will have a larger mean hydraulic radius. The actual velocity of the gas will be greatest at the walls, and the gas flow through the main mass of packing will be slower than if this "wall effect" were not present. Consequently, the pressure drop through such a column will be considerably less than in a tower where the ratio of particle size to tower diameter is small. This effect is allowed for by the "wall-effect factor," A_w, which is unity for a larger tower packed with small particles. In plotting Fig. 40, Chilton and Colburn used the values of A_w computed by Furnas[66] and plotted in Fig. 41 as A_w *vs.* the ratio of particle diameter to tower diameter. This plot should be used in connection with Fig. 40 for computing pressure drops in small towers. The upper curve applies below $d_p u_0 \rho/\mu = 40$, and the lower curve should be used when $d_p u_0 \rho/\mu$ is greater than 40.

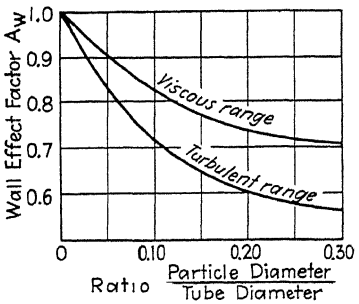

FIG. 41.—Wall-effect factor [Eq. (129)].

As would be expected, the pressure drop through beds of hollow particles, such as Raschig rings, is much less than for solid particles of the same nominal sizes. Using the data of Blake[16] and of Arnould,[6] Chilton and Colburn showed the pressure drop for 1-in. Raschig rings to be only 26 to 28 per cent of that for 1-in. solid particles, but gave no general correlation for rings or other

hollow particles, because of the lack of data. Since the appearance of their paper, White[193] has published data on hollow rings of various sizes and suggests the use of a factor A_p by which the calculated pressure drop for solid particles should be multiplied to obtain the pressure drop for hollow particles of the same nominal size. For hollow particles the wall-effect factor A_w may be expected to be less important than for solid particles, and was taken as unity by White in correlating the available data. Figure 42 shows the data collected by White, replotted as A_p *vs.* d_p. The various data on dry rings and Berl "saddles,"[13] corrected by the use of this plot of A_p, fall in a narrow band along the

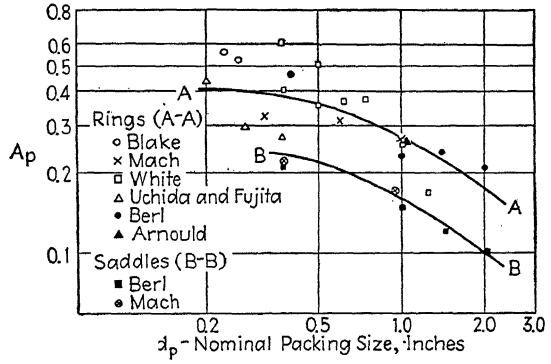

FIG. 42.—Correction factor A_p for rings and Berl saddles (dumped). In using this plot A_w should be taken as 1.0.

Chilton and Colburn line of Fig. 40. The data cover cylindrical (Raschig) rings from 1/4 to 2 in., and three sizes of rings with single internal webs (Lessing rings). Mach[134] used carbon dioxide and illuminating gas, as well as air. The data of Arnould[6] shown on Fig. 42 have been added to White's original plot.

The early data of Zeisberg[200] cover a variety of commercial packings, but are reported in terms of a factor analogous to f' and the range of gas velocities covered is not given. His results have been compared with Chilton and Colburn's curve on the assumption that they apply at a superficial velocity of 1 ft./sec., and the resulting values of A_p tabulated in Table VIII. For the solid packings A_p should be 1.0 by definition, and the poor agreement for the 2-in. quartz and 3-in. coke is evident from the

table. The values of A_p for the hollow packings run considerably higher than those plotted in Fig. 42 for rings, and should be used in preference to the latter plot only for the diaphragm and spiral rings.

TABLE VIII.—DATA OF ZEISBERG

Packing	A_p, dry			A_L Water circulation 660 lb. (hr.) (sq. ft.)		
	Dumped	Stacked	Packed	Dumped	Stacked	Packed
Quartz, 6 in.	1.05	....	....	1.03	....	....
Quartz, 3 in.	0.80	....	....	1.38	....	....
Quartz, 2 in.	1.92	....	....	1.12	....	....
Quartz, 1/2 in. to 1 in.	1.10	....	....	1.63	....	....
Coke, 3 in.	0.60	....	....	1.23	....	....
4-in. × 3-in. smooth diaphragm rings.	0.50	0.24	....	1.23	1.52	....
3- × 3-in. corrugated diaphragm rings.	0.40	0.24	0.20	1.23	1.87	1.08
3-in. × 3-in. corrugated spiral rings.	0.35	0.43	....	1.40	1.13	....
6-in. × 6-in. corrugated spiral rings.	....	0.69	0.43	....	1.31	1.46
6-in. corrugated Hechenbleikner blocks	0.29	0.64	0.47	2.25	1.08	1.08
1-in. Raschig rings	0.8	....	....	1.0	....	....
Tile on edge, staggered 6.4 sq. ft./cu. ft.	....	....	....	....	....	1.72
Tile on edge, staggered 10.5 sq. ft./cu. ft.	....	....	....	....	....	1.39
Tile on edge, staggered 14.0 sq. ft./cu. ft.	....	....	....	....	....	1.72

Summarizing the data for dry packing, Fig. 40 may be employed to obtain the factor f' to be used in Eq. (129). For solid particles, the wall-effect factor is obtained from Fig. 41, and A_p taken as unity. For hollow particles the wall-effect factor A_w is taken as unity and A_p obtained from Fig. 42. By definition, A_L is 1.0 for dry packing.

In the ordinary operation of a packed tower the liquid circulated over the packing occupies an appreciable fraction of the voids and reduces the mean free cross section open to passage of the gas. At a constant superficial gas velocity, therefore, the actual gas velocity is increased, and the pressure drop is appreciably greater than when the packing is dry. This was shown by the early data of Zeisberg, who found that for small particle sizes, the pressure drop through packing wet, but with no liquid circulating, was nearly three times as great as when the same

packing was dry. The effect was found to be small, however, for particle sizes above 2 in. Zeisberg also obtained data for various packings with liquid being circulated at the rate of

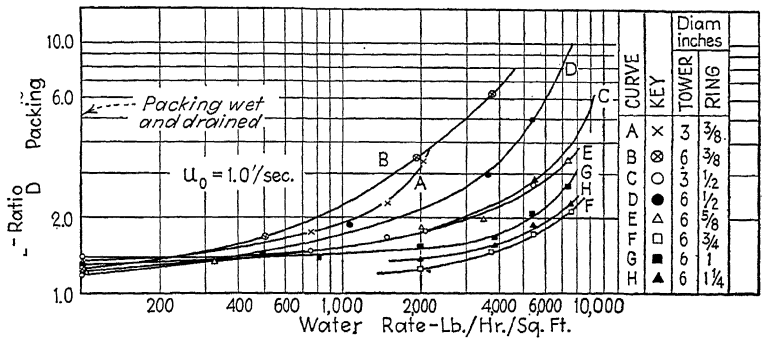

FIG. 43.—Effect of liquid rate on pressure drop through dumped ring packings at a superficial gas velocity of 1.0 ft./sec.

660 lb./(hr.)(sq. ft.) but does not report the gas rates. Apparently the only data with known liquor and gas rates are those for hollow cylinders reported by White,[193] and a few data by Arnould for rings, triangles, and spirals.

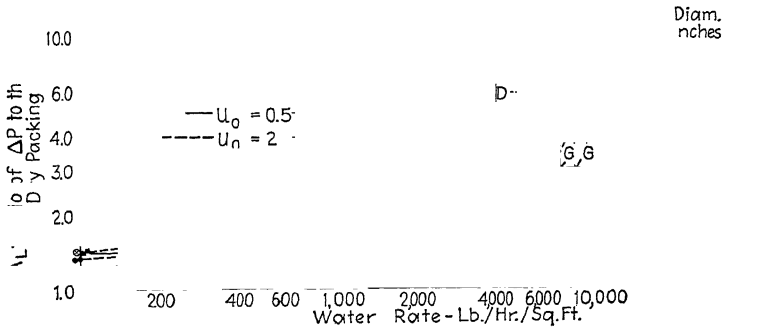

FIG. 44.—Effect of liquor rate on pressure drop through dumped ring packings at superficial gas rates of 0.5 and 2.0 ft./sec.

White's data have been replotted as A_L *vs.* liquor (water) rate, as shown in Figs. 43 and 44. A_L represents the ratio of the observed pressure drop to that obtained with the same packing dry, and at the same gas (air) velocity. The points at the

extreme left represent packing wet and drained, with no water actually being circulated. At the extreme right the curves turn up sharply and if continued would be asymptotic to the abscissa representing the flooding velocity. In general, A_L decreases with increased particle size and increases with liquor rate. It increases sharply as either gas or liquor velocity corresponding to flooding conditions is approached. For the larger particle sizes A_L is almost independent of gas velocity in the range covered, but for the smaller sizes it increases with gas velocity. It is somewhat larger for large towers than for small towers containing the same size packing, although this effect is probably important only for ratios of tower to particle diameters less than 10.

Values of A_L from Zeisberg's data for a water rate of 660 lb./(hr.)(sq. ft.) are given in Table VIII and are seen to be in general agreement with the curves of Fig. 43 for packings of similar sizes.

Arnould found values of A_L from 1.6 to 1.8 for 1-in. rings at a liquor rate of 750 lb./(hr.)(sq. ft.). For these conditions White obtained values of 1.3 to 1.5, as shown by Fig. 44. For 1-in. triangular rings at a liquor rate of 1,850 Arnould obtained A_L = 1.2 to 1.5. The effect of liquor rate was much greater with 1-in. wire spirals, A_L being from 2.7 to 4.7 at a liquor rate of 1,230, but decreasing with increased air flow.

It should be emphasized that the data on A_L plotted in Figs. 43 and 44 are for water only and do not apply when the liquor circulated is viscous or has physical properties differing widely from those of water.

Illustration 17.—Estimate the pressure drop through 10 ft. of packing in a tower 1 ft. in diameter packed with 1-in. Raschig rings. Assume the gas to be air at 70°F. flowing at a superficial velocity of 1.2 ft./sec. and the liquor to be practically pure water flowing at the rate of 1,200 lb./(hr.)(sq. ft.) of tower cross section.

Solution.—Referring to Eq. (129), u_0 is 1.2 and g is 32.2. The abscissa of Fig. 40 is $6{,}170 \times 1/12 \times 1.2 = 617$. From Fig. 40, f' is 15, and A_w is taken as 1.0 for hollow packings. A_p is 0.27 from Fig. 42, and A_L is 1.4 from Figs. 43 and 44. Hence,

$$\Delta P = \frac{2 \times 15 \times 1.0 \times 0.27 \times 1.4 \times 0.075 \times 1.2^2 \times 10}{32.2 \times \frac{1}{12}}$$

$$= 4.6 \text{ lb./sq. ft.}$$

$$= 4.6 \times \frac{12}{62.3} = 0.88 \text{ in. water}$$

PRESSURE DROP IN WOOD GRID PACKINGS

The recent data of Johnstone are available for the estimating of pressure drop in gas flow through various types of wood grid and corrugated-sheet packings. The results may be summarized in the form of a table of values of the constant f_0 in the equation

(130)

TABLE IX.—DATA OF JOHNSTONE ON PRESSURE DROP FOR AIR FLOW THROUGH VARIOUS SHEET AND GRID PACKINGS

Type of packing	Height, in.	Pitch, in.	Arrangement	$f_0 \times 10^8$ [see Eq. (130)]
Wood grids	1	0.625	Staggered	21.4
Wood grids	1	0.625	Nonstaggered	18.9
Wood grids	2	0.625	Staggered	14.6
Wood grids	2	0.625	Nonstaggered	13.7
Wood grids	4	0.625	Staggered	10.2
Wood grids	4	0.625	Nonstaggered	8.3
Wood grids	8	0.625	Staggered	6.4
Wood grids	8	0.625	Nonstaggered	5.7
Wood grids	4	1.25	Nonstaggered	2.43
Wood grids	8	1.25	Nonstaggered	79
Wood grids	4	1.75	Staggered	75
Wood grids	4	1.75	Nonstaggered	73
Wood grids	12	1.25	Nonstaggered	20
Wood grids	16	1.25	Nonstaggered	17
Wood grids	8	1.75	Nonstaggered	16
Wood grids	8	1.75	Staggered	04
Wood grids	12	1.75	Staggered	0.99
Wood grids	12	1.75	Nonstaggered	0.95
Wood grids	16	1.75	Nonstaggered	0.87
Wood grids	16	1.75	Staggered	0.82
Wood grids	4	2.25	Nonstaggered	0.87
Wood grids	8	2.25	Nonstaggered	0.68
Wood grids	12	2.25	Nonstaggered	0.63
Wood grids	16	2.25	Nonstaggered	0.61
Smooth sheets	96	1.0	Parallel	0.21
Smooth sheets	96	2.0	Parallel	0.124
1¼-in. corrugated sheets	96	1.0	Parallel	2.11
2⅝-in. corrugated sheets	96	1.0	Parallel	1.88
2⅝-in. corrugated sheets	96	2.0	Parallel	1.07
2⅝-in. corrugated sheets	96	3.0	Parallel	0.56

where Δh = pressure drop as inches of water per foot of height.
G = superficial mass velocity of the gas as lb./(hr.) (sq. ft. total cross section).

The data obtained cover the range of G from 700 to 4,400, for air flowing at 55 to 85°F. over grids wet with water circulated at 0.08 to 0.136 g.p.m. per ft. of wetted perimeter. The various grids were made of wood 1/4 in. thick, arranged vertically in different ways. By "pitch" is meant the horizontal distance or clearance between parallel grids. The "height" is the height of each individual grid. The successive sections were placed one above the other so that the grids were at right angles to those in the adjacent sections. The alternate sections were said to be arranged in a "staggered" or "nonstaggered" fashion, respectively, according to whether each grid fell directly in the middle of the next parallel channel, or directly over the grids in the parallel sections. This nomenclature is used in Table IX, which gives the values of f_0 obtained from Johnstone's data.

ALLOWABLE LIQUOR AND GAS RATES IN PACKED COLUMNS

As pointed out in a previous section, the height of an absorption tower determines its absorption efficiency, and the cross section determines the capacity, or the quantity of gas which can be treated. For design purposes it is obviously important to have information on the allowable gas and liquor rates per square foot of tower cross section.

In packed towers the gas and liquor rates are limited by the tendency of the column to flood. As either liquor or gas velocity is increased, the liquid hold-up in the packing increases, the free area for gas flow decreases, and the pressure drop through the column increases (see Fig. 42). A point is finally reached when the gas bubbles violently through the liquid, the pressure drop rises extremely sharply with the slightest increase in gas velocity, and much liquid is carried off mechanically by the gas leaving the top of the packing. This point is called the flooding point and is determined by both gas and liquor rates. At any given gas rate there is a definite liquor rate above which the column will flood. Similarly, at any given liquor rate there is a definite gas rate above which the column will flood.

"Loading point" and "load point" are sometimes used synonomously with "flooding point." White, however, defines the

"loading point" as the point above which the pressure drop becomes proportional to an exponent greater than 2.0 on the gas rate. As gas or liquor rate is increased, the loading point is reached somewhat before the flooding point. White recommends operating slightly below the loading point and well below the flooding point. The best operation should be determined by an economic balance of the costs involved, since power for the blower, as well as height and cross section of the tower are all involved. As a rough rule it is suggested that the operation should be such

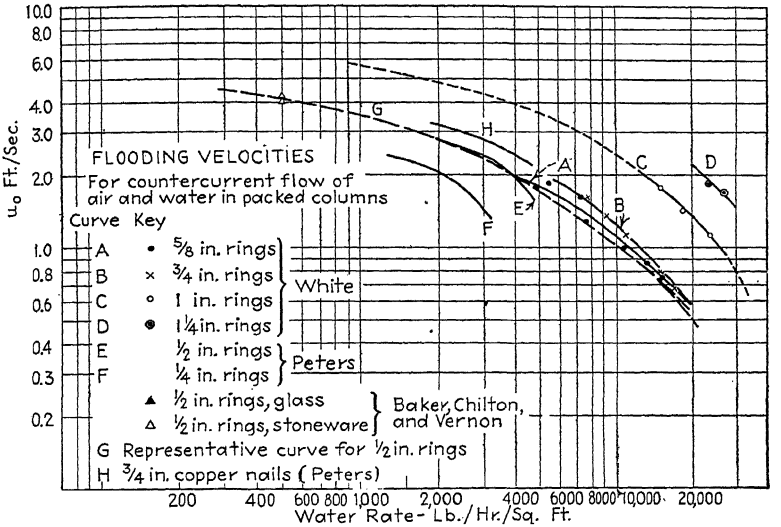

FIG. 45.—Flooding velocities for ring packings.

that A_L is less than 2.0. Referring to Fig. 43 it will be seen that this corresponds to operation safely below the flooding velocity, since the vertical asymptotes to the curves plotted represent the liquor rates corresponding to the flooding point.

Actual data on flooding velocities are not plentiful. Those of White[193] and of Peters[153] plotted in Fig. 45 as superficial gas velocity, u_o, *vs.* liquor rate, are seen to be in good agreement. Two points of Baker, Chilton, and Vernon are used to extend the representative curve for 1/2-in. rings, shown dotted (curve *G*). Higher gas and liquor rates are required to produce flooding in the larger sizes of packings, as would be expected. The data

TABLE X.—CHARACTERISTICS OF VARIOUS PACKINGS, AND FLOODING VELOCITIES (AIR) WITH WATER CIRCULATION OF 500 LB./(HR.)(SQ. FT.)

Packing	Nominal size, in.	Apparent density lb./cu. ft.	Hold-up with no circulation. Water volume as a percentage of tower volume	Pieces per cu. ft.	Mean dimensions, in.	Estimated surface, sq. ft./cu. ft.	Percentage voids	Superficial air velocity at flooding point, ft./sec.	Remarks
Broken stone	1/4	95.5	6.1	67,700	0.5 × 0.3 × 0.15	150	41	1.5	Carefully screened
Broken stone	1/2	90.5	4.7	14,750	0.87 × 0.43 × 0.25	94	43	2.8	Carefully screened
Broken stone	3/4	88.3	3.3	3,560	1.24 × 0.67 × 0.55	52	54	3.6	Carefully screened
Clay spheres	1/2	84.9	3.8	20,200	0.457	92	46	2.3	Uniform
Clay spheres	3/4	81.2	2.6	4,700	0.736	57	51	3.2	Uniform
Clay spheres	1	77.1	2.0	1,950	0.99	41	50	4.7	Uniform
Jack chain	3/16	104.4	....	3,900 linear ft.	.....	198	79	5.3	
Carborundum	1/2	59	12.1	7,360	1 × 0.375	...	60	4.3	Fairly uniform
Glass rings	1/4	34.5	3.2	77,250	0.27 × 0.27	188	75	4.1	Uniform
Glass rings	1/2	26.5	1.2	16,000	0.45 × 0.45	133	82	4.2	Uniform
Bregeat spirals	1/2	57.2	3.3	9,350	0.875 × 0.5	144	83	7	1/16-in. wire—4 spirals
Bregeat spirals	1 1/4	45.2	1.6	620	1.25 × 1.25	81	91	12	
Lessing rings	1	35.0	0.5	1,145	1 × 1	66	92	4	
Stoneware rings	1/2	48.8	2.3	11,000	0.5 × 0.5	132	68	4	
Twisted fence wire	1/2	.....	....	103	0.5 × 36.0	43	..	25	

given by White show some evidence of a wall effect, the flooding point being reached sooner in large than in small columns with the same size packing. The data plotted were all obtained using air and water. Peters found that with alcohol the velocities necessary to produce flooding were appreciably greater than when using water in the same packing. The flooding velocities are doubtless related to liquid holdup, and for oils are probably less than for water.

In addition to the data shown in Fig. 45, there are available a few data reported by Baker, Chilton, and Vernon on the air rates

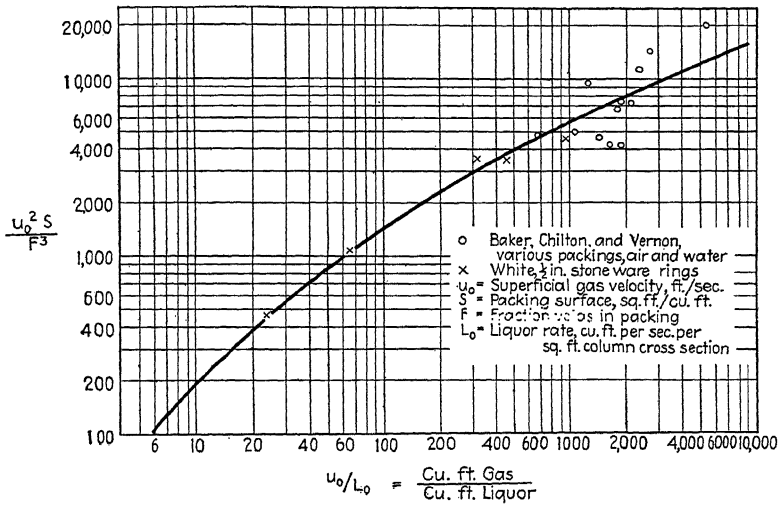

FIG. 46.—General correlation of data on flooding velocities for various packings.

at which flooding occurs in various packings over which water was circulated at the rate of 500 lb./(hr.)(sq. ft.). These are tabulated in Table X.

For various types of packings other than the rings covered by Fig. 45, an estimate of the flooding velocity may be obtained from Fig. 46, which is based on a method of correlation recently suggested. The abscissa is the volumetric ratio of gas to liquor, a quantity ordinarily fixed by the absorption conditions to be fulfilled. The ordinate is the square of the mean velocity through the packing divided by the hydraulic mean radius, and is written as $u_0^2 S/F^3$, where u_0 is the superficial gas velocity, feet per

second, S is the packing surface per cubic foot of tower volume, and F is the fraction free space in the packing. The circles represent the data of Baker, Chilton, and Vernon given in Table X, and the crosses represent the data reported by White for 1/2-in. stoneware rings.

PLATE TOWERS

Plate towers are frequently employed in cases where the solvent and gas are noncorrosive and ordinary steel construction is satisfactory. Their use is borrowed from distillation practice and they are operated very much like rectifying columns. The gas to be treated enters at the bottom, passing up through the tower

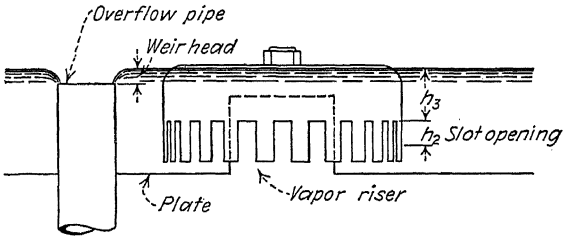

FIG. 47.—Diagrammatic sketch of plate and bubble cap.

and bubbling through the liquid on each plate. The solvent is fed at the top, and overflows from plate to plate through vertical overflow pipes connecting each plate with that next below. Figure 47 shows a diagrammatic sketch of a plate and a single bubble cap. Although some columns are built with a single large cap as much as 2 ft. in diameter, it is more common to have a number of small 4- to 6-in. caps on each plate. The gas from below enters the caps through the risers, and depressing the liquid level inside the caps, escapes into the liquid on the plate through the notches cut in the periphery of each cap. The gas passes through these notches at high speed and passes into, and up through, the liquor pool in the form of irregular bubbles of all sizes and shapes. The gas is broken up into sufficiently small bubbles so that the interphase surface is large and rapid absorption is promoted. Furthermore, the violent agitation of the liquid and the escape of gas from its surfaces causes considerable

splashing, so that the gas space between plates operates as a spray chamber.

A wide variety of caps is available, from small 3-in. caps with vertical 3/16-in. notches, to large cast-iron hemispherical caps with 2-in. V-notches designed for use with slurries which would clog the small slots. In addition to caps, sieve and porous plates may be used to obtain a similar bubbling action. Sieve plates are metal sheets punched with small holes, and must be held absolutely level or serious channeling will result. Furthermore, they operate properly only within a rather narrow range of gas velocities. Porous plates are used for aerating sewage and are extremely effective in breaking up the gas into fine bubbles. Most of the pressure drop is through the plate and not through the liquid, so the importance of maintaining the plate level is not so great as for the sieve plates. Most porous plates now available give a high pressure drop. The overflow pipes dip into a liquid seal on each plate, but if the pressure drop through the plate is greater than the liquid head between plates, the vapor will go up the overflow pipes and the column cease to function. At a superficial velocity of 1.0 ft./sec. the pressure drop through a commercial "coarse" ceramic plate is about 25 in. of water, which means that the plates in the column would have to be spaced at least this far apart, making the tower very tall. The usual plate spacing is from 6 in. to 3 ft. depending on the tendency of the liquid to foam and splash from one plate to the next. In the larger columns the shell may be provided with manholes at each plate to allow occasional cleaning of the tower.

The liquid overflow pipes on successive plates are usually placed at alternate sides of the column. Thus the liquor overflowing from the plate above must pass across the plate to reach the overflow weir. Even with this arrangement there is some tendency for "short-circuiting" of the liquor directly from one overflow pipe to the next. This difficulty may be at least partially overcome by various baffle arrangements designed to guide the liquor across the plate.

At high gas rates in a plate column the mechanical entrainment of liquid from one plate to the next becomes serious, resulting in a dilution of the liquor which has just been concentrated. Data reported by F. J. Jenny and the author[167] show the quantitative effect of entrainment of water by air in an 18-in. column with

seven 4-in. caps placed on 5 1/4-in. centers. With a plate spacing of 9 in., the entrainment was found to be a little greater than 0.1 lb. water per lb. air at a superficial velocity of 3 ft./sec. It was shown that this amount of entrainment would have relatively little effect on the performance of the column. It seems probable that entrainment plays no important role in plate-column absorbers at any gas velocity below that at which the column ceases to function because of priming (foaming of the liquid up through the column from one plate to the next), or because of liquor backing up the overflow pipes.

The liquor rate in a plate tower is limited by the capacity of the overflow pipes. For high liquor rates several overflow pipes may be installed, although "short-circuiting" of the liquor across the plate may be more serious when the distance traveled by the liquor is small. For the absorption of light hydrocarbons from lean refinery gases the oil rates are frequently very high, and a special design may be employed in which each cap has an overflow pipe at its center. This arrangement not only provides capacity for a high liquor rate, but forces the liquor to flow radially toward the center of the cap, passing directly over the stream of bubbles rising from the submerged outer periphery of the cap.

COMPARISON OF PLATE AND PACKED TOWERS FOR GAS ABSORPTION

The relative merits of the plate tower and packed tower for a given purpose are properly determined only by comparison of the cost figures resulting from detailed designs for each type. However, it may be worth while to summarize in a general way their relative advantages and disadvantages. This may be done briefly as follows:

1. For acids and other highly corrosive solutions the packed tower is simpler and cheaper to construct than the plate tower built of glass, acid-resisting alloy steel, or other material.

2. The pressure drop of the gas in passing through the packed tower can be considerably less than for a plate tower designed for the same duty.

3. The plate column avoids serious channeling difficulties of gas and liquor streams.

4. The plate column can be designed to handle liquor rates which would flood the ordinary packing.

5. A plate tower fitted with manholes can be cleaned of accumulated sediment which would clog many packing materials and make necessary costly removal and refilling of the tower.

6. The plate tower lends itself readily to cooling of the liquor to remove a large heat of dilution, either by cooling coils on the plates or by external coolers through which the liquor is passed in flowing from one plate to the next.

7. The liquor holdup in the packed tower is considerably less than in the plate tower.

8. The total weight of the plate tower is usually less than for the packed tower designed for the same duty.

9. Temperature changes are apt to do more damage to the packed tower than to the plate tower.

PRESSURE DROP AND LIMITING VELOCITIES IN PLATE COLUMNS

Although large pressure drop is one of the principal disadvantages of the plate column, there is little published information on the subject. Referring to Fig. 47, it is evident that the total pressure drop incurred by the gas or vapor in passing from one vapor space to the next should be the sum of:

1. The loss in the riser (vapor nipple) and cap, h_1.

2. The depression of the liquid inside the cap, equal to the vertical slot opening, h_2.

3. The liquid level above the top of the slots, h_3, corresponding to the conditions of no gas flow.

There is no question but that the first is negligible in ordinary designs. The second has been obtained experimentally by Griswold[73] and by Rogers and Thiele,[160] and correlated on the basis of a modified orifice equation. Griswold gives

$$h_2 = 1.81 V_s^{\frac{2}{3}} \left(\frac{\rho_2}{\rho_1}\right)^{\frac{1}{3}} \text{in.} \tag{131}$$

for rectangular slots, and for similar slots Rogers and Thiele give

$$h_2 = 2.08 V_s^{\frac{2}{3}} \left(\frac{\rho_2}{\rho_1 - \rho_2}\right)^{\frac{1}{3}} \text{in.} \tag{132}$$

For triangular slots the last authors give

$$h_2 = 2.25 \left(\frac{V_s'}{\alpha}\right)^{0.4} \left(\frac{\rho_2}{\rho_1 - \rho_2}\right)^{0.2} \text{in.} \tag{133}$$

where ρ_2 = density of the gas.
ρ_1 = density of the liquid.
V_s = gas rate, cu. ft./(min.)(in.) of slot width.
V_s' = gas rate, cu. ft. per min. per slot.
α = ratio of maximum slot width to total slot height for triangular slots.

Both equations apply only when the slots are not fully opened.

The liquid level above the top of the slots is the vertical distance from the top of the slots to the overflow weir edge, plus

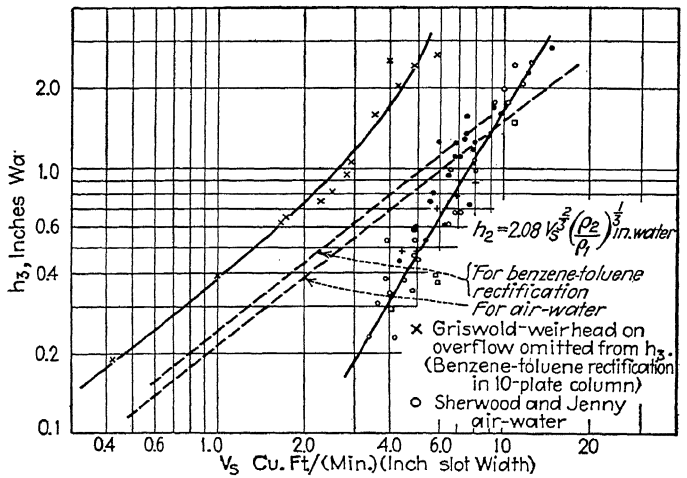

FIG. 48.—Data on pressure drop through slots in bubble cap.

the weir head. The first is fixed by the design, and the second may be estimated roughly from the known liquor rate using the weir formula, although no adequate study of the usual circular weirs has been made.

Actually, it is found that the calculated pressure drop cannot be relied on with any assurance, as indicated by the data of Griswold,[73] and of Jenny,[167] plotted in Fig. 48. The top curve represents the observed pressure drop per plate in Griswold's experimental column, less the vertical distance from the top of the slots to the weir edge. The ordinate should represent the weir head plus the slot opening, and does fall from 0.1 to 2.0 in. water above the calculated curve for the slot opening h_2. The discrepancy is greatest at the high vapor rates, where the weir

head would also be large. Griswold obtained these data in the course of making benzene-toluene rectification runs, in a 10-plate column 8 in. in diameter, with 6.4 sq. in. of column cross section per sq. in. of total slot area (wide open).

The lower solid curve represents the data of Jenny, obtained by blowing air through caps on a plate covered with water, but with no overflow. Since there was no weir head, h_3 represents the distance from the top of the slots to the liquid surface in the quiescent pool, and $\Delta p - h_3$ should check the calculated lower dotted curve. The necessary correction term is apparently negative, as suggested by Rogers and Thiele. Jenny's data are for 4-in. caps in an 18-in. column, and the points shown represent runs with liquid levels from 0.26 to 1.01 in. above the tops of the slots, with one, four, and seven caps per plate. The various arrangements corresponded to 55, 13.8, and 7.9 sq. in. column cross section per square inch total slot area (wide open).

Although the correlation obtained in Fig. 48 is not encouraging, it indicates that the equations for slot opening may be used as a means of obtaining an approximate value of h_2 in the estimation of the total pressure drop.

MISCELLANEOUS TYPES OF ABSORPTION EQUIPMENT

In addition to the more or less standard packed and plate towers, there are many other designs which have been used or proposed. Of these the spray tower is the most common. Most of the other miscellaneous types have been designed for special uses, and no attempt will be made to describe them in detail.

Spray towers are usually square or cylindrical empty towers made of concrete, steel, or masonry, and have the important advantage of operating with very low pressure drop. The absorbing liquid is sprayed in at the top and the gas to be treated enters at the bottom. Sprays are now available which distribute the liquor uniformly in a solid cone and lessen the tendency for channeling. Although it is desirable that the spray break the liquid stream into small drops, too fine a spray will result in excessive entrainment. With proper sprays the total interphase surface per cubic foot is doubtless greater than in most packed towers, but the tendency of the gas to pass up one side and the liquor spray down the other side may offset the advantage of the larger surface. Spray towers are common in the recovery of

ammonia from coke-oven gas, and are also used in making bleach for sulfite pulp by the absorption of chlorine in milk of lime. In the latter case the suspended material in the milk-of-lime solution would tend to clog an atomizing spray, so a coarse spray is produced by dropping a stream of liquor onto a bowl, the liquor being projected as a broken sheet from the edge. This same distributing device is sometimes used to distribute liquor at the top of a packed tower. Sprays are also commonly used for humidification and for spray-drying of liquids.

Where high pressure drop must be avoided, a modification of the plate tower called the "disk and doughnut" is sometimes used. Every other plate or tray is a plain horizontal plate with a large hole in the middle. The plates in between are horizontal disks supported in the center of the column, with diameters somewhat larger than the central holes in the other plates. The liquor cascades down the column, dropping through the large central hole of one plate onto the central disk below. From the periphery of the disk it then falls to the annular plate next below the disk, and so on. The liquor thus tends to fall from one plate to the next as a vertical cylindrical sheet, through which the gas must force its way. In the Schneible column tangential vanes are introduced to give the gas a swirling motion as it passes up the tower, thus improving the contact with the falling liquor.

The gas industry has contributed a wide variety of special types of absorption equipment, most of which are not of general applicability. For example, an English process for drying illuminating gas with glycerin employs a contact device consisting of a number of large parallel disks spaced a few inches apart and fitted to a horizontal shaft. The shaft rotates slowly, turning the disks through a bath of glycerin, the level of which is about even with the shaft. The gas is blown between the disks above the shaft, coming in contact with the surfaces wet with fresh absorbent each revolution. The various types of towers requiring mechanical drives to create the interphase surface have not proved generally popular since they require one drive in addition to the gas blower and liquor pump, and frequently consume considerably more power.

As pointed out in a previous chapter, the heat of solution of the gas being absorbed may be so large that its dissipation presents a serious problem. During the war mustard gas was produced

by the reaction of ethylene with sulfur chloride in large lead-lined reactors fitted with lead cooling coils. Absorption and reaction took place simultaneously, the ethylene being introduced through gas injector nozzles at the bottom of the reactor. The rate of absorption was limited by the rate at which the heat of reaction would be dissipated, since it was important to keep the temperature below about 40°C. until near the end of the operation. Although the absorption capacity was not high, the production was limited by the rate of heat transfer across the cooling surface. This situation is not uncommon in industrial practice where large heat effects are involved.

An important large-scale industrial absorption process in which large quantities of heat are liberated is the absorption of hydro-

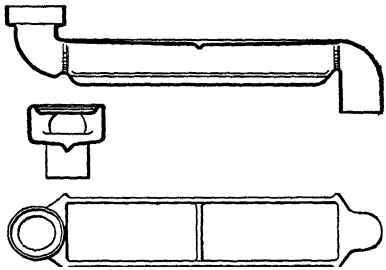

FIG. 49.—Tyler fused-silica absorption units, externally cooled.

chloric acid gas. This was formerly carried out in a series of stoneware tourills or Woulff bottles, acid being condensed and collected as well as absorbed by water flowing countercurrently. The absorption capacity of each tourill was small, and the heat dissipation to the surroundings was poor. Consequently, this system has been largely replaced by ring-filled packed towers with acid coolers between towers. The towers are constructed of stoneware sections packed with stoneware plain or spiral rings, and operated with countercurrent flow of gas and acid. The acid leaving the bottom of each tower passes to a vessel in which it is cooled by a stoneware cooling coil supplied with cooling water. The gas is drawn through the system by an exhaust fan, so placed to insure air leakage into the system rather than gas leakage out.

An alternative system for hydrochloric acid is the Tyler vitreosil absorber[64,183] illustrated in Fig. 49. Its construction is similar

to that of the ordinary trombone cooler, and cooling water cascades from one section to another over the outer surfaces. The gas to be absorbed passes inside these sections, coming in contact with acid retained in shallow pools in the recessed bottoms of each section. At the lower end of each section the acid overflows a dam and drops to the unit below. Because of the high thermal conductivity of the fused silica from which the sections are made, and the excellent heat-transfer coefficients on the outer surface, the cooling capacity of these units is high. The interphase surface for absorption is small, however, so that it is sometimes necessary to increase the absorption capacity by introducing a packing in short vertical sections between the horizontal units.

The Tyler system is one of many developed to accomplish simultaneous absorption of a gas and cooling of gas and liquor. Various other types have been proposed, some of which involve internally cooled packed or plate columns, etc. It should be clear that the most desirable system is that in which adequate cooling is provided for and in which the absorption capacity and cooling capacity are properly balanced to give the most economical operation.

Nomenclature for Chapter V

a = area of interphase contact, sq. ft./cu. ft. of packed volume.
A_L = correction factor [Eq. (129)] for wetting of packing by solvent circulated = unity for dry packing.
A_p = correction factor for hollow packing [Eq. (129)].
A_w = correction factor for wall effect [Eq. (129)].
d_p = nominal particle size of packing, ft.
f' = friction factor for gas flow through packing.
f_0 = constant in Eq. (130).
g = acceleration of gravity = 32.2 ft./(sec.)^2.
h_1 = pressure drop of gas flowing through riser (vapor nipple) and cap, in. of liquid.
h_2 = depression of liquid inside the cap equal to the vertical slot opening, in. of liquid.
h_3 = liquid level above the top of the bubble-cap slots, corresponding to conditions of no gas flow, in.
h = height of tower, ft.
Δh = pressure drop through wood grid tower, in. water/ft. height.
ΔP = pressure drop through packed columns in the height h, lb./sq. ft.
S = surface of dry packing per cu. ft. of tower volume, sq. ft./cu. ft. of packed volume.

u_0 = linear velocity of gas based on total cross section, ft./sec.
V_s = gas rate as cu. ft./(min.)(in. of slot width).
V_s' = gas rate as cu. ft./min. per slot.
α = ratio of maximum slot width to total slot height, for triangular slots.
ρ = gas density, lb./cu. ft.
ρ_2 = gas density, lb./cu. ft.
ρ_1 = liquid density, lb./cu. ft.
μ = gas viscosity, lb./(sec.)(ft.).

CHAPTER VI

PERFORMANCE OF ABSORPTION EQUIPMENT

As is common in many chemical-engineering problems, the design of absorption equipment involves data and calculations on three fundamental phases of the problem as a whole: the stoichiometry, relating the quantities of the materials; the equilibria involved; and the rate of the controlling process whether it be mass transfer or chemical reaction. The first requires the application of the laws of conservation of matter and of chemical combining weights, the second necessitates the availability of data on chemical equilibria as well as on physical equilibria between phases (solubility), and the third requires performance data in the form of capacity coefficients on the particular form of absorption equipment considered. The stoichiometry of absorption processes presents no serious difficulties to well-trained chemical engineers, although the importance of the conclusions which may sometimes be made on the basis of the stoichiometry alone is frequently overlooked. Most of the important equilibrium data are available in the literature, especially in the standard handbooks* of physical constants such as the International Critical Tables, and will not be reproduced here. Vapor-liquid equilibrium data for hydrocarbon systems are given in Table VI of Chap. IV. It is the purpose of the present chapter to present a summary of the more important of the available performance data on typical absorption equipment. Such data are not plentiful, and it is to be hoped that much more data on plant performance may become available in the future.

DATA ON WETTED-WALL COLUMNS

The performance of wetted-wall columns is of interest, not only because of the direct utility of the data in many problems of

* The first printing only of Perry's "Chemical Engineers' Handbook," in Section 10 on Gas Absorption, quoted the I.C.T. incorrectly. The numerical values of the Henry's law constant for a number of gases are quoted directly, but it is stated that these constants apply to Henry's law with pressure in *atmospheres*, whereas pressure in *millimeters of mercury* should be used.

engineering design, but because the results obtained with such columns throw light on the mechanism of mass transfer for the systems studied. The interfacial area is fixed and definite, and the turbulence conditions in the gas stream are standard and reproducible. In this connection the correlation of Gilliland's data on the vaporization of various liquids in a wetted-wall column have been presented in Chap. II. It will be recalled that for turbulent flow of gas through a round pipe, Gilliland's data were represented by the equation

$$\frac{d}{x} = 0.023\left(\frac{du\rho}{\mu}\right)^{0.83}\left(\frac{\mu}{\rho D}\right)^{0.44} = 0.023\left(\frac{dG}{\mu}\right)^{0.83}\left(\frac{\mu}{\rho D}\right)^{0.44} \tag{58}$$

where d represents the diameter of the tube, D the diffusivity for the system, μ, ρ, and u the viscosity, density, and linear velocity, respectively, for the gas stream, $G = u\rho$ = mass velocity, and x is the effective film thickness for diffusion, to be used in the equation

$$N_A = \frac{Dp}{RTx}\frac{\Delta p}{p_{BM}} = k_G \Delta p \tag{16}$$

An equation of the same form as Eq. (58) has been employed by Fallah[61] and by Uchida.[184] Fallah added another dimensionless group to allow for entrance turbulence in short towers without calming sections, and obtained a correlation of the data of Haslam, Ryan, and Weber,[80] Haslam, Hershey, and Kean,[79] Greenewalt,[71] and certain of his own data on the absorption of ammonia from air and from butane. The resulting equation employed an exponent of 0.8 on the Reynolds group, as well as on the group $\mu/\rho D$. Because the experimental results are quite sensitive to the degree of entrance turbulence, as shown by Greenewalt, it seems probable that Fallah's correlation, based on data from several different towers is not to be considered as reliable as that represented by Eq. (58). Uchida suggests an equation not only similar in form to Eq. (58) but also with similar constants.

The gas-film coefficient k_G may be obtained by combining Eqs. (58) and (16). For the special case of a dilute mixture of solute gas in air at 1 atm. and 68°F., for which μ and ρ may be taken as for air, and p_{BM} may be taken as 1 atm., there results

$$k_G = 0.0 \frac{D^{0.56}}{} \tag{134}$$

in c.g.s. units (k_G as g. mols/(sec.)(cm.^{2})(atm.). In English units, with k_G as lb. mols/(hr.)(sq. ft.)(atm.) this may be written

$$k_G = 0.0013 \frac{D^{0.56}}{d^{0.17} G^{0.83}} \tag{135}$$

where d is in feet, G in lb./(hr.)(sq. ft.), but for convenience D is still as cm.^{2}/sec., as given by Eq. (31).

These equations may be used for absorption or vaporization in a wetted-wall column with gas-film resistance controlling, providing the flow is turbulent and normal turbulence conditions exist as in a long straight pipe. If extra turbulence exists due to flow conditions at the gas inlet or to turbulence promoters in the gas stream, the values of k_G will be higher. Greenewalt[73] studied the effect of various inlet gas nozzles in the absorption of water vapor from air by sulfuric acid in a wetted-wall tower, and found that for a given air flow there was a definite trend in k_G with the degree of turbulence induced by the inlet nozzle used. Certain of his data are shown in Fig. 50, the four upper lines representing the data obtained with four different nozzles. The uppermost line was obtained using a header pierced with several small holes to supply the air at the bottom of the column. The lowest of the four curves was obtained with a venturi-type inlet nozzle, used to minimize entrance turbulence. The tower was only 31 in. long, however, and even this latter inlet tube induced enough turbulence to give results somewhat higher than predicted by Eq. (135), represented by the lower dotted line. Greenewalt's data for the venturi-type inlet nozzle shows a marked break at a mass velocity of 230, corresponding to a Reynolds number of about 900. This is doubtless the critical velocity for the apparatus, the flow being streamline or viscous at lower air rates.

Figure 50 also shows the data of Cogan and Cogan[37] for the absorption of ammonia from air by water in a 1.6-in. i.d. wetted-wall tower provided with a calming section to eliminate entrance turbulence effects. These data fall approximately 20 per cent below the line predicted by Eq. (135). (See Illustration 5, page 40.) The group of points at a mass velocity of 1,600 to 1,700 represents a series of runs with varying ammonia concentrations in the gas, obtained at approximately the same Reynolds number.

It was found that k_G increased with ammonia concentration in the gas, an effect only partially explained by the decreased partial pressure of air in the film, p_{BM}.

The equations given above apply only when the liquid-film resistance is negligible, and the gas-film resistance controls. When the resistances of both films are involved, as in the absorption of moderately soluble gases, it is convenient to employ the

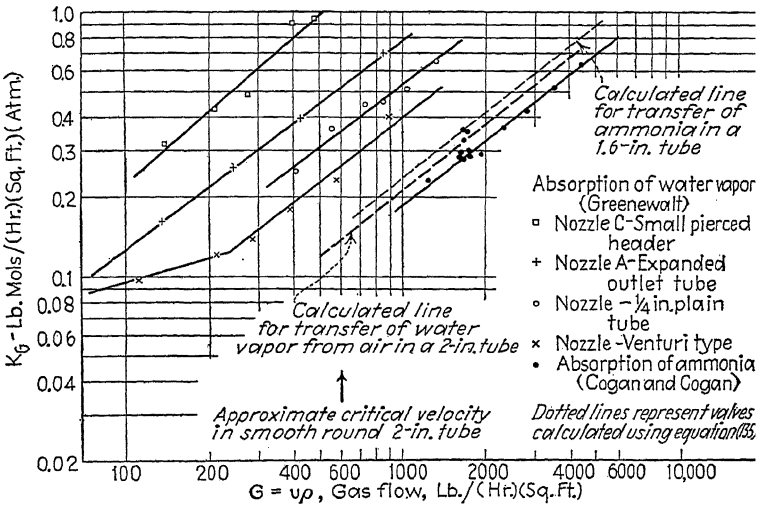

FIG. 50.—Comparison of data on absorption in wetted-wall columns.

method of plotting suggested by Haslam, Ryan, and Weber.[80] Assuming k_G to be proportional approximately to the 0.8 power of the gas velocity, we may write

$$\frac{1}{K_G} = \frac{1}{k_G} \quad \frac{1}{Hk_L} \quad \frac{1}{\gamma G^{0.8}} + \frac{1}{Hk} \tag{136}$$

where $G = u\rho$ = mass velocity of gas flow. Assuming k_L to be independent of gas velocity, a plot of the over-all resistance $1/K_G$ *vs.* $1/G^{0.8}$ should be a straight line with a positive intercept representing the liquid-film resistance $1/Hk_L$. When air is the carrier gas, the slope $1/\gamma$ involves principally the diffusivity D and the tower diameter, as indicated by Eq. (135). If the liquid-film resistance is negligible, the data should be represented by an

approximately straight line passing through the origin. If the gas-film resistance is negligible, a horizontal line should result.

Data plotted in this way are shown in Fig. 51.* The three sets of data on the absorption of ammonia fall on curves passing through the origin, or very nearly so, indicating a negligible liquid-

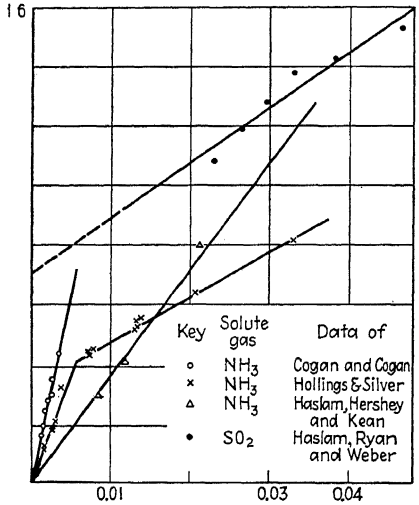

FIG. 51.—Reciprocal method of plotting applied to data on wetted-wall columns.

film resistance $1/Hk_L$, as is to be expected because of the high solubility of ammonia in water. Cogan and Cogan's apparatus had a straight approach or calming section, and their data accordingly fall high, indicating a larger gas-film resistance. The break in the curve of Hollings and Silver's data[93] probably represents the critical velocity for their apparatus. To the right

* No attempt will be made to present and correlate all of the existing data on absorption and vaporization in wetted-wall towers. Such data are of interest primarily because of the light they throw on the factors influencing k_G and k_L, and representative data will be discussed with this in mind. As a general correlation for the gas-film coefficient, Eq. (135) is doubtless the best available, although this relation applies only when there is a minimum of turbulence caused by the gas entering the tower. When entrance turbulence is appreciable, k_G may be expected to be larger. No general correlation has been proposed for the liquid-film resistance in wetted-wall towers.

of the break the flow is probably viscous, and k_G is not proportional to $G^{0.8}$. The data on SO_2 also fall on a straight line, but a definite intercept is indicated, corresponding to the liquid-film resistance $1/Hk_L$. At the lower gas velocities (at the right of the plot) the gas-film resistance is seen to be somewhat greater than the liquid-film resistance.

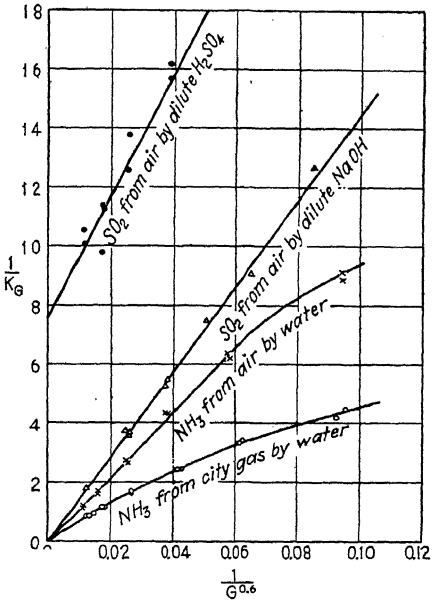

FIG. 52.—Data of Hollings and Silver on absorption in a wetted-wall column fitted with an internal helix.

Figure 52 represents the data of Hollings and Silver obtained with a wetted-wall tower fitted with an internal helix to promote gas turbulence throughout the apparatus. With such a device k_G is proportional to some power of G less than 0.8, and the abscissa is taken as $1/G^{0.6}$ in order that the resulting lines will be approximately straight. As in the last plot, the data on the highly soluble gases (NH_3 in water, SO_2 in dilute NaOH) are represented by lines passing through the origin, and it is evident that the liquid-film resistances for these cases must be very small. SO_2 is only slightly soluble in dilute H_2SO_4, however, and a definite

intercept is indicated. The intercept is large principally because H is small, but also because k_L is less in the more viscous acid solution. The slopes of the three lines passing through the origin are in inverse order of the diffusivities for the gas systems involved and so support qualitatively the conclusion that k_G is proportional to the 0.56 power of the diffusivity. The two lines for SO_2 absorp-

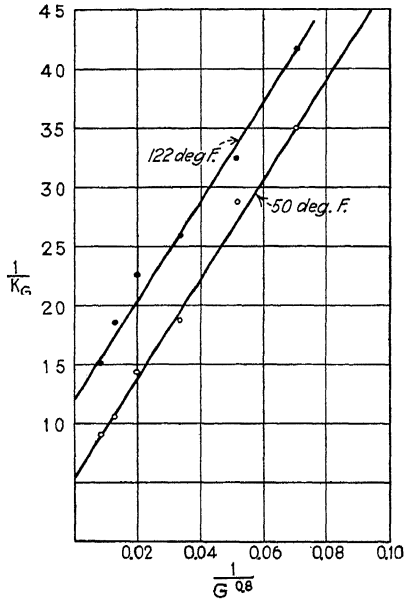

FIG. 53.—Effect of temperature on SO_2 absorption in a wetted-wall column.

tion should be parallel, but it is evident that their slopes are only approximately the same.

The effect of temperature on the absorption of SO_2 by water in a wetted-wall column is indicated by the data of Haslam, Hershey, and Kean,[79] shown in Fig. 53. For a given Reynolds number the gas-film thickness x should be independent of temperature, since $\mu/\rho D$ is independent of temperature. Hence, k_G should vary as the square root of the absolute temperature, since k_G is proportional to D/T, and D is proportional to $T^{\frac{3}{2}}$. It

follows that k_G should increase about 7 per cent in the range from 50 to 122°F., and this increase should be practically independent of gas velocity. The lines for 50 and 122°F. are approximately parallel, but the values of $1/K_G$ differ by more than 7 per cent because of the effect of temperature change on the intercept $1/Hk_L$. Increased temperature increases k_L because the diffusivity in the liquid phase is markedly affected by the temperature, but H decreases with increasing temperature. The net effect is not large in this case, although the liquid-film resistance $1/Hk_L$ is definitely increased by raising the temperature.

The factors which affect k_G are indicated by Eqs. (58) and (16), together with the empirical correlation of gas diffusivities (Eq. (31)). The conclusions, which are supported by the data on wetted-wall towers, are as follows:

k_G is: (*a*) Proportional to the 0.56 power of the diffusivity.

(*b*) Proportional to approximately the 0.8 power of the mass velocity of the gas.

(*c*) Inversely to approximately the 0.2 power of the tower diameter.

(*d*) Independent of the total pressure at a given mass velocity.

(*e*) Proportional to the square root of the absolute temperature at a given Reynolds number.

(*f*) Inversely proportional to the mean partial pressure of inert gas p_{BM}.

Relatively little is known regarding the factors which influence the liquid-film resistance in wetted-wall towers. Conclusions regarding the liquid film are of less interest, however, since the special conditions in a thin film of liquid flowing down a vertical wall make the results less applicable to other types of absorption equipment than the general conclusions given above regarding gas-film coefficients. When the liquid rate is low, the flow is streamline, and the solute must diffuse in without the aid of eddy motion. The mathematics which should apply are analogous to those presented in Chap. II for streamline flow of the gas in a wetted-wall tower, and have been discussed by Hatta and Katori.[85] As pointed out above, k_L probably increases rapidly with temperature, but the liquid-film resistance $1/Hk_L$, employing a driving force in pressure units, may not vary appreciably with temperature, because of the counterbalancing effect of the variation in H.

SPRAY TOWERS

Atomization of the absorbing liquid provides a very large surface of contact with the gas, and various types of spray equipment are used for gas absorption, particularly for the recovery of ammonia from manufactured gas. The large surface of contact is partially offset by the fact that the drops settle out quickly, allowing little time for the solute to diffuse into the interior of the individual drops. The surface of each drop tends to become saturated with solute, and the absorption stops unless the liquid is collected and sprayed again. Consequently, spray towers are best suited to the absorption of very soluble gases. They are also widely used for humidification and dehumidification, where no liquid-side diffusion problem is encountered.

The mechanism of absorption by a falling drop has been studied by Whitman, Long, and Wang,[197] who allowed drops of water to fall through a column of gas. They obtained values of k_G of 2.64 lb. mols/(hr.)(sq. ft.)(atm.) for the absorption of ammonia, 2.05 for the evaporation of water into air, and 0.019 in the same units for the absorption of CO_2. The similarity of the results for water vapor and for ammonia indicate that gas-film resistance is controlling in both cases. The low value for CO_2 indicates clearly the influence of a large liquid-film resistance and shows why spray towers are undesirable for the less soluble gases. Whitman, Long, and Wang interpret their results with CO_2 in terms of liquid-film coefficients, but point out that the penetration of CO_2 into the liquid drop is a case of unsteady-state diffusion, analogous to the heating of a sphere by suddenly placing it in a hot fluid. A further study of absorption by a falling drop has been made by Hatta, Ueda, and Baba.[84]

Figure 54 shows representative data from several sources on the performance of spray towers used for gas absorption. Although the correlation is not good, it is perhaps better than might be expected in view of the variation in the degree of atomization obtained with different sprays. Kowalke, Hougen, and Watson[110] absorbed ammonia in a tower 18 in. in diameter and 4 ft. high. Water was supplied at the top through five "Vermorel" sprays arranged in an 8-in. circle. K_Ga was found to be proportional to approximately the 0.7 power of the gas rate, over the range from 3 to 126 lb./(hr.)(sq. ft.). K_Ga increased with water rate

up to about $L = 500$ lb./(hr.)(sq. ft.), but it remained essentially constant as the water rate was further increased to 800 lb./(hr.)(sq. ft.). These conclusions are supported by considerably more data than shown in Fig. 54, which is intended only for comparison of representative data of several investigators.

Hixon and Scott[92] employed a tower 2 7/8 in. i.d. fitted with a single nozzle consisting of a brass plate drilled with thirty-seven 0.028-in. holes. Liquor rate, gas rate, and tower height were varied and data obtained on the absorption of NH_3 by water, SO_2 by water, and benzene by straw oil. The liquid running down the walls was collected separately from that falling as a spray.

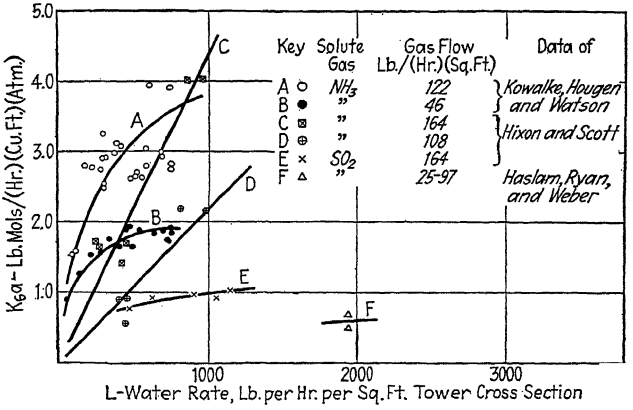

FIG. 54.—Data on absorption in spray towers.

and the values of K_Ga calculated for the central spray core. The data plotted on Fig. 54 were obtained in this way, using a 54-in. tower. In general, Hixon and Scott found that for each gas K_Ga was nearly directly proportional to the liquor rate, proportional to approximately the 0.8 power of the gas flow, and inversely proportional to the square root of the tower height. Their data covered the range of gas rates from 81 to 164 lb./(hr.)(sq. ft.), liquor rates from 200 to 1,400 lb./(hr.)(sq. ft.), and tower heights from 19 to 54 in. Their general correlation shows K_Ga for NH_3 to be approximately 2.3 times that for SO_2 at comparable gas and liquor rates. This is somewhat larger than the 0.56 power of the ratio of diffusivities of the two gases, and so it may be assumed that the liquid film contributed appreciably to the total resistance

in the absorption of SO_2. The values of K_Ga for absorption of benzene by oil using the same tower height of 54 in. were but a small fraction of those obtaining for ammonia absorption, the difference probably being explainable on the grounds that the atomization of the liquid by the spray head was much less effective.

The data of Haslam, Ryan, and Weber,[80] also shown in Fig. 54, were obtained with a small spray tower 8 in. in diameter and 30 in. high used to absorb SO_2 in water. Although no attempt was made to eliminate the wall effect in calculating the results, the principal reason for the discrepancy between these data and those of Hixon and Scott is probably the difference in the effectiveness of the sprays used.

In the manufacture of the bleach used in sulfite pulp mills, chlorine is absorbed in milk of lime in concrete spray towers. The spray is quite coarse, being formed by allowing the solution to drop onto a concave plate, from which it splashes into the empty tower. In one unit of such a tower system, 1.7 by 4 ft. by 14.5 ft. tall, several tests[138] gave an average K_Ga of 0.43 lb. mols/(hr.)(cu. ft.)(atm.), at liquor rates averaging 9,200 lb./(hr.)(sq. ft.) and an average gas rate of 58 lb./(hr.)(sq. ft.). The crude spray is used because lime tends to clog nozzle-type sprays, and the coarseness of the spray is partially offset by the high liquor rate.

Although published data on large-scale spray-type absorption systems is almost completely lacking, it is possible to estimate the coefficient for the absorption of very soluble gases from available data on similar equipment used for humidification of air. Where the original data are available, it is best to calculate k_Ga for water vapor in air, and then estimate the desired value on the assumption that k_Ga is proportional to the 0.56 power of the diffusivity D. If the test results are reported in terms of the heat transfer coefficient ha, B.t.u./(hr.)(cu. ft.)(°F.), this may be converted to k_Ga by means of the Chilton-Colburn relation between heat transfer and absorption, using Eq. (57).

PACKED TOWERS

The published performance data on packed towers consists principally of laboratory data on small experimental equipment. Actual plant data, or even data on moderately large pilot plants

are not plentiful. The available laboratory data fall in two classes: those obtained in towers less than 6 in. in diameter, packed with 1/2-in. or smaller packing, and data on towers 6 in. to 3 ft. in diameter packed with material 1/2 to 4 in. nominal size. The former are of relatively little value for design purposes, but the latter if used properly serve as a reasonably adequate basis for large-scale plant design.

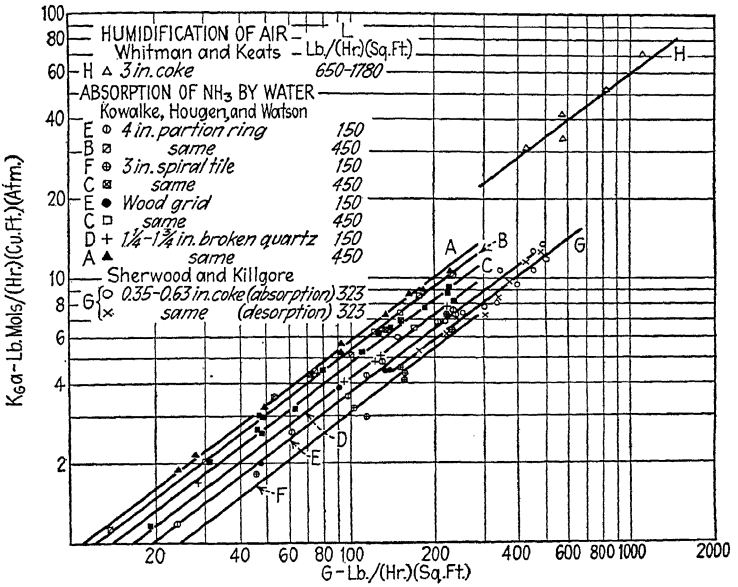

FIG. 55.—Data on packed towers for cases where gas-film resistance is controlling.

Various data on capacity coefficients have been collected from the literature and are presented below in a common set of units. Cases where gas film is controlling are typified by the absorption of ammonia in water; the absorption of CO_2 in water is a case in which the resistance of the liquid film is controlling. Intermediate cases in which the absorption of both films are involved to an appreciable extent are typified by the absorption of SO_2 by water.

Various Packings—Gas Film Controlling.—The most extensive data on the absorption of ammonia are those of Kowalke, Hougen, and Watson.[110] These investigators used a metal tower

4 ft. in height and 16 in. in diameter, packed with four different typical packing materials. Data were obtained at various gas and water rates for each packing, and a few runs were made with one packing in a study of the effect of temperature. Figure 55 shows representative data from their tests, plotted as K_Ga *vs.* G on logarithmic coordinates. Two curves are shown for each packing, for water rates of 150 and 450 lb./(hr.)/(sq. ft.), respectively. Each set of data can be fitted by a straight line having a slope of approximately 0.8 and the data for the various packings fall surprisingly close together.

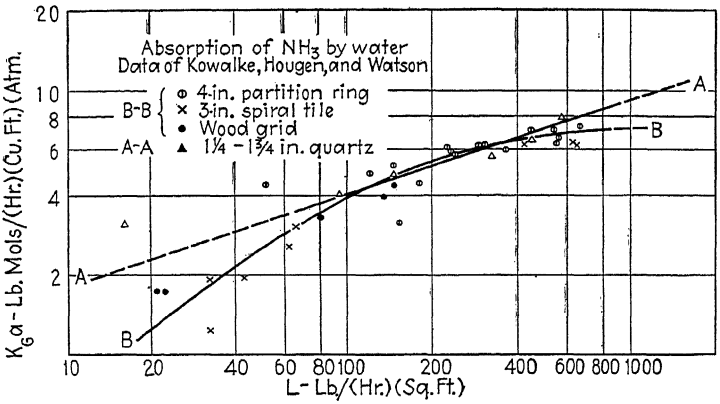

FIG. 56.—Effect of water rate on absorption of ammonia in packed towers.

Increased water rate increases K_Ga as indicated by the fact that the lines for water rates of 450 lb./(hr.)(sq. ft.) fall 40 to 50 per cent higher than those for water rates of 150 lb./(hr.)(sq. ft.). The effect of water rate is made clearer by Fig. 56, which shows K_Ga plotted *vs.* water rate for a constant gas rate of 120 lb./(hr.)(sq. ft.). It is evident that the increase in K_Ga with water rate becomes very small at high water rates, and it is probable that K_Ga does not increase appreciably with further increases of water rate above about 700 lb./(hr.)(sq. ft.) for the wood grid, partition ring, and spiral-tile packings. There is indication of a steady increase of K_Ga with water rate for the broken-quartz packing, as indicated by the line AA, but it is probably safest to assume that K_Ga reaches a maximum value at a water rate of about 1,000 lb./(hr.)(sq. ft.).

At low water rates the packing is only partially wetted, and increasing water rate increases K_Ga mainly because of the increase in wetted surface. After the packing surface has become almost completely wetted, further increase in water rate serves only to increase the thickness of the water layer running down over the surface of the packing, and has relatively little effect on K_Ga in cases where gas film is controlling. If the water rate is increased to the flooding point, K_Ga may be expected to decrease sharply. The irregular shape of the quartz packing particles may cause the maximum K_Ga to be reached at higher water rates than for the other packings, but the data available do not appear to be adequate to determine the exact relation.

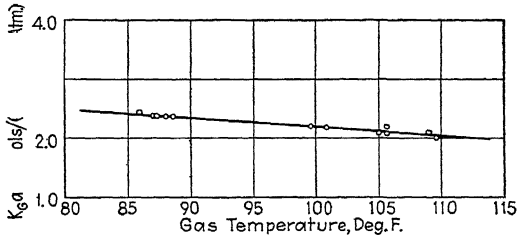

FIG. 57.--Effect of temperature on absorption of ammonia in quartz-packed towers ($G = 46$, $L = 150$).

The effect of temperature was studied over a limited range by Kowalke, Hougen, and Watson using the quartz packing, with a gas rate of 46 and a water rate of 150 lb./(hr.)(sq. ft.). These data are plotted in Fig. 57 as K_Ga *vs.* gas temperature, and it is seen that the latter variable has quite a small effect over the range covered. This is supported by the data of Haslam, Hershey, and Kean, who found K_G to decrease approximately 20 per cent for the absorption of ammonia from air in their wetted-wall column as the temperature was increased from 50° to 122°F. As pointed out above, k_G should increase as the square root of the absolute temperature for a constant Reynolds number. Figure 57 is for a constant mass velocity of air flow, so an additional effect of air viscosity is involved. It would appear that the effect of increasing air viscosity with temperature more than offsets the increase in k_G due to increased diffusivity.

The process of desorption, or stripping by means of an air current, is essentially similar to that of gas absorption. That

the K_Ga's for the two processes are the same is shown by the data of Sherwood and Killgore,[168] represented by curve G of Fig. 55. The results were obtained for absorption and desorption of ammonia in a 4-in. i.d. column packed with 0.35- to 0.63-in. coke. These data fall in with Kowalke, Hougen, and Watson's data for larger packing.

Figure 55 also shows the data of Whitman and Keats[196] obtained for the humidification of air by water in a tower 1 ft. in diameter packed with 3-in. coke. These values of K_Ga are considerably higher than the extrapolation of Kowalke, Hougen, and Watson's lines, apparently because of the very high water rates employed. The diffusivity of water vapor in air is about 18 per cent greater than that for ammonia, which would explain an increase in K_Ga of about 10 per cent.

The data of Fig. 55 may be represented by simple empirical equations, which may be expected to apply for absorption or desorption of ammonia with air as the carrier gas and water as the solvent. The equations given below are based on the data of Fig. 55, all obtained at room temperature (55° to 85°F.).

For the absorption of ammonia at a water rate of 500 lb./(hr.)(sq. ft.):

$$K_Ga = 0.135G^{0.8} \text{ for 4-in. partition rings (Fig. 39)} \quad (137)$$

$$K_Ga = 0.122G^{0.8} \text{ for 3-in. spiral tile (Fig. 39), and for paraffined wood grids (3- by 1/2-in. slats placed on edge with 1/2-in. spaces between)} \quad (138)$$

$$K_Ga = 0.147G^{0.8} \text{ for 1 1/4 to 1 3/4-in. broken quartz} \quad (139)$$

For these packings the effect of water rate may be estimated by Fig. 56, from which the ratio of K_Ga at the desired water rate to that at 500 lb./(hr.)(sq. ft.) may be obtained. To be conservative, the line B-B should be used for this purpose.

For the 0.35- to 0.63-in. coke at a water rate of 323 lb./(hr.)(sq. ft.)

$$K_Ga = 0.083G^{0.8} \quad (140)$$

No data on the effect of water rate for this packing are available.

For humidification of air in 3-in. coke at water rates of 650 to 1,780 lb./(hr.)(sq. ft.),

$$K_Ga = 0.23G^{0.8} \quad (141)$$

Variation in water rate in this high range appears to have little influence on K_Ga.

In addition to the data on ammonia absorption quoted above, Chilton[33] has studied the absorption of ammonia by water in towers packed with three sizes of crushed stone and three sizes of solid balls. He gives values of K_Ga obtained with these packings in towers 3 in. and 6 in. in diameter, at a water rate of 500 lb./(hr.)(sq. ft.) and at a gas velocity of 2 ft./sec. ($G = 120$). The results are tabulated in Table XI for the 6-in tower. The results for the 3-in. tower ran from 0 to 30 per cent higher.

Tests on plant equipment for ammonia absorption are almost completely lacking. Kowalke, Hougen, and Watson report the results of Dexheimer on the operation of a system of gas scrubbers at the Milwaukee Gas and Coke Company, but they do not describe the equipment completely. Values of K_Ga from 0.3 to 1.3 lb. mols/(hr.)(cu. ft.)(atm.) were obtained at water rates of 230 to 590 lb./(hr.)(sq. ft.) and gas rates of 460 lb./(hr.)(sq. ft.) in eight towers packed with "wooden grid, coke, and stoneware."

Wohrley[199] reports data on large Doherty scrubbers, from which Lewis and McAdams[123] have calculated capacity coefficients. The towers were 3 ft. 8 in. in diameter packed for 15 ft. 6 in. with 1/4 by 6-in. wooden slats on edge, spaced 3/8 in. apart. An average K_Ga of 1.8 lb. mols/(hr.)(cu. ft.)(atm.) was obtained at a gas rate of 850 and a liquor rate of 380 lb./(hr.)(sq. ft.). It is not evident why this result should fall so much lower than Kowalke, Hougen, and Watson's data for a similar packing.

A series of tests on the absorption of benzene by a light wash oil have been reported by Simmons[170] and his various coworkers. Unfortunately, these tests were conducted in small towers (2.8 to 3.6 in. i.d.) with small-size packing materials, and the results cannot be used with confidence for the design of large-scale equipment. Most of the data have been recalculated and are shown on Fig. 58, which includes the data of Osborne and Simmons on the absorption of ethylene dichloride by wash oil. For purposes of comparison, the data of Kowalke, Hougen, and Watson on the absorption of NH_3 in 3-in. spiral tile at a water rate of 150 lb./(hr.)(sq. ft.) are also shown. The various data of Simmons and coworkers might be represented by a single straight line, but as benzene is very soluble in the oil used, gas film is probably controlling, and it seems reasonable to expect that K_Ga should be

proportional to $G^{0.8}$. Consequently, straight lines with slopes of 0.8 have been drawn, and the different intercepts must be explained by the differences in the packings and in the oil rates. In the case of the coke packing the oil rate was increased progressively with the gas rate, which explains the tendency of the points to cross the line drawn. The diffusivity of ethylene dichloride in air is less than 10 per cent greater than for benzene in air, so

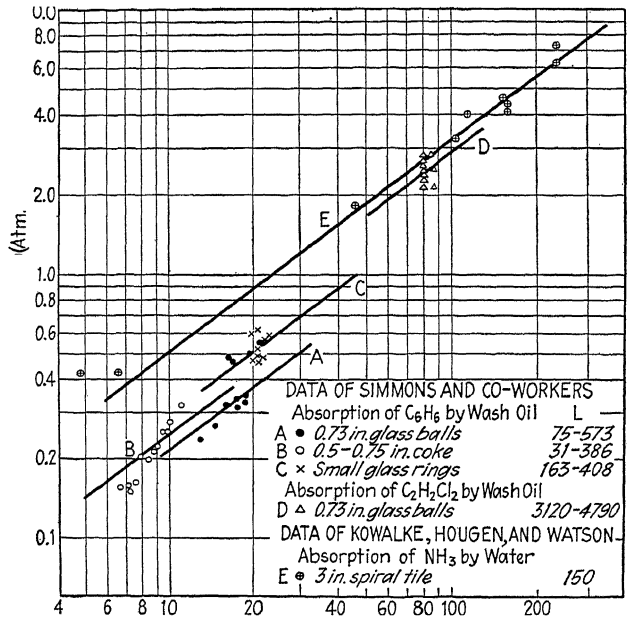

FIG. 58.—Absorption of benzene and ethylene dichloride by wash oil.

in the same packing the $K_G a$ would be expected to be practically the same for both solutes. Since the surface per cubic foot is large for these small packing materials, it might be expected that $K_G a$ would be large in proportion. The fact that the data fall below those for ammonia absorption in the large 3-in. spiral tile is no doubt due principally to the relatively viscous solvent (wash oil), which blocks some of the packing surface by accummulating at the points of contact of the packing particles, and so

reduces the area of contact between phases, even though the rate may be sufficient to wet the packing thoroughly.

In connection with the foregoing data on benzene absorption it is interesting to note that several tests[138] on large scrubbers for the removal of light oil (benzene, toluenes, xylenes) from coke-oven gas gave an average $K_G a$ of 0.6 lb. mol/(hr.)(cu. ft.) (atm.) when operating at a gas rate of 240 lb./(hr.)(sq. ft.) and an oil rate of 680 lb./(hr.)(sq. ft.). This tower, 15 ft. 6 in. in diameter and 111 ft. tall, was packed with 7-in. by 1/4-in. wooden slats spaced 1/2 in. apart on edge. In order to keep the pressure drop at a minimum the slats were not spaced close together, and the resulting $K_G a$ is considerably smaller than obtained with the small-size packings described above.

A comparison of the data for the various cases where gas film should be controlling may be made by tabulating the constant in the equation

$$K_G a = \gamma G^{0.8} \tag{142}$$

This has been done in Table XI, which serves as a useful comparison of various packings, although it is not possible to tabulate the results for a common liquor rate. Where possible, the values are tabulated for a liquor rate of 500 lb./(hr.)(sq. ft.). It is evident that γ bears no direct relation to the packing surface per cubic foot. As pointed out above, the effective area of contact between phases is a function not only of the actual dry surface of the packing material, but of the gas and liquor rates, the liquor viscosity, etc. It would appear that in general the greater surface of the smaller packing tends to be offset by the lower ratio of interfacial to total packing surface, at reasonable liquor rates.

Wood-grid Packings.—The recent data of Johnstone[105] provide a basis for the design of towers packed with slats or wood grids for systems where the gas-film resistance is controlling. The corresponding data on pressure drop have already been presented.

In the course of his work Johnstone tested a number of different types of wood grids, as well as flat and corrugated vertical sheets, using the apparatus to absorb SO_2 from air by a dilute caustic-soda solution, to absorb ammonia from air by dilute acetic acid, and to humidify air. The results are correlated by the Chilton-Colburn modification of the Reynolds analogy (see page 35) and

TABLE XI.—COMPARISON OF PACKINGS FOR MASS TRANSFER WITH GAS-FILM CONTROLLING
Carrier-gas Air at Room Temperature

Packing	Solute	Solvent	Estimated surface, sq. ft./cu. ft.	Liquor rate, lb./(hr.)(sq. ft.)	Constant in relation $K_G a = \gamma G^{0.8}$	Investigators
0.25 in. × 0.4-in. glass rings	Benzene	Wash oil	...	163–408	0.046	Simmons and Long[170]
0.5- to 0.75-in. coke	Benzene	Wash oil	...	500	0.057	Simmons and Osborne[171]
0.73-in. glass balls	Benzene	Wash oil	...	75–573	0.034	Simmons and Osborne[171]
0.73-in. glass balls	Ethylene Dichloride	Wash oil	...	3,120–4,790	0.071	Osborne and Simmons[150]
0.35 to 0.63-in. coke	Ammonia	Water	...	323	0.083	Sherwood and Killgore[168]
0.25-in. crushed stone	Ammonia	Water	123	500	0.116	Chilton[33]
0.50-in. crushed stone	Ammonia	Water	79	500	0.105	Chilton
0.75-in. crushed stone	Ammonia	Water	53	500	0.071	Chilton
0.50-in. balls	Ammonia	Water	94	500	0.103	Chilton
0.75–in. balls	Ammonia	Water	64	500	0.058	Chilton
1.0-in. balls	Ammonia	Water	55	500	0.057	Chilton
1 1/4- to 1 3/4-in. broken quartz	Ammonia	Water	30	500	0.147	Kowalke, Hougen, and Watson[110]
3-in. spiral tile	Ammonia	Water	30	500	0.122	Kowalke, Hougen, and Watson[110]
4-in. partition ring	Ammonia	Water	22	500	0.135	Kowalke, Hougen, and Watson[110]
Wood grid, 3 in. × 1/2 in. spaced 1/2 in. apart	Ammonia	Water	32	500	0.122	Kowalke, Hougen, and Watson[110]
3-in. coke	Water	Water	...	650–1,780	0.23	Whitman and Keats[196]

expressed on a common basis as k_G for SO_2 absorption. In each case the gas-film resistance was controlling, since the reactions of SO_2 with caustic and ammonia with acetic acid are so rapid that the liquid-film resistance is negligible. In the case of the humidification tests the water was supplied essentially at the wet-bulb temperature of the air leaving and did not change in temperature appreciably in passing through the tower. These results were then converted to values of k_G for SO_2 by means of Eq. (57). The values of k_G for ammonia absorption were converted to corresponding values for SO_2 by multiplying by the 2/3 power of the ratio of the diffusivity of SO_2 to that for ammonia (note that Eq. (134) would call for the 0.56 power). The correlation of k_G's obtained by the three methods was found to be excellent.

Three different rectangular towers were employed, designed to accommodate the various packing. For the vertical smooth and corrugated sheets the tower used was 96 in. tall by 16 in. wide, the third (narrow) dimension being variable. The grids were tested in a tower 48 in. tall and 5 1/2 by 15 1/2 in. in cross section. Water or solution was distributed over the grid packings by sprays, and over the vertical sheets by perforated-bottom distributor boxes. The temperature range covered was 55 to 85°F.

The various grids were made of wood 1/4 in. thick, arranged vertically in different ways. By "pitch" is meant the horizontal distance or clearance between parallel grids. The "height" is the height of each individual grid. The successive sections were placed one above the other so that the grids were at right angles to those in the adjacent sections. The alternate sections were said to be arranged in a "staggered" or "nonstaggered" fashion, respectively, according to whether each grid fell directly in the middle of the next parallel channel, or directly over the parallel grids in the parallel sections. This nomenclature is used in describing the packings in the summary of the data given below.

The results of the tests for any one packing may be represented by the simple relation

$$k_G \text{ (for } SO_2) = \gamma_0 G^{0.8} \tag{143}$$

where k_G is expressed in the usual units of lb. mols SO_2/(hr.)(sq. ft.)(atm.), G is the superficial mass velocity of the gas as lb./(hr.)(sq. ft. total cross section). Values of the constant γ_0

are summarized in Table XII and may be assumed to hold over a range of G from 1,000 to 4,400.

The value of k_G estimated is to be used in connection with the calculated total area of the *vertical* surfaces (neglecting the surface of the horizontal 1/4 in. edges) in predicting the performance of towers packed with similar grids. This assumes that the surfaces are completely wetted, which was observed to be true provided a water rate of at least 0.045 g.p.m. per foot of wetted grid perimeter was used. The tests described were run with water rates

TABLE XII.—DATA OF JOHNSTONE ON k_G FOR ABSORPTION OF SO_2 USING VARIOUS SHEET AND GRID PACKINGS—GAS FILM CONTROLLING

Type of packing	Height, in.	Pitch, in.	Arrangement	γ_0 [See Eq. (143)]
Wood grids		0.625	Staggered	0.00524
Wood grids		0.625	Nonstaggered	0.00512
Wood grids		0.625	Nonstaggered	0.00454
Wood grids		0.625		0.00362
Wood grids		.25	Nonstaggered	0.00255
Wood grids		.75	Staggered	0.00223
Wood grids		.75	Nonstaggered	0.00215
Wood grids		.75	Nonstaggered	0.00250
Wood grids		.75	Staggered	0.00274
Wood grids		2.25	Nonstaggered	0.00333
Smooth sheets		1.0	Parallel	0.00088
Smooth sheets		2.0	Parallel	0.00077
1 1/4-in. corrugated sheets		1.0	Parallel	0.00127
2 5/8-in. corrugated sheets	96	1.0	Parallel	0.00133
2 5/8-in. corrugated sheets	96	2.0	Parallel	0.00129
2 5/8-in. corrugated sheets	96	3.0	Parallel	0.00092

from 0.08 to 0.172 g.p.m. per foot, and variations of twofold in water rate showed no effect on k_G. Entrainment from the wetted walls was noted at values of G above about 3,600.

Although the data are expressed by Johnstone in terms of k_G for SO_2, the results may be used to predict k_G for other gases by the method previously described. The procedure is simply to multiply the value of k_G obtained from Table XII by the 0.56 power of the ratio of the diffusivity of the new gas to the diffusivity of SO_2. Values of D may be obtained from Table III, page 35, or from Eq. (31).

Comparison of these data with the data on pressure drop for the same packings (page 145) shows that both the absorption coefficient and the pressure drop increases as the "pitch" and "height" of the section decreases. This comparison indicates the advantages of streamlined sections, which, as discussed on page 134, greatly reduce friction losses without proportionate reductions in film coefficients. The optimum packing can properly be determined only by an economic balance of power and fixed costs.

As a general correlation of these data on wood grids, Johnstone proposes the empirical equation

$$k_G \text{ (for } SO_2) = \frac{6.7 \times 10^{-4}}{d_S^{0.4} d_G^{0.2}} \left[\frac{G(d_S + d_T)}{d_S} \right]^{0.8} \qquad (143a)$$

where k_G and G have the units given above; d_S represents the pitch or clearance between grids, ft.; d_G represents the height of the individual grid section, ft.; and d_T is the thickness of the grid slats, ft.

Liquid Film Controlling.—The absorption of CO_2 in water in the usual packings is a typical case of interphase transfer with liquid film controlling. The recent data of Draemel and Ruckman[50] on desorption of CO_2 from water are the most interesting of those available, as excellent material balances were obtained in their tests, and the carbon-ring packing used was one of definite interest for practical design problems. Although Henry's law applies to CO_2 in water, making it permissible to express the data either as $K_G a$'s or as $K_L a$'s, the results are plotted on Fig. 59 as $K_L a$ *vs.* water rate. It may be assumed that these results apply equally well to absorption of CO_2 by water, as it was found before that absorption data agreed with desorption data for the case of ammonia and water.

The points representing Draemel and Ruckman's data are seen to fall on a straight line having a slope of 0.92. No trend of $K_L a$ with gas velocity was noticed, although G was varied from 57 to 314 lb./(hr.)(sq. ft.). The tower used was 10 in. in diameter, dumped-packed to a height of 56 in. with 1-in. carbon Raschig rings. The CO_2-water solution was distributed evenly over the packing by means of a "Christmas tree" of 1/4-in. copper tubing. Gas and liquid temperatures were between 69° and 79°F. in all runs. The equation of the line drawn is

$$K_L a = 0.016 L^{0.92} \qquad (144)$$

which applies only for a water temperature of 74°F. These results contradict the conclusions of Drane,[51] who found a large effect of gas velocity and no effect of water rate on the absorption of CO_2 by water in a tower packed with 4-in. "propeller" units. Drane does not give his original data, however, so it is not possible to determine where the discrepancy lies.

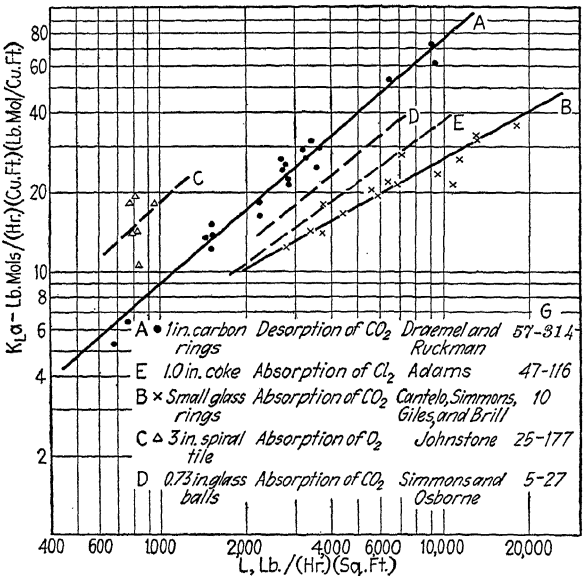

FIG. 59.—Data on absorption in packed towers for cases where liquid-film resistance is controlling.

Curve *B* of Fig. 59 represents the data of Cantelo, Simmons, Giles, and Brill[30] on the absorption of CO_2 in water in a 3.5-in. tower packed to a height of 33 in. with rings 0.4 in. long cut from 0.25-in. o.d. glass tubing. The lower values of $K_L a$ and the smaller slope of the line are probably both due to the difference in the character of the water flow over the smaller packing, in which greater channeling may have occurred and in which the actual interfacial surface was a very much smaller fraction of the dry-packing surface than in the case of the 1-in. rings.

Curve *D* represents the scattered data of Simmons and Osborne[171] on the absorption of CO_2 by water in a similar tower packed with 0.73-in. glass spheres. Although it would appear from these three sets of data on CO_2 absorption and desorption that the coefficients increase with packing size, it does not follow that K_La would continue to increase as the packing size is increased above 1 in. It is probable that a maximum is reached with rings of about 1 to 3 in., and that K_La for larger rings would be smaller because of the smaller packing surface per cubic foot.

Although not indicated by the data of Fig. 59, the effect of temperature on k_L is known to be very marked. The diffusivities of solutes in liquids increase much faster with increased temperature than do diffusivities in gas systems, and the decreased liquid viscosity decreases the effective film thickness. As shown below, the coefficients for the absorption of SO_2 by water increase rapidly with temperature even though the gas film represents an appreciable fraction of the total resistance. The scattering of the points representing Draemel and Ruckman's data is largely explained by the variation in water temperature from 69 to 79°F. in the course of their work. Almost without exception the points above the line *A* are for water temperatures of 74 to 79°F., and those below the line represent tests in which the water temperature was 69 to 74°F.

With liquid film controlling the effect of temperature is so large that an increase in temperature over a limited range may increase K_La sufficiently to offset the increased vapor pressure of the solute over the solution. Under such conditions there is an optimum operating temperature at which the absorption should be carried out. This optimum may be well above room temperature, so it should not be stated as a general rule, as sometimes given, that absorption processes should always be carried out at temperatures as low as are practical.

Curve *E* represents the data of Adams and Edmonds[2a] on the absorption of chlorine from air in a 6-in. tower packed to a height of 4 ft. with 1-in. coke. No effect of gas rate was observed and it is evident that the case is one of liquid film controlling. Although the diffusion coefficient for chlorine in water is less than for CO_2 in water (Table II, page 24), it is probable that the principal reason these data fail to check curve *A* is the difference in the nature of the packing. Adams and Edmonds

also give a summary and correlation of the best available data on the solubility of chlorine in water.

As a matter of interest, Fig. 59 also shows the data on oxygen absorption obtained by Johnstone,[103] whose work is discussed in Chap. VII. Flue gas was scrubbed to remove its SO_2 content, using a tower 42 in. in diameter and 66 in. high, packed with 3-in. spiral tile. The solvent used was an aqueous solution containing small amounts of dissolved iron or manganese salts which effected rapid oxidation of the SO_2 in solution to sulfuric acid. The oxygen necessary to oxidize the SO_2 absorbed was calculated and values of K_La for oxygen absorption were obtained, by using the solubility data for oxygen in water to obtain C_e. The calculation of the data as coefficients for oxygen absorption appears justified by Johnstone's conclusion that the process as a whole is controlled by the rate of oxygen absorption rather than that of SO_2.

The values of K_La are seen to be about twice those for CO_2 with 1-in. rings. Since the oxygen reacts with SO_2 to form acid in the liquid film, the effective liquid-film thickness is reduced, and the results would be expected to be high. The case is similar to the absorption of methyl formate by NaOH studied by Jenny, and discussed in Chap. VII.

Although data on the absorption of CO_2 by water is of considerable value in showing the influence of those factors which affect the liquid-film resistance, the absorption of CO_2 by lye solutions, however, is of considerably more industrial interest. For this case the data of Byrne and Carlson[29] are available. These investigators absorbed CO_2 from a CO_2-rich flue gas, using a tower 1.0 ft. in diameter and 12 ft. high, packed with 3-in. coke. The apparatus was set up in a commercial liquid CO_2 plant and lye solution was taken from the supply going to the large-plant absorbers. The tests made covered a range of temperatures as well as gas and liquor rates. The results have been recalculated employing the product, sodium normality times fraction conversion to bicarbonate, as the driving force. The capacity coefficient as lb. mols CO_2/(hr.)(cu. ft.)(unit driving force) with driving force expressed in these units will be designated as $K_L''a$. The results are well represented by the empirical equation

$$K_L''a = 0.000074t + 0.0000048L - 0.0055 \qquad (145)$$

where t is in °F., and L represents the lye rate as lb./(hr.)(sq. ft.).

This should be used only over the range of variables covered by the data, *i.e.*, from 84 to 138°F. and lye rates from 110 to 760 lb./(hr.)(sq. ft.). No effect was noted due to variation of gas rate, which was varied from 13 to 175 lb./(hr.)(sq. ft.). Design calculations indicate that the above relation compares closely with the performance of commercial absorbers.

The large effect of temperature on the capacity coefficient makes it desirable to absorb at a temperature above room temperature, in spite of the adverse effect of the larger back pressure of CO_2 over the solution. With lye feed containing bicarbonate present equivalent to 30 per cent of the total sodium, and lye removed containing 70 per cent of the sodium as bicarbonate, the optimum temperature is in the vicinity of 105°F. Equilibrium data for the system are given in Chap. VII.

Illustration 18.—It is desired to estimate the size of the absorption tower required for the recovery of CO_2 from flue gas in a plant manufacturing liquid carbon dioxide. A steel tower packed with 3-in. coke will be used, and it is specified that the CO_2 recovery shall be 80 per cent. The flue gas contains 17 per cent CO_2, 4 per cent O_2, and 79 per cent N_2. A sodium carbonate-bicarbonate solution will be supplied to the tower at the rate of 780 lb./(hr.)(sq. ft.). This solution will be $1.5N$ in sodium and 40 per cent converted to bicarbonate. The gas-feed rate will be 460 cu. ft. (70°F., 1 atm.)/(hr.)(sq. ft.) on a dry basis. Neglecting temperature changes within the tower, calculate the optimum temperature for absorption, and the corresponding tower height.

Solution.—Equation (145) will be used to obtain $K_L''a$, and values of the required tower height will be calculated at each of several temperatures. Basis: 1 sq. ft. tower cross section.

$$CO_2 \text{ adsorbed} = \frac{460}{359} \times \frac{492}{530} \times 0.17 \times 0.80 = 0.162 \text{ lb. mol/hr.}$$

CO_2 equivalent of sodium in liquor feed to tower (assume density of 67.2 lb./cu. ft.) =

$$\frac{780}{67.2} \times 28.35 \frac{\text{l./hr.}}{\frac{1.5}{454 \times 2}} = 0.543 \text{ lb. mol/hr.}$$

Percentage conversion to bicarbonate in tower

$$= \frac{0.162}{0.543} \times 100 = 29.8 \text{ per cent}$$

Conversion to bicarbonate at liquor outlet (bottom of tower) =

$$40 + 29.8 = 69.8 \text{ per cent}$$

$$\text{Inert-gas rate} = \frac{460}{359} \times \frac{492}{530} \times 0.83 = 0.987 \text{ lb. mol/hr.}$$

Let Y' represent the mols CO_2 per mol inert gas, and f the fraction conversion to bicarbonate, then a material balance gives

$$0.987(Y' - Y_0') = 0.543(f - f_0)$$

which is the equation of the operating line. This is represented by a straight line on a plot of Y' *vs.* f, with $f_1 = 0.698$,

$$f_0 = 0.40, \qquad Y_1' = \frac{0.17}{0.83} = 0.205, \qquad Y_0 = 0.17 \times \frac{0.2}{0.83} = 0.041$$

Equilibrium data are obtained from Eq. (175), page 209, and a family of curves of Y' *vs.* f plotted for a number of different temperatures. From the definition of $K_L''a$,

$$0.543\, df = K_L''a \times 1.5(f_e - f)\, dh$$

or,

$$h = \frac{0.543}{1.5K_L''a}\int_{0.4}^{0.698} \frac{df}{(f_e - f)} \text{ height in feet}$$

Values of $(f_e - f)$ are obtained from the curves plotted, and the integration performed graphically. The results are tabulated below:

t, °F.	$\int df/(f_e - f)$	$K_L''a$	h, ft.
68	1.13	0.00328	125
86	1.23	0.00460	97
104	1.43	0.00593	87
122	1.96	0.00726	97
140	3.14	0.00861	132

The optimum temperature is about 106°F., at which the required tower height is 86 ft.

Intermediate Cases Involving the Resistances of Both Films.—In the absorption of the majority of industrial gases either the gas or liquid film presents such a large fraction of the total resistance that the resistance of the other film may be neglected. Intermediate cases are encountered, however, for which the resistance of both films must be allowed for. These cases are relatively easy to handle if Henry's law holds, as K_La and K_Ga will then be related by a constant proportionality. If Henry's law does not apply, they are considerably more difficult to treat, since both K_La and K_Ga will vary with solute concentration. This latter is true for sulfur dioxide and water, dilute mixtures of which obey Henry's law only approximately.

Figure 60 shows Adams's data[2] on the effect of water rate for the absorption of SO_2 from burner gas in an 18-in. tile tower

packed with 3-in. spiral tile. The deviations of the points from line A do not fall in order of the gas rate, which was varied about threefold in this series of runs. The slope of the line is 0.9 and the values of $K_L a$ fall approximately 50 per cent below those of Fig. 59 for the desorption of CO_2 from water in 1-in. carbon rings. The large effect of water rate and the lack of any noticeable effect of gas rate suggest that liquid film is controlling. Another series of runs, however, obtained at a constant water rate with the same apparatus, indicates that the gas-film resistance may be more than

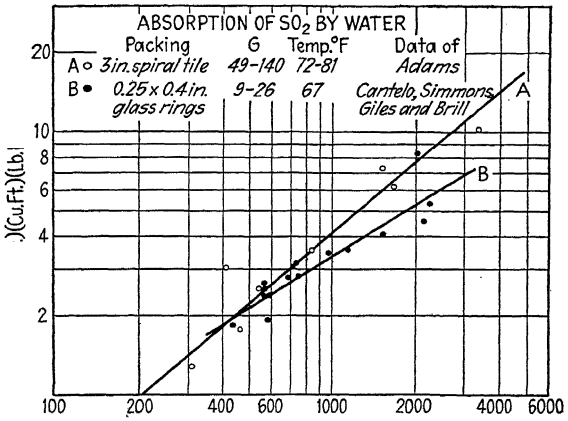

FIG. 60.—Absorption of SO_2 by water in packed towers.

half of the total. This second series is plotted in Fig. 61 as $1/K_L a$ *vs.* $1/G^{0.8}$, following the method of plotting described in connection with the data on wetted-wall columns. If the liquid-film resistance is assumed to be independent of gas rate, the intercept at $1/G^{0.8} = 0$ should represent the resistance $1/k_L a$, and the remainder of the ordinate should represent the gas-film resistance H/k_G. The small intercept indicates that the liquid film presents only 20 to 35 per cent of the total resistance, which conclusion is compatible with the data of the previous figure only if gas rate is assumed to affect the liquid-film resistance.

Figure 60 shows the data of Cantelo, Simmons, Giles, and Brill[30] on SO_2 absorption in 0.25- by 0.4-in. glass rings. As in the case of CO_2, the small rings gave smaller coefficients in spite of the larger packing surface per cubic foot. The relative slopes and

the location of the intersection of the lines for CO_2 and for SO_2 agree closely. Figure 61 also shows the data of Haslam, Ryan, and Weber on the absorption of SO_2 in water in an 8-in. tower packed with 3-in. spiral tile, and with 1-in. coke. The data on the 3-in. tile compare fairly well with those of Adams, although the intercept is much higher, indicating the liquid film to be a much higher fraction of the total resistance. Except for one point, the data on the 1-in. coke fall on a line having a simi-

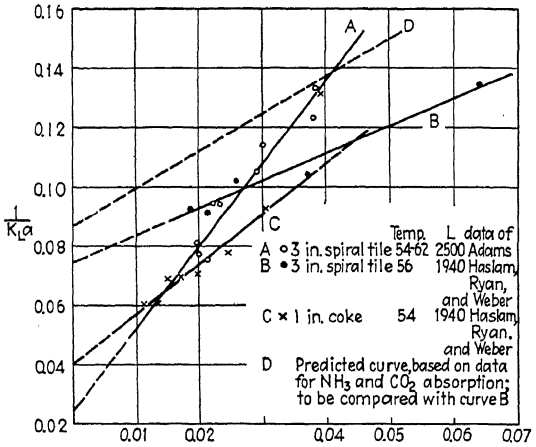

FIG. 61.—Reciprocal method of plotting applied to data on absorption of SO_2 in packed towers.

lar slope, giving an intercept representing a large liquid-film resistance.

Adams studied the effect of temperature on the over-all coefficient and found a rapid decrease of K_La with increased temperature. The effect of temperature was somewhat larger at the low gas rates, but in general the coefficient K_La was halved by an increase of temperature of roughly 50°F. The effect of temperature is much larger than and in the opposite direction from that observed for ammonia absorption.

Although some of the results are difficult to explain, it would appear that most of the evidence favors the conclusion that liquid-film resistance is controlling over the range of variables covered by the data shown. The large effect of liquor rate and

the general similarity of the results to those for CO_2, together with the important effect of temperature, all point strongly toward this conclusion. On the other hand, the smallness of the intercept of curves *A* and *C* of Fig. 61, and the fact that temperature appears to have a larger effect at low gas rates, is difficult to explain on this basis, unless it is assumed that gas rate has a large effect on the liquid-film resistance. It is possible, of course, that such an effect of gas rate exists in the 3-in. spiral tile, even though it was not found for CO_2 desorption in 1-in. rings.

In passing it may be noted that the effect of temperature on K_Ga is different than on K_La. Since $K_Ga = HK_La$, it is possible for K_Ga to decrease and K_La to increase with increase in temperature (H decreases with increased temperature). A comparison of the data of Haslam, Hershey, and Kean, presented in Fig. 53, with the temperature effect on K_La observed by Adams, shows this result.

ESTIMATION OF ABSORPTION COEFFICIENTS FROM DATA ON CO_2 AND NH_3

The factors which affect the gas-film resistance have been discussed in detail, and it should be possible to estimate the gas-film coefficient k_Ga for any packing for which data on ammonia absorption are available. The factors which affect k_La are not so well understood, but preliminary data indicate the k_L for a water-solute system does not vary appreciably with the solute. For purposes of estimation, therefore, k_La may be taken directly from data on CO_2 absorption. The two coefficients may be combined, using the relations

$$\frac{1}{K_La} = \frac{1}{k_La} + \frac{H}{k_Ga} \tag{145a}$$

$$\frac{1}{K_Ga} = \frac{1}{k_Ga} + \frac{1}{Hk_La} \tag{146}$$

Unfortunately, sufficient basic data to make this method of real value are not available.

As an example, suppose it is desired to estimate K_La for the absorption of SO_2 by water in 3-in. spiral tile at a water rate of 1,940 lb./(hr.)(sq. ft.) and at 56°F. The liquid-film coefficient k_La is assumed to be equal to K_La for CO_2, and as no data on spiral tile are available, the data of Fig. 59 for 1-in. rings will be used. Thus at $L = 1940$, k_La is 16.5. These CO_2 data, how-

ever, were obtained at an average water temperature of 75°F. and would probably be some 30 per cent less, say 11.5, at 56°F. From Table XI K_Ga for NH_3 in this packing is $0.122G^{0.8}$ at $L = 500$, which should be increased about 10 per cent to allow for the higher water rate (see Fig. 56). For NH_3 absorption K_Ga is assumed equal to k_Ga. The ratio of the diffusivities for SO_2 and NH_3 in air is 0.103/0.170 (see Table III). Consequently, for SO_2,

$$k_Ga = 0.122\left(\frac{0.103}{0.170}\right)^{0.56} \times 1.10G^{0.8} = 0.101G^{0.8}$$

No correction for p_{BM} is introduced, as it is assumed that the mean partial pressure of air in the case for which the K_La for SO_2 is desired will be approximately the same as in the tests of Kowalke, Hougen, and Watson from which k_Ga for NH_3 was obtained. At 56°F., H for SO_2 is approximately 0.13 lb. mol/(cu. ft.)(atm.), (I.C.T.). Hence, for SO_2

$$\frac{1}{K_La} \qquad \frac{0.13}{0.101G^{0.8}} = 0.087 + \frac{1.28}{G^{0.8}}$$

This relation, plotted as the dotted curve D of Fig. 61, may be compared with curve B, representing the data of Haslam, Ryan, and Weber obtained for SO_2 absorption in 3-in. spiral tile under the stated conditions.

PLATE COLUMNS

The performance of plate columns is most conveniently expressed in terms of plate efficiencies, which may be used in connection with the calculation of the required number of theoretical or perfect plates to determine the number of actual plates. The concept of plate efficiencies has been discussed in Chap. III, and the "over-all" and "Murphree" efficiencies defined. It will be recalled that the over-all efficiency is the ratio of the number of theoretical plates to the number of actual plates required in a column as a whole. The Murphree efficiency applies to an individual plate, and represents the fractional approach to equilibrium with the liquid leaving the plate. The relation between the two efficiencies is discussed by W. K. Lewis, Jr.,[127] who points out that they are equal when the equilibrium and operating lines are parallel.

In commercial rectifying columns for binary mixtures it is common to obtain over-all plate efficiencies from 65 to 95 per cent. Similar efficiencies are obtained in the rectification of multicomponent mixtures, as in gasoline stabilizers.[74] In natural gasoline and refinery gas absorbers the over-all efficiencies run much lower (see page 121). These low efficiencies are probably not to be expected with aqueous solutions used to absorb relatively soluble gases.

Reynolds and Sanders[158] studied the absorption of ammonia by water in an experimental single-plate apparatus fitted with five 3-in. bubble caps. Murphree efficiencies, defined as the percentage approach to equilibrium with the liquid *leaving* the plate, varied from 65 to 85 per cent, averaging about 75 per cent. The liquid level on the plate was varied from 1.65 to 4.0 in., but no trend of plate efficiencies was apparent.

Whitman and Davis[195] report data on the absorption of CO_2 by a sodium carbonate-lye solution in a 15-plate bubble-cap column having one bubble cap per plate. Complete data are given on one run, which has been used to calculate the over-all plate efficiency. A plot of operating and equilibrium curves, using the equilibrium data given in Chap. VII, shows that the separation obtained corresponded to the performance of just one theoretical plate, and as the column had 15 actual plates the over-all plate efficiency was 1/15, or 7 per cent.

Somewhat higher efficiencies are obtained by calculating the data of McCabe and Swanson[130] on the absorption of SO_2 from burner gas, using milk of lime in a Paulson acid absorber (see page 234). Equilibrium data for the system are given by Beuschlein and Conrad.[14] The calculations give individual or Murphree efficiencies varying from 20 to 100 per cent, averaging about 55 per cent. Since the temperature of the test was not given, it was assumed that the liquor temperatures were 70°F., and this may explain the erratic results. The average efficiency of 55 per cent is relatively low in spite of the fact that the liquor levels in this apparatus were approximately 2 ft. on each plate.

Nomenclature for Chapter VI

a = area of interphase contact, sq. ft./cu. ft. of packed volume.
d = diameter of tube, ft.
d_G = height of individual grid section, ft.
d_S = pitch, or clearance between grids, ft.

d_T = thickness of grid slats, ft.
D = diffusion coefficient or diffusivity, cm.^{2}/sec.
G = superficial mass velocity of gas, lb./(hr.)(sq. ft. of total cross section).
h = tower height, ft.
ha = volume coefficient of heat transfer, B.t.u./(hr.)(cu. ft.)(°F.).
H = Henry's law constant, lb. mols/(cu. ft.)(atm.).
k_G = gas-film coefficient of material transfer, lb. mols/(hr.)(sq. ft.)(atm.).
k_Ga = gas-film coefficient, lb. mols/(hr.)(cu. ft.)(atm.).
k_L = liquid-film coefficient of material transfer, lb. mols/(hr.)(sq. ft.)(lb. mol/cu. ft.).
k_La = liquid-film coefficient, lb. mols/(hr.)(cu. ft.)(lb. mol/cu. ft.).
K_G = over-all coefficient of mass transfer, lb. mols/(hr.)(sq. ft.)(atm.).
: over-all coefficient of mass transfer, lb. mols/(hr.)(cu. ft.)(atm.).
: over-all coefficient of mass transfer, lb. mols/(hr.)(sq. ft.)(lb. mol/cu. ft.).
: over-all coefficient of mass transfer, lb. mols/(hr.)(cu. ft.)(lb. mol/cu. ft.).
$K_L''a$ = coefficient in Eq. (145), lb. mols CO_2/(hr.)(cu. ft.) [(sodium normality) (fraction conversion to bicarbonate)].
L = superficial liquid rate, lb./(hr.)(sq. ft. of total cross section).
N_A = diffusion rate, mols per unit time per unit area.
P = total pressure, atm.
Δp = driving force in terms of pressures, atm.
p_{BM} = log mean partial pressure of inerts at film boundaries, atm.
R = gas constant.
t = temperature, °F.
T = absolute temperature.
u = superficial linear velocity of gas, ft./sec.
x = effective gas-film thickness.

$$\gamma = \frac{K_Ga}{G^{0.8}} = \frac{K_Ga}{(u\rho)^{0.8}}$$

$$\gamma_0 = \frac{k_G}{G^{0.8}} = \frac{k_G}{(u\rho)^{0.8}}$$

μ = gas viscosity, lb./(sec.)(ft.).
ρ = gas density, lb./(cu. ft.).

CHAPTER VII

SIMULTANEOUS ABSORPTION AND CHEMICAL REACTION

The purpose of industrial absorption equipment is very often to transfer the solute gas to the liquid phase, in order that a subsequent chemical reaction may be carried out. Occasionally, also, it is necessary to carry out a chemical reaction in the gas phase before absorption will occur. For example, nitric oxide is oxidized in the gas phase in order that the absorption as peroxide may occur readily, and the absorbed peroxide reacts to form nitric acid with the water used as absorbent. The simultaneous occurrence of chemical reactions and physical absorption complicates the treatment of the problem, and the simple laws of physical absorption must be modified very considerably.

In the absorption of some industrial gases it is advantageous to use as an absorbent a liquid compound or a solution which reacts chemically with the gas to be absorbed, forming a loose chemical compound which may easily be decomposed by heating. In the manufacture of liquid and solid carbon dioxide, for example, the solvent is usually a solution of sodium carbonate and sodium bicarbonate. The absorbed CO_2 reacts with the carbonate present, increasing the bicarbonate concentration. The resulting solution, high in bicarbonate, is heated to the boiling point, causing decomposition of the bicarbonate, which gives off CO_2 and reverts to the carbonate. The water vapor evolved with the CO_2 is condensed and the resulting gas is nearly pure CO_2. The hot carbonate solution is cooled and used again to absorb more CO_2. The reaction involved is

$$Na_2CO_3 + CO_2 + H_2O \rightleftarrows 2NaHCO_3.$$

Sodium carbonate may also be employed as an absorbent for hydrogen sulfide, the operation being very similar to the absorption of CO_2. In this the reaction is

$$Na_2CO_3 + H_2S \rightleftarrows NaHCO_3 \quad NaHS$$

H_2S is recovered by blowing air through the resulting solution without heating.

In recent years carbonate solutions for the absorption of CO_2 have been replaced in some installations by aqueous solutions of diethenolamine or triethanolamine.[19] These compounds combine with CO_2 to form unstable carbonates, as follows:

$$2RNH_2 + CO_2 + H_2O \rightleftarrows (RNH_2)_2H_2CO_3.$$

The carbonate decomposes on heating above 122°F., liberating CO_2. The same compounds may be used in a similar way to absorb H_2S. They are nonvolatile and have a high absorption capacity. They have been used to remove CO_2 from water gas in the manufacture of hydrogen for hydrogenation processes, but some corrosion troubles have been encountered in their use for this purpose.

In any absorption process involving a chemical reaction, the reaction may be looked upon as an additional resistance placed in series with the diffusional resistances. If the reaction takes place slowly, the "chemical resistance" may be considered large compared with the diffusional resistance, and is controlling. The rate of absorption is then equal to the rate of reaction. If the reaction is rapid, the chemical resistance is small and the diffusional resistances are controlling, just as though no chemical reaction were involved. The mechanism is more complicated, however, because of the occurrence of multiple films, discussed below. Frequently the occurrence of a chemical reaction reduces one or more of the diffusional resistances, and so may increase the over-all mass-transfer rate.

ABSORPTION FOLLOWED BY A RAPID IRREVERSIBLE REACTION IN THE LIQUID PHASE

In the case of a rapid chemical reaction in the liquid phase, the conditions in the film are complicated by the fact that it is within the liquid film that the reaction occurs. For example, assume that a solute gas A is absorbed from a gas mixture by a solution of a substance B, which combines with A according to the equation

$$A + B \rightarrow AB$$

As the solution is first brought into contact with the gas, A will dissolve and react immediately with B at the phase boundary.

The product AB produced will begin to diffuse toward the main body of liquid. The liquid near the surface will soon be depleted of B, which will begin to diffuse from the main body of the liquid toward the interface. The rapid removal of B from the zone near the surface makes it necessary for the incoming A to diffuse through part of the liquid film to meet the substance B diffusing in the opposite direction. The zone of reaction between A and B will thus move away from the gas-liquid interface, taking up a position such that the rate of diffusion of A from the gas phase is equal (mol for mol) to the rate of diffusion of B from the main body of the liquid. This process requires only a very short time, during which the absorption rate falls rapidly. Within a few seconds at the most, the reaction zone reaches this equilibrium position. Figure 62 is a diagrammatic sketch of the resulting concentration gradients. Pressures or concentrations are plotted as ordinates, and the abscissa represents the position in the film. PQ represents the plane of the interface between gas and liquid phases. VW and UT are the outer boundaries of gas and liquid films, respectively. SR represents the equilibrium position of the reaction zone, to which A and B diffuse, and from which the product AB diffuses toward the main body of the liquid. A diffuses through the gas film under the influence of the driving force $p_G - p_i$ and diffuses to the reaction zone owing to the driving force C_i in the liquid phase. B diffuses from the main body of the liquid to the reaction zone under the influence of the driving force q, and the reaction product AB diffuses back to the main body of the liquid owing to the potential $m - (n - q)$. The solution is n-normal in free plus combined B, q-normal in B, and consequently the normality with respect to AB is $n - q$. The reaction product tends to diffuse from reaction zone toward the gas phase as well as toward the main body of the liquid, but AB is assumed nonvolatile, and the concentration of AB is soon equalized through the section QS of the liquid film.

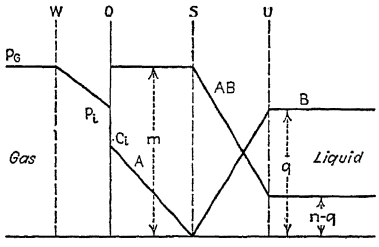

FIG. 62.—Idealized sketch of gradients in double film with irreversible instantaneous reaction occurring at SR.

The diffusion equations derived in the previous chapters may be applied to the gas film and to both sections of the liquid film. Thus, for the gas film

$$N_A = k_G(p_G - p_i) \tag{73}$$

Assuming the solvent concentration to be large compared with the concentrations of A, B, and AB, Eq. (72) may be written

$$N_A = \frac{D_A}{x_L'}(C_i - O) \tag{147}$$

for the first section of the liquid film. For the second section SU,

$$-N_B = \frac{D_B}{x_L''}(q - o) = +N_A \tag{148}$$

and

$$N_{AB} = \frac{D_{AB}}{x_L''}(m - n + q) = N_A \tag{149}$$

As before, the gas and liquid phases at the actual interface QP may be assumed to be in equilibrium, and since A does not react in the section of the film QS but dissolves physically, the equilibrium may be assumed to follow Henry's law approximately,

$$C_i = Hp_i \tag{150}$$

Since the molal diffusion rates of B and AB are equal, the potentials $m - (n - q)$ and q must be in inverse proportion to the respective diffusivities of AB and B, as found by combining Eqs. (148) and (149):

$$m - (n - q) = \frac{D_B}{D_{AB}}q \tag{151}$$

Equations (73), (147), (148), (149), and (150) may be combined algebraically to eliminate p_i, C_i, m, n, x_L' and x_L''. The result is

$$N_A = \frac{\frac{D_B}{D_A}q + Hp_G}{\frac{x_L}{D_A} + \frac{H}{k_G}} \tag{152}$$

This equation states that the rate of absorption is proportional to the over-all driving force, as expressed by the sum of the two terms in the numerator, and inversely proportional to the over-all resistance, as expressed by the denominator. The first term

of the denominator represents the combined resistances of both sections of the liquid film, and the second term represents the resistance of the gas film. It states further that for a constant gas composition and constant film conditions, the rate should be a linear function of the residual concentration of B in the liquid.

Since it is impossible for p_i to be negative, Eq. (73) cannot be expected to apply for conditions where p_i is less than zero. Solving Eqs. (73) and (152) for p_i,

$$p_i = \frac{k_G p_G - \dfrac{D_B q}{x_L}}{k_G + \dfrac{H D_A}{x_L}} > 0 \tag{153}$$

Hence

$$q < \frac{x_L k_G p_G}{D_B} \tag{154}$$

which is a necessary condition for the application of Eq. (152). When q is greater than $x_L k_G p_G / D_B$, p_i approaches zero, and absorption takes place at constant rate;

$$N_A = k_G p_G \tag{155}$$

The condition (154) expresses the critical value of q. If absorption is started using a solution in which the concentration of B is greater than this critical value, the rate of absorption will be constant as q decreases to the critical value. The rate will then fall off linearly with q as indicated by Eq. (152), assuming, of course, that p_G and other conditions are held constant. Just this behavior has been observed experimentally for the absorption of CO_2.

Brunner[22] was apparently the first to picture the double film as illustrated by Fig. 62. The concept was developed to a considerable extent by Weber and Nilsson[191] and later by Hatta[81] and by Davis and Crandall.[43] The derivation of Eq. (152) follows that of Hatta who was interested in the absorption of CO_2 by KOH solutions (see below).

Although the double liquid film pictured in Fig. 62 represents only a hypothesis as to the actual mechanism, the concept is supported by a number of observed facts. For example, the calcium carbonate precipitated on the absorption of CO_2 by milk

of lime is in the form of an exceedingly fine precipitate. It is well known that fine precipitates are formed when the concentrations of the reacting substances are very low, as in the middle of the double film where the reacting substances meet.

REACTION IN TWO STAGES IN THE LIQUID PHASE

The case illustrated by Fig. 62 is representative of the complications encountered in absorption followed by chemical reactions. More complicated cases are not uncommon: where a gas is absorbed by a solution containing more than one reacting solute; where the reaction results in precipitation in the film; or where

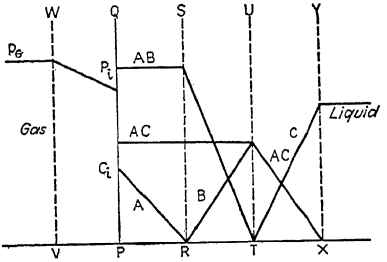

FIG. 63.—Idealized sketch of film conditions for absorption followed by chain reactions.

the reaction occurs in two stages. Figure 63 illustrates the gradients set up in the last case, for the reactions

$$A + B = AB$$
$$AB + C = AC + B$$

A is the solute gas, and C is the reacting substance in solution. A diffuses through the section QS where it reacts with the product B of the second reaction. AB diffuses through SU to UT, where it reacts with C diffusing in from the main body of the solution.

The still more complicated case of absorption into a solution of two reacting substances, as in the absorption of CO_2 by a solution of calcium hydroxide to which NaOH has been added, is discussed by Weber and Nilsson.[191]

REACTION PROMOTED BY A SUSPENDED CATALYST

This interesting case has been investigated by Davis, Thomson, and Crandall[44] who measured the rate of hydrogen absorption

by alcoholic solutions of several olefins containing a suspended platinum-platinum oxide catalyst. The solutions were shaken in a closed bottle in an atmosphere of hydrogen, and the rate of absorption calculated from the observed rate of decrease of hydrogen pressure. The hydrogen diffused through gas and liquid films at the gas-liquid interface and reached the main body of the solution, from which it reached the catalyst surface by

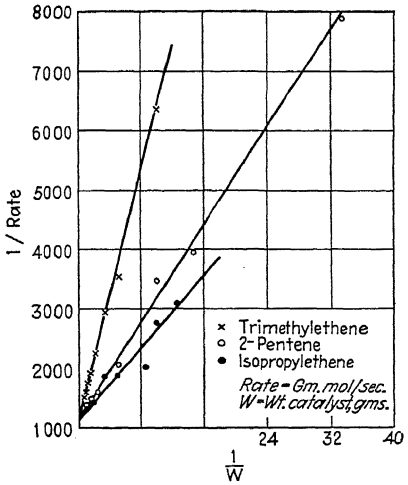

FIG. 64.—Data of Davis, Thompson, and Crandall on hydrogen absorption by olefins in alcoholic solution, with suspended platinum catalyst.

diffusion through a surface liquid film on the catalyst. At constant temperature and rate of shaking, the resistance of gas and liquid films at the gas-liquid interface remained constant, and the rate varied only with the amount of catalyst. The liquid film on the surface of the catalyst may be looked upon as a diffusional resistance in series with the others. Its magnitude should be inversely proportional to the catalyst surface and so to the amount of catalyst per unit volume. The rate of absorption, therefore, may be expressed

$$N_A = \frac{C_e - C_{cat.}}{w} \tag{156}$$

where C_e = equilibrium liquid concentration corresponding to the hydrogen pressure in the gas phase.
$C_{cat.}$ = hydrogen concentration at the surface of the catalyst.
R_1 = combined diffusional resistance of gas film, total liquid film, and main body of liquid.
r_2/w = resistance of the liquid film at the catalyst surface.
w = weight of catalyst per unit volume of solution.
r_2 = a constant.

Equation (156) states that the rate of absorption for the case in question is directly proportional to the over-all driving force from gas to catalyst, and inversely proportional to the sum of two resistances, one of which varies inversely as the catalyst concentration. Davis, Thomson, and Crandall carried out experiments using various quantities of catalyst in a solution of 150 cc. alcohol with 10 cc. olefin. Figure 64 shows their results, plotted as reciprocal of rate *vs.* reciprocal of catalyst concentration. The points fall approximately on straight lines as called for by Eq. (156), and the common intercept indicates that the resistance R_1 is independent of catalyst concentration, as might be expected. The differences between the results for the three olefins is presumably due to differences in the hydrogen pressure $C_{cat.}$ at the catalyst.

CHEMICAL REACTION WHICH TAKES PLACE IN THE LIQUID PHASE AT A MODERATE VELOCITY

If the liquid-phase reaction is rapid, it will occur within the liquid film in a narrow region parallel to the interface. It is in this region that the gas diffusing into the liquid meets the solute diffusing out toward the gas phase (see Fig. 62). If the reaction is slow, however, the diffusing substance is not eliminated at a plane or narrow region, but reacts as it diffuses into the liquid. If the reaction is relatively rapid, the substance absorbed from the gas may react completely before reaching the main body of the liquid. If the reaction is very slow, the amount of solute reacting in the liquid film will be negligible, practically all of it reaching the main body of the liquid before reacting.

In the general case the conditions in the film will be somewhat as pictured in Fig. 65. This figure and the derivation given below are based on the work of Hatta,[82] modified to make the treatment more general. The solute A diffuses through the gas film under

the influence of the driving force $p_G - p_i$. After entering the liquid phase, it starts to diffuse toward the main body of the liquid, but immediately begins to react with the dissolved substance B. Since the diffusing current is being depleted as it diffuses into the liquid, the gradient will be concave upward as shown.

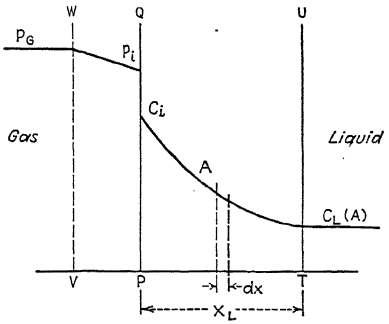

FIG. 65.—Idealized sketch of film conditions for absorption followed by chemical reaction in liquid phase.

If the rate equation for the reaction is known, the conditions of the process may be expressed mathematically. Assume for example, that the reaction is first order,* and that the rate of elimination of A is proportional to the concentration of A at any point, *i.e.*,

$$-\frac{dA}{d\theta} = k_c C V \qquad (157)$$

where k_c is the specific rate of reaction constant, C is the variable concentration of A, and V is the liquid volume considered. Consider now a differential element dx of the liquid film x_L. The rate of diffusion into this element will be

$$N_A = -D_A\left(\frac{dC}{dx}\right) \qquad (158)$$

at $x = x$. The rate of diffusion out of this element, at $x = x + dx$ will be

$$N_A = -D_A\left(\frac{dC}{dx} + \frac{d^2C}{dx^2}\,dx\right) \qquad (159)$$

The disappearance of A within the element, owing to reaction with B, is

$$\frac{dA}{d\theta} = -k_c C\,dx \qquad (160)$$

since the volume of the element is dx. The difference in diffusion rates in and out of the element must equal the rate of elimination of A by reaction with B, whence

$$\frac{d^2C}{dx^2} = \frac{k_c}{D_A} C \qquad (161)$$

Assuming k_c constant throughout the film, the solution of this equation may be given as

$$C = A_1 e^{a_0 x} + A_2 e^{-a_0 x} \qquad (162)$$

* This may not be possible in any actual case, but is sometimes approximated in practice, and will be assumed here for illustrative purposes.

where $a_0 = \sqrt{k_c/D_A}$. Substituting the limits $C = C_i$ at $x = 0$, and $C = C_L$ at $x = x_L$, the constants A_1 and A_2 are obtained and the solution becomes

$$C = \frac{C_L \sinh a_0 x + C_i \sinh a_0(x_L - x)}{\sinh a_0 x_L} \tag{163}$$

For the special case of $C_L = 0$, this reduces to

$$C = \frac{\sinh a_0(x_L - x)}{\sinh a_0 x_L} C_i \tag{164}$$

It is of interest that this equation is mathematically similar to the solution of the problem of heat conduction along a fin, maintained at a constant temperature at the base, with heat dissipation along the fin proportional to the temperature of the fin.[132]

The slope of the concentration curve is obtained by differentiating Eq. (163):

$$\frac{dC}{dx} = \frac{a_0 C_L \cosh a_0 x + C_i \cosh a_0(x_L - x)}{\sinh a_0 x_L} \tag{165}$$

The rate of diffusion into the liquid is obtained by multiplying the slope at $x = 0$ by the diffusivity D_A:

$$N_A = -D_A\left(\frac{dc}{dx}\right)_{x=0} = \frac{D_A a_0(C_i \cosh a_0 x_L + C_L)}{\sinh a_0 x_L} \tag{166}$$

and the rate of diffusion of A into the main body of the liquid is obtained similarly by substituting $x = x_L$,

$$N_A' = -D_A\left(\frac{dc}{dx}\right)_{x=x_L} = \frac{a_0 D_A(C_i + C_L \cosh a_0 x_L)}{\sinh a_0 x_L} \tag{167}$$

Of the solute A entering the liquid phase, the fraction F reaching the main body of the liquid without reacting is given by

$$F = \frac{N_A'}{N_A} = \frac{\cosh a_0 x_L + C_i}{+ C_i \cosh} \tag{168}$$

In the special case where the concentration of A in the main body of liquid is low, Eq. (166) may be written

$$N_A = \frac{bD_A(C_i - C_L)}{x_L} \tag{169}$$

where

$$b = \frac{\quad x_L}{\tanh a_0 x_L} \tag{170}$$

Equation (169) is similar to Eq. (73), with k_L replaced by bD_A/x_L. Equation (79), for over-all resistance, becomes

$$\frac{1}{K_L} = \frac{x_L}{bD_A} + \frac{H}{k_G} \tag{171}$$

whence

$$N_A = \frac{C_e - C_L}{\frac{x_L}{bD_A} + \frac{H}{k_G}} \tag{172}$$

This is the same as the equation for absorption through combined gas- and liquid-film resistances, except that the factor b has been introduced into the term representing liquid-film resistance. Figure 66 shows F and b plotted *vs.* a_0x_L, as calculated from Eqs. (168) and (170) for the case of $C_L = 0$. When C_L becomes an appreciable fraction of C_i, F may still be calculated by Eq. (168), but Eq. (172) no longer applies, and Eq. (166) must be employed.

Figure 66 indicates that F, the fraction of the diffusing material getting through the film without reacting, decreases rapidly as a_0x_L increases. Low diffusivity, large film thickness, or high rate of reaction tends to increase the value of a_0x_L, and most of the reaction occurs within the liquid film.

If the reaction rate is low, F is nearly unity, indicating that most of the diffusing material passes through the film without reacting. The variation in b is equally interesting. At high values of a_0x_L, b becomes equal to a_0x_L, and Eq. (172) reduces to

$$N_A = \frac{C_e - C_L}{\dfrac{1}{\sqrt{k_c D_A}} + \dfrac{H}{k_G}} \qquad (173)$$

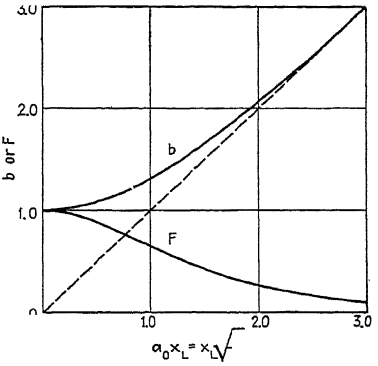

FIG. 66.

which indicates that if a_0x_L is large because k_c is large, the gas film may become controlling. At low values of a_0x_L, the factor b approaches unity, and Eq. (172) reduces to

$$N_A = \frac{C_e - C_L}{\dfrac{x_L}{D_A} + \dfrac{H}{k_G}} = \frac{C_e - C_I}{\dfrac{1}{k_L} + \dfrac{H}{k_G}} \qquad (152) \text{ and } (76)$$

Thus if the chemical reaction is slow, the absorption process becomes the same as for pure physical absorption, and the reaction takes place in the main body of the liquid.

The effect of the speed of the chemical reaction is illustrated by the recent work of Jenny,[102] who absorbed ethyl acetate and methyl formate in water and in caustic solutions. The data were obtained by batch experiments in a small cylindrical container containing 700 cc. of absorbing liquid, and fitted with stirrers in both gas and liquid phases. A mixture of air and ester was fed

continuously through the gas space, and liquid samples removed at frequent intervals, analyzed for residual caustic by means of a conductivity cell, and returned to the reactor.

Jenny found that for both esters the rate of absorption remained constant throughout the run, which in some cases was continued until the residual OH^- normality was less than 0.01. In the case of the ethyl acetate runs, appreciable time was required to obtain a constant reading in the conductivity cell, indicating the presence of unreacted ester in the sample withdrawn. The results obtained with the two esters are summarized in Table XIII. For comparison, the results of a test absorbing ammonia by water from air in the same apparatus are included.

TABLE XIII.—RATE OF ABSORPTION OF ESTERS BY NaOH SOLUTIONS (DATA OF JENNY)

Vapor	Initial NaOH normality	Partial pressure of solute in gas, atm.	Absorption rate, g. mols/(hr.)(cm.^{2})	K_G, g. mols/(hr.)(cm.^{2})(atm.)
Ethyl acetate.....	0 (water)	0.095	0.00145	0.0153
Ethyl acetate.....	0.5	0.046	0.00070	0.0152
Ethyl acetate.....	0.5	0.087	0.00125	0.0144
Ethyl acetate.....	0.5	0.095	0.00127	0.0134
Ethyl acetate.....	1.0	0.092	0.00135	0.0147
Methyl formate.....	0 (water)	0.094	0.0015	0.016
Methyl formate.....	0.5	0.088	0.00285	0.032
Methyl formate.....	0.5	0.090	0.0029	0.032
Methyl formate.....	0.5	0.130	0.00366	0.028
Methyl formate.....	1.0	0.084	0.0044	0.052
Ammonia.....	0 (water)	0.052	0.0048	0.092

For ammonia the gas-film resistance is presumably controlling, because of the high solubility. Since for each ester the value of K_G for absorption by water is much less than for ammonia, it is apparent that the liquid film must represent a large part of the over-all resistance. In the case of the ethyl acetate the differences obtained with various strengths of caustic are probably within the experimental error, and it may be concluded that the occurrence of the chemical reaction does not affect the rate of absorption. The reaction is sufficiently slow to permit the ester to diffuse through the liquid film before reacting, and the result

corresponds to the last case above, in which F is unity, and the theoretical relation reduces to Eq. (76).

Methyl formate is absorbed by water at practically the same rate as is ethyl acetate, and it seems probable that the liquid-film resistance is again controlling. The reaction rate constant for methyl formate and caustic is very much larger than for ethyl acetate and caustic, and the increase in caustic strength results in a marked increase in K_G. The results thus lend qualitative support to the derivation given above for a first-order reaction, and the higher absorption rates may be explained on the basis of chemical reaction within the liquid film, and consequently a shorter distance for the ester to diffuse.

ABSORPTION OF CARBON DIOXIDE BY ALKALI HYDROXIDE AND CARBONATE SOLUTIONS

The manufacture of liquid and solid carbon dioxide is an industry of considerable importance. Liquid carbon dioxide has long been used in manufactured beverages, and the solid form has come into prominence in recent years as a valuable refrigerant. Liquid carbon dioxide is shipped in heavy steel cylinders built to withstand the high vapor pressure of the product at ordinary temperatures. Solid carbon dioxide vaporizes at 1 atm. at −110°F., and is necessarily shipped in heavily insulated containers, trucks, or freight cars. Because both forms are expensive to handle and to ship, manufacturing plants have been constructed in relatively large numbers, the individual plants being only large enough to serve the localities within the relatively small economic shipping distance. In the large majority of these plants the source of CO_2 is flue gas obtained by burning coke under boilers. By careful control of the combustion process, employing thick fuel beds and regulating carefully the amount of secondary air, a gas containing 17 to 18 per cent CO_2 is obtained, from which CO_2 is recovered by absorption in a solution of carbonate and bicarbonate of either sodium or potassium. As explained in the preceding chapter, the carbonate is converted into bicarbonate, which liberates CO_2 when heated to 220°F. The gas so formed is dried, purified, and compressed to 55 to 75 atm. The liquefied product is either distributed as liquid in steel cylinders, or cooled and expanded to form the solid. A flow sheet of the process is shown diagrammatically in Fig. 67.[156] This

method of manufacture has become fairly well standardized and is used more widely than any other. It may be divided into two parts: the production of pure dry CO_2 at 1 atm. pressure, and the manufacture of the liquid or solid product starting with the low-pressure pure gas. It is in the first part of the process that absorption plays such an important role.

Although most of the existing plants use flue gas as a source of CO_2, fermentation gases and lime-kiln gases are also employed

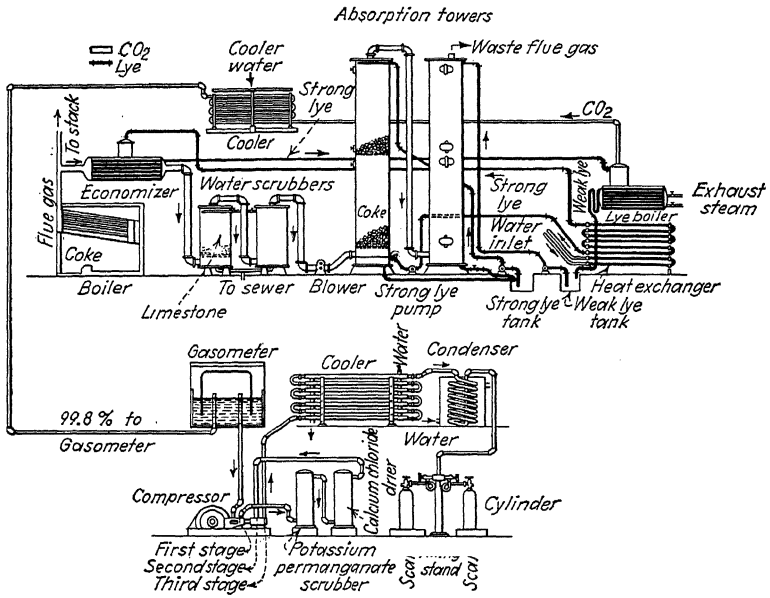

FIG. 67.—Standard CO_2 absorption system. (*Courtesy of G. C. Reich, and Chemical and Metallurgical Engineering.*)

as raw materials. The gas obtained on burning limestone contains approximately 40 per cent CO_2, and the higher CO_2 concentration makes the absorption problem somewhat simpler and less expensive than when flue gas is used. Waste gases from fermentation processes frequently contain still higher CO_2 contents. The solution employed as absorbent is most commonly a mixture of sodium carbonate and sodium bicarbonate, although in the past the potassium carbonates were sometimes employed. The lye concentrations are frequently expressed as lb. K_2CO_3 per

cu. ft. solution, although sodium carbonate is actually being used, and "8 lb./cu. ft." means a soda-lye solution of a strength chemically equivalent to that of a potash-lye solution containing 8 lb. K_2CO_3/cu. ft. The use of ethanolamines as absorbents for CO_2 has been mentioned.

In the industrial manufacture of hydrogen, water gas containing principally CO_2 and hydrogen is treated to remove the CO_2. It frequently happens that the manufactured hydrogen is to be used under considerable pressure for hydrogenation or other purposes, so the CO_2 removal by absorption is carried out under pressure in order to reduce the size of the necessary absorption equipment, and simplify the absorption problem. The pressure at which the absorption unit operates is determined by the relative costs of compression and absorption, since with increasing pressure the cost of compressing the unwanted CO_2 increases. As in the manufacture of liquid and solid CO_2, soda lye is the most common absorbent, although the ethanolamines have also been used. (See also page 221.)

The following deals with the absorption of CO_2 by carbonate solutions, as in the absorption processes outlined above. Although of less industrial importance, the absorption of CO_2 by sodium and potassium hydroxides will also be discussed, because of its bearing on the mechanism of the diffusional processes involved.

EQUILIBRIA IN CO_2-LYE SOLUTIONS

Before dealing with the mechanism of the absorption of CO_2 in various solutions, it is necessary to present briefly the principal data available on the equilibria involved.

The solubility of CO_2 in pure water is given in Table XIV, which tabulates values of the Henry's law constant as given by the International Critical Tables,[98] expressed as the ratio of mol fraction CO_2 in aqueous solution to the CO_2 partial pressure in mm. Hg. In the same table are given values of the solubility as g. mols CO_2/l. of solution at a CO_2 pressure of 1 atm., quoted by Harte, Baker, and Purcell[77] from Seidell's Solubility Tables. Both sets of data are probably based on the same original source. That CO_2 is only sparingly soluble in water is indicated by these figures, since the solubility at 59°F. is only 2.0 g. CO_2/l. at a CO_2 partial pressure of 1 atm.

Relatively few data are available on the equilibria between CO_2 and various carbonate solutions. The early work of McCoy,[133] however, provides a basis of correlation of such data as do exist, so that interpolation and extrapolation may be carried out with reasonable safety over a fairly wide range of conditions. McCoy combined the dissociation constants of the reactions between sodium carbonate, bicarbonate, hydroxide, and water and derived the expression

$$p_{CO_2} = \frac{f^2 N}{S K_{McC.}(1 - f)} \tag{174}$$

where N = sodium normality.
p_{CO_2} = the partial pressure of CO_2, mm. Hg.
f = the fraction total base present as bicarbonate.
S = solubility of CO_2 in water under a pressure of 1 atm. of CO_2, g. mols CO_2/l.
$K_{McC.}$ = "McCoy" constant.

TABLE XIV.—SOLUBILITY OF CO_2 IN WATER

Temperature		$\frac{\text{Mol fraction } CO_2}{\text{Partial pressure } CO_2 \text{ mm. Hg}}$ (I.C.T.)	S = g. mols CO_2/l. at 1 atm. CO_2 (as used by Harte, Baker, and Purcell)
°C.	°F.		
5	41	1.501×10^{-6}	.....
10	50	1.263×10^{-6}	.....
15	59	1.076×10^{-6}	0.0455
20	68	0.926×10^{-6}	.....
25	77	0.804×10^{-6}	0.0336
35	95	.....	0.0262
45	113	.....	0.0215
55	131	.....	0.0175
63	145.4	.....	0.0151
75	167	.....	0.0120
85	185	.....	0.0090
100	212	.....	0.0065

The experimental work of McCoy on sodium carbonate and that of Sieverts and Fritzsche[169] on potassium carbonate-bicarbonate mixtures support the use of this equation, but indicate that $K_{McC.}$, while independent of p_{CO_2} and f, varies with both temperature and base normality.

Recently Harte, Baker, and Purcell[77] obtained additional data on the sodium carbonate-bicarbonate system. They found that their data, together with the data of McCoy, could be correlated empirically by the equation

$$p_{CO_2} = \frac{137 f^2 N^{1.29}}{S(1 - f)(365 - t)} \qquad (175)$$

where t represents the temperature in °F. and the other symbols are as defined above. This equation is known to hold only over the range from 65 to 150°F., and for *sodium* normalities from 0.5 to 2.0. This covers the range of the commercial lyes, which are in the vicinity of 1.0N. Figure 68 represents a plot of values calculated from Eq. (175) for a solution 1.0N in sodium. Since Harte, Baker, and Purcell used Seidel's values of S in deriving Eq. (175), these same values of S, given in Table XIV, should be employed when using the equation.

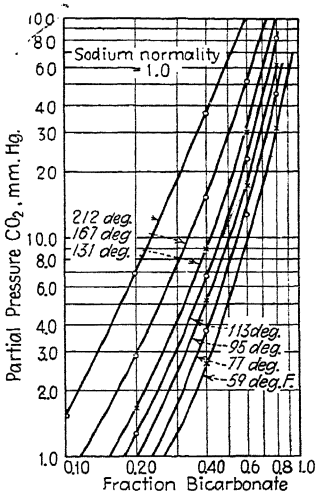

FIG. 68.—Partial pressure of CO_2 over 1.0 N sodium carbonate-bicarbonate solutions.

Sieverts and Fritzsche's data on the potassium system may be approximated by Eq. (175) if the constant 137 be replaced by 45, and the constant 365 be replaced by 302, thus:

$$p_{CO_2} = \frac{45 f^2 N^{1.29}}{S(1 - f)(302 - t)} \qquad (176)$$

which holds reasonably well over the temperature range from 30° to 100°F., and for *potassium* normalities from 1.0 to 2.0. The data are not sufficient to test the 1.29 exponent on N, which is borrowed from the previous equation for the sodium system. Values of S are again those given by Table XIV. Figure 68 may be employed for the potassium system, if values of p_{CO_2} are read from the curve corresponding to $t + 63$, and the result multiplied by 45/137.

Data on the equilibrium between CO_2 and the ethanolamines are given by Mason and Dodge.[137]

ABSORPTION OF CO_2 BY CAUSTIC SOLUTIONS

The absorption of CO_2 by solutions of KOH and NaOH has been studied by a number of investigators. Under certain conditions the gas film is found to be controlling, but in the majority of cases the rate of diffusion in the liquid phase or the rate of the chemical reactions occurring in the liquid phase very evidently determine the over-all rate of absorption. The problem of determining the true mechanism is difficult, because the principal factors which affect the liquid-film resistance have a similar effect on the rate of chemical reaction. Temperature, for example, has a large effect on diffusivities in liquids and on the effective thickness of liquid films (owing to viscosity), and the combined effect of these variables is quantitatively similar to the effect of temperature on rate of chemical reaction. The observed effects of temperature consequently are of little value in distinguishing between processes controlled by diffusion and processes controlled by the rate of a chemical reaction. The determination of the mechanism is further complicated because the chemical kinetics and, in fact, the actual chemistry of the process, are not well understood.

Payne and Dodge[151] list eight reactions which may be involved in the absorption process:

$$CO_2\ (\text{gas}) \rightleftarrows CO_2\ (\text{dissolved}) \qquad (a)$$

$$CO_2\ (\text{dissolved}) + H_2O \rightleftarrows H_2CO_3 \qquad (b)$$

$$H_2CO_3 \rightleftarrows H^+ + HCO_3^- \qquad (c)$$

$$HCO_3^- \rightleftarrows H^+ + CO_3^{--} \qquad (d)$$

$$H^+ + OH^- \rightleftarrows H_2O \qquad (e)$$

$$CO_2 + OH^- \rightleftarrows HCO_3^- \qquad (f)$$

$$HCO_3^- + OH^- \rightleftarrows CO_3^{--} + H_2O \qquad (g)$$

$$CO_2 + 2OH^- \rightleftarrows CO_3^{--} + H_2O \qquad (h)$$

The ionic reactions are believed to be very rapid, but the rates of the other reactions, which are not all independent, are not well known.

Various assumptions as to which of these reactions may be controlling lead to different pictures of the mechanism of the absorption process. Thus Hatta[81] assumes that the reactions are (*a*), (*f*), and (*g*), and that (*g*) is much more rapid than (*f*). Accordingly, he pictures the mechanism to be that illustrated by

Fig. 69, which is similar to Fig. 62. The gas-liquid interface is represented by *QP*, and the ordinates represent concentrations or pressures. In the gas phase CO_2 diffuses under the influence of the potential $p_G - p_i$. In the first zone of the liquid film CO_2 diffuses through a carbonate solution, meeting OH^- ions at *SR*, where the reaction to CO_3^{--} ions takes place. The latter diffuse through the second zone of the liquid film, and out into the main body of the solution where the CO_3^{--} concentration is $(n - q)/2$ (n represents the initial OH^- concentration). Hatta assumes negligible reaction of CO_2 and carbonate in the first zone, where the OH^- concentration is quite low. If the diffusivities of CO_2 and OH^- ions in the liquid are assumed equal, the equation may be written:

$$N_A = \frac{D}{x_L'} C_i = \frac{1}{2} \frac{D}{x_L''} q \qquad (177)$$

where x_L' and x_L'' represent the effective thicknesses of the zones *PR* and *RT*, respectively, q represents the OH^- concentration in the main body of the solution, and C_i represents the CO_2 concentration in the liquid at the interface. This may be written

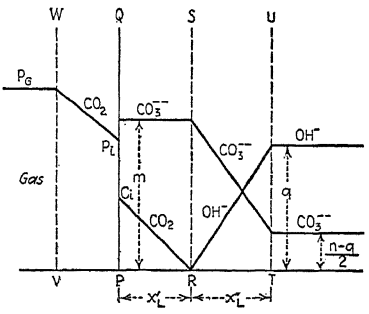

FIG. 69.—Absorption of CO_2 by KOH. (*Hatta.*)

$$N_A = \frac{D}{x_L}\left(C_i + \frac{q}{2}\right) \qquad (178)$$

since $x_L' + x_L'' = x_L$. Equation (178) is fundamentally the same as the equations given by Hatta[81] and by Davis and Crandall.[43] The maximum value of C_i is the solubility of CO_2 corresponding to the pressure p_G, and is small compared with q, except in very weak caustic solutions. The equation states, therefore, that the rate of absorption should be nearly proportional to the OH^- concentration. In caustic solutions, the OH^- concentration is practically proportional to the residual free hydroxide.

Equation (178) may be compared with the data of Hitchcock,[90] which are perhaps the best available data on the batch absorption of CO_2 by caustic solutions under constant CO_2 pressure. The

caustic solution was placed in the lower part of a vertical glass cylinder having an inside diameter of 5 cm., and agitated by a glass stirrer driven from below. A constant CO_2 pressure of 1 atm. over the solution was maintained automatically by addition of CO_2 gas. The rate of absorption was calculated from the observed rate at which CO_2 was added to maintain this constant pressure. Data were obtained at 86°F. using both KOH and NaOH solutions of various strengths. In any one batch experiment, it was found that the rate of absorption fell off rapidly

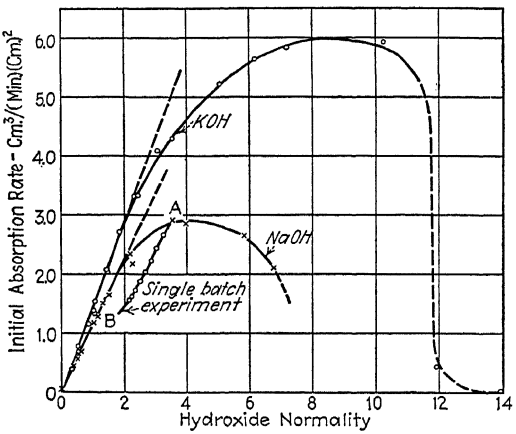

FIG. 70.—Data of Hitchcock on absorption of pure CO_2 by KOH and NaOH solutions.

as CO_2 was absorbed and carbonate formed. Extrapolation of the observed rates back to zero carbonate concentration yielded initial rates corresponding to absorption by pure hydroxide. The initial rates obtained in this way were somewhat lower than the true initial rates prevailing in the first second or so when the film gradients were first being set up. The initial rates obtained by extrapolation are shown in Fig. 70, in which the ordinate represents the initial rate of absorption and the abscissa represents the initial hydroxide normality. Equation (178) is supported by the linear relation between rate and hydroxide normalities below $2N$. The deviations from a straight line above $2N$ are attributed by Hitchcock to the increase of viscosity with normality. It is notable, for example, that the viscosity of NaOH solutions is

somewhat greater than for KOH solutions. It seems probable, however, that the proportionally low rates at very high normalities are due principally to the precipitation of bicarbonate in the surface carbonate layer. Hitchcock states that in the runs using 12*N* and 14*N* KOH, crystals clogged the surface and stopped absorption. Furthermore, Davis and Crandall, observing the surface through a microscope, report some crystal formation at the surface in solutions as low as 1.5*N*. Mitsukuri[144] and Ledig and Weaver[114] also found the rate of CO_2 absorption to go through a maximum as the hydroxide normality was increased.

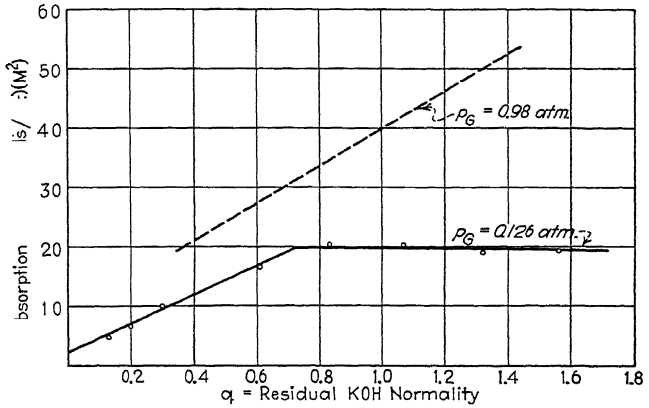

FIG. 71.—Data of Hatta on absorption of CO_2 by KOH solutions.

Hatta[81] carried out experiments similar to those of Hitchcock, but in most cases used a mixture of CO_2 and air in place of pure CO_2. The curves of Fig. 71 are illustrative of the results obtained. The rate of absorption is shown plotted *vs.* the residual free KOH, each curve representing a single run. It will be noted that this is not the same method of plotting as used in Fig. 70, where each point represented the initial absorption rate for a single run. When using high gas concentrations, Hatta found the rate to be very nearly a linear function of the concentration, as indicated by the upper dashed line. Hitchcock's data, if plotted in this way for each run, would show similar curves, approximately straight lines, but actually somewhat S-shaped. Hitchcock's curves, however, intersect the ordinate scale very near the origin, whereas Hatta's data indicate much higher

absorption rates at zero residual KOH. The line AB on Fig. 70 indicates the type of curve obtained by Hitchcock in the course of a single run. When using mixtures of CO_2 and air containing 2 to 20 per cent CO_2 Hatta obtained quite different curves, as illustrated by the lower curve of Fig. 71. As the run progressed, the rate of absorption remained constant over a considerable concentration range, but suddenly began to fall off at some critical value of the residual free KOH, after which the rate was found to be linear in concentration and the curve quite similar to those obtained using high gas concentration. Curves of this type were not obtained by Hitchcock, who did not use mixtures of CO_2 with an inert gas.

Hatta explains his results on the basis of the two-zone liquid film, as discussed previously. The analysis given above is, in fact, a generalization of Hatta's derivations for the absorption of CO_2 by KOH. Hatta assumes the reactions involved to be

$$CO_2 + OH^- \rightleftarrows HCO_3^- \qquad (f)$$

$$HCO_3^- + OH^- \rightleftarrows H_2O + CO_3^{--} \qquad (g)$$

and further assumes that (g) is very rapid. Eucken and Grutzner[57] conclude that the over-all reaction

$$CO_2 + 2OH^- \rightleftarrows H_2O + CO_3^{--} \qquad (h)$$

goes directly in the presence of free hydroxide, and that the rate of reaction is very rapid. Whether or not the reaction occurs in one or two stages does not affect Hatta's subsequent derivation.

Equation (152) becomes

$$N_A = \frac{\frac{D_B}{D_A}\frac{q}{2} + Hp_G}{\frac{x_L}{D_A} + \frac{H}{k_G}} \qquad (179)$$

and Eq. (154) for the critical value of q becomes

$$q = \frac{2x_L k_G p_G}{D_B} \qquad (180)$$

In these equations the subscript A refers to CO_2, and B to OH^- ions. The similarity of Eq. (152) and Davis and Crandall's equation has been pointed out above. Equation (180) specifies

the value of q above which p_i is zero and the rate of absorption is given by

$$N_A = k_G p_G \tag{155}$$

From Eq. (179) it follows that in any one batch absorption test under such conditions, the rate should be linear in q, as found by both Hatta and Hitchcock to be approximately the case for low values of q. Above some critical value of q given by Eq. (180) the rate should be constant, as indicated by Eq. (155). As stated above, Hatta found the rate to be constant at high values of q, in those runs where the CO_2 was mixed with an inert gas. According to Eq. (180), the critical value of q should be proportional to p_G, other variables remaining constant. Hatta does not tabulate his results, but his plotted data indicate this to be at least qualitatively true. The rates obtained at values of q above the critical should be proportional to p_G. The data show this to be very nearly true for values of p_G from 0.0227 to 0.383 atm. when using solutions having initial KOH normalities of 1, 2, and 4. The ratio of rate to p_G, in the region above the critical q, was found to increase with increase in the speed of the stirrer in the gas space, supporting the conclusion that the gas film is controlling in this region. For low values of q, where Eq. (179) should hold, agitation of the liquid should affect x_L and cause a variation of the slope of the rate curve. Experiments in which the stirrer in the liquid was operated at various speeds, but all with the same gas concentration, showed the slope of the rate curve to increase progressively with the r.p.m. of the stirrer. Each of these curves intersected the abscissa scale at the same point, to the left of the rate axis. This result agrees with Eq. (179), which indicates that the intercept on the q-axis should be $-2Hp_GD_A/D_B$, which should be independent of agitation of the liquid. The slope of the rate curve for the absorption of pure gas by $4N$ KOH was abnormally low, indicating that the initial rates may have passed through a maximum with increasing KOH normality, as found by Hitchcock. The effect of temperature was similar to the effect of the speed of the liquid stirrer. The slopes of the rate curves increased rapidly with temperature (approximately as the fifth power of the absolute temperature from 32 to 122°F.) and the negative intercept with the q-axis increased with temperature. Temperature should affect x_L, H,

D_A and D_B, so that the slope, the intercept with the rate axis, and the negative intercept with the q-axis should all increase with temperature.

The agreement of the data with the theory on so many points, is quite remarkable, particularly in view of the assumptions on which the derivation is based. The theory is weakened, however, by the results of Jenny[102] who carried out experiments similar to those of Hatta, absorbing CO_2 from CO_2-air mixtures, using NaOH solutions of various strengths. Jenny confirmed Hatta's results in that he obtained rate curves made up of two straight lines, as shown by the lower curve of Fig. 71. Table XV summarizes certain of Jenny's data for the constant-rate periods.

TABLE XV.—RATE OF ABSORPTION OF CO_2 BY NaOH SOLUTIONS IN CONSTANT-RATE PERIOD (DATA OF JENNY)

Initial NaOH normality	Partial pressure of CO_2 in gas, atm.	Absorption rate, g. mols/(hr.)(cm.^{2})	K_G g. mols/(hr.)(cm.^{2})(atm.)
0.25	0.05	0.00034	0.0068
0.50	0.09	0.00084	0.0093
1.0	0.04	0.00089	0.022
1.0	0.10	0.0013	0.013
1.0	0.14	0.0017	0.012
1.0	0.19	0.0018	0.0096
2.0	0.10	0.00140	0.0140

The principal weakness in Hatta's theory, as indicated by these data, is the effect of NaOH normality. According to Hatta, the gas-film resistance is controlling in the constant-rate period, and K_G should be independent of concentrations or other conditions in the liquid phase. Jenny finds K_G essentially independent of NaOH normality between 1 and $2N$, as did Hatta, but finds a marked effect at low normalities. That liquid-film resistance is involved is also indicated by the fact that K_G is so much smaller than the value obtained for ammonia in the same apparatus (see Table XIII).

These and various other discrepancies between his data and the Hatta theory led Jenny to suggest that the principal error in the theory lay in the assumption of an instantaneous reaction in the film. A real understanding of the mechanism of the process

will probably have to be postponed until more is known of the mechanism and kinetics of the reaction between CO_2 and caustic.

ABSORPTION OF CO_2 BY CARBONATE SOLUTIONS

The rate of absorption of CO_2 by a solution containing both carbonate and bicarbonate is very much less than when free hydroxide is present. In a batch-absorption experiment, starting with KOH, for example, the initial high rate drops off rapidly as KOH is converted to K_2CO_3, and then falls off more slowly as K_2CO_3 is converted to $KHCO_3$. Typical results of absorption-rate measurements over the range from hydroxide to bicarbonate are shown in Fig. 72. The data of Harte[78] were obtained using a glass wetted-wall column 2.4 cm. i.d. and 127 cm. long, through which the solution recirculated, running in a thin film down the inner wall. The temperature was maintained at 77°F. and both 0.5 and 1.25*N* NaOH were used. The results for the two normalities did not differ appreciably. Since the gas concentration was maintained constant the values of K_G plotted are very nearly proportional to absorption rate. Williamson and Mathews[198] employed somewhat the same technique, but used a 7.6-cm. column fitted with a number of small baffles over which the liquid flowed. Their data using 0.6*N* KOH is shown plotted as rate of absorption as cu. ft. CO_2/min. The abscissa is the ratio of combined CO_2 to total base. This ratio is, of course, zero for KOH, 0.5 for K_2CO_3, and unity for $KHCO_3$. Hatta obtained similar results using 1.0*N* KOH in batch-absorption experiments in which the solution was stirred but not circulated. The low rate of absorption by carbonate-bicarbonate solutions supports Hatta's assumption that no appreciable chemical reaction takes place as CO_2 diffuses physically through the surface carbonate zone into a hydroxide solution.

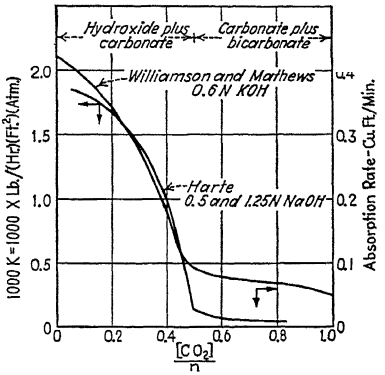

FIG. 72.—Relative rates of absorption of CO_2 by hydroxide and carbonate solutions.

The curves of Fig. 72 bear a rather striking resemblance to the curve representing the OH^- concentration in alkaline solutions. Figure 73 shows the latter relation, as calculated using the recent values of MacInnes and Belcher[135] for the first and second dissociation constants of carbonic acid. Although it is evident from Figs. 72 and 73 that the absorption rate is not proportional to the OH^- concentration, the relation between the two is of interest. The data of several investigators have been plotted in Fig. 74, as absorption rate *vs.* log OH^-. Payne and Dodge[151] employed a

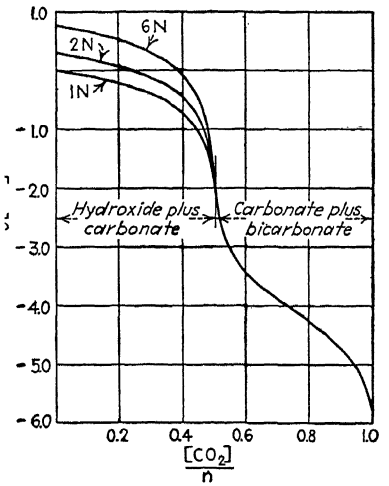

FIG. 73.—OH^- concentration in aqueous solutions of hydroxide, carbonate, and bicarbonate at 77°F.

packed tower, consisting of a 7.2-cm. i.d. glass tube packed for 326 cm. of its length with glass rings 1.0 cm. o.d. by 0.8 cm. i.d. by 1.0 cm. long. The data plotted are for those runs at 77°F. using inlet gas containing 19.5 to 21 per cent CO_2. The liquor rate was constant at either 453 or 480 l./(min.)(m.^{2}). The values actually plotted are 100 times the absorption coefficient in g./(hr.)(cc.)(atm.), but in the section of the tower on which the calculations were based the mean driving force was approximately constant, and the coefficient and absorption rate are roughly proportional. Hitchcock[90] absorbed pure CO_2 by stirred KOH solutions in a closed container. The values plotted are l. (86°F., 1 atm.)/(min.)(m.^{2}). The data were obtained at 86°F.,

using a solution initially 3.54*N* in KOH. Williamson and Mathews used a baffle tower with circulating solutions, as described above, and the data plotted are those of Fig. 72 for a 0.6*N* KOH solution. Hatta[83] absorbed CO_2 by K_2CO_3 solutions, using the same apparatus as for his previous work with KOH, described above. The data plotted are those of the only run tabulated in detail, which was carried out at 86°F. using 1.0*N* KOH. The values plotted are g. mols CO_2/(hr.)(m.^{2}). Harte's experiments have been described briefly above. The data plotted are those of Fig. 72, for absorption by NaOH solutions

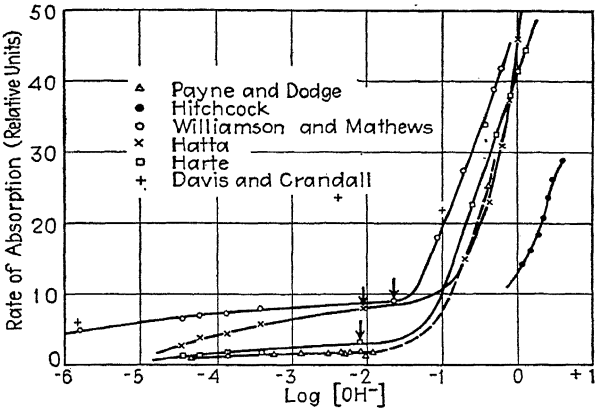

FIG. 74.--Comparison of various data on rates of absorption of CO_2 by carbonate-bicarbonate and by caustic solutions.

at 77°F. Davis and Crandall[43] data were obtained using a technique somewhat similar to that of Hatta and of Hitchcock. Initial rates of absorption were obtained using 0.1*N* NaOH, Na_2CO_3, and $NaHCO_3$. These three points are plotted on Fig. 74, in which the ordinate represents g. mol/(sec.)(cm.^{2}) $\times 10^8$. No attempt was made to recalculate these various data to a common basis, since the types of apparatus represented differed so widely.

The data agree in showing the rate to be roughly proportional to the OH^- concentration in the hydroxide-carbonate region. Except for the single point of Davis and Crandall's, the rates in the carbonate-bicarbonate region are very much lower and are relatively insensitive to OH^- concentration. The Davis and

Crandall points are for initial rates, whereas the other data, with the exception of those of Payne and Dodge, represent instantaneous rates in the course of a change from hydroxide to bicarbonate in the solution. This difference might be the explanation for the apparent discrepancy, although the rates reported by Davis and Crandall are stated to pertain to conditions after practically stationary concentration gradients had been set up in the liquid film.

The absorption rates reported by Williamson and Matthews for the carbonate-bicarbonate region are greater in proportion to the corresponding rates in the hydroxide-carbonate region than for any other set of data. It is perhaps pertinent that in their baffle-plate tower the agitation of the liquid phase was probably greater than in any of the other types of apparatus. Their results also show a sharper break in the curve at the OH^- concentration corresponding to the normal carbonate (indicated by the vertical arrows on Fig. 74).

Payne and Dodge found that gas velocity had no effect on the absorption coefficient, and that substitution of hydrogen for air as the carrier gas likewise was without effect. They found also that both liquid rate and temperature had a marked effect on the coefficient. Williamson and Matthews, Hatta, and Harte also found a marked increase of absorption rate with temperature. These results show conclusively that either diffusion or rate of chemical reaction in the liquid phase must be controlling under practically all conditions when absorbing CO_2 by alkaline solutions. In fact, the only experiments in which the gas-film resistance was found to be controlling were those of Hatta, when absorbing CO_2 from air-CO_2 mixtures by solutions containing appreciable amounts of residual free KOH.

COMMERCIAL ABSORPTION OF CO_2 IN THE MANUFACTURE OF HYDROGEN

As pointed out above, hydrogen is manufactured commercially by the pressure absorption of CO_2 from an impure gas containing principally CO_2 and hydrogen. The solvent used is a material which combines chemically with CO_2 and which can be regenerated by heating. Figures 74*a* and 74*b* illustrate a recent installation for the removal of CO_2 from a gas obtained by the catalytic reaction of steam with butane, using a solution of diamino-isopropanol as absorbent.

The gas treated contains approximately 76 per cent hydrogen, 18 per cent CO_2, with small amounts of methane, nitrogen, and

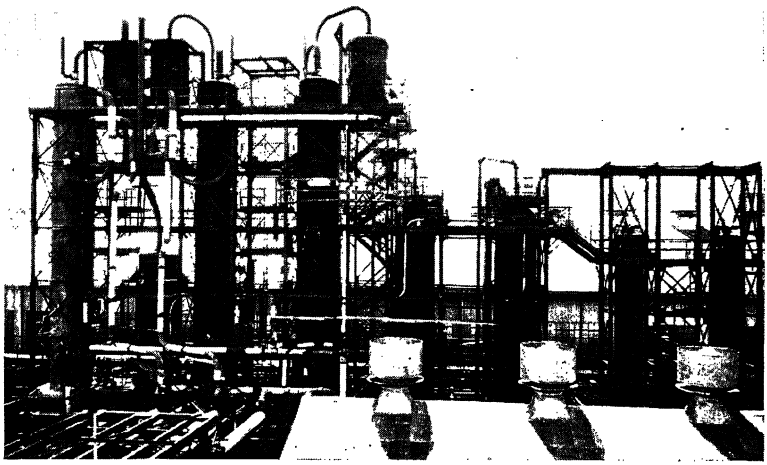

FIG. 74*a*.—Plant for the production of 13,000,000 cu. ft. per day of CO_2-free hydrogen. (*Courtesy of The Standard Oil Development Company and the Girdler Corporation.*)

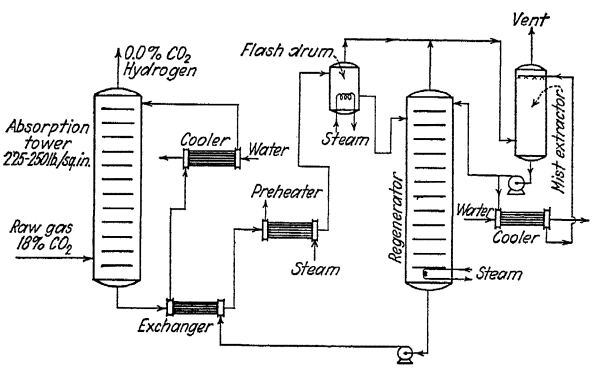

FIG. 74*b*.—Flow sheet of CO_2 absorption system using a solution of diaminoisopropanol as absorbent. (*Courtesy of The Standard Oil Development Company and the Girdler Corporation.*)

carbon monoxide. Two systems are operated in parallel to produce 13,000,000 cu. ft. per day of CO_2-free hydrogen. Each complete system consists of a bubble-plate absorption tower,

heat exchangers, preheaters, bubble-plate regenerating tower, coolers, and a vent-gas contactor. The flow sheet is indicated diagrammatically in Fig. 74*b*.

The raw gas enters the bottom of the absorption tower which operates at a pressure of 225 to 250 lb. per sq. in. The scrubbing fluid enters the top of the tower and the "foul" liquor from the base of the scrubber then passes through heat exchangers and steam preheaters to a disengaging drum where it is flashed at essentially atmospheric pressure, thereby releasing part of its absorbed CO_2. The liquid from the flash drum enters the top of the regenerator and is heated by steam coils in the bottom of the tower. The "fresh" fluid leaving the bottom of the tower is pumped through exchangers and coolers back to the top of the gas scrubber. The gas and steam leaving the flash drum and regenerator pass into a direct-contact cooler. This cooler is packed with spiral tile and water is sprayed over the tile and cooled in external shell-and-tube type coolers. The contact cooler serves the following two purposes: (1) steam leaving the system is condensed and returned to the system, thereby maintaining a constant solution concentration; (2) amine losses are reduced in that the CO_2 gas is continuously washed to remove small quantities of amine.

ABSORPTION OF NITROGEN OXIDES

The absorption of nitrogen oxides to produce nitric acid, nitrites, or nitrates is an industrial problem of major importance. That it is also a technical problem of considerable complexity is witnessed by the enormous literature on the subject. It is significant, however, that most of the research on the mechanism of the process has been by chemists working primarily on the chemical aspects of the problem, relatively little attention having been paid to the importance of the diffusional resistance to interphase transfer.

Until a very few years ago the standard process for the production of nitric acid was the reaction of sulfuric acid with sodium nitrate in a heated iron pot. The gases formed, consisting principally of HNO_3, NO_2, NO, and water vapor, pass to a condenser serving to collect the "drip acid," and so to a series of absorption towers in which the nitrogen oxides are absorbed to form 50 to 65 per cent nitric acid. Since the development of the

various processes for the fixation of atmospheric nitrogen, however, nitric acid is more conveniently produced by the catalytic oxidation of ammonia, with subsequent absorption of the nitrogen oxides formed, which are present to the extent of 7 to 9 per cent in the gases to be treated. In the arc process for the direct oxidation of atmospheric nitrogen a dilute gas is produced containing only 1.2 to 1.8 per cent NO, which must be oxidized and the NO_2 absorbed. The absorption of this dilute gas requires such enormous equipment that the absorption towers represent over 40 per cent of the capital cost of the plant.[111] The absorption of nitrogen oxides is also of importance in the recovery of nitric acid from spent mixed acid, where gases containing up to 20 per cent nitrogen oxides are treated.

The oxides of importance are nitric oxide, NO, nitrogen peroxide, NO_2, the trioxide, N_2O_3, and the tetroxide, N_2O_4. Nitrous oxide, N_2O, is not ordinarily encountered in the processes mentioned. NO does not react with water and must be oxidized before absorption occurs. It combines with NO_2, however, forming N_2O_3, which reacts with water to form nitrous acid. NO_2 is stable at ordinary temperatures, being only 5 per cent dissociated into NO and oxygen at 430°F. It polymerizes readily to the tetroxide, and at ordinary temperatures exists in the polymer form to an appreciable extent. At 77°F. and 1 atm., for example, a gas containing 10 per cent total NO_2 plus N_2O_4 will contain 6.75 per cent NO_2 and 3.25 N_2O_4. This equilibrium is reached very rapidly, as is also that between NO_2, NO, and N_2O_3. For a 10-per cent gas the latter equilibrium at 77°F. corresponds to approximately 0.16 per cent N_2O_3, 4.9 per cent NO, and 4.9 per cent NO_2.

The principal reactions involved in the absorption process are probably the following:

$$2NO + O_2 \rightleftarrows 2NO_2 \qquad (a)$$

$$2NO_2 \text{ (or } N_2O_4) + H_2O \rightleftarrows HNO_3 + HNO_2 \qquad (c)$$

$$3HNO_2 \rightleftarrows HNO_3 + 2NO + H_2O \qquad (d)$$

The oxidation of NO is a trimolecular reaction with a negative temperature coefficient. It proceeds relatively slowly, the homogeneous reaction rate constants having been obtained by Bodenstein.[17] There is no agreement as to whether NO_2 or

N_2O_4, or both, react with water; Webb,[190] for example, believes that only N_2O_4 is absorbed, since the rate of absorption is very low at high temperatures corresponding to nearly complete dissociation to NO_2. The decomposition of the nitrous acid occurs rapidly, particularly if the solution is agitated. That reaction (*d*) does not hold up the nitric acid formation is evidenced by the fact that the acid product leaving the absorption towers contains only 0.2 to 0.3 per cent HNO_2. In addition to the above reactions, it is probable that N_2O_3 is absorbed and hydrolized directly to nitrous acid. A part of the NO liberated by the decomposition of nitrous acid may be oxidized in the liquid phase by oxygen diffusing in from the gas, although oxygen absorption is so slow that this is probably not important.

It should be evident from this brief summary of the chemistry of the process that there are three parts which may possibly control the rate of the over-all absorption. These are

1. The oxidation of NO to NO_2 in the gas phase.
2. The physical diffusion of the reacting oxides from gas to liquid phase.
3. The chemical reaction in the liquid phase.

When the solvent is water or weak nitric acid, the oxidation of NO is the controlling reaction. Using a wetted-wall tower with water as the absorbent, Bolshakoff[18] found the rate of absorption to decrease with increasing gas rate when the gas feed consisted of a freshly mixed mixture of NO and air containing 10 per cent NO. The decreased absorption is explained by the shorter time for oxidation in contact with water at the high gas rates. Taylor, Chilton, and Handforth[181] state that they were able to calculate the performance of commercial absorption units using formulas involving the rate constant for NO oxidation and the available equilibrium data for reactions (*c*) and (*d*). The only rate constants available in the literature are for the homogeneous gas-phase reaction, and it would appear that these could not be applied to the reaction taking place in an absorption tower, since Burdick[23] found water vapor, charcoal, and other surfaces to affect the reaction rate.

An oxidation chamber placed before the absorption towers to promote the oxidation of the NO is recommended by Webb. This recommendation is supported by the results of Bolshakoff, who obtained over 10 times as much total absorption when the

NO-air mixture was passed through an empty vessel before going to the wetted-wall tower. Webb does not, however, recommend alternate absorption and oxidation chamber, as proposed by Moscicki.[145] If the original gas fed to the absorption system is thoroughly oxidized, the only subsequent oxidation involved is that of the NO liberated by reaction (*d*). This will take place in the free space in the absorption equipment, and some of the reabsorption will probably occur as N_2O_3. This is not particularly desirable, since every three mols of N_2O_3 form directly only two mols of nitric acid with the liberation of four mols of NO, whereas three mols of N_2O_4 absorbed form directly four mols of nitric acid with the liberation of only two mols of NO to be reoxidized. The $NO\text{-}NO_2\text{-}N_2O_3$ equilibrium, however, allows only a small amount of N_2O_3 to form. The net result is probably a greater capacity if all of the volume is used for absorption instead of using part for absorption and part for oxidation. Modern plants employ bubble-cap plate absorbers operating under pressure, and the space between plates probably provides some time for oxidation.

When gas containing only NO_2 and N_2O_4, with no NO, is brought in contact with water, dilute nitric acid, or a caustic solution, the rate of absorption is controlled by the diffusional resistance to transfer between phases, and the gas-film resistance is probably controlling. This is shown by the work of Bolshakoff, quoted above, who found that with a mixture of NO_2 (and N_2O_4) and nitrogen, in a wetted-wall tower, the rate of absorption increased nearly as the 0.8 power of the gas velocity. Under such conditions the absorption of the nitrogen oxides reduces to the ordinary case of gas absorption treated in Chap. III.

When NO_2 is absorbed, there is a simultaneous absorption of N_2O_4. Applying the diffusion equations to the transfer of both gases across the film we may write

$$N_A = -\frac{D_A P}{RT\, p_{BM}} \frac{dp_A}{dx} = -K_A \frac{dp_A}{dx}$$

and

$$N_C = -\frac{D_C P}{RT\, p_{BM}} \frac{dp_c}{dx} = -K_C \frac{dp_c}{dx}$$

where the subscript A refers to NO_2 and C to N_2O_4. As an approximation, the equations for the diffusion of a single gas are used in place of the more

complex relation for the simultaneous diffusion of two gases, and a constant partial pressure of inerts p_{BM} is taken as being equal for both cases. At a distance $x + dx$ through the film

$$N_A + dN_A = -K_A\left[\frac{dp_A}{dx} + \frac{d}{dx}\left(\frac{dp_A}{dx}\right) dx\right]$$

whence

$$dN_A = -K_A\frac{d}{dx}\left(\frac{dp_A}{dx}\right) dx$$

Similarly

$$dN_C = -K_C\frac{d}{dx}\left(\frac{dp_C}{dx}\right) dx$$

N_2O_4 will dissociate into NO_2 in the film, so that by a material balance, $dN_C = -\frac{1}{2}\,dN_A$, and

$$-K_C\frac{d^2p_C}{dx^2} = \frac{K_A}{2}\frac{d^2p_A}{dx^2} \tag{181}$$

If it is assumed that the equilibrium between NO_2 and N_2O_4 is reached instantaneously, the relation between p_A and p_C is given by the equilibrium equation

$$p_A{}^2 = kp_C$$

Differentiating,

$$k\,dp_C = 2p_A\,dp_A \tag{182}$$

Substituting this in (181), there results the basic differential equation

$$\left(\frac{K_Ak}{4K_C} + p_A\right)\frac{d^2p_A}{dx^2} + \left(\frac{dp_A}{dx}\right)^2 = 0 \tag{183}$$

This has been integrated by Roberts[159] to give

$$\left(\frac{K_Ak}{4K_C} + p_A\right)^2 = \left(p_{AG} + \frac{K_Ak}{4K_C}\right)^2 - \left(p_{AG}{}^2 + p_{AG}\frac{K_Ak}{2K_C}\right)\frac{x}{x_F} \tag{184}$$

where p_{AG} = partial pressure of NO_2 in the main body of the gas.
x_F = effective film thickness.
x = distance through the film.

At $x = x_F$, *i.e.*, at the liquid interface,

$$\left(\frac{dp_A}{dx}\right)_{x=x_F} = -\frac{2p_{AG}{}^2K_C}{x_FK_Ak} - \frac{p_{AG}}{x_F} \tag{185}$$

which gives a finite value for the rate of transfer of NO_2 at the interface, *i.e.*, for the rate of absorption of NO_2. Since from Eq. (182),

$$\frac{dp_C}{dx} = \frac{2p_A}{k}\frac{dp_A}{dx}$$

it follows that if there is no vapor pressure of NO_2 over the solution, so that p_A is zero at the interface, then the N_2O_4 partial pressure gradient dp_C/dx at the interface must be zero and no N_2O_4 can be absorbed. Under these conditions of no NO_2 back pressure, N_2O_4 will diffuse toward the interface, but will be completely dissociated to NO_2 in the film, and will be absorbed wholly as NO_2.

Substituting the gradient from Eq. (185) in the original diffusion equation, the final absorption equation is obtained for $p_{Ai} = 0$, as

$$N_A = \frac{P}{RTx_F p_{BM}}\left[\frac{2p_{AG}^2 D_C}{k} + D_A p_{AG}\right] \tag{186}$$

This result is the same as would be obtained by adding N_A and $2N_B$ calculated as though the diffusion of each occurred independently of the other.

Roberts[159] carried out batch-absorption experiments in a beaker-type absorption apparatus, with stirrers in both gas and liquid phases. Tests absorbing ammonia from air in which the gas film was assumed to be controlling, served to determine the value of the effective film thickness, x_F. The same apparatus was then used to absorb NC_2 from nitrogen, using $0.1N$ sodium hydroxide in one test, and 63 per cent H_2SO_4 in a second. The rate of absorption by caustic was approximately five times as fast as by the sulfuric acid. Using the value of x_F calculated from the ammonia runs, the rate of absorption was calculated by Eq. (186), and the calculated value was found to check within 17 per cent of the observed value for the absorption in caustic. These data not only indicate the value of Eq. (186) for cases where gas film is controlling, but show that the gas-film resistance can be but a small fraction of the total when NO_2 is absorbed by 63 per cent H_2SO_4.

The rate of absorption falls off rapidly as the concentration of nitric acid in the absorbing solution increases above 40 per cent HNO_3. The equilibrium approached is indicated by the resultant of reactions (*c*) and (*d*):

$$3N_2O_4 + 2H_2O \rightleftarrows 4HNO_3 + 2NO \qquad (e)$$

for which the equilibrium data of Burdick and Freed[24] and of Abel, Schmid, and Stein[1] are available. These data do not agree at low HNO_3 concentrations, but there is agreement that a maximum of about 68 per cent HNO_3 is obtainable in absorption at atmospheric pressure at ordinary temperatures. As the equilibrium concentration is approached, the rate of absorption falls off rapidly, probably owing to the increasing vapor pressure of NO_2 over the solution, and the resulting decrease in driving force causing diffusion from gas to liquid. It seems probable that

the rate of absorption is controlled by the reaction (*e*) through the effect of its equilibrium on the diffusion potential.

Summarizing, therefore, it may be said that the absorption to form HNO_3 is controlled by chemical reaction in the gas phase (NO oxidation) when NO and oxygen are brought in contact with dilute caustic or dilute nitric acid solutions; that interphase diffusion controls when NO_2 and N_2O_4 are absorbed by the same solutions; and that chemical reaction in the liquid phase controls the rate when either NO and oxygen, or NO_2 and N_2O_4, are absorbed by strong nitric acid.

In the older process for the manufacture of nitric acid by absorption of the gases from the niter pot, it is common to operate several towers with countercurrent flow of gas and acid. If a large number of towers are employed, a strong acid is produced, and in such a case the rate of absorption goes through a maximum in the middle of the absorption system. The rate is low in the first tower because the acid strength is approaching its equilibrium value, and the rate is low in the last tower because the gases are dilute. In the ordinary system making acid of concentrations of less than 60 per cent nitric acid, this maximum may not be noted, as the high gas strength in the first tower more than offsets the effect of increasing acid strength and results in a maximum absorption in the first tower. This effect is noted in the data on such a system quoted in Table XVI from the results of Hall, Jaques, and Leslie.[75]

TABLE XVI.—ABSORPTION IN EIGHT-TOWER SYSTEM TREATING GASES FROM NITRIC ACID STILL

Tower	Percentage HNO_3, liquor leaving		HNO_3 formed, lb./hr.	
	Test 1	Test 6	Test 1	Test 6
1	66.4	58.2	31.4	73.5
2	62.0	46.5	41.9	53.0
3	54.7	34.6	49.1	24.3
4	43.3	27.7	23.4	10.7
5	36.2	24.3	27.6	14.3
6	25.9	19.3	17.5	12.8
7	17.9	14.2	11.1	16.7
8	12.0	7.0	19.2	14.1

Test 1 shows the maximum referred to above. The absorption in the first tower was less than in the second because of the high strength of the acid (62.0 per cent) supplied to it. Although the data are somewhat erratic, a definite minimum is indicated at about the sixth or seventh tower. This is explained by Hall, Jaques, and Leslie on the basis of certain reactions of chlorine compounds introduced by the sodium chloride impurity in the nitrate used.

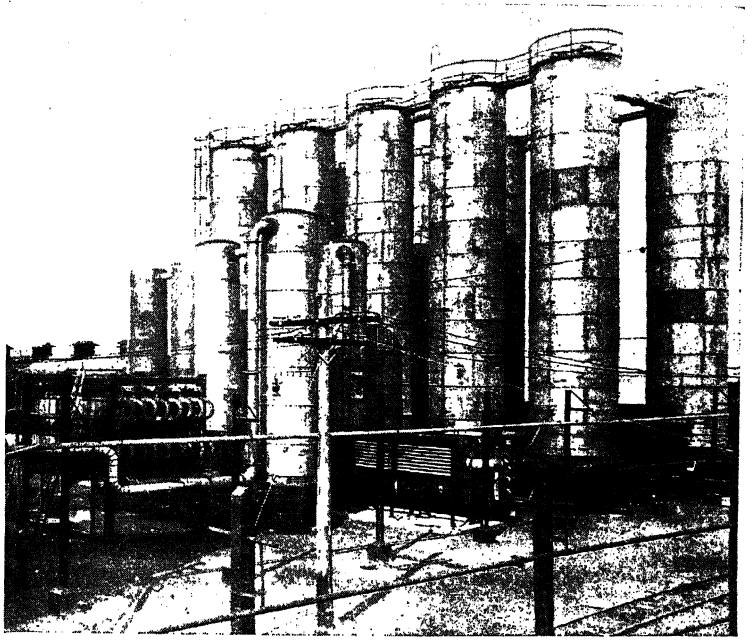

FIG. 75.—Atmospheric pressure absorption towers for nitric acid. (*Courtesy of T. H. Chilton.*)

Effect of Temperature and Pressure.—Unlike most homogeneous gas-phase reactions, the oxidation of NO proceeds more rapidly at low than at high temperatures. Insofar as NO oxidation is controlling, it is desirable to have the absorption proceed at as low a temperature as may be practicable. Furthermore, the process of physical absorption is favored by low temperature because the solubility of NO_2 in nitric acid increases with decreasing temperature and the transfer across the liquid film is

speeded up by the higher NO_2 concentration at the liquid-gas interface. The chemical reactions (*c*) and (*d*) in the liquid phase are retarded at low temperatures, but as these are relatively rapid anyway, the net result of low temperature is beneficial. The equilibrium fixing the maximum strength of nitric acid is not appreciably influenced by temperature.[24]

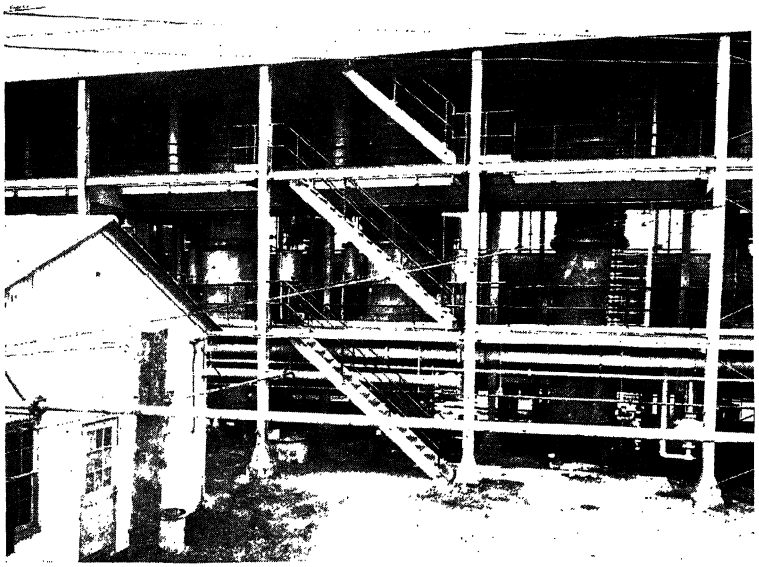

FIG. 76.—High-pressure chrome-iron towers for nitric acid. (*Courtesy of T. H. Chilton.*)

Modern plate-column absorbers are fitted with tubular coolers for the removal of the heat of reaction by cooling the acid on each plate. Although cooling in this way with available cooling water results in an appreciable increase in absorption capacity, Taylor, Chilton, and Handforth[181] state that the cost of additional cooling by artificial refrigeration is not ordinarily warranted.

The important advantages of increasing the total pressure on the absorption system have long been recognized,[62,181,190] but until recently acid-resisting materials of construction capable of withstanding high pressure have not been available. The development of the art of fabricating chrome-steel vessels, how-

ever, has made possible the construction of large absorption towers of alloy steel capable of resisting both nitric acid and the desired high pressure. At a given gas concentration the rate of oxidation of NO increases as the square of the total pressure, and the rate of physical absorption also increases rapidly with pressure, provided the liquid film represents an appreciable fraction of the total resistance to diffusion. (See Illustration 6, page 44.) Furthermore, the chemical equilibrium is shifted favorably by increased pressure, making higher acid strengths possible. Taylor, Chilton, and Handforth describe the operation of a pilot plant operating at 100 lb. pressure, producing 5 tons of 60 per cent nitric acid, requiring an absorption system of only 1/20 the volume of an atmospheric-pressure plant producing the same amount of 50 per cent nitric acid. Figure 75 shows the absorption system of a plant producing 25 tons of nitric acid at atmospheric pressure, requiring 10 towers each 10 ft. in diameter and 50 ft. tall. The last two towers make sodium nitrite. Operating at 100 lb. pressure it is necessary to have only one tower 5 1/4 ft. in diameter 40 ft. high, which will produce 25 tons of 60 per cent acid per day. Figure 76 shows several such units in a large nitric acid plant. In this case the nitric oxide is obtained by the oxidation of ammonia, this latter step also being carried out under pressure.

REMOVAL OF SULFUR DIOXIDE FROM FLUE GAS

The generally increasing interest in air conditioning and in the prevention of smoke nuisance in cities makes it appear probable that power plants located in thickly populated centers may in the future be required to remove sulfur dioxide as well as dust from their stack gases. The Battersea station of the London Power Company has an installation now in operation for SO_2 removal, made necessary by the requirements of the Port of London Authority. In this country the problem has received the attention of Chicago public utilities, who have financed a research problem carried out by Johnstone and coworkers at the University of Illinois.[108]

The SO_2 content of stack gases from the combustion of coal varies from 0.05 to 0.5 per cent, depending on the sulfur content of the fuel. The obvious procedure of scrubbing with water is relatively expensive because of the low solubility of SO_2 and the necessity of using enormous quantities of water. Approximately

11 tons of water at 68°F. per ton of coal containing 1.0 per cent sulfur is the theoretical minimum for the recovery of 85 per cent of the SO_2 from a gas containing 0.3 per cent SO_2. Furthermore, the extremely low driving force available makes it necessary to employ an absorption apparatus having an enormous volume. The type of absorber used in any practical process for the treatment of stack gases must involve very low pressure drop, which adds to the difficulty of the problem.

In spite of these difficulties the London Power Company has installed a gas-washing plant using water as the principal solvent.[87] This plant consists of a series of spray chambers and towers partially filled with wood slats, the total scrubber volume being nearly 1,600,000 cu. ft. It is designed to treat the gas from coal burned at the rate of 133 tons/hr. with an SO_2 removal of approximately 90 per cent. The last of the banks of scrubbers is fed with a milk-of-lime solution, and no attempt is made to utilize the SO_2 in the resulting solutions. The washing system and related accessories added nearly one million dollars to the plant investment, which cost corresponds to approximately 13 cents per ton of coal if the total fixed charges be taken as 10 per cent per year. About 20 tons of water and 10 to 20 lb. of lime are used per ton of coal, representing an additional cost of 6 cents per ton of coal for pumping and for lime. The total cost of treating the gas is in the vicinity of 30 to 40 cents per ton of coal burned. This installation is very probably the largest gas-absorption unit in existence.

Johnstone's work has been directed primarily toward the discovery of addition agents which might serve to increase the solubility of SO_2 in water. He found[103] that small amounts of ferric or manganese sulfates catalyzed the liquid-phase oxidation of the SO_2 absorbed, and greatly increased the absorption capacity of the solution. Treating a gas containing 0.325 per cent SO_2 in a single porous-plate absorber, he obtained recoveries of more than 95 per cent of the SO_2 with only 1 gal. of water per 4,000 cu. ft. of gas. The oxidation of the SO_2 absorbed produces sulfuric acid which was obtained in concentrations as high as 40 per cent. With the catalyst present in the liquid, the liquid-film resistance was reduced to such an extent that oxygen and not SO_2 absorption became controlling. Although the required absorption volume was still quite large, this process appeared very promising until

it was discovered that ordinary stack gases contain unknown inhibitors (probably phenol and other organic compounds) which stop the catalytic action of the added salts after the solution has been used but a few hours. Liquid-phase oxidation of SO_2 by dissolved catalysts may prove to be of commercial importance in the recovery of SO_2 from waste gases where such inhibitors are not present.

Johnstone also discusses the possible use of other solutions which give promise of being economical. With milk of lime there is no necessity of absorbing oxygen, and the rate of absorption is much higher. Regeneration of the SO_2 is not feasible, however, and the calcium bisulfite formed is not valuable, so fresh lime must be supplied at the rate of about 140 lb./ton of coal containing 3 per cent sulfur. Buffered solutions of ammonium hydroxide appear much more promising,[104] as SO_2 can be recovered by heating the solution produced, decomposing the ammonium sulfite formed. Reduction of the SO_2 content in flue gas has been accomplished by absorption with such a solution, yielding a sulfite liquor which will give up 5 to 7 per cent of its weight of SO_2 when heated to 158°F. Because the capacity of the hydroxide solution to take up SO_2 is so large, the amount of solution to be circulated is not excessive. The size of the required absorption unit is still large, although much smaller than when using water or when using the oxidation process. Johnstone[104] and Johnstone and Keyes[106] report data on the SO_2-NH_3-H_2O equilibrium necessary in designing both absorber and stripper. Some rectification is necessary in the stripping operation to prevent loss of ammonia. As no large installation has been made for the removal of SO_2 from flue gas by means of an ammonia solution as solvent, it is not possible to compare the cost of the process with the costs at the Battersea station in London. It seems probable that the ammonia process may prove practical where the SO_2 recovered can be liquefied and sold.

The Howden-I.C.I. process, developed in England[152] since the erection of the Battersea plant, is a noneffluent water system. The gases are scrubbed with a solution of milk of lime or a slurry of powdered chalk, and the pH carefully controlled to allow supersaturation with respect to calcium sulfate within the scrubber. From the scrubber the solution goes to a "delay tank" in which calcium sulfate precipitates, and from which the solution is

returned to the scrubber. By using the correct shape and material as packing, and by careful control of the liquor system, precipitation on the packing surface is avoided.

The packing employed is a wood grid fabricated of laths 1 in. wide and 1/8 in. thick. It is claimed that this packing gives a low pressure drop for the gas flow, resists precipitation of sulfates, and removes most of the flue dust. With a depth of packing of 3 ft. 6 in., 98 per cent SO_2 removal is claimed at a superficial gas velocity of 4.5 ft./sec.

SO_2 ABSORPTION FOR BISULFITE COOKING LIQUOR

Two absorption systems are commonly used for the production of the calcium bisulfite solution used in the manufacture of sulfite pulp. In the Barker milk-of-lime system burner gas from the combustion of sulfur is passed into a combination packed and sieve-plate tower. The lower part of the tower is packed with a large-size ceramic manufactured packing material and in the upper part are several perforated plates. Milk-of-lime solution is fed to the top plate and the acid liquor is withdrawn from the bottom. Deep liquid seals are maintained on each plate and the pressure drop through the tower is about 5 lb./sq. in. The strength of the liquor and the fraction of the total SO_2 present in the combined form is regulated by the amount and strength of lime water fed. The absorption is relatively rapid and the recovery good. Where dolomitic limestone is used, there is a greater sludge formation and the tendency to clog the sieve plates is greater. This clogging is avoided by the Paulson acid absorber, which employs a single large bubble-cap on each plate. In these towers the liquor seals are 2 ft. and a tower 27 ft. high and 8 ft. in diameter is said to be ample for a 100-ton pulp mill. Equilibrium data for the system CaO-SO_2-H_2O are given by Beuschlein and Conrad.[14]

The other absorption system employs towers packed with broken limestone. Water is supplied at the top and runs down over the stone, the latter providing not only the surface of contact between gas and liquid, but also supplying the source of calcium. Limestone is attacked by sulfurous acid and goes into solution as bisulfite with the liberation of CO_2. The stone is gradually dissolved and replaced by more stone introduced at the top of the tower. Accumulation of insoluble residue tends to clog the gas passage and necessitates removal of the stone and refilling.

RECOVERY OF SO_2 FROM SMELTER GASES

The recovery of SO_2 from gases of intermediate concentrations (1 to 10 per cent) is relatively costly, not because of the difficulty of absorption by water, but because the resulting solutions are so dilute that the heat requirements for stripping the SO_2 are frequently excessive. A recent German process[192] uses a mixture of equal parts of xylidine and water as a solvent, with sodium carbonate to convert any xylidine sulfate to sodium sulfate, and heats the rich liquor to 175 to 212°F. in order to drive off the recovered SO_2 as a practically pure gas. The mixture of xylidine and water consists of two immiscible layers, but the xylidine sulfite formed is soluble in water and the rich liquor going to the still is a single layer of xylidine sulfite dissolved in water. Toluidine may also be used.

Nomenclature for Chapter VII

a = area of interphase contact, sq. ft./cu. ft. of packed volume.

$a_0 = \sqrt{\frac{k_c}{D_A}}$

$b = \frac{a_0 x_L}{\tanh a_0 x_L}$

C = concentration of solute in the liquid, mols/unit volume.

C_e = solute concentration in the liquid, corresponding to equilibrium with the partial pressure of solute in the main body of gas, mols/unit volume.

C_i = solute concentration in the liquid at the gas-liquid interface, mols/unit volume.

C_L = solute concentration in the main body of liquid, mols/unit volume.

D_A = diffusion coefficient for component A.

D_{AB} = diffusion coefficient for reaction product AB, in the liquid phase.

D_B = diffusion coefficient for component B.

D_C = diffusion coefficient for component C.

e = base of natural logarithms.

f = fraction total base present as bicarbonate.

$= \frac{N_A'}{N_A}$ = fraction of solute entering the liquid phase which reaches the main body of solution without reacting chemically.

H = Henry's law constant.

k = equilibrium constant for reaction $2NO_2 \rightleftarrows N_2O_4$.

k_c = specific rate of reaction constant for the reaction $A + B \rightleftarrows AB$.

k_G = gas-film coefficient of material transfer, g. mols/(sec.)(cm.^{2})(atm.); or lb. mols/(hr.)(sq. ft.)(atm.).

k_L = liquid-film coefficient of material transfer, g. mols/(sec.)(cm.^{2})(g. mol/l.); or lb. mols/(hr.)(sq. ft.)(lb. mol/cu. ft.).

K_A = coefficient for absorption of gas A, g. mols/(sec.)(cm.)(atm.); or lb. mols/(hr.)(ft.)(atm.).
K_C = coefficient for absorption of gas C, g. mols/(sec.) (cm.) (atm.); or lb. mols/(hr.)(ft.)(atm.).
K_G = gas-film coefficient, g. mols/(sec.)(cm.^{2}) (atm.); or lb. mols/(hr.)(sq. ft.)(atm.).
= gas-film coefficient, g. mols/(hr.)(cc.)(atm.); or lb. mols/(hr.)(cu. ft.)(atm.).
= "McCoy" constant. See Eq. (174).
m = concentration of reaction product AB in the liquid film, between the gas-liquid interface and reaction zone. See Fig. 62.
n = normality of solution in free plus combined B (or total sodium). See Fig. 62.
N = normality of base in Eqs. (174), (175), and (176).
N_A = diffusion rate of A, mols/(unit time)(unit area).
N_A' = diffusion rate of A at the boundary between the main body of liquid and liquid film, mols/(unit time)(unit area).
N_{AB} = diffusion rate of AB, mols/(unit time)(unit area).
N_B = diffusion rate of B, mols/(unit time)(unit area).
P = total pressure on system, atm.
p_A = variable partial pressure of NO_2 in gas film, atm.
p_{AG} = partial pressure of NO_2 in main body of gas, atm.
p_{Ai} = partial pressure of NO_2 at gas-liquid interface, atm.
p_{BM} = log mean of inert gas pressures at film boundaries, atm.
p_C = variable partial pressure of N_2O_4 in the gas film, atm.
p_{CO_2} = partial pressure of CO_2, mm. Hg.
p_G = partial pressure of solute in main gas stream, atm.
p_i = partial pressure of solute at liquid-gas interface, atm.
q = in the case of absorption and chemical reaction, the concentration in the main body of solution of the substance reacting with the solute.
r_2 = a constant in Eq. (156).
R = gas-law constant.
R_1 = total diffusional resistance of the gas film, total liquid film, and the main body of solution.
S = solubility of CO_2 in H_2O, g. mols/l. at 1 atm. CO_2 pressure.
t = temperature, °F.
T = absolute temperature.
V = liquid volume.
w = weight of catalyst per unit volume of solution.
x = effective thickness of liquid film.
x_F = effective thickness of gas film.
x_L = $x_L' + x_L''$ = effective thickness of liquid film.
x_L' = effective thickness of liquid film from gas-liquid interface to reaction zone.
x_L'' = effective thickness of liquid film from reaction zone to main body of liquid.
θ = time.

CHAPTER VIII

SOLVENT EXTRACTION

Solvent extraction refers to the separation of the components of a liquid solution by treatment with an immiscible solvent in which one or more of the components of the solution are soluble. In many cases distillation is cheaper and more effective than extraction, but it is also true that separation by the latter method is sometimes practicable where ordinary distillation is uneconomical or actually impossible. Acetic acid may be removed from a dilute solution of acetic acid in water by distillation or by extraction with toluene, in which the acid is soluble and the water insoluble. On the other hand, close-boiling petroleum fractions, differing chemically, may be almost impossible to separate by distillation but easily separable by solvent extraction. Extraction finds its widest application in the separation of compounds differing in chemical type, but which may be hard to separate by distillation because their volatilities do not differ greatly.

The extraction process involves the three operations of (*a*) bringing solvent and solution into intimate contact, (*b*) separation of the resulting phases, and (*c*) removal and recovery of solvent from each phase, usually by distillation. Contacting may be accomplished in any of the several types of equipment, such as baffle-plate mixers, impinging jets of the two liquid streams, agitated vessels containing the liquids, plate columns, or packed towers. Separation may be accomplished by simple settling tanks or by means of centrifuges. The difficulty encountered in separating the phases is usually greatest when the phases are dispersed to a high degree in the contacting equipment. A large difference between the densities of the two phases tends to make separation easy, but the presence of emulsifying agents may cause more trouble in the separation process than a small density difference. After separation of the phases, the solvent is usually recovered by ordinary distillation of the solvent layer, termed the "extract," and of the treated solution, termed the "raffinate."

METHODS OF OPERATION

Single Contact.—The simplest type of operation is the single contact, in which the solvent and solution are brought together for a single-batch extraction. Solute is transferred from one phase to the other, and the concentrations in the two phases approach equilibrium. The amount of solute extracted is determined by the amount of solvent employed, the equilibrium relations for the system (solution-solute-solvent) involved, and the extent to which it is possible to approach equilibrium.

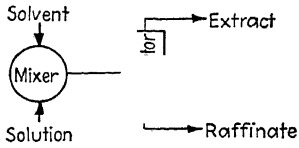

FIG. 77.—Single-contact extraction.

The equipment employed for a single-contact extraction is shown diagrammatically in Fig. 77. As indicated above, the contacting equipment may be any one of a variety of types. In mixers of the jet or agitator types, the contact between phases may be so good that equilibrium is approached closely. The final extract and raffinate from a single-contact operation are essentially

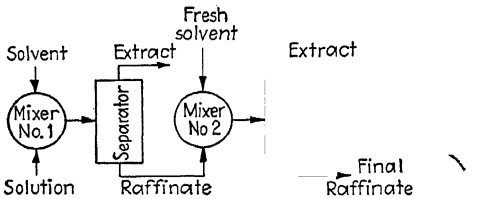

FIG. 78.—Multiple-contact extraction using fresh solvent in each contact.

in equilibrium with each other, and the amount of solute which may be extracted with a given amount of solvent is definitely limited. Because the efficiency permitted by the equilibrium involved is usually low, this type of operation is seldom employed for large-scale work.

Multiple-contact Extraction, Using Fresh Solvent in Each Contact.—Figure 78 shows an obvious improvement over the single-contact operation, the extraction being repeated on the raffinate from the first contact. The reduction of solute content of the raffinate may be improved to any desired extent by increasing the number of contacts, or stages. The concentration of solute from the second and later separators is low, however, and this method of operation is uneconomical of solvent. Provided

the distribution law (see below) holds, the maximum efficiency is obtained when the total solvent to be used is divided in equal parts,[173] the same quantity being employed in each stage. Thus if one volume of solution is to be extracted with six volumes of solvent, the best results are obtained by using three volumes of solvent in each mixer if the operation is two-stage, two volumes in each mixer if three-stage, or one volume in each mixer if six-stage.

Countercurrent Multiple-contact Extraction.—If fresh solvent is used in each stage, the extract leaving the later stages is quite dilute and could be used in place of fresh solvent in treating the original solution. The operation illustrated in Fig. 78, which is inefficient because it fails to utilize the solvent properties of the weaker extracts, may be greatly improved if solution and solvent

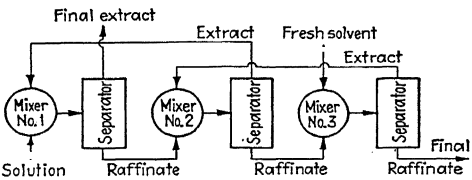

FIG. 79.—Three-stage countercurrent multiple-contact extraction.

are passed through the system in opposite directions. Figure 79 shows the type of operation employing this principle. The system illustrated involves three stages, although any number may be used. The solution to be treated enters the first mixer, as before, but all of the fresh solvent enters the last mixer. The two streams pass in a countercurrent direction, the original solution being treated with extract from the second stage, and so on, the final extract being removed from the first separator and the final raffinate from the last separator. All of the solvent passes through each stage, and the over-all efficiency, for a given amount of solvent and number of stages, is appreciably better than when part of the fresh solvent is used in each stage.

This type of operation, with from two to five stages, is the one most commonly employed for commercial solvent extraction. The operation may be either batch or continuous, as exemplified by systems of batch mixers and settlers on the one hand, or by the bubble-cap plate column on the other. At first glance the

latter would appear to be an example of continuous countercurrent flow but in reality should be classified as continuous multiple contact, since each plate acts as a combined mixer and settling chamber.

Continuous Countercurrent Extraction.—The maximum extraction efficiency would be obtained if it were possible to obtain intimate contact between phases in an apparatus in which the two liquid phases passed continuously in opposite directions. Such operation is difficult to get in practice because the best contact is obtained by violent mixing of the phases. Towers packed with Raschig rings or other filling may be employed, however, the heavier liquid flowing downward and the lighter liquid passing upward. The liquids cannot be pumped past each other, the flow resulting only from the difference in density of the two phases. The intimacy of contact obtained in jet mixers is not possible, but the apparatus is simple and reasonably cheap, and the theoretical maximum efficiency of this type of operation is higher than in the case of the countercurrent batch systems. The most recent developments in extraction equipment are along the lines of improving the performance of such countercurrent columns.

In the case of batch extractions employing jet- or agitator-type mixers, the contact is so good that equilibrium between phases is closely approached, and the rate of interphase diffusion does not govern performance. The efficiencies which may be obtained can consequently be calculated by simple stoichiometry from the equilibrium data, as shown below. In the case of countercurrent-packed columns, the solute can theoretically be completely extracted, but equilibrium is not reached because of the poorer contact between phases. The rate of solute transfer between phases governs the operation, and the analytical treatment of the performance of such equipment follows closely the methods employed for gas absorption, discussed in Chap. III.

PHASE EQUILIBRIA

In the case of two immiscible liquids, the equilibrium concentrations of a third component in each of the two phases are ordinarily related by the so-called "distribution law":

$$y = K'x \tag{187}$$

where y = solute concentration, in one liquid (extract) phase.
x = solute concentration, in the other (raffinate) phase.
K' = the "distribution coefficient."

Equilibrium data for such systems are usually reported[100] in terms of the distribution coefficients, which are analogous to Henry's law constants (see page 64). For most systems, however, K' varies considerably with concentration, and the relation (187) can hardly be called a "law." For example, if y represents the concentration of acetic acid in water as g./l., and x the equilibrium concentration of acetic acid in chloroform as g./l., K' at 77°F. is found to vary from 36 to 7 over the range of acetic acid in chloroform molalities from 0.002 to 0.21.

In cases where the solute is associated in one or the other phase, forming double or triple molecules, the mass action and equilibrium laws may be combined[95] to give the equilibrium relation. Thus if the solute tends to form triple molecules in the extract phase, then by the mass-action law,

$$y_3 = ky_1^3 \tag{188}$$

where y_3 = concentration of triple molecules.
y_1 = concentration of single molecules.
k = mass-action constant.

The total concentration y_T is given by

$$y_T = y_1 + 3y_3 = y_1 + 3ky_1^3 \tag{189}$$

The distribution law may be assumed for the single molecules:

$$y_1 = K'x$$

whence

$$\begin{aligned} y_T &= K'x + 3k(K'x)^3 \\ &= (K' + 3kK'^3x^2)x \end{aligned} \tag{190}$$

which is the new equilibrium expression. Because of the limited applicability of the distribution law, however, this treatment is seldom justified.

TRIANGULAR GRAPHS OF EQUILIBRIUM DATA

When two of the liquid phases are partially or wholly miscible, the equilibrium relations for a three-component system are best expressed by means of a triangular graph. Several possible types of such diagrams will be considered.

1. *Component A is miscible in all proportions with B, likewise with C, but B and C are but partially miscible.* This case is illustrated by Fig. 80. Point *A* represents 100 per cent *A*, *B* represents 100 per cent *B*, and *C* 100 per cent *C*. Any point *H* within the triangle represents a mixture of the three components, in relative amounts given by the perpendiculars *HL*, *HJ*, and *HK*. The geometry of the figure requires that these three percentages always add to 100. *BN* represents the solubility of *C* in *B*, and *MC* the solubility of *B* in *C*. The region *NPFQM* is the unstable or two-phase region, mixtures such as *O* automatically splitting into two layers of compositions *P* and *Q*. The "tie lines," of which *PQ* is one, connect the points representing compositions of two phases in equilibrium. The compositions of the two phases approach each other as *O* is moved vertically, and become equal (and so revert to one phase) at *F*, the "plait-point." For extraction calculations, it is necessary to have both the solubility curve *NPFQM* and the data on concentrations of phases in equilibrium as given by the tie lines.

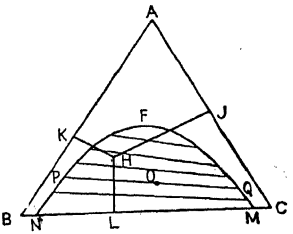

FIG. 80.—Triangular diagram for representing equilibrium data on three-component system.

Instead of a family of tie lines, a single conjugate line may be used to represent the data on equilibrium between phases. A second triangle is drawn having a base common to the first and the conjugate line located as *DR* in the lower triangle of Fig. 81. Starting at any point *P* on the solubility curve, the equilibrium concentration in the other phase is obtained by following a line parallel to the side *BD* of the lower triangle until the conjugate line is reached at *T*, and then turning back along a line parallel to the other side *DC* of the lower triangle until the desired point *Q* on the other branch of the solubility curve is located. This procedure is indicated by the dotted lines *PT* and *TQ* of Fig. 81.

Another type of conjugate line, not requiring the lower second triangle, is represented by the curve *FSN* of Fig. 81. To use this type of line, pass from a point *Q* on the right branch along a line *QS* parallel to the base *BC* to the point *S* on the conjugate line, and then up to the left parallel to *AC*, intersecting the left branch at the desired equilibrium point *P*. Conjugate lines can be

plotted if a few tie lines are known, and are helpful for purposes of interpolation.

2. *Component A is miscible in all proportions with B, but B and C, and A and C, are but partially miscible.* This case is illustrated by Fig. 82, in which region *a* and *c* are single-phase and region *b* is two-phase. A mixture of composition represented by point *O* will automatically split into two layers of compositions *P* and *Q*, as indicated by the tie line.

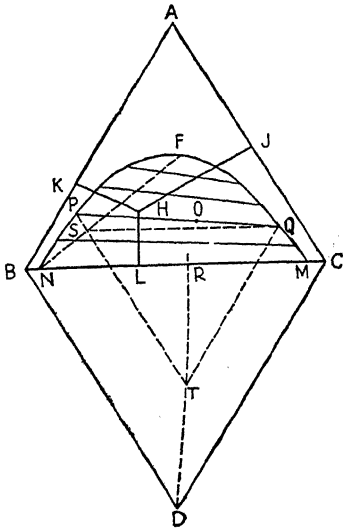

FIG. 81.—Two types of conjugate lines for representing equilibria between phases.

3. *Each component is only partially miscible with each of the other two.* Referring to Fig. 83, regions *a*, *a*, *a* are single phase, *b*, *b*, *b* are two phase; and *c* is the three-phase region. Any point in region *c* represents a mixture which spontaneously splits into

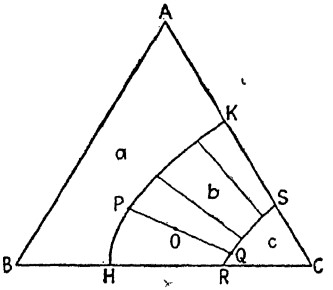

FIG. 82.

three phases of compositions *E*, *F*, and *G*. Mixtures such as *H*, represented by points in region *b*, split into two layers of compositions *J* and *K*, as indicated by the appropriate tie line.

4. *One component is a solid.* Since the solubility of a liquid in a solid is negligible, the lines representing the phase boundaries pass directly to the apex of the triangle corresponding to the solid composition. In Fig. 82, for example, if *C* were a solid, the curve *RS* would disappear into the apex *C*, with the result shown in Fig. 84. Solutions of varying compositions along *HK* would all be in equilibrium with the solid *C*. Tie lines, such as *PC*, are obviously unnecessary.

Other cases are encountered, such as when one component of Fig. 83 is solid, but the diagrams are simply modifications of those given for three liquids and will not be discussed in detail.

STOICHIOMETRIC CALCULATIONS

As pointed out above, a number of different types of equipment are used to bring the two liquid phases in contact. In several of these, the intimacy of contact is excellent and the phases, after separation, are very nearly in equilibrium. The calculation of the result of any specified system of operation with such equipment is, therefore, merely a matter of stoichiometry, with the aid of the equilibrium data. Because the equilibrium data are frequently difficult to express algebraically, the computations are

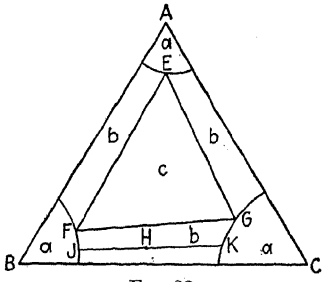

FIG. 83.

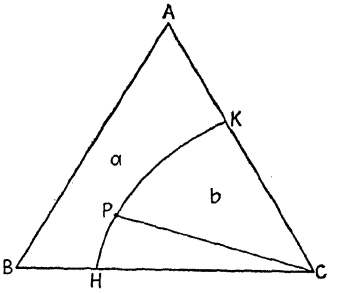

FIG. 84.

apt to involve time-consuming trial and error, unless a graphical procedure is followed. Graphical methods have been developed for use with both ordinary and triangular graphs of the equilibrium data and are described below.

In cases where equilibrium is not reached in the contacting equipment, the methods described may be used to calculate the number of "equilibrium contacts" necessary to accomplish the separation actually effected in practice. A comparison of this number with the actual number of contacts employed affords a useful index of the efficiency of the contacting equipment and a basis for the computation of any proposed method of extraction using similar equipment.

1. Solvent Completely Immiscible with Solution to Be Treated.[94]—In Fig. 85, curve *OP* represents the general type of equilibrium relation for this case. The ordinate y represents the

solute concentration in the extract layer, and x the concentration in the raffinate layer, each expressed as lb. solute per lb. of solvent (or g. solute per g. solvent). Where the distribution law (Eq. (187)) holds, OP is approximately straight.

Assume that an original solution of composition x_0 containing a lb. of solvent A, is to be treated with b lb. of pure solvent B. The resulting mixture separates into two layers of composition x_1 and y_1, in equilibrium. By a material balance,

$$ax_0 = ax_1 + by_1 \tag{191}$$

or

$$\frac{y_1}{x_1 - x_0} = -\frac{a}{b} \tag{192}$$

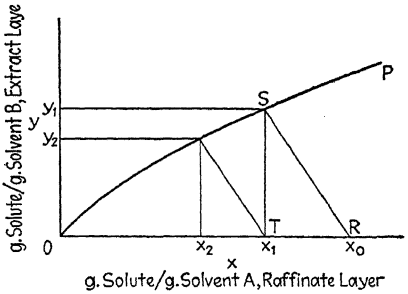

FIG. 85.—Graphical construction using immiscible liquids; multiple contact using fresh solvent B in each stage.

The composition of the original solution is represented by the point R; the compositions x_1 and y_1 are obtained from the equilibrium curve OP by the intersection at S of a line drawn through R with a slope $-a/b$, so that $y_1/(x_1 - x_0)$ will be equal to $-a/b$. Further extraction of the raffinate T with pure solvent will give raffinate and extract of compositions x_2 and y_2, found by the same method.

If OP is straight, $(y = K'x)$, then the graphical construction is unnecessary, since

$$ax_0 = ax_1 + by_1 = ax_1 + bK'x_1 \tag{193}$$

whence

$$x_1 = \left(\frac{a}{a + bK'}\right)x_0 \tag{194}$$

If the same amount of fresh solvent is used in each subsequent extraction, then

$$x_2 = \left(\frac{a}{a + bK'}\right)x_1 = \left(\frac{a}{a + bK}\right)^2 x_0$$

and

$$x_n = \left(\frac{a}{a + bK'}\right)^n x_0 \tag{195}$$

It can be shown that x_n will be a minimum for any given number of stages and for a given total quantity of fresh solvent, if equal quantities of solvent are used in each extraction, *i.e.*, if the total solvent is divided into n equal portions.

For countercurrent multiple-contact extraction, the material balance on the first stage (extract leaving, raffinate entering) is

$$by_2 + ax_0 = by_1 + ax_1 \tag{196}$$

and for the nth stage,

$$by_{n+1} + ax_{n-1} = by_n + ax_n \tag{197}$$

where the subscripts refer to the stage which the solution is leaving. By drawing a material balance around the first n stages it follows that

$$ax_0 + by_{n+1} = ax_n + by_1$$

$$y_{n+1} = \frac{a}{b}(x_n - x_0) + y_1 \tag{198}$$

The composition of the extract entering the nth stage is a linear function of the composition of the raffinate leaving the nth stage. The line representing this relation on a plot of y *vs.* x is the "operating line" and is based solely on the stoichiometry of the process.

Figure 86 represents the construction for a three stage countercurrent extraction effecting the reduction of the raffinate concentration from x_0 to x_3; y_3 is 0, since a pure solvent is used. The line EF is the operating line, drawn with a slope a/b.

If the initial and the desired final raffinate concentrations x_0 and x_n are specified, then the number of equilibrium stages required, using a given solvent ratio a/b, is obtained by stepping

off the intervals GH, KL, MF, etc., after first placing the equilibrium curve and drawing the "operating line" EF through E with a slope a/b. The point E has the coordinates y_n, x_n, where y_n is the solute concentration in the fresh solvent (zero in the diagram) and x_n is the final raffinate concentration.

If the number of equilibrium stages is specified, then the calculation of the required solvent ratio for a specified x_n, or the calculation of the resulting concentration x_n using a specified solvent ratio, is necessarily carried out by trial and error, but is not time consuming.

If it can be assumed that the two phases leaving each stage of the contacting equipment are essentially in equilibrium, then

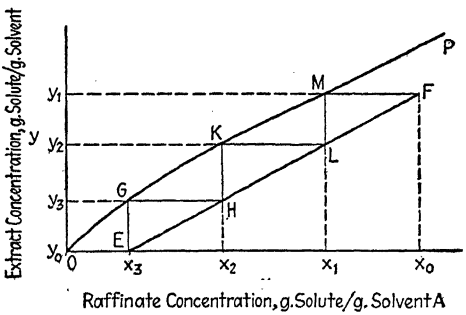

FIG. 86.—Graphical construction using immiscible liquids; countercurrent multiple-contact extraction.

the number of equilibrium stages will be equal to the number of actual stages. If equilibrium cannot be assumed, because of inadequate contact of the phases, then a "stage efficiency" may be introduced. Several "efficiencies" might be defined, such as an analogue of the Murphree efficiency as applied to fractionating columns, but the simple over-all efficiency is probably adequate for analysis of extraction data. This is defined as the ratio of the calculated number of equilibrium stages to the number of actual stages or contacts required. Thus with an over-all efficiency of 50 per cent, the concentration x_0 would be reduced to x_3 in six stages, whereas Fig. 86 shows that only three equilibrium stages would be required.

2. Solvent Partially Miscible with the Solution to Be Treated. In this general case the equilibrium is best represented by a triangular diagram. The stoichiometric computations are con-

veniently carried out by graphical construction on such a diagram, as has been explained by Hunter and Nash,[96] and by Evans.[58] An alternative method, based on the graphical method of Ponchon, is discussed by Thiele.[182]

Before this procedure is described, it is important to point out certain properties of triangular diagrams. Figure 87 shows a diagram similar to Fig. 80, with the solubility curve and the tie lines. It is not difficult to prove that if a mixture of A, B, and C, represented by the point P, be mixed with a solution of composition R, the composition of the resulting mixture will be represented by a point Q lying on a straight line connecting P with R. Furthermore, the position of Q will be such that the distances PQ and QR are in the ratio of the amounts of R and P mixed, *i.e.*,

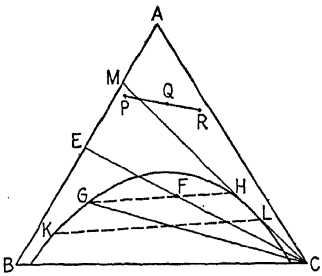

FIG. 87.—Graphical construction for stoichiometric computations.

$$\frac{PQ}{QR} \quad \frac{\text{amount of } R}{\text{amount of } P} \tag{199}$$

If the point Q should fall within the two-phase region on the diagram, then the resulting mixture will split into two phases having the compositions indicated by the points at the ends of the tie line through Q. The amount of each resulting phase will be in inverse proportion to the distance of Q from the end of the tie line.

Figure 87 shows the construction for a two-stage multiple-contact extraction using fresh solvent in each stage. The material to be treated has a composition represented by the point E and is brought in contact with solvent C. The resulting mixture F, lying within the two-phase region, will separate into two layers of compositions G and H, as determined by the tie line through F. The raffinate G is treated with further solvent, and the final raffinate K obtained. The compositions of the two extracts are given by points H and L. The amounts of each material may be determined from the known amounts of original solution and of solvent used, and by a calculation of the amounts of the phases separated, using the rule represented by Eq. (199).

Figure 88 represents the construction for a two-stage countercurrent multiple-contact system, employing the solvent C to treat the original solution E. The procedure is by trial and error, and may be started in various ways. Assume, for example, that the final extract is to have a composition H. Then for the extraction process as a whole,

$$E + C = H + K = F$$

where the letters represent *both amount and composition* of the several mixtures. Point F lies on EC and its position is determined by the relative amounts of solution E and solvent C used. The final raffinate K is determined as the intersection of HF with

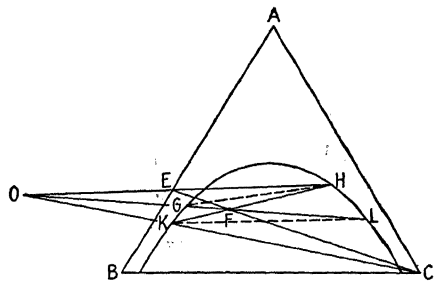

FIG. 88.—Construction for two-stage countercurrent multiple-contact extraction.

the solubility curve. The intermediate raffinate and extract have compositions G and L, as yet undetermined. By material balances on the separate stages it follows that

$$E + L = G + H, \qquad \text{and} \qquad G + C = K + L$$

whence $K - C = G - L = E - H$.

Application of the rule of Eq. (199) shows that the straight lines HE, LG, and CK will intersect in a common point O. Point O represents a mixture having a negative-solvent content and hence is of geometric significance only.

Since the location of H has been assumed, K may be located by extending HF. Point O is then located as the intersection of CK and HE. Point G is located at the other end of the tie line through H, and L is obtained by extending OG. Points L and K should then be found to lie on a common tie line; if not, point H

was incorrectly assumed, and the procedure must be repeated with another assumed composition of the final extract. With three or more stages the construction is the same, but employing a correspondingly greater number of tie lines and construction lines through *O*.

Referring again to Figure 87, the material obtained by removing the solvent from the extract has a composition represented by the intersection on *AB* of a straight line from the apex *C* through the point representing the composition of the extract. With systems of the type illustrated in Fig. 87, the maximum concentration of *A* in the distilled extract will be represented by *M*, where *CM* is tangent to the solubility curve.

The final raffinate *K*, after two extractions, may be compared with the original solution *E*. It is evident that the separation effected, and the completeness of the removal of *A* from the raffinate, will depend to a large extent on the position of the tie lines. Had the tie lines sloped more steeply up to the right, the separation would have been easier in that *K* would have been lower. Conversely, if the tie lines had sloped down to the right, *K* would have fallen on the solubility curve nearer to the line *EC*. In the latter case, *C* would be a poor solvent for the separation of *A* and *B*, but *B* would be an excellent solvent for the separation of *A* and *C*.

An alternative graphical method of calculation, based on the use of an operating line, has been developed by I. L. Murray.[149] An equation for the operating line is obtained from the usual material balances, and the line plotted on the triangular equilibrium diagram. Having placed this line, it is a simple matter to "step off" the number of equilibrium contacts between this and the conjugate lines. As a trial-and-error calculation is apparently required to locate the coordinates of each point on the curved operating line, the method is not easier to use than the trial-and-error graphical method described above.

The analogy between distillation and extraction and methods of employing "reflux" in continuous extraction processes are discussed by Saal and Van Dyck[162] and by Thiele.[182]

3. Complex Hydrocarbon-solvent Systems.—In the solvent refining of lubricating oils, the object is to separate in the extract a high proportion of the undesirable "naphthenic" compounds, leaving a raffinate containing an increased proportion of

the "paraffinic" compounds. The improvement of the raffinate is measured by the change of any one of several criteria, such as the viscosity index* (V.I.), or viscosity gravity coefficient† (V.G.C.). Oils having a high V.I. have a low temperature coefficient of viscosity, a property desirable in automotive lubricating oils. The V.G.C. is reduced by proper solvent refining, the better oils having low values of this criterion.

The problem is no longer that of the relatively simple ternary system, but involves a complex system of solvent and a large number of different and unknown hydrocarbons. A method of attack proposed by Hunter and Nash[95] appears to have considerable promise, and will be described briefly.

It is first assumed that the V.G.C. of a mixture of two oils will be a weighted mean of the two values of the V.G.C. for the two oils. This assumption does not appear to have been proved directly, but is borne out by the comparison of experimental and calculated results for various cases of solvent treating. A ternary diagram is constructed, the three apexes representing respectively the solvent, an oil with a low V.G.C. (say 0.80), and an oil with a high V.G.C. (say 0.90.). Such a diagram is represented in Fig. 89. Laboratory extractions then serve to determine the solubility curves and the tie lines, as in the case of a normal ternary system. For example, suppose one volume of an oil having a V.G.C. of A is shaken with an equal volume of solvent. The mixture will be represented by point F, located on a straight line AP and midway between A and P. A raffinate and extract are obtained, and the solvent content of each is determined. Also, the V.G.C. of each solvent-free layer is measured. Point E representing the composition of the extract is then located on a straight line connecting P with B, the V.G.C. of the solvent-free extract, at a position determined by the measured solvent-oil ratio in the extract. Similarly, point D is located from the

* The viscosity index is an empirical measure of the temperature coefficient of viscosity. It is defined arbitrarily in terms of the viscosities at 100°F. and 210°F. in such a way that a standard good Pennsylvania-base lubricating oil has a V.I. of 100, and a standard poor oil has a V.I. of 0. (See Dean and Davis,[46] also Davis, Lapeyrouse and Dean.[45])

† The viscosity gravity constant is a constant in an empirical relation between the specific gravity and the viscosity. Paraffinic oils exhibit a low specific gravity and a low V.G.C., and the naphthenic oils a high specific gravity and a high V.G.C. for any given viscosity. (Hill and Coats.[88])

V.G.C. of the solvent-free raffinate C, and the solvent-oil ratio CD/DP of the raffinate. Thus one tie line and two points on the solubility curve are determined. Similar tests serve to locate other tie lines and other points on the solubility curve, and the result is a diagram similar to Fig. 89. Using this diagram, the stoichiometric computations are entirely similar to those described for actual ternary systems.

As an example of the results obtained using this method of computation, Hunter and Nash[97] compare the calculated and observed results of the multiple extraction of a naphthenic-distillate lubricating oil with nitrobenzene at 50°F. One hundred volumes of oil were treated with 100 volumes of nitrobenzene, giving raffinate A and extract A. Raffinate A was then treated with 120 volumes of nitrobenzene, yielding raffinate B and a

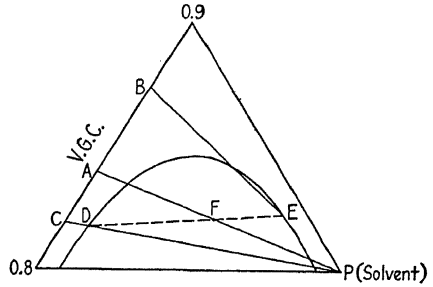

FIG. 89.—Ternary diagram for representation of complex hydrocarbon-solvent equilibria.

second extract which was mixed with extract A to give extract B. Raffinate B was treated with 173 volumes of nitrobenzene, giving raffinate C and an extract which was mixed with extract B to give extract C. Table XVII compares the amounts and V.G.C.'s of the various fractions as determined experimentally, with the calculated values obtained using the graphical method described above.

The comparison is not particularly good in the third stage, but the discrepancies may be blamed in part on the inadequate equilibrium data available for this oil.

Using this method of calculation, it is necessary to obtain equilibrium data for each oil to be considered. Such data not only allow the calculation of the results for a given extraction procedure, but also give immediate indication of the practicability

of the particular solvent. A straight line through the solvent apex, and tangent to the solubility curve intersects the V.G.C. axis at the maximum V.G.C. obtainable in the solvent-free extract.

TABLE XVII.—COMPARISON OF EXPERIMENTAL AND CALCULATED RESULTS OF THE MULTIPLE EXTRACTION OF AN OIL WITH NITROBENZENE

	Solvent-free oil vol. percentage of original stock		V.G.C. of solvent-free oil		Vol. percentage solvent	
	Actual	Calculated	Actual	Calculated	Actual	Calculated
Raffinate *A*.....	49.0	49.7	0.840	0.838	19.5	19.5
B.....	27.3	31.0	0.811	0.811	12.5	15.0
C.....	15.6	20.7	0.802	0.805	16.6	16.0
Extract *A*.....	50.7	50.6	0.911	0.911		
B.....	72.7	69.3	0.898	0.904		
C.....	84.4	79.6	0.887	0.893		

Illustration 19.—It is desired to treat a Mid-Continent semiparaffinic oil with nitrobenzene in order to improve its lubricating qualities, as indicated by a reduced V.G.C. Using the following data, compute the solvent content of the extract and the raffinate for a three-stage countercurrent extraction of the oil, and determine the V.G.C. of each product after removal of solvent. Equal volumes of solvent and oil will be used. Compare the calculated results with the experimental results determined by Hunter and Nash, given below:

Solvent content of final extract = 64.8 per cent
Solvent content of final raffinate = 12.5 per cent
V.G.C. of final solvent-free extract = 0.895
V.G.C. of final solvent-free oil = 0.811

Ferris, Berkheimer, and Henderson[63] report the results shown on page 254 of single-contact extractions by nitrobenzene at 50°F., for the oil used by Hunter and Nash.[97]

Solution.—Using triangular coordinates, let one apex represent an oil having a V.G.C. of 0.80, another apex represent an oil having a V.G.C. of 0.90, and the third apex represent the pure solvent, nitrobenzene.

Locate the solubility curve from the data of Ferris, Berkheimer, and Henderson in the following manner. On a straight line connecting the V.G.C. of the solvent-free extract and the solvent apex (Y) place a point corresponding to the solvent content of the solvent-oil mixture. Thus,

point *E* (Fig. 90) on the curve *EA* is obtained for an extract layer having 70.2 per cent solvent, the V.G.C. of the solvent-free extract being 0.894. Data on the raffinate layer are used in the same manner, to determine the solubility curve *UTS-DEBA*. Points such as *n* on the conjugate line *HnA* are located from the data below as at the intersection of two lines, one through a point on the raffinate side of the curve and parallel to *XY*, the other through a point representing the equilibrium extract and parallel to *XZ*.

Vols. solvent per 100 vols. oil	Raffinate layer		Extract layer	
	Percentage solvent	V.G.C.*	Percentage solvent	V.G.C.*
50	20.6	0.842	58.4	0.899
100	17.4	0.830	70.2	0.894
300	12.5	0.815	84.4	0.880
500	12.7	0.807	86.7	0.868

* Of solvent-free oil.

The line *RY* is now drawn, *R* representing the V.G.C. of the feed oil. Since equal volumes of oil and solvent are specified, point *F* at the middle of *RY* represents the composition of the oil-solvent mixture. The rest of the procedure is by trial and error. First, an estimate of the compositions of the final extract and final raffinate, represented by *D* and *U*, is made. *D* and *U* must lie on the ends of a line through *F*. Point *O* is then located at the intersection of *RD* and *UY*. By means of the conjugate line the other end of the tie line through *D* is located, as shown on the figure by point *S*. The line *OS* is next drawn, and point *C* is located on the equilibrium curve. Point *T* is located at the other end of the tie line through *C*, and *TO* is drawn, its intersection with the equilibrium curve fixing point *B*. Then, if the assumed value of *U* lies on the other end of the tie line through *B*, *D* and *U* have been correctly chosen, and the diagram gives the compositions and extract. If *U* and *B* do not lie on the same tie line, another estimate of *U* and *D* must be made, and the procedure repeated.

The values read from Fig. 90 are compared below with the experimental results:

	Experimental	Calculated
Solvent content of final extract....	64.8 per cent	65 per cent
Solvent content of final raffinate...	12.5 per cent	13 per cent
V.G.C. of final solvent-free extract	0.895	0.898
V.G.C. of final solvent-free oil.....	0.811	0.807

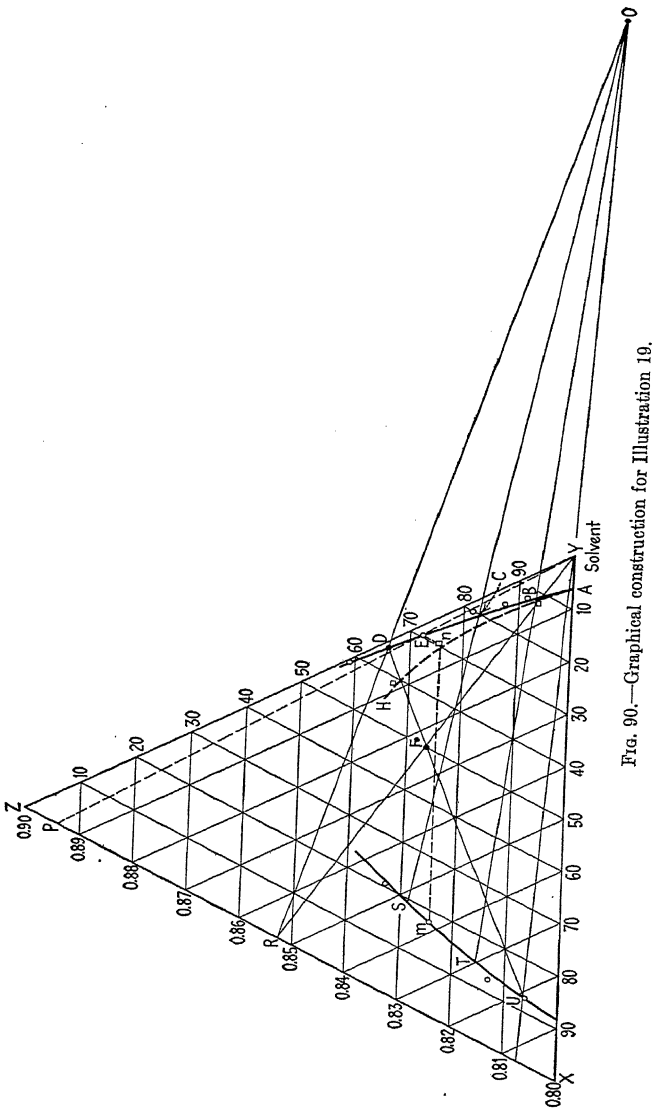

FIG. 90.—Graphical construction for Illustration 19.

CONTINUOUS EXTRACTION IN PACKED COLUMNS

The recent data of Demo and Ewing[48] serve to indicate the results obtainable with packed columns used for extraction, and the methods which may be employed for interpretation of the data. The apparatus used was a 3.55-in. i.d. glass column packed to a depth of 5 ft. with 1/2-in. carbon rings. Water-acetic mixtures containing 10 to 12 per cent acetic acid were fed at the top, and extracted by benzene fed continuously at the bottom. The benzene-acetic acid extract was removed at the top, and the water-acetic acid raffinate removed from the bottom. The equilibrium concentration of acid in water is roughly 15 times that in the benzene phase, so that even though high benzene rates were used, acid extracted was only 7 to 24 per cent of that in the feed. The results are summarized in Table XVIII.

TABLE XVIII.*—DATA OF DEMO AND EWING ON EXTRACTION OF ACETIC ACID FROM WATER BY BENZENE IN A TOWER PACKED WITH 1/2-IN. RINGS

Disperse phase	Water rate, cu. ft./(hr.) (sq. ft.)	Benzene rate, cu. ft./(hr.) (sq. ft.)	K_Wa	K_Ba	$(H.T.U)_W$, ft.	$(H.T.U)_B$, ft.
Benzene....	3.52	9.9	0.29	4.86	12.0	2.1
Benzene....	3.52	16.1	0.39	6.45	8.9	2.5
Benzene....	3.52	20.3	0.46	6.66	7.6	3.0
Benzene....	1.77	16.1	0.30	4.90	5.9	3.3
Benzene....	5.90	12.5	0.44	7.18	13.3	1.7
Benzene....	5.90	16.1	0.74	11.6	8.0	1.4
Benzene....	5.90	17.8	0.16	17.3	37.8	1.0
Water.....	1.77	16.1	0.16	1.89	13.0	8.5
Water.....	3.52	16.1	0.15	2.22	23.4	7.3
Water.....	5.90	16.1	0.23	3.04	25.0	5.3
Water.....	3.52	9.9	0.11	1.64	32.3	6.0
Water.....	3.52	20.3	0.17	2.60	20.8	7.8

* Ka = lb. mols/(hr.)(cu. ft.)(lb. mol/cu. ft.).

Subscript W refers to values based on flow of water phase and concentrations of acid in the water phase.

Subscript B refers to values based on flow of benzene phase and concentrations of acid in the benzene phase.

As in the case of gas absorption, the results may be interpreted in the form of a capacity coefficient, the height of a theoretical

plate, or the height of a transfer unit (H.T.U.). By analogy to Eq. (115), page 91, the H.T.U. is defined by the equation

$$\text{H.T.U.} = \frac{h}{\int_{C_0}^{C_1} \frac{dC}{\Delta C}} = \frac{L}{Ka} \tag{200}$$

where h is the height of the packed section in feet, C is the concentration of solute in one phase, lb. mols/(cu. ft.), and L is the volume rate of flow of the *same phase*, cu. ft./(hr.)(sq. ft. tower cross section). The driving force ΔC is the actual concentration in one phase minus the equilibrium concentration in the same phase corresponding to the actual concentration in the other phase. Ka represents the capacity coefficient as lb. mols/(hr.)(cu. ft.)(lb. mol/cu. ft.). Subscript B refers to values obtained where L represents the benzene rate and C the concentration in the benzene phase; subscript W refers to values obtained using the water rate and the concentrations in the water phase.

Since the distribution coefficient favors the water phase, and since the individual film coefficients for the two phases are probably about the same, it seems reasonable that the benzene film offers the major resistance to acid transfer. Consequently the values based on the concentrations in the benzene phase are probably the more reliable. There is no more reason to expect that the results on the two bases should be the same than there is to expect $K_G a$ to be the same as $K_L a$ for absorption of SO_2 from air. The difference between the results on the two bases illustrates the error in assuming that H.T.U. (or the H.E.T.P.) should always be the same for a given packing material, independent of the system involved.

It follows from Eq. (200) that the H.T.U. will increase if Ka increases less rapidly than the first power of the flow of the phase on which the calculations are based. The first three runs show $(\text{H.T.U.})_B$ increasing from 2.1 to 3.0 ft. as the benzene rate is increased from 9.9 to 20.3 cu. ft./(hr.)(sq. ft.), indicating that $K_b a$ does not increase in proportion to the benzene rate. With benzene the dispersed phase the three runs at a benzene rate of 16.1 show $(\text{H.T.U.})_W$ passing through a maximum, indicating that at high flow rates Ka may increase in proportion to the flow rate raised to a power greater than unity. It seems probable that the major variable is the interfacial surface a, which is greatly

affected by the rates of flow of the two phases. As the velocity of the continuous phase is increased, the dispersed phase is held back, and there are more drops per unit volume. Furthermore, as more of the dispersed phase is present in the column, the actual linear velocity is further increased, accentuating this effect.

No data on flooding velocities were obtained, but it appeared evident from the action in the column that flooding was approached closely in the seventh run tabulated, in which the flow rates were at a maximum.

Data on extraction using the system benzene-ethyl alcohol-water in a small 0.55-in. i.d. tower packed with small chain and 5/32-in. wire packing are reported by Varteressian and Fenske.[186] A packed height of 10 ft. gave results corresponding to 2.1 to 4.0 equilibrium contacts, when operated with parallel flow. The data are not particularly significant for large-scale design purposes because of the small size of tower and packing, but they are of interest as a case where the two phases are miscible to a considerable extent. In such a system there is a simultaneous diffusion of solute and of one of the two solvents.

TABLE XIX.*—DATA OF ELGIN AND BROWNING ON EXTRACTION OF ACETIC ACID FROM ISO-PROPYL ETHER IN AN UNPACKED SPRAY TOWER

Disperse phase	Water rate, cu. ft./(hr.) (sq. ft.)	Ether rate, cu. ft./(hr.) (sq. ft.)	$K_W a$	$(H.T.U.)_W$, (ft.)
Ether	103	58	4.9	21.0
Ether	99	93	8.8	11.3
Ether	101	127	11.2	9.1
Ether	101	178	15.4	6.6
Ether	37	72	6.2	6.0
Ether	223	72	7.3	30.6
Ether	494	71	10.7	46.3
Water	100	31	7.4	13.6
Water	99	68	13.8	7.2
Water	100	85	17.3	5.8
Water	102	38	7.8	13.1
Water	102	66	12.3	8.3
Water	102	111	18.2	5.6

* $K_W a$ = lb. mols acetic acid/(hr.)(cu. ft.)(lb. mol acetic acid/cu. ft. water phase).

Elgin and Browning[55] report data on the extraction of acetic acid by water from iso-propyl ether solutions, and extraction of

acetic acid by iso-propyl ether from water solution, using an unpacked tower 2.03 in i.d. and 48.75 in. high. Table XIX gives a summary of representative data[56] on extraction by water. The distribution coefficients favor the water phase, so the ether film is probably controlling, and the results should be calculated in terms of concentrations in the ether phase. The distribution coefficient is fairly constant, however, and $K_W a$ and $K_E a$ are almost proportional. The values of $(\text{H.T.U.})_E$ are approximately constant at about 2.4 ft. when the dispersed phase is ether, and about 1.1 ft. when the dispersed phase is water. The flow rates are much higher than those employed by Demo and Ewing, indicating the greater capacity of the unpacked column.

In the case of the unpacked column the results are largely dependent on the type of spray by which the dispersed phase is introduced, and on the physical properties such as surface tension which affect the drop size and "settling" rate. In the packed tower these factors are probably secondary to the action of the packing in determining the nature of the contact between the phases.

SOLVENT REFINING OF PETROLEUM OILS

The last few years have seen the rapid development of extraction processes for the refining of lubricating oils. The principal value of these processes has been their ability to produce high V.I. oils comparable with those obtained from good Pennsylvania stocks from various Mid-Continent and Coastal crudes. A wide variety of solvents is employed, but the majority of the extraction processes themselves are quite similar.

Since the object of extraction is the separation of the naphthenic and paraffinic constituents the solvent should be highly "selective," *i.e.*, it should be a good solvent for the naphthenic and a poor solvent for the paraffinic fractions. Both the character and yield of raffinate depend on the selectivity of the solvent. It should be relatively insoluble in the oil, so that recovery costs may not be too high. It should obviously be chemically stable and noncorrosive to ordinary materials of construction. Its specific gravity should be materially different from that of the oil, so that separation may be easily effected. (In this connection, however, it should be noted that ease of separation is by no means proportional to the difference in densities of the two phases, since

natural emulsifying agents present in the oils cause much more trouble with some solvents than with others.) The solvent should have a low boiling point so that solvent recovery may be carried out without injuring the product. It should operate most effectively at ordinary temperatures in order that costs of heat exchangers, refrigeration, etc., will not be large. It should preferably be nontoxic. Since there is necessarily some solvent loss, it should be cheap.

The important solvents now in use include furfural, nitrobenzene, phenol, crotonaldehyde, β-β-dichloroethyl ether ("chlorex"), cresylic acid, and a mixture of SO_2 and benzene. The action of the various solvents is similar, the raffinate usually showing an increased viscosity index, a decreased viscosity, an improved color, a greater resistance to sludging, a reduced tendency toward carbon deposition, and an increased pour point.

As might be expected, the yield is less the greater the improvement in the physical properties of the raffinate. Thus a 100 V.I. oil (equivalent to a good Pennsylvania-stock lubricating oil) may be obtained from a good Mid-Continent distillate with a yield of perhaps 70 per cent, but the same product would be obtained from a distillate from a Coastal crude with a yield of possibly only 30 to 40 per cent. These figures are but roughly indicative of the difference, since the yields vary widely with the stock to be treated, as well as with the solvent-oil ratio employed, the number of stages, the type of solvent, etc. Large solvent ratios mean good separation and a good product, but also result in poor yields. Extraction efficiencies are improved and better yields obtained if less solvent is used with a greater number of extraction stages. More than seven stages, however, are practically never economical.

Figure 91 shows a typical flow sheet for a four-stage extraction process. The oil to be treated enters the system through the exchanger *M* and passes with extract from 2 through the U-shaped baffle-plate mixer into the first settling tank, 1. The raffinate, lighter than the extract, is decanted off and with extract from 3 goes through a second baffle-plate mixer into a second settling tank 2. Thus the four units shown operate as a four-stage countercurrent multiple-contact system. The final extract, drawn from the bottom of 1, passes through the heat exchangers *A* and *B* and from the steam preheater *C* to the vacuum steam

stripping still *E*. This still is supplied with steam at the bottom, and the solvent-free extract is removed through the exchanger *A*. The solvent vapors pass through the exchanger *B* and a condenser *H* to the receiver *K*.

The final raffinate from the extraction system, removed from the top of 4, passes through the exchangers *D* and *F* and the steam preheater *G* to the vacuum still *R*. The final raffinate from the system leaves this still through the exchanger *D*.

The solvent vapors from *R* are condensed in *H* and pass to *K*, where they mix with condensate from the extract still *E*. Solvent

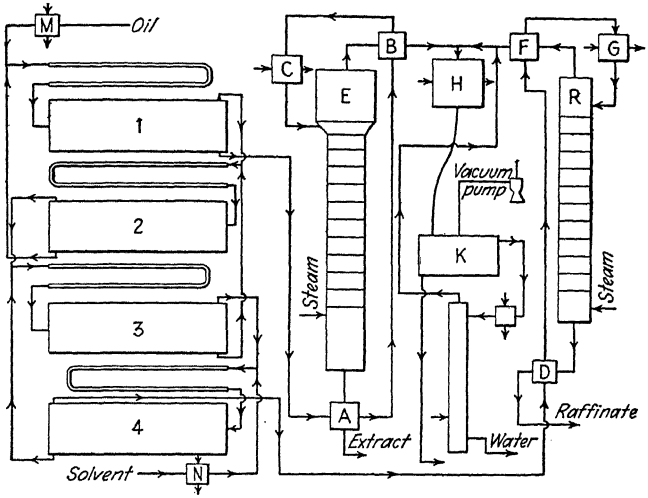

FIG. 91.—Typical flow sheet of extraction process.

drained from the bottom* of the receiver *K* is returned to storage and reused. The water layer drained from the top of *K* passes to a small atmospheric steam stripper whence the wet recovered solvent passes as vapor back to *H*. The water leaving the bottom is essentially solvent-free and is discarded.

Most of the earlier systems installed employed an extraction unit consisting of some type of mixer followed by a settling tank. It has been found, however, that the benefits of continuous

* The problems encountered in separating solvents and water are discussed in a recent paper by Smoley and Kraft.[174]

countercurrent extraction may be obtained by using a tower packed with Raschig rings or similar filling. The heavier phase passes down and the lighter phase passes up, each issuing from the tower essentially free from the other. Towers of reasonable height (30 to 40 ft.) are equivalent to three to six equilibrium stages. The capacity is limited, however, and depends considerably on the difference in density of the two phases. It has been found that an experimental tower 12 ft. high packed with 1-in. Raschig rings and using furfural at 200° to 220°F., will handle from 400 to 1,700 gal. of oil/(hr.)(sq. ft.) of tower cross section.

One commercial process operates on a somewhat different principle than that described above, and should be mentioned. This is the Duo-Sol process, which, as its name indicates, employs two solvents. These are usually propane and a mixture consisting principally of cresylic acid. Propane enters the extraction system at one end, the naphthenic solvent at the other end, and the feed is introduced near the middle. At the feed point the feed is treated with both solvents and two layers separated. The propane layer is taken out through several extraction stages countercurrent to the incoming cresylic acid, and its naphthenic content reduced. The naphthenic layer is taken out through several extraction stages and its paraffinic content largely recovered by the incoming propane.

LEACHING AND WASHING

The leaching of a solid is a special case of extraction, involving the diffusion of the solute through the liquid film on the solid surface. The prediction of the leaching rate is complicated by the fact that the interfacial area decreases as leaching proceeds. A few data are given by Watson,[189] Donnan,[49] Deerr,[47] Roller,[161] and by Hixon and Crowell.[91]

Washing refers to the extraction of a solute already in solution in a liquid, held mechanically by a porous solid or sludge. The calculations for this process, based simply on stoichiometry, have been treated extensively in the literature. See Hawley,[86] Sanders,[163] Griffin,[72] Baker,[10] and Ravenscroft.[155]

A graphical method of handling the stoichiometric calculations of both leaching and washing problems has been developed by Elgin.[54a] The method employs a triangular diagram, and is analogous to that described above for extraction calculations.

Nomenclature for Chapter VIII

a = amount of one solvent in solution to be extracted, lb.
b = amount of second solvent in treating agent, lb.
C = solute concentration, lb. mols/cu. ft.
h = tower height, ft.
K' = distribution coefficient $= \frac{y}{x}$.
Ka = over-all coefficient, lb. mols/(hr.)(cu. ft.)(lb. mol/cu. ft.).
L = rate of flow of liquid, cu. ft./(hr.) (sq. ft.).
x = solute concentration in raffinate phase.
y = solute concentration in extract phase.

Subscripts

0, 1, n refer to the extraction stage from which the solution is withdrawn.
B pertaining to benzene phase.
E pertaining to ether phase.
W pertaining to water phase.

BIBLIOGRAPHY

1. ABEL, E., H. SCHMID, and M. STEIN: Z. *Elektrochem.*, **36**, 692 (1930).
2. ADAMS, F. W.: *Trans. Am. Inst. Chem. Eng.*, **28**, 162 (1932); also *Ind. Eng. Chem.*, **25**, 424 (1933).

2*a*. ADAMS, F. W., and R. G. EDMONDS: Paper to appear in *Ind. Eng. Chem.*

3. ARNOLD, J. H.: *Ind. Eng. Chem.*, **22**, 1091 (1930).
4. ARNOLD, J. H.: *J. Am. Chem. Soc.*, **52**, 3937 (1930).
5. ARNOLD, J. H.: *Physics*, **4**, 255 (1933).
6. ARNOULD, J.: *Chimie et Ind.*, **21**, 478 (1930).
7. ATKINS, G. T., and W. B. FRANKLIN: *Refiner*, **15**, No. 1, p. 30 (1936).
8. AWBERY, J. H., and E. GRIFFITHS: *Proc. Phys. Soc.* (London) **44**, pt. 2, 132 (1932).
9. BADGER, W. L., and W. L. MCCABE: "Elements of Chemical Engineering," 1st ed., McGraw-Hill Book Company, Inc. New York, 1931.
10. BAKER, E. M.: *Trans. Am. Inst. Chem. Eng.*, **32**, 62 (1936).
11. BAKER, T. C.: *Ind. Eng. Chem.*, **27**, 977 (1935).
12. BAKER, T. C., T. H. CHILTON, and H. C. VERNON: *Trans. Am. Inst. Chem. Eng.*, **31**, 296 (1935).
13. BERL, E.: *Chem. Fabrik.*, **8**, 186 (1932).
14. BEUSCHLEIN, W. L., and R. H. CONRAD: *Paper Trade J.*, **99**, Sept. 20, 1934, p. 75.
15. BLACK, W. C., and L. A. MONROE: S. M. Thesis in Chemical Engineering, M.I.T., 1933.
16. BLAKE, F. C.: *Trans. Am. Inst. Chem. Eng.*, **14**, 415 (1922).
17. BODENSTEIN, M.: *Helv. Chim. Acta*, **18**, 743 (1935).
18. BOLSHAKOFF, P. E.: S. M. Thesis in Chemical Engineering, M.I.T. (1934).
19. BOTTOMS, R. R.: *Ind. Eng. Chem.*, **23**, 501 (1931).
20. BROWN, G. G., M. SOUDERS, JR., and R. L. SMITH: *Ind. Eng. Chem.*, **24**, 513 (1932).
21. BROWN, G. G., and M. SOUDERS, JR.: *Oil and Gas J.*, **31**, No. 5, 34 (1932).
22. BRUNNER, E.: *Z. Physik Chem.*, **47**, 67 et seq. (1904).
23. BURDICK, C. L.: *J. Am. Chem. Soc.*, **44**, 244 (1922).
24. BURDICK, C. L., and E. W. FREED: *J. Am. Chem. Soc.*, **43**, 518 (1921).
25. BURKE, S. P., and W. B. PLUMMER: *Ind. Eng. Chem.*, **20**, 1196 (1928).
26. BUTCHER, C. H.: *Ind. Chemist*, **4**, 446 (1928).
27. BUTCHER, C. H.: *Ind. Chemist*, **5**, 455 (1929).
28. BUTCHER, C. H.: *Ind. Chemist*, **8**, 131 (1932).
29. BYRNE, P. J., and C. E. CARLSON: Thesis in Chemical Engineering, M.I.T., 1921.

30. CANTELO, R. C., C. W. SIMMONS, E. M. GILES, and F. A. BRILL: *Ind. Eng. Chem.*, **19**, 989 (1927).
31. CARRIER, W. H.: *Trans. A.S.M.E.*, **33**, 1005 (1911).
32. CHAPMAN, W.: *Phil. Trans. Roy. Soc.*, (London) **A217**, 165 (1917).
33. CHILTON, T. H.: Private Communication, 1934.
34. CHILTON, T. H., and A. P. COLBURN: *Trans. Am. Inst. Chem. Eng.*, **26**, 178 (1931).
35. CHILTON, T. H., and A. P. COLBURN: *Ind. Eng. Chem.*, **26**, 1183 (1934).
36. CHILTON, T. H., and A. P. COLBURN: *Ind. Eng. Chem.*, **27**, 255 (1935).
37. COGAN, J. C., and J. P. COGAN: Thesis in Chemical Engineering, M.I.T. (1932).
38. COLBURN, A. P.: *Ind. Eng. Chem.*, **22**, 967 (1930).
39. COLBURN, A. P.: *Trans. Am. Inst. Chem. Eng.*, **28**, 105 (1932).
40. COLBURN, A. P., *Trans. Am. Inst. Chem. Eng.*, **29**, 174 (1933).
41. COMBS, L. N., and L. G. SIMONS: S. M. Thesis in Chemical Engineering M.I.T., 1932.
42. COPE, J. Q., W. K. LEWIS, and H. C. WEBER: *Ind. Eng. Chem.*, **23**, 887 (1931).
43. DAVIS, H. S., and G. S. CRANDALL: *J. Am. Chem. Soc.*, **52**, 3757, 3769 (1930).
44. DAVIS, H. S., G. THOMSON, and G. S. CRANDALL: *J. Am. Chem. Soc.*, **54**, 2340 (1932).
45. DAVIS, G. H. B., M. LAPEYROUSE, and E. W. DEAN: *Oil and Gas J.*, p. 92, March 31, 1932.
46. DEAN, E. W., and G. H. B. DAVIS: *Chem. Met. Eng.*, **36**, 618 (1929).
47. DEERR, N.: *Int. Sugar J.*, **33**, 167 (1931).
48. DEMO, J. J., and R. EWING: Thesis in Chemical Engineering, M.I.T. (1936).
49. DONNAN, F. G.: *J. Soc. Chem. Ind., Chem. Eng. Group*, **5**, 15 (1923–1924).
50. DRAEMEL, F. C., and N. E. RUCKMAN: Thesis in Chemical Engineering, M.I.T., 1936.
51. DRANE, H. S.: *J. Soc. Chem. Ind.*, **43**, 329*T* (1924).
52. DREW, T. B.: *Trans. Am. Inst. Chem. Eng.*, **26**, 26 (1931).
53. DREW, T. B., J. J. HOGAN, and W. H. MCADAMS: *Ind. Eng. Chem.*, **23**, 936 (1931).
54. DREW, T. B., E. C. KOO, and W. H. MCADAMS: *Trans. Am. Inst. Chem. Eng.*, **28**, 56 (1932).
54*a*. ELGIN, J. C.: Paper presented at the Baltimore meeting of the Am. Inst. Chem. Eng., November, 1936.
55 ELGIN, J. C., and F. M. BROWNING: *Trans. Am. Inst. Chem. Eng.*, **31**, 639 (1935).
56. ELGIN, J. C., and F. M. BROWNING: *Trans. Am. Inst. Chem. Eng.*, **32**, 105 (1936).
57. EUCKEN, A., and H. G. GRÜTZNER: *Z. physik. Chem.*, **125**, 385 (1927).
58. EVANS, T. W.: *Ind. Eng. Chem.*, **26**, 439 (1934).
59. FAGE, A., and H. C. H. TOWNEND: *Great Griain, Aero. Res. Com. Rep. and Mem.*, No. 1474, (1932); see also *Proc. Roy. Soc. A.*, **135**, 656 (1932).

60. FAIRLIE, A. M.: *Chem. Met. Eng.*, **39**, 76 (1932).
61. FALLAH, R., *J. Soc. Chem. Ind.*, **53**, 262T (1934).
62. FAUSER, G.: *Chem. Met. Eng.*, **35**, 474 (1928).
63. FERRIS, S. W., E. R. BIRKHEIMER, and L. M. HENDERSON: *Ind. Eng. Chem.*, **23**, 753 (1931).
64. FRITZ, H. E., and J. R. WITHROW: *Trans. Am. Inst. Chem. Eng.*, **15**, 217 (1923).
65. FROLICH, P. K., E. J. TAUCH, J. J. HOGAN, and A. A. PEER: *Ind. Eng. Chem.*, **23**, 548 (1934).
66. FURNAS, C. C.: *U.S. Bur. Mines Bull.*, 307 (1929).
67. GILLILAND, E. R.: Private Communication, February, 1932.
68. GILLILAND, E. R.: *Ind. Eng. Chem.*, **26**, 681 (1934).
69. GILLILAND, E. R., and T. K. SHERWOOD: *Ind. Eng. Chem.*, **26**, 516 (1934).
70. GRAETZ, VON L.: *Ann. Physik*, **18**, 79 (1883); **25**, 337 (1885).
71. GREENEWALT, C. H.: *Ind. Eng. Chem.*, **18**, 1291 (1926).
72. GRIFFIN, C. W.: *Ind. Eng. Chem., Anal. Ed.*, **6**, 40 (1934).
73. GRISWOLD, J.: Sc. D. Thesis in Chemical Engineering, M.I.T., 1931.
74. GUNNESS, R. C.: Sc. D. Thesis in Chemical Engineering, M.I.T., 1936.
75. HALL, J. A., A. JAQUES, and M. S. LESLIE: *Trans. Soc. Chem. Ind.*, **41**, 285 (1922).
76. HANKS, W. V., and W. H. MCADAMS: *Ind. Eng. Chem.*, **21**, 1034 (1929).
77. HARTE, C. R., E. M. BAKER, and H. H. PURCELL: *Ind. Eng. Chem.*, **25**, 528 (1933).
78. HARTE, C. R., and E. M. BAKER: *Ind. Eng. Chem.*, **25**, 1128 (1933).
79. HASLAM, R. T., R. L. HERSHEY, and R. H. KEAN: *Ind. Eng. Chem.*, **16**, 1224 (1924).
80. HASLAM, R. T., W. P. RYAN, and H. C. WEBER: *Trans. Am. Inst. Chem. Eng.*, **15**, Pt. I, 177 (1923).
81. HATTA, S.: *Tech. Rep. Tohoku Imp. Univ.*, **8**, 1 (1928–1929).
82. HATTA, S.: *Tech. Rep. Tohoku Imp. Univ.*, **10**, 119 (1932).
83. HATTA, S.: *Tech. Rep. Tohoku Imp. Univ.*, **10**, 136 (1932).
84. HATTA, S., and A. BABA: *J. Soc. Chem. Ind.* (Japan), **38**, 544B (1935).
85. HATTA, S., and M. KATORI: *J. Soc. Chem. Ind.*, (Japan), **37**, 280B (1934).
86. HAWLEY, L. F.: *Ind. Eng. Chem.*, **9**, 866 (1917); **12**, 493 (1920).
87. HEWSON, G. H., S. L. PEARCE, A. POLLITT, and R. L. REES: *J. Soc. Chem. Ind.*, **52**, 593 (1933).
88. HILL, J. B., and H. B. COATS: *Ind. Eng. Chem.*, **20**, 641 (1928).
89. HILPERT, R.: *Forschung*, Forschungsheft **355**, p. 21, July–August (1932).
90. HITCHCOCK, L. B.: Sc. D. Thesis in Chemical Engineering, M.I.T., 1933; see also *Ind. Eng. Chem.*, **26**, 1158 (1934); **27**, 461 (1935); **27**, 728 (1935); and *Trans. Am. Inst. Chem. Eng.*, **36**, 347 (1935).
91. HIXSON, A. W., and J. H. CROWELL: *Ind. Eng. Chem.*, **23**, 923 (1931).
92. HIXSON, A. W., and C. E. SCOTT: *Ind. Eng. Chem.*, **27**, 307 (1935).
93. HOLLINGS, H., and L. SILVER: *Trans. Inst. Chem. Eng.*, **12**, 49 (1934).
94. HUNTER, T. G., and A. W. NASH: *J. Soc. Chem. Ind.*, **51**, 285T (1932).
95. HUNTER, T. G., and A. W. NASH: *World Petroleum Congress*, **2**, 340 (1933).

96. HUNTER, T. G., and A. W. NASH: *J. Soc. Chem. Ind.*, **51**, 95T (1934).
97. HUNTER, T. G., and A. W. NASH: *Ind. Eng. Chem.*, **27**, 836 (1935).
98. International Critical Tables, McGraw-Hill Book Company, Inc., New York, 1927.
99. International Critical Tables, **3**, p. 248, McGraw-Hill Book Company Inc., New York, 1928.
100. International Critical Tables, **3**, p. 418, McGraw-Hill Book Company, Inc., New York, 1928.
101. JEANS, J. H.: "The Dynamical Theory of Gases," 3d ed., Chap. XIII, p. 307, Cambridge University Press, Cambridge, Eng., 1921.
102. JENNY, F. J.: Thesis in Chemical Engineering, M.I.T., 1936.
103. JOHNSTONE, H. F.: *Combustion*, **5**, No. 2, p. 19 (1933).
104. JOHNSTONE, H. F.: *Ind. Eng. Chem.*, **27**, 587 (1935).
105. JOHNSTONE, H. F.: Private Communication, 1936.
106. JOHNSTONE, H. F., and D. B. KEYES: *Ind. Eng. Chem.*, **27**, 659 (1935).
107. KAY, W. C.: Private Communication, April, 1934.
108. KEYES, D. B.: *J. Soc. Chem. Ind.*, **53**, 692 (1934).
109. KIRSCHBAUM, *Z. Ver. deut. Ing.*, **75**, 1212 (1931).
110. KOWALKE, O. L., O. A. HOUGEN, and K. M. WATSON: *Bull. Univ. Wisconsin Eng. Exp. Sta.*, **68** (June, 1925).
111. KRASE, N. W.: "Fixed Nitrogen," Edited by H. A. Curtis, Chemical Catalogue Company, New York, 1932.
112. KREMSER, A.: *Nat. Pet. News*, **22**, No. 21, p. 42 (May 21, 1930).
113. LAWRENCE, A. E., and J. J. HOGAN: *Ind. Eng. Chem.*, **24**, 1318 (1932).
114. LEDIG, P. G., and E. R. WEAVER: *J. Am. Chem. Soc.*, **46**, 650 (1924).
115. LEWIS, G. N., and M. RANDALL: "Thermodynamics," p. 190, McGraw-Hill Book Company, New York (1923).
116. LEWIS, W. K.: *Trans. A.S.M.E.*, **44**, 329 (1922).
117. LEWIS, W. K. *Trans. Am. Inst. Chem. Eng.*, **20**, 1 (1927).
118. LEWIS, W. K. *Mech. Eng.*, **55**, 567 (1933).
119. LEWIS, W. K.: *Ind. Eng. Chem.*, **28**, 257 (1936).
120. LEWIS, W. K., and K. C. CHANG: *Trans. Am. Inst. Chem. Eng.*, **21**, 127 (1928).
121. LEWIS, W. K., and W. C. KAY: *Oil and Gas J.*, March 29, 1934.
122. LEWIS, W. K., and C. D. LUKE: *Trans. A. S. M. E.*, **54**, 55 (1932).
123. LEWIS, W. K., and W. H. MCADAMS: *Proc. Am. Gas. Assoc.*, **5**, 1143 (1923).
124. LEWIS, W. K., L. SQUIRES, and C. E. SANDERS: *Ind. Eng. Chem.*, **27**, 1395 (1935).
125. LEWIS, W. K., and L. SQUIRES: Article to appear in *Ind. Eng. Chem.*
126. LEWIS, W. K., and W. G. WHITMAN: *Ind. Eng. Chem.*, **16**, 1215 (1924).
127. LEWIS, W. K., JR.: *Ind. Eng. Chem.*, **28**, 399 (1936).
128. LOHRISCH, W.: *Mitt. Forschungsarb.*, **322**, 46 (1929).
129. LUKE, C. D.: Sc. D. Thesis in Chemical Engineering, M.I.T. (1934).
130. MCCABE, W. L., and W. H. SWANSON: *Paper Trade J.*, **92**, No. 26, p. 48 (1931).
131. MCADAMS, W. H.: "Heat Transmission," McGraw-Hill Book Company, Inc., New York, 1934.

132. McAdams, W. H.: "Heat Transmission," McGraw-Hill Book Company, Inc., New York, p. 234, 1934.
133. McCoy, H. N.: *Am. Chem. J.*, **29**, 437 (1903).
134. Mach: *Dechema*, **6**, 38 (1934). (Taken from White.)
135. MacInnes, D. A., and D. Belcher: *J. Am. Chem. Soc.*, **55**, 2630 (1933).
136. Mark, J. G.: Data presented by Sherwood, *Trans. Am. Inst. Chem. Eng.*, **28**, 107 (1932).
137. Mason, J. W., and B. F. Dodge: *Trans. Am. Inst. Chem. Eng.*, **32**, 27 (1936).
138. Mass. Inst. Tech., School of Chem. Eng. Practice, *Reports*.
139. Maxwell, J. C.: *Scientific Papers*, **2**, p. 57, Cambridge University Press, Cambridge, Eng., 1890.
140. Maxwell, J. C.: *Scientific Papers*, **2**, p. 343, Cambridge University Press, Cambridge, Eng., 1890.
141. Maxwell, J. C.: *Scientific Papers*, **2**, p. 625, Cambridge University Press, Cambridge, Eng., 1890. Reprinted from Encyclopedia Britannica, article on "Diffusion," 9th ed., 1877.
142. Mayo, F., T. G. Hunter, and A. W. Nash: *J. Soc. Chem. Ind.*, **54**, 375T (1935).
143. Meyer, O. E.: "Kinetic Theory of Gases," Transl. from the 2d rev. ed., Longmans, Green, & Company, London, 1899.
144. Mitsukuri, S.: *Sci. Rep. Tohoku Imp. Univ.*, **18**, 245 (1929).
145. Moscicki, I.: *Chimie et Industrie*, **2**, 1303 (1919).
146. Mullaly, J. M., and H. Jacques: *Phil. Mag.*, **48**, 1105 (1924).
147. Murphree, E. V.: *Ind. Eng. Chem.*, **17**, 747 (1925).
148. Murphree, E. V.: *Ind. Eng. Chem.*, **24**, 726 (1932).
149. Murray, I. L.: Private Communication, 1936.
150. Osborne, H. B., and C. W. Simmons: *Ind. Eng. Chem.*, **26**, 856 (1934).
151. Payne, J. W., and B. W. Dodge: *Ind. Eng. Chem.*, **24**, 630 (1932).
152. Pearson, J. L., G. Nonhebel, and P. H. N. Ulander: *J. Inst. Fuel*, **8**, 119 (1935).
153. Peters, W. A., Jr.: *Ind. Eng. Chem.*, **14**, 476 (1922).
154. Prandtl, L.: *Z. Physik*, **11**, 1072 (1910).
155. Ravenscroft, E. A.: *Ind. Eng. Chem.*, **28**, 851 (1936).
156. Reich, G. T.: *Chem. Met. Eng.*, **38**, No. 3 (1931).
157. Reiher, H.: *Mitt. Forschungsarb.*, **269**, 20 (1925).
158. Reynolds, B. M., and F. W. Sanders: Thesis in Chemical Engineering, M.I.T., 1920.
159. Roberts, J. B.: Thesis in Chemical Engineering, M.I.T. (1936).
160. Rogers, M. C., and E. W. Thiele: *Ind. Eng. Chem.*, **26**, 524 (1934).
161. Roller, P. S.: *J. Phys. Chem.*, **36**, 1202 (1932).
162. Saal, R. N. J., and W. J. D. VanDyck: *World Petroleum Congress*, **2**, 352 (1933).
163. Sanders, M. T.: *Chem. Met. Eng.*, **39**, 161 (1932).
164. Sandstrom, C. O.: *Chem. Met. Eng.*, **39**, 270 (1932).
165. Selheimer, C. W., M. Souders, R. L. Smith, and G. G. Brown: *Ind. Eng. Chem.*, **24**, 515 (1932).

166. SHERWOOD, T. K., and E. W. COMINGS: *Trans. Am. Inst. Chem. Eng.*, **28**, 88 (1932).
167. SHERWOOD, T. K., and F. J. JENNY: *Ind. Eng. Chem.*, **27**, 265 (1935).
168. SHERWOOD, T. K., and A. J. KILLGORE: *Ind. Eng. Chem.*, **18**, 744 (1926).
169. SIEVERTS, A., and A. FRIZSCHE: *Z. anorg. allgem. Chem.*, **133**, 1 (1924).
170. SIMMONS, C. W., and J. D. LONG: *Ind. Eng. Chem.*, **22**, 718 (1930).
171. SIMMONS, C. W., and H. B. OSBORN: *Ind. Eng. Chem.*, **26**, 529 (1934).
172. SMITH, A. S.: *Ind. Eng. Chem.*, **26**, 1167 (1934).
173. SMITH, E. L.: *J. Soc. Chem. Ind.*: **47**, 159T (1928).
174. SMOLEY, E. R., and W. W. KRAFT: *Trans. Am. Inst. Chem. Eng.*, **31**, 671 (1935).
175. SOUDERS, M., and G. G. BROWN: *Ind. Eng. Chem.*, **24**, 519 (1932).
176. SOUDERS, M., C. W. SELHEIMER, and G. G. BROWN: *Ind. Eng. Chem.*, **24**, 517 (1932).
177. STEFAN: *Sitz. Akad. Wiss. Wien*, **63**, (2), 63 (1871).
178. STEFAN: *Sitz. Akad. Wiss. Wien*, **65**, (2) 323 (1872).
179. STEFAN: *Sitz. Akad. Wiss. Wien*, **65**, (2) 161 (1879).
180. SUTHERLAND, W.: *Phil. Mag.*, **38**, 1 (1894).
181. TAYLOR, G. B., T. H. CHILTON, and S. L. HANDFORTH: *Ind. Eng. Chem.*, **23**, 860 (1931).
182. THIELE, E. W.: *Ind. Eng. Chem.*, **27**, 392 (1935).
183. TYLER, S. L.: *Trans. Am. Inst. Chem. Eng.*, **17**, 75 (1925).
184. UCHIDA, S.: *J. Soc. Chem. Ind.* (Japan), **37**, 456B (1934).
185. UCHIDA, S., and S. FUJITA: *J. Soc. Chem. Ind.* (Japan), 37, 724B, 791B (1934).
186. VARTERESSIAN, K. A., and M. R. FENSKE: *Ind. Eng. Chem.*, **28**, 928 (1936).
187. VINT, A. W.: Thesis in Chemical Engineering, M.I.T., 1932.
188. WALKER, W. H., W. K. LEWIS, and W. H. MCADAMS: "Principles of Chemical Engineering," 2nd. ed., McGraw-Hill Book Company, 1927.
189. WATSON, K. M.: *Ind. Eng. Chem.*, **23**, 1146 (1931).
190. WEBB, H. W.: "Absorption of Nitrous Gases," Edward Arnold & Company, London, 1923.
191. WEBER, H. C., and K. NILSSON: *Ind. Eng. Chem.*, **18**, 1070 (1926).
192. WEIDMANN, H., and ROESNER, G.: *Ind. Eng. Chem.*, News Edition, **14**, 105 (1936).
193. WHITE, A. M.: *Trans. Am. Inst. Chem. Eng.*, **31**, No. 2,390 (1935).
194. WHITMAN, W. G.: *Chem. Met. Eng.*, **29**, No. 4, July 23, 1923.
195. WHITMAN, W. G., and G. H. B. DAVIS: *Ind. Eng. Chem.*, **18**, 264 (1926).
196. WHITMAN, W. G., and J. L. KEATS: *Ind. Eng. Chem.*, **14**, 186 (1922).
197. WHITMAN, W. G., L. LONG, and W. Y. WANG: *Ind. Eng. Chem.*, **18**: 363 (1926).
198. WILLIAMSON, R. V., and J. H. MATHEWS: *Ind. Eng. Chem.*, **16**, 1157 (1924).
199. WOHRLEY, J. R.: *Proc. Am. Gas. Assoc.*, **4**, 349 (1922).
200. ZEISBERG, F. C.: *Trans. Am. Inst. Chem. Eng.*, **12**, 231 (1919).

INDEX

D